Université de Montréal

Transcriptional regulation of temporal identity transitions in retinal progenitor cells

par Awais Javed

Programme de biologie moléculaire

Faculté de médecine

Thèse présentée

en vue de l'obtention du grade de *Philosophiae doctor* (Ph.D)

en biologie moléculaire

option générale

Avril, 2021

A été évalué par un jury composé des personnes suivantes

Dr. Hideto Takahashi

Président

Dr. Michel Cayouette

Directeur de recherche

Dr. Adriana Di Polo

Membre du jury

Dr. May Griffith

Représentant de la Doyenne

Dr. Valerie Wallace

Examinateur externe

Résumé

La manière dont la diversité neuronale du système nerveux central est établie au cours du développement est une question d'un grand intérêt depuis plus d'un siècle. Les progéniteurs neuronaux sont contrôlés dans l'espace et dans le temps afin de générer un ensemble diversifié de neurones. Les composants moléculaires du contrôle spatial chez les vertébrés soient bien compris, mais le cadre moléculaire du contrôle temporel chez les vertébrés n'a été que peu exploré. Les travaux réalisés, au cours de la dernière décennie, sur le développement de la rétine chez la souris ont révélé l'existence de deux importants facteurs de transcription temporels (tTF). Ikzf1 confère une compétence temporelle précoce alors que Casz1 confère une compétence temporelle tardive aux cellules progénitrices de la rétine (RPC) des mammifères. Cependant, sur les sept types cellulaires présents dans la rétine, ces tTFs ne régulent pas la capacité de générer les cônes nés précocement ni pour les cellules gliales de Müller nées tardivement, suggérant la présence d'autres tTFs non identifiés. L'objectif principal de cette thèse a été de découvrir les mécanismes moléculaires contrôlant la production des cônes au cours de la rétinogenèse précoce ainsi que la production tardive des cellules gliales de Müller. Dans cette thèse, Pou2f1 a été découvert comme un tTF qui confère aux RPCs une compétence temporelle à générer des cônes. Pou2f1 active l'expression de Pou2f2, qui permet ensuite de favoriser la production de cônes en réprimant l'expression du facteur de transcription Nrl. Ikzf1 active l'expression de Pou2f1 dans les RPC alors que Pou2f1 réprime le tTF tardif Casz1, suggérant une boucle d'autorégulation transcriptionnelle entre ces différents tTF. De plus, Ikzf4, un autre membre de la famille Ikzf, s'est avéré important pour la spécification des cônes et des cellules gliales de Müller. Ikzf4 active l'expression de Pou2f1/Pou2f2 lorsqu'il est surexprimé dans des RPC tardifs, suggérant qu'il permet la production de cônes en activant directement l'expression de Pou2f1/Pou2f2. Ikzf4 était également lié à de nombreux gènes de la voie de signalisation de Notch, qui sont impliqués dans la production de cellules gliales de Müller au cours de la rétinogenèse. Ce travail établi des bases pouvant inspirer de futures études dans d'autres parties du SNC, où des tTF similaires pourraient aussi contrôler la production de différents types cellulaires en fonction du temps. Enfin, cette thèse propose de nouveaux tTF comme outils thérapeutiques pour améliorer l'efficacité de production des cônes à partir de cellules souches.

Mots-clés: compétence temporelle, rétine, développement de cône, développement de glie de Müller, Pou2f1, Pou2f2, Ikzf4

Abstract

How neural diversity is established in the developing central nervous system has been a question of great interest for more than a century. Neural progenitors are spatially and temporally patterned to generate a diverse set of neurons. Although molecular components of spatial patterning in vertebrates are well understood, the molecular framework behind temporal patterning in vertebrates has been largely unexplored. Work done in the past decade on mouse retinal development has revealed insights on how temporal patterning could be established in the CNS. Retinal neurons and glia are born in a sequential but overlapping manner from a pool of multipotent retinal progenitor cells (RPCs), consisting of an early embryonic and late post-natal window of cell birth. Two temporal transcription factors (tTFs), Ikzf1 and Casz1, confer early and late temporal competence to retinal progenitor cells (RPCs), respectively. However, out of the seven cell types in the retina, these tTFs do not regulate the competence for early born cones and late born Müller glia, suggesting the presence of other unidentified tTFs. The prime goal of this thesis was to uncover the molecular mechanisms controlling cone specification during early, and Müller glia specification during late retinal development. In this thesis, Pou2f1 was discovered as a novel tTF that confers temporal competence to RPCs to generate cones. Pou2f1 activates Pou2f2, which binds to the promoter of Nrl, a key rod specification gene, and represses its expression. Early tTF Ikzf1 activates Pou2f1, whereas Pou2f1 represses late tTF Casz1 in RPCs. Additionally, Ikzf4 was discovered as an important regulator of cone specification early, and Müller glia specification late during retinal development. Ikzf4 binds to genomic regions near *Pou2f1/Pou2f2* gene bodies and activates their expression during early retinogenesis. During late retinogenesis, Ikzf4 binds to promoters of Notch signaling genes and activates their expression to promote Müller glia differentiation. Taken together, these results reveal important insights on how cone and Müller glia production is temporally controlled during early and late retinogenesis. This work lays the groundwork for future studies in other parts of the developing CNS that could employ similar tTFs for temporal patterning. Finally, this thesis proposes novel tTFs as therapeutic tools to efficiently generate cones from ESC-derived retinal organoids and sheets.

Keywords: Temporal competence, Retina, Cone development, Müller glia development, Pou2f1, Pou2f2, Ikzf4

Table of Contents

List of figures and tables

List of abbreviations

A.C: Amacrine cell

A.k.a: Also known as

AAV: Adeno-associated virus

AMD: Aged related macular degeneration

B.C: Bipolar cell

bHLH: Basic helix loop helix

C: Cone

ChIP: Chromatin Immunoprecipitation

cKO: Conditional knockout

CMZ: Ciliary marginal zone

CNS: Central nervous system

CRM: Cis regulatory module

CUT&RUN: Cleavage under target and release under nuclease

D: Dichaete

D-D: Differentiated cell – Differentiated cell

DIV: Days in vitro

Ey: Eyeless

FGF: Fibroblast growth factor

FW: Fetal week

GCL: Ganglion cell layer

GMC: Ganglion mother cell

GO: Gene ontology

Grh: Grainyhead

GRN: Gene regulatory network

H.C: Horizontal cell

HAA: High acuity area

Hb: Hunchback

Hth: Homothorax

INL: Inner nuclear layer

IPL: Inner plexiform layer

Klu: Klumpfuss

Kr: Krüppel

M.G: Müller glia

MITF: Melanocyte inducing transcription factor

MN: Motor neurons

mpNrl: mutated promoter Nrl

NFL: Neurofilament layer

NuRD: Nucleosome remodeling and deacetylase

ONL: Outer nuclear layer

P-D: Progenitor- Differentiated cell

POU: Pit-Oct-Unc

P-P: Progenitor-Progenitor

RT: Room temperature

RA: Retinoic acid

RGC: Retinal ganglion cell

RPC: Retinal progenitor cell

RPE: Retinal pigmented epithelium

Slp: Sloppy paired 1 and 2

TF: Transcription factor

Tll: Tailless

TSS: Transcription start site

tTF: Temporal transcription factor

VNC: Ventral nerve cord

VZ: Ventricular zone

‘دیر آئے درست آئے’

‘It took some time, but what matters is that you arrived safely.’

- South Asian proverb.

Acknowledgements

First of all, I'd like to thank Dr. Michel Cayouette for his constant support and guidance during my Ph.D. When I started in the lab, I was a total mess of a student. An example of this is my first lab meeting. I exited the meeting room multiple times to drink water and calm myself down. Before any big talk, Michel went over it with me multiple times while sitting patiently and repeatedly saying, 'go again'. I spent the first 6 months of my time in the lab cloning one vector because, well, it was cloning. At times, I did not know if I had it in me to complete a Ph.D. Michel took a chance on me despite all of this and I am forever grateful for not only his kindness but also his patience in helping me grow. I feel like many would have given up on me and not have accepted me as a Ph.D student in their lab at the time. It is truly a sign of a great leader and a mentor, rather than a boss, to nurture persistent growth in their trainees.

I would like to thank Dr. Pierre Mattar who would spend hours on end to discuss any question I had about the science. He taught me to never shy away from a tough experiment and explore even the craziest of ideas. He was, and still is, a constant source of inspiration and an amazing role model. I am forever grateful to you.

Thank you to the Cayouette lab members, both past and present: Adele, Benoit, Camille, Carine, Christine, Fatima, Ko, Maeva, Marine, Marie-Claude, Megan, Michel Jr., Mike, Maude, Sepideh, Sarah, Shaz, Thomas and Yulia. Without these people, everyday at the bench would have been boring and tiresome. I would also like to thank all neurolab members at the IRCM and especially, Farin, Lukas and Shannon. Growing as a scientist and an individual with these people is truly an unforgettable experience and I will always cherish the times we argued about everything we possibly could.

Although I still have a long way to go, I am incredibly grateful to my committee members who pushed me to become a more critical and better scientist over the years: Dr. Frédéric Charron, Dr. Jacques Drouin, Dr. Maxime Bouchard, Dr. Hideto Takahashi, Dr. Artur Kania, Dr. Rod Bremner and Dr. Robin Ali. I am also grateful to the anonymous reviewers that granted me the FRQS scholarship and the reviewers in the past 4 attempts that gave me feedback on my application.

I would like to thank my father, Javed Iqbal, for his relentless support and being a constant role model for hard work and persistence. Your struggles are the reason why I am where I am today. My mother, Shamim Akhtar, who showed me the meaning of sacrifice and to always dream big. Ammi ji, thank you for always believing in me. My brother, Osama, who always had my side, even in the toughest of times when I was not necessarily the best brother. You relentlessly defended my crazy decision to pursue a Ph.D and I do not know if I would have started it if it was not for you. My sister, Noora, who makes me want to be the best possible person I can be. I have not been the best brother to you because I was totally consumed with work these past few years, but you only mildly complained. I truly would not have done any of this without you all. Thank you for supporting me in the pursuit of my dream. I hope I have made you proud.

Maraika. One would think 13 months of a pandemic lockdown with anyone would be a recipe for disaster. Thank you for everything.

Finally, this thesis is dedicated to the Pakistani diaspora all over the world. My parents come from two small villages in Pakistan, Varpal and Lambanwali. I am the first person in my entire family to pursue a Ph.D. I hope this thesis inspires others from a similar background to think about a career in research. I thank the generations before mine for their struggles and sacrifices.

1 Introduction

The development of the central nervous system is an intricate and fascinating process that has stimulated countless questions in the field of biology. How does a pool of neural stem cells or progenitors differentiate and diversify to form such a complex architecture of neurons and glia? How do these neurons and glia communicate with each other to grant us abilities, from feeling our simplest emotions to addressing the largest quandaries of our existence? Going as far back as the birth of these neurons and glia, how do the neural stem cells know where to migrate, where to interact, and where to connect? How do these progenitors know exactly what kind of neurons to produce at the right time and place, so that they synapse with their appropriate targets before development ends? What happens when these stem cells lose their identity? The answers to these questions lie in the molecular machinery that guides every cell to not only become a distinct functional unit in an organ, but also have a distinct cellular identity.

1.1 Generation of neural diversity: Space and time

The development of the central nervous system begins when the naïve neural plate is first defined by the dorsal mesoderm, also called the organizer in frogs or Henson's node in chicks. Cells from the organizer release neural inducing signals, which inhibit BMP activity in the surrounding tissue, reviewed in (Harland, 2000). The inhibition of BMP in the surrounding ectoderm of the animal pole leads to the specification of this region into the neural plate. Subsequently, the neural plate invaginates to form the primitive streak at the rostral most region and moves towards the caudal most region. These events activate Hox gene expression across the developing neural tube that instructs the rostro-caudal identity, reviewed in (Philippidou and Dasen, 2013). On the other hand, the organizer cells become the notochord that release ventralizing signals to the neural tube, whereas the surrounding non-neural ectoderm release dorsalizing signals that establish the dorso-ventral axes (Pituello, 1997). Therefore, positional information instructs the progenitor cells in the neural tube to form distinct parts of the central nervous system, the rostral most being the forebrain and the caudal most being the spinal cord (Jessell, 2000). Once the neural tissue has been specified, the neural progenitors in each sub-region such as forebrain,

hindbrain, and the spinal cord, require another level of positioning information within the same tissue. This is called spatial patterning, which allows the neural progenitors to know where they are in space.

1.1.1 Spatial patterning in the vertebrate CNS

One of the most well-studied vertebrate systems for understanding spatial identity and patterning is the developing mouse rostral neural tube that becomes the spinal cord. After neural induction in the rostro-caudal axis, the neural tube is spatially patterned on the dorso-ventral axis by a combination of morphogens, BMP/Wnt from the roof plate and Shh from the floor plate (Echelard et al., 1993; Liem et al., 1997) (Fig. 1.1A). Low BMP/Wnt and high Shh combination promotes the adoption of ventral-most identity and vice versa. Taking the example of the developing mouse spinal cord, progenitor domains constituting of distinct dorso-ventral spatial identity are established due to these opposing morphogen gradients (Fig. 1.1B). In the ventral half of the developing spinal cord, p0-3 and pMN progenitor sub-domains are formed closer to the floor plate and defined by high Shh concentration gradient that progressively reduces as it is diffuses more dorsally (Chamberlain et al., 2008). This allows the progenitors to acquire a specific regional identity in the developing spinal cord. After differentiation, these progenitors give rise to V1-3 and MN neurons, which then innervate their own set of targets, reviewed in (Hori and Hoshino, 2012). Therefore, Shh and BMP/Wnt establish important spatial identity information for the progenitors in the dorso-ventral axis of the developing spinal cord.

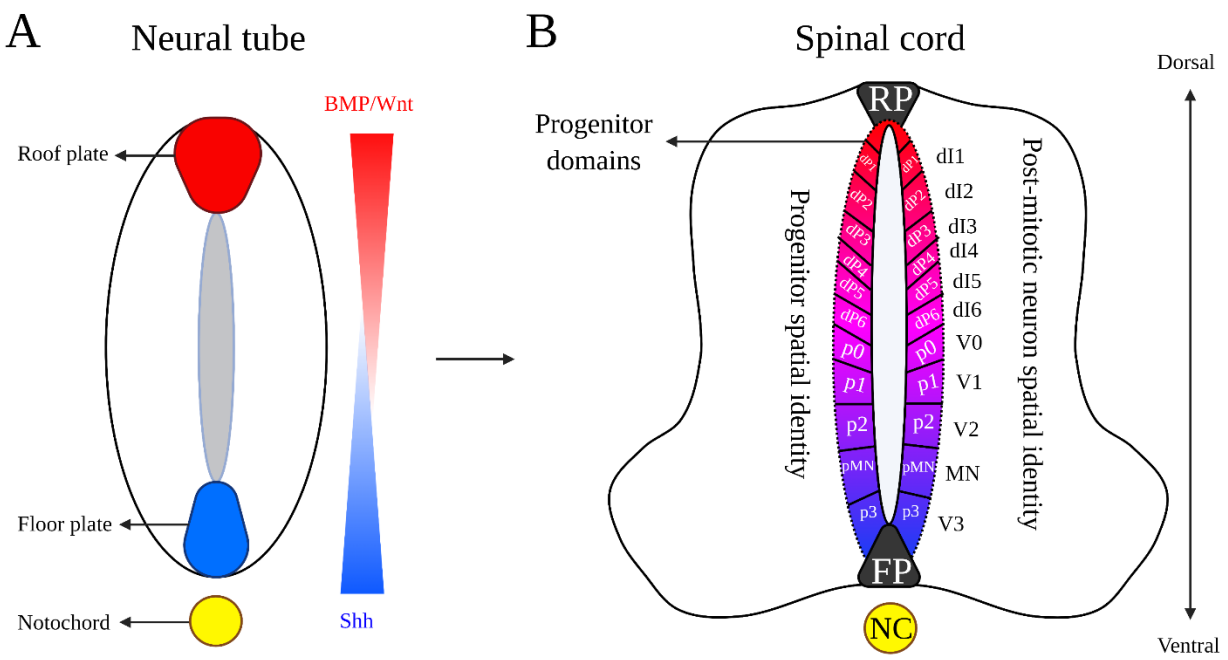

Figure 1.1: Spatial patterning the developing spinal cord. (A) Illustration of a developing neural tube. Roof plate domain is colored red to depict the high morphogen gradient of BMP/Wnt, whereas the Floor plate is colored blue to emphasize high Shh gradient, adapted from (Zannino and Sagerstrom, 2015). (B) Schematic of the developing spinal cord. Progenitor domain is colored in a gradient: dorsal most region with high BMP/Wnt as red, low BMP/Wnt and Shh as magenta, and ventral most region with high Shh as blue. Progenitor domains contain progenitors with spatial identity ranging from dP1-6 to p0-3/pMN. Progeny of these progenitors give rise to neurons made from the same spatial identity ranging from dI1-6 to V0-3/MN. The dorso-ventral axis is labelled on the right, adapted from (Hori and Hoshino, 2012). RP: Roof plate. FP: Floor plate. NC: notochord.

1.1.1.1 Spatially restricted transcription factors of the spinal cord progenitors

As the morphogen gradients set up positional information for the neural progenitors, certain transcription factors are expressed in a spatially restricted manner of the progenitor domain. Basic Helix Loop Helix (bHLH) transcription factors, Olig2/3, Atoh1, Neurog1/2, Ascl1 and Ptf1a define spatial identity to the progenitors in their subdomains (Bermingham et al., 2001; Gowan et al., 2001; Mizuguchi et al., 2006; Mizuguchi et al., 2001; Muller et al., 2005; Novitch et al., 2001; Takebayashi et al., 2002). In the various progenitor sub-domains, these bHLH transcription factor are specifically expressed in a tightly regulated gene regulatory network. Atoh1 expression is restricted in the dorsal most dP1 progenitor domain and represses Neurog1/2 (Bermingham et al.,

2001; Gowan et al., 2001) (Fig. 1.2). Moreover, Ascl1 regulates dP3 and dP5 progenitor domain identity by repressing Neurog2 whereas Ptf1a establishes the dP4 domain due to a cross inhibitory mechanism with Ascl1 (Helms et al., 2005; Mizuguchi et al., 2006). Finally, Neurog1/2 expression defines the dP2 domain whereas combinatorial expression of Olig3 defines p0, p2 and p3 domains (Mizuguchi et al., 2001). Olig2 and Olig3 are expressed in a non-overlapping manner in the ventral progenitor domains p2, pMN and p3 which also provides precision in the acquisition of spatial identity in these progenitor domains (Takebayashi et al., 2002). Finally, there are other classes of transcription factors such as PR containing transcription factors (Prdm8, Prdm13), homeodomain (Lhx3, Dbx1/2, Nkx 2.2, Nkx6.1/2) and paired box (Pax3/6/7) proteins that also define these progenitor domains based on their combinatorial expression (Briscoe et al., 2000; Chang et al., 2013; Ericson et al., 1997; Komai et al., 2009; Thelie et al., 2015). Therefore, a tightly controlled gene regulatory network consisting of sequential or combinatorial expression of transcription factors is essential to set up distinct progenitor subdomains.

1.1.1.2 Spatially restricted transcription factors of spinal cord neurons

Once the progenitor domain has been classified, there is an additional level of specification of post-mitotic cells based on the expression of downstream transcription factors, primarily belonging to the homeodomain and paired box transcription factor classes. This leads to the establishment of the post-mitotic cell domains, where each post-mitotic neuron made from the progenitor in the respective domain has a distinct spatial identity. In the dorsal half of the post-mitotic cell domain, Lhx2/9 expression in post-mitotic cells generated from dP1 progenitors leads to the differentiation of dorsal most dI1 neurons (Wilson et al., 2008) (summarized in Fig. 1.2). Lhx1/5 define dI2 and dI4 neurons (Pillai et al., 2007), Gsx1/2 define dI3-6 (Kriks et al., 2005; Mizuguchi et al., 2006), Lbx1 defines dI4-6 (Muller et al., 2002), Pax2 defines dI4, dI6 and V0-1 neurons (Burrill et al., 1997; Cheng et al., 2004b; Glasgow et al., 2005) and Tlx1 defines dI6 neurons (Cheng et al., 2004b; Qian et al., 2002). On the ventral axis, Dbx1/2, Evx1/2, En1, Nkx6.2, Lhx2, Vsx2, Gata2/3, Tal1 and Sim1 define the V0-3 and MN neuron subtypes originating from the progenitors in their respective domains (Debrulle et al., 2020; Fan et al., 1996; Francius et al., 2013; Francius et al., 2015; Moran-Rivard et al., 2001; Pierani et al., 1999; Pierani et al., 2001). Similar to the progenitor domains, many of these transcription factors have overlapping and non-overlapping expression, thereby forming a combinatorial code of expression that classify each cell

based on their position in the developing spinal cord. This is how spatial identity is coded into progenitors and post-mitotic cells to generate neuronal diversity in the rodent spinal cord. However, progenitors generate different neurons as the spinal cord neurogenesis proceeds in developmental time (Nornes and Das, 1972). Using temporal labeling of [^{3}H]thymidine, it was shown that motor neurons (MN) are generated the earliest, followed by the neurons in the intermediate gray (V0-2) and substantia gelatinosa neurons are the latest to be born (dI1-6) (Nornes and Das, 1974). If not spatial patterning, what other mechanism could explain the temporal order of neuron birth in the developing spinal cord?

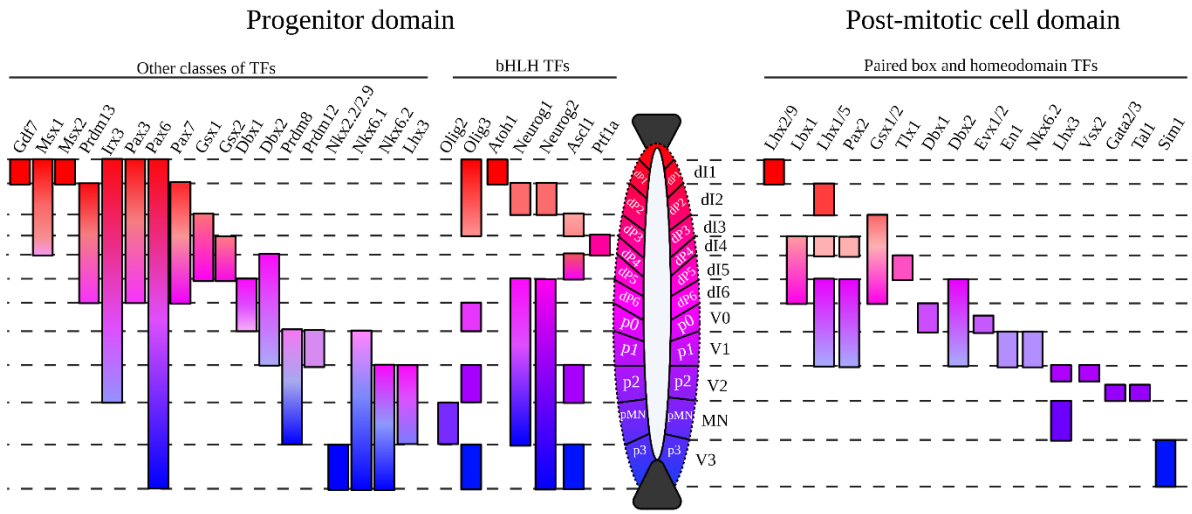

Figure 1.2: Combinatorial code of transcription factors in spinal cord development. Different classes of TFs are expressed in the progenitor domain on the left (gradient colored as red for dorsal most progenitor, magenta for middle and blue for ventral most). Paired box and homeodomain TFs are expressed in post-mitotic cell domains listed as dI1-6, V0-3 and MN on the right. Adapted from (Hori and Hoshino, 2012; Lai et al., 2016). TF: Transcription factors.

1.1.2 Temporal patterning in the vertebrate CNS: A poorly understood mechanism

Within the same spatially restricted domain of neural progenitors of the CNS, there is another level of patterning that relies on time to produce neurons. Neurons produced from the same progenitors are different earlier during development compared to late during development. This type of patterning is called temporal patterning in which the neural progenitors modulate their neuron specification potential, as they move forward in developmental time. In addition to the spinal cord, another striking example of temporal patterning is observed in the developing neocortex where a pool of neural progenitors give rise to deeper layer neurons early and superficial layer neurons late (Berry and Rogers, 1965). Although the existence of the birth order of cortical neurons has been known for many decades, the mechanism by which this is established and the factors that regulate the shift in early to late temporal identity of the neural progenitors, remains poorly understood in vertebrates. However, a proposed model of a transcription factor cascade has been discovered in *Drosophila melanogaster* CNS development, that could explain how temporal patterning is established in the developing vertebrate CNS.

1.1.3 *Drosophila melanogaster* CNS development

Development of the *Drosophila melanogaster* CNS initiates when the neuroectoderm is specified by the action of morphogens *dpp* and *sog* that pattern the embryo in the dorso-ventral axis (Araujo and Bier, 2000; Biehs et al., 1996). Once the neuroectoderm has been established, subsequent expression of maternal coordinate genes, gap genes, pair-rule genes and segment polarity genes spatially specify the dorso-ventral and anterior posterior axis, reviewed in (Umulis et al., 2008). The combination of these genes set up column and rows of neural progenitors, also called neuroblasts, that give rise to neurons with distinct spatial identity. Neuroblasts acquire the apico-basal positional information through *mirror*, *wingless*, *hedgehog*, *gooseberry* and *engrailed* genes (Bhat and Schedl, 1997; Chu-LaGraff and Doe, 1993; Matsuzaki and Saigo, 1996; McDonald and Doe, 1997; Skeath et al., 1995; Urbach and Technau, 2003; Zhang et al., 1994). These genes, also known as segmentation genes, are expressed in stripes in their respective domains. This establishes spatial identity of the neuroblast based on which row they are located in. For example, *wingless* is required for the specification of the rows 4 and 6, whereas *gooseberry*

is required for the specification of row 5 (Chu-LaGraff and Doe, 1993; Skeath et al., 1995; Zhang et al., 1994). Misexpression in other rows or loss of expression in their respective rows leads to a shift in spatial identity of the neuroblast, highlighting the importance of these genes in providing positional information to the neuroblast. As the *Drosophila melanogaster* ventral nerve cord (VNC) is spatially specified, neuroblast in the VNC delaminate (Fig. 1.3). Following delamination, NB are further diversified to produce distinct sets of neurons in a time dependent manner, depending on the mode of cell division. There are three main modes of cell division in NBs. Type I division which leads to the production of a NB and a ganglion mother cell (GMC), that further divides to produce two neurons, reviewed in (Homem et al., 2015). Type II NB divisions give rise to a NB and an intermediate neural progenitor that produces a GMC (Bello et al., 2008; Boone and Doe, 2008; Bowman et al., 2008). Additionally, there is Type 0 division, primarily present in the larval stage of the brain lobe, that gives rise to a NB and a neuron (Baumgardt et al., 2014; Baumgardt et al., 2009; Karcavich and Doe, 2005).

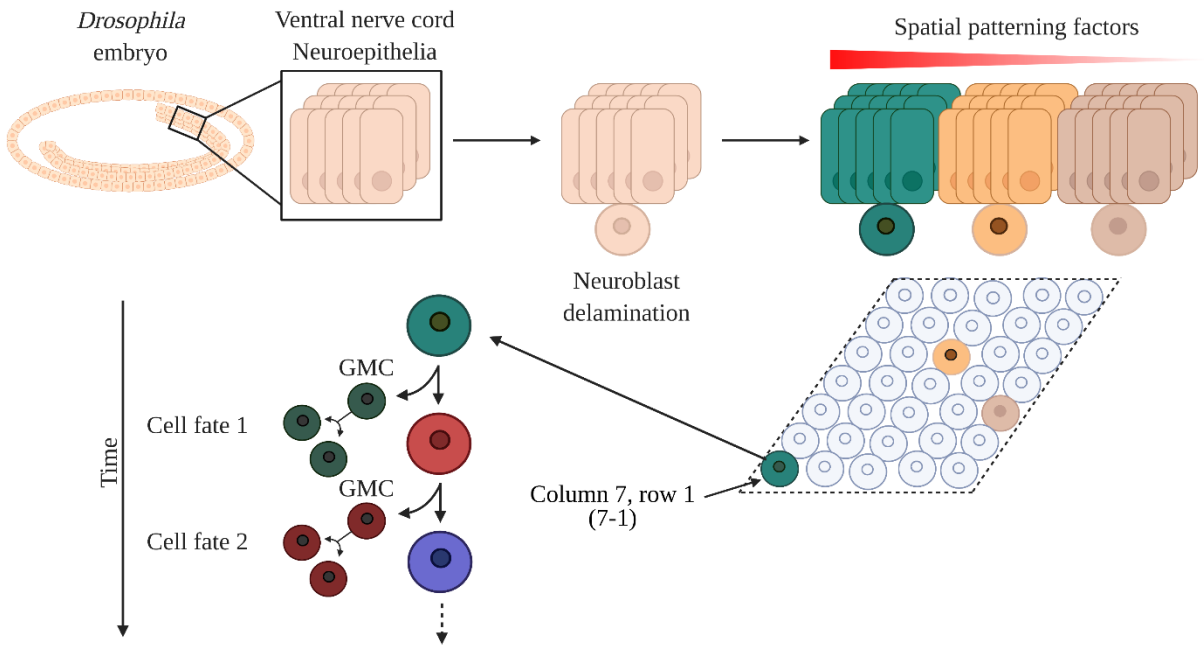

Figure 1.3: Development of the *Drosophila melanogaster* VNC. Neuroblasts delaminate from the neuroepithelia leading to arrangement in columns and rows, adapted from (Kohwi and Doe, 2013). Each NB in a particular column and row produces the same stereotypical lineage after cell division in different flies. NB: Neuroblast.

1.1.3.1 Ventral nerve cord temporal order of neuron birth

In the fly, intrinsic genetic cues establish the temporal order by which a neuron is formed at the specific time. In the fly VNC, consisting of three thoracic and eight abdominal segments, 30 neuroblasts delaminate from the neuroepithelium and are arranged in columns and rows established by spatial patterning factors (Broadus et al., 1995; Hartenstein et al., 1994) (Fig. 1.3). Interestingly, the lineage from each of the neuroblast belonging to a particular column and row always undergoes a stereotypic differentiation, leading to the formation of the same neurons between different flies. In the example of column 7 row 1 annotated as 7-1, the mode of division is Type-I which means that NBs asymmetrically divide to give rise to a NB and ganglion mother cell (GMC), that inherits cell fate determinants such as Numb, Prospero and Brat (Betschinger et al., 2006; Lee et al., 2006; Lu et al., 1998; Matsuzaki et al., 1998; Shen et al., 1998). The asymmetric localization of cell fate determinants instructs the GMC to produce specific neurons. Subsequently, the GMC produces a dorsal motor neuron early, and a ventral motor neuron later in the division, labelled as U1-5 neurons spanning the thoracic T3, T2 and abdominal segment A1 (Lee and Luo, 1999). The deeper layer neurons U1-2 have bipolar morphology with contralateral dendrites and axons (Schmid et al., 1999). Their projections innervate the dorsal body wall muscles. The superficial neurons U3-5 have monopolar morphology with ipsilateral dendrites and axons that innervate the ventral body wall (Bossing et al., 1996; Pearson and Doe, 2003; Schmid et al., 1999; Schmidt et al., 1997; Seroka and Doe, 2019). Therefore, each of the neurons produced after a successive division has a distinct temporal identity and innervates a different set of targets. After the first five divisions, the 7-1 NBs switch from producing motor neurons to interneurons. These first five divisions have been a source of great interest in the past due to the stereotypical nature of these divisions.

1.1.3.2 Temporal competence factors of the NB 7-1 lineage

A set of transcription factors known as temporal transcription factors (tTFs) set up a cascade in the dividing NBs that establish the temporal order of neurogenesis in VNC development. In the first division of the NBs following delamination in the 7-1 lineage, high Hunchback (Hb) expression confers the competence to the NBs to generate the earliest born U1 neurons (Brody and Odenwald, 2000; Isshiki et al., 2001; Kambadur et al., 1998) (Fig. 1.4A). After

asymmetric cell division, NBs generate one GMC and another NB that has lower expression of Hb. The GMC undergoes another round of division leading to the production of two neurons. NB with low Hb expression undergoes another round of asymmetric cell division and produces a self-renewing NB and GMC. U2 neurons are produced from the GMC, whereas the NB now expresses the next tTF in the cascade, Krüppel (Kr). In the 7-1 and other NB lineages such as 7-3, the second division is initiated by Svp, which promotes the transition from Hb to Kr (Kanai et al., 2005). This NB divides again, generating another NB and GMC, which produces U3 neurons. During the subsequent divisions, each NB upregulates the next tTF in the cascade, *nub/pdm2* (collectively called *Pdm*) and *Cas* that each lead to the production of a self-renewing NB and a GMC (Grosskortenhaus et al., 2006). As with the previous GMC divisions, the daughter cells from the GMC gives rise to different motor neurons, namely U4 and U5. Therefore, tTFs open the temporal window conducive to produce a particular neuron, thereby acting permissively. This allows other factors, such as cell fate determinants, to then instruct the production of a particular cell fate in the temporal window established by tTFs. This is one of the key differences between tTFs and classical fate determinants observed in other parts of the CNS. Finally, the expression of the tTFs in the cascade progresses in the same manner when isolated NBs are cultured *in vitro* (Brody and Odenwald, 2000; Grosskortenhaus et al., 2005). This highlights the importance of a cell intrinsic temporal program that is independent of environmental signals. Therefore, a temporal competence cascade in the NBs is completed from Hb > Kr > Pdm > Cas.

1.1.3.3 Deterministic model of temporal competence in VNC neuroblasts

The role of the tTFs in cell fate competence of the fly NBs is a deterministic process. In a WT cascade, each division leads to the production of U1-5 motor neurons successively (Fig. 1.4B). If Hb is genetically knocked out, the NBs only lose competence to generate the earliest born neurons associated with the Hb competence window. However, the cascade keeps moving forward, as the rest of the neurons are generated normally (Isshiki et al., 2001; Novotny et al., 2002; Pearson and Doe, 2003). Conversely, sustained expression of Hb leads to overproduction of neurons with U1 identity at the expense of U2-5 neurons. Loss of Kr leads to the loss of U3 neurons, whereas sustained expression of Kr in the NBs leads to the overproduction of U3 neurons in the subsequent divisions, respectively (Cleary and Doe, 2006; Isshiki et al., 2001; Kanai et al., 2005). Similarly, Pdm and Cas are also sufficient and required for their respective motor neurons fates by regulating

temporal competence in the NBs (Grosskortenhaus et al., 2006). Interestingly, if Hb expression is maintained for a short period of time, the NBs revert to the intrinsic progression of the temporal cascade (Isshiki et al., 2001). This highlights the importance of maintained tTF expression to ensure temporal competence window conducive to produce a particular set of neurons is established. Nevertheless, each competence window is associated with the expression of its respective tTF, governed by a deterministic decision to produce one neuron over another. This also suggests that there could be a cross-regulatory mechanism present in the NBs to ensure the expression of each tTF is tightly controlled in its respective window. This could explain why the progression of the temporal cascade always moves forward even if one of the tTFs is deleted.

1.1.3.4 Cross regulation of temporal transcription factors in the VNC neuroblasts

Indeed, such a cross-regulatory mechanism exists in the NBs (Fig. 1.4C). In the 7-1 lineage, Hb activates Kr after the second NB division, which leads to high Kr expression (Grosskortenhaus et al., 2006; Isshiki et al., 2001; Kanai et al., 2005; Nakajima et al., 2010). High Kr expression represses Hb expression in the NB. As the NB divides, Kr activates Pdm, which then represses Kr. Similarly, Pdm activates Cas, which represses Pdm (Kambadur et al., 1998). Additionally, Hb represses Pdm and Cas, whereas Kr represses Cas, the tTFs expressed in the following NB divisions. This is important to maintain the expression of Kr in the NB while ensuring that the other competence factors are not precociously expressed. Cross-repression of tTFs is essential for the appropriate transition of NB temporal identity. This is evidenced by the ectopic expression of a form of Hb that can only acts as a transcriptional activator, which is not able to extend the Hb competence window (Tran et al., 2010). Therefore, a tightly controlled and temporally dependent cross-regulatory network exists between the tTFs during VNC development.

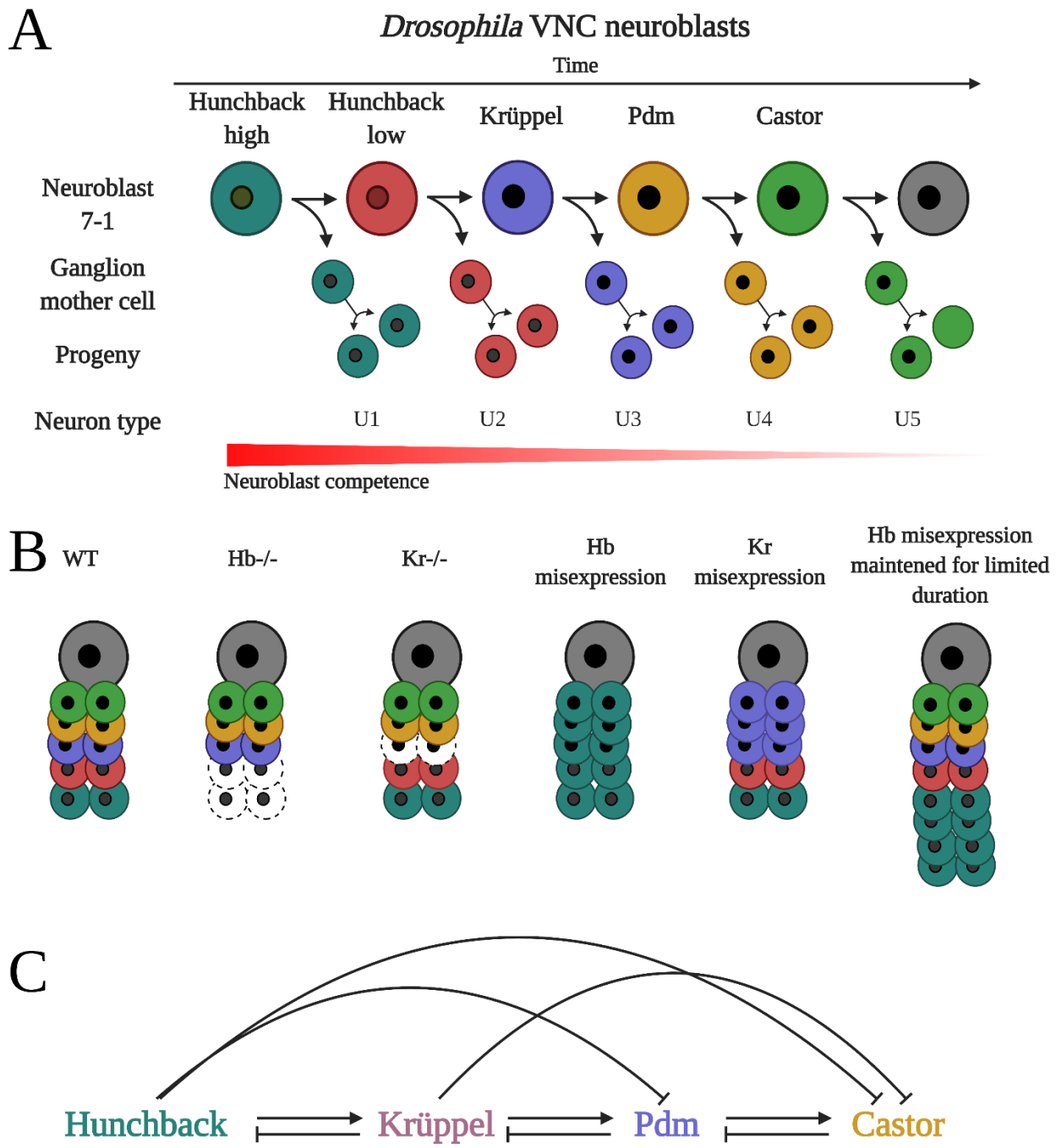

Figure 1.4: Temporal patterning in *Drosophila melanogaster* VNC. (A) Example of neuroblast 7-1 division in which sequential expression of temporal transcription factors (tTFs) Hunchback, Krüppel, Pdm and Castor leads to the generation of distinct neuronal fates, adapted from (Kohwi and Doe, 2013). (B) Loss of function and gain of function experiments illustrating the importance of tTFs expression in their respective windows, adapted from (Egger et al., 2008). (C) Schematic representing cross-regulation of tTFs in the fly VNC, adapted from (Doe, 2017).

1.1.3.5 Is the same temporal cascade present in other NB lineages?

The same tTF cascade acts in other NB lineages with a few variations. For example, in the 7-3 lineage, these NBs generate EW1-3 motor neurons, but Cas is never expressed in the late NBs and the temporal cascade is only made up of Hb > Kr > Pdm (Isshiki et al., 2001; Novotny et al., 2002). On the other hand, the 3-1 lineage has the same temporal cascade as 7-1. These NBs generate RP1, RP4, RP3, RP5 motor neurons from the first four competence windows regulated by Hb^{high}, Hb^{low}, Kr, Pdm and an interneuron from the fifth competence window regulated by Cas (Tran and Doe, 2008). Finally, in some cases such as 5-5 lineage, Hb or Kr are not expressed in the earliest NBs and instead, the temporal cascade is set up by Pdm, Cas and another tTF *grainyhead* (Grh) producing abdominal leucokinergic neurons (Benito-Sipos et al., 2010). Therefore, the main tTFs are similar in various NB lineage, the neurons produced after asymmetric division are different.

1.1.3.6 Diversity in temporal transcription factors

In other parts of the fly CNS, different sets of tTFs can collaborate to form a temporal competence cascade, producing completely different sets of neurons. One of the most well studied examples of this are the ~800 optic lobe NB present in the central brain at the larval stage that each give rise to different neurons and glia in a stereotypic manner. Instead of the Hb > Kr > Pdm > Cas cascade, the optic lobe employs a temporal cascade made up of Homothorax (Hth), Klumpfuss (Klu), Eyeless (Ey), Sloppy paired 1 and 2 (Slp), Dichaete (D) and Tailless (Tll) (Li et al., 2013; Suzuki et al., 2013). The cascade has generally the same characteristics as found in the VNC neuroblasts. During each successive NB division, tTF expression is activated in the order: Hth > Klu > Ey > Slp > D > Tll, leading to the production of a GMC that gives rise to two daughter cells. Interestingly, one of the two daughter cells express Notch ($Notch^{ON}$), whereas the other daughter cell does not express Notch ($Notch^{OFF}$). Due to this, each of these daughter cell become a different type of neuron, thereby adding another level of diversity in neuron specification (Li et al., 2013). This feature is not present in VNC NBs as GMCs produce the same types of neurons. Moreover, in the optic lobe, there is also evidence of cross-regulation of tTFs, albeit partially (Li et al., 2013).

In addition to these two tTF cascades, there is another temporal cascade that regulates competence in the larval thoracic NBs. These NBs have a temporal order of neuronal birth

producing Chimno^{+ve} early born proximal motor neurons and Br-C^{+ve} late born distal motor neurons sequentially (Maurange et al., 2008). Cas and Svp set up the early and late temporal phase of competence producing Chimno^{+ve} neurons and Br-C^{+ve} neurons, respectively. Therefore, in the fly CNS, there are multiple temporal competence cascades that confer competence to developing NBs to generate a wide variety of cells depending on the temporal and spatial context.

Understanding how cell fate is regulated by tTFs in the fly system has been extensively studied but important questions in the field of vertebrate neurogenesis remain: Is the temporal cascade also conserved between invertebrates and vertebrates? Do vertebrates also utilize the same tTFs? To answer these questions, our lab and others use the developing mouse retina as a model system to study temporal patterning in vertebrates.

1.2 Mouse retina: A molecular window into CNS development

Similar to the rest of the CNS, the mouse retina is derived from the neural tube. Firstly, the anterior neuroepithelium protrudes towards the surface ectoderm to form the optic vesicle, reviewed in (Heavner and Pevny, 2012). Once the optic vesicle is formed, the surface ectoderm invaginates towards the neuroepithelium to form a cup-like shape, known as the optic cup. The surface ectoderm cells become the lens placode cells and release fibroblast growth factor (FGF) to instruct the neighboring neuroepithelium to become the neural retina (Hyer et al., 1998; Mikami, 1939). On the other hand, the outer layer of the neuroepithelium becomes retinal pigmented epithelium (RPE) through activation of MITF (Nguyen and Arnheiter, 2000). As the invagination increases, the tips of the optic cup meet to complete a circular boundary of the lens vesicle. The developing RPE closes onto the developing neural retina to complete a bilayer consisting of the neural retina and RPE. The extreme region of the bilayer where the neural retina and the lens primordium meet, is specified into the ciliary marginal zone (CMZ). The CMZ generate the ciliary body and contributes to the production of retinal cell types in the periphery of the developing retina (Belanger et al., 2017; Fischer et al., 2013; Marcucci et al., 2016). Finally, after lens vesicle formation, the surface ectoderm becomes the corneal epithelium.

The neurons and glia are generated from a pool of multipotent retinal progenitor cells (RPCs) located in the retinal progenitor layer (RPL) of the nascent retina. The spatial patterning

and morphogenesis events listed above lead to the specification of the neural retina and activate expression of many transcription factors involved in RPC proliferation and maintenance. Pax6, Rax, Vsx2, Sox2, Lhx2,Six3 and Six6 are factors that grants multipotency to the RPCs in a highly conserved GRN (detailed in section 1.3) (Carl et al., 2002; Chow et al., 1999; Jean et al., 1999; Liu et al., 1994; Loosli et al., 1999; Mathers et al., 1997; Oliver et al., 1995; Taranova et al., 2006; Zuber et al., 2003; Zuber et al., 1999). Loss of function mutations of these genes leads to anophthalmia or similar defects of eye morphogenesis in humans (Ferda Percin et al., 2000; Gallardo et al., 1999; Gallardo et al., 2004; Glaser et al., 1994; Voronina et al., 2004). This highlights the importance of these transcription factors in specifying the retina in the eye field, which is initially orchestrated by spatial patterning factors, reminiscent of the developing spinal cord.

1.2.1 Cell type birth order in the mouse retina

In the developing mouse retina as early as embryonic day 10 (E10), retinal ganglion cells (RGCs) are the earliest cells to be born from the pool of multipotent RPCs. This is followed by horizontal cells, cone photoreceptors and amacrine cells, all of which are born predominantly in the embryonic window (Carter-Dawson and LaVail, 1979a; Rapaport et al., 2004; Turner and Cepko, 1987; Turner et al., 1990; Young, 1985a, b). Rod photoreceptors, bipolar cells and Müller glia are born from postnatal day 0 (P0) to P10 and retinogenesis is completed by P14 (Fig. 1.5A). Postnatal RPCs generally undergo terminal divisions, giving rise to either neurons or glia. This temporal birth order is highly conserved in vertebrates, from fish to humans (Hendrickson, 2016; Hendrickson et al., 2016; Hendrickson and Yuodelis, 1984; Johns and Easter, 1977; La Vail et al., 1991). In addition to the seven general mouse retinal cell types, there are 2 subtypes of cones, around 40 subtypes of RGCs, around 60 subtypes of amacrines, and around 15 subtypes of bipolar cells characterized so far from either morphological or transcriptomic analyses (Rheaume et al., 2018; Shekhar et al., 2016; Yan et al., 2020).

1.2.2 Anatomy of the mouse retina

In the fully developed adult retina, rod and cone photoreceptors are arranged in the outer nuclear layer (ONL) and are responsible for light detection (Fig. 1.5B), reviewed in (Wässle and

Boycott, 1991). The inner segments of the photoreceptors contain the mitochondria, whereas the outer segments are comprised of membrane disks that contact the RPE cells. There are two types of cones in mice, M- and S-cones, whereas three types of cones in humans namely, L-, M- and S-cones. Each of these subtypes of cones can detect certain wavelengths of light depending on the expression of the G-protein coupled receptor opsin protein, reviewed in (Kolb, 1995). Short wavelength opsin (S-opsin) detects light in the 400nm to 450nm range, mid wavelength opsin (M-opsin) detects light in the 500nm to 575nm, and long wavelength opsin (L-opsin) detects light in the 525 to 625nm range. The diversity in the types of opsins in cones allows detection of colours in daylight conditions. On the other hand, the opsin expressed in rods is called Rhodopsin that can detect light in the 475 to 525nm range. Rods can only detect one photon of light at a time (Kefalov et al., 2003). Therefore, although they have both photoreceptors, rods are the primary source of light detection in nocturnal animals that rely on vision in dim-light conditions.

Photoreceptors synapse with bipolar cells at the outer plexiform layer, whereas the cell bodies of the bipolar cells are located in the inner nuclear layer (INL) (Kolb, 1995). At the other end, bipolar cells synapse with RGCs at the inner plexiform layer (IPL). Cell bodies of RGCs are located in the ganglion cell layer (GCL). Therefore, bipolar cells mainly relay the electrical signal from photoreceptors to RGCs. RGCs send their projections to the brain through the neurofilament layer (NFL) that bundles into the optic nerve in the central retina. Horizontal and amacrine cells are located in the INL, with their dendrites spanning the OPL and IPL, respectively. These cells modulate the electrical activity generated by the phototransduction cascade in photoreceptors. The cell bodies of the Müller glia are also present in the INL, although the processes of these glia span the entire length of the retina. Müller glia are critical for homeostasis and structural support of the retina. Therefore, due to the precise organization of the retina, the temporal birth order of retinal cell types is important for the correct establishment of the circuitry responsible for light detection. In addition to the retinal cells born from RPCs, microglia and astrocytes are also present in the IPL and NFL, respectively, that migrate into the retina, reviewed in (Vecino et al., 2016). Since they originate from outside the retina, this will not be discussed in the context of temporal patterning.

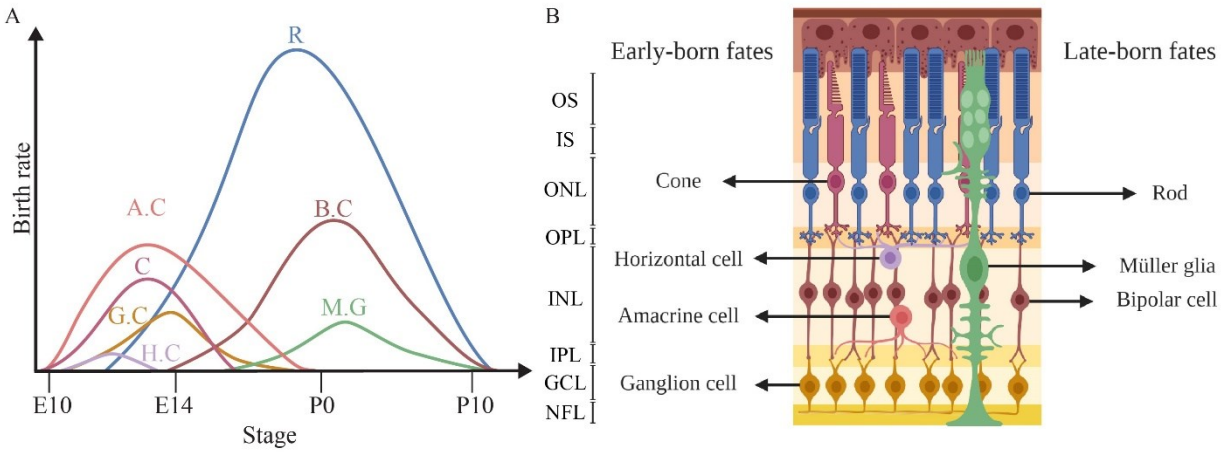

Figure 1.5: Composition of the mouse retina. (A) Birth order of retinal cell types during retinogenesis, adapted from (Carter-Dawson and LaVail, 1979a, b; Rapaport et al., 2004; Young, 1985a, b). (B) Seven cell types of the retina arranged in three distinct nuclear and synaptic layers. Created with Biorender.com. OS: Outer segment. IS: Inner segment. ONL: Outer nuclear layer. OPL: Outer plexiform layer. INL: Inner nuclear layer. IPL: Inner plexiform layer. GCL: Ganglion cell layer. NFL: Neurofilament layer. G.C: Ganglion cells. A.C: Amacrine cells. H.C: Horizontal cells. C: Cones. R: Rods. B.C: Bipolar cells. M.G: Müller glia.

1.2.3 Mouse retina as a model to study temporal patterning

The mouse retina is an elegant model to study neurogenesis and temporal patterning for several reasons. The genetic tools available for experiments in mice are very extensive, which allows for thorough characterization of function for a particular gene or pathway from genotype to phenotype. There are two retinas per animal which allows for efficient experimental design. Moreover, the retinas are easily accessible for experimentation and not essential for the survival of the mouse. This allows *in vivo* experiments to be performed without risking the health of the mouse. The number of cell types are relatively few compared to the enormous types of neurons present in the central brain regions such as the neocortex. There are also many known cell-type specific markers for each retinal cell type, which allows accurate identification. The temporal order of birth in the retina is generally divided in two main stages, an early embryonic and late post-natal window. This is useful for efficient experimental design to study novel candidate tTFs involved in temporal patterning.

In the past, many labs have uncovered the important events of RPC differentiation in the developing retina. There are many questions of immense interest in the retinogenesis field: 1) How

is the retina temporally patterned? 2) Do environmental factor shape the cell fate output from an RPC? 3) What are the tTFs, if any, expressed and functioning in the developing mouse retina? 4) How different are the principles behind RPC differentiation in the mouse retina and NB differentiation in the fly VNC? To answer these questions, this next part will discuss what is known about the molecular components of cell fate determination in the mouse retina.

1.3 Cell fate determination in the retina

As there is an overlapping sequence of birth between the various cell types of the retina, a simple deterministic model such as the one present in the fly VNC neuroblasts does not fully explain how cell fate determination takes place in the retina. Some late born cell types are born in the early window whereas some early born cell types are born in the late window, albeit there being a discrete boundary between the peak production timing of early and late born cell types (Carter-Dawson and LaVail, 1979a, b; Young, 1985a, b). This implies that a single RPC in the early window has the competence to generate all seven cell types in the embryonic stage. If not a deterministic model, what could explain the overlap in the temporal order of cell birth? What factors are involved in cell fate determination of the retinal cell types from RPCs?

1.3.1 Retinal progenitor cells

As mentioned earlier, seven retinal cell types are formed from the same pools of multipotent RPCs and this feature is well conserved between vertebrate species (Fekete et al., 1994; Holt et al., 1988; Reese et al., 1999; Turner and Cepko, 1987; Turner et al., 1990). Do environmental signals play a role in modulating the types of neuron RPCs produce or is it completely governed by a cell intrinsic mechanism? To answer this question, heterochronic experiments performed by culturing the embryonic RPCs with the postnatal retina and vice versa, to assess whether co-culturing with a retina belonging to a different temporal stage could affect cell fate specification (Belliveau and Cepko, 1999). Interestingly, there was a decrease in the early cell types generated from the early RPCs when cultured with a postnatal retina. However, these RPCs do not precociously generate late cell types outside their temporal window of birth. This suggests that environmental signals might affect proportions of the cells made in a particular window, but they do not alter the temporal birth windows. Many such environmental signals have

been discovered such as CNTF, EGF, FGF, TGFα, TGFβII and Shh that modulate either rod or RGC production in their respective windows (Altshuler and Cepko, 1992; Altshuler et al., 1993; Belliveau et al., 2000; Ezzeddine et al., 1997; Kelley et al., 1994; Kim et al., 2005; Kirsch et al., 1996; Kirsch et al., 1998; Levine et al., 1997; Lillien, 1995; Ma et al., 2007; Neophytou et al., 1997; Ozawa et al., 2007; Wang et al., 2005; Yu et al., 2006). This suggests that an intrinsic mechanism must be in place in RPCs that controls the temporal window of birth.

Clonal density cultures of individual RPCs that cannot contact each other, grown in a general culture medium, and imaged overtime using time-lapse, have demonstrated that RPCs can generate the same types of cells, although the temporal order of birth was not assessed (Jensen and Raff, 1997). A follow up study, expectedly, showed that clones produced by RPCs in clonal density cultures are of the same size and composition as clones that develop in retinal tissue explants (Cayouette et al., 2003). This suggests that without the influence of environmental signals, RPCs can generate the similar proportions of retinal cells compared to retinal explants, possibly through an intrinsic program of cell fate determination.

1.3.2 Stochastic model of cell fate determination

Murine RPC potential cannot be probed the same way as *Drosophila melanogaster* NBs because it is not known whether the same individual RPC in a particular region of the retina would lead to the same lineage in different animals. This is mainly due to the lack of tools in rodent models available to specifically label the same progenitor between different animals, which is possible with flies due to the stereotypic arrangement of the NBs in columns and rows. On a general population level, it has been shown that RPC differentiation initiates in the central retina and progresses peripherally (Wong et al., 2002). A stochastic model of cell fate determination has been developed to explain how RPC differentiation takes place at a population level. The stochastic model dictates that RPCs differentiate in a biasing manner, where the probability of acquiring one cell fate over the other is based on the variations that exist in the cell, whether genetic or environmental (Gomes et al., 2011; He et al., 2012). Time-lapse imaging and lineage reconstruction of rat RPCs, a similar rodent model to mouse RPCs, demonstrated that RPCs undergo three main modes of divisions: Progenitor-Progenitor (P-P), Progenitor-Differentiated cell (P-D), or Differentiated cell- Differentiated cell (D-D) (Gomes et al., 2011). RPCs were

counted as they underwent a P-P, P-D, or D-D divisions and the lineages associated with the divisions were re-constructed to statistically test the possibility of a stochastic mechanism (Gomes et al., 2011). Interestingly, when compared to a computer-generated stochastic model of fixed probabilities projected from the published birth-dating data, the reconstructed lineages showed a similar distribution. This suggests that RPCs likely decide the cell fate of the daughter on a population level stochastically. A similar stochastic mode of RPC differentiation was detected from lineage re-construction of zebrafish RPCs *in vivo* (He et al., 2012). From this model, it can be postulated that intrinsic temporal competence of an RPC, along with certain extrinsic signals and a mechanism of stochastic cell fate choice could all collaborate to determine the fate of the daughter cell.

A combinatorial model could also help explain why there is heterogeneity between different RPCs at the same age. For example, not all RPCs at the late-stage are similar to each other as demonstrated by a previous microarray study and recently by scRNA-seq (Clark et al., 2019; Trimarchi et al., 2008). Generally, this stochastic model applies to RPCs undergoing PD divisions. However, there has been evidence of restricted lineages of RPCs that only generate the same types of cells after terminal division, thereby undergoing DD divisions.

1.3.3 Fate restricted RPCs

One of the most well studied examples of restricted RPCs is a population of bHLH transcription factor Olig2^{+ve} RPCs present throughout retinogenesis. By employing an elegant TVA-dependent gammaretroviral lineage tracing strategy, it was shown that the terminally dividing Olig2^{+ve} RPCs always generate cones and horizontal cells after their division during the early embryonic period (Hafler et al., 2012). In contrast, during postnatal retinogenesis, terminally dividing Olig2^{+ve} RPCs could only generate rods and bipolar cells. This raised the possibility of the presence of fate restricted RPCs that always generate the same types of cells. This lineage tracing strategy also revealed that these restricted RPCs are generated from multipotent RPCs. Similarly, Atoh7 and Ascl1 are other bHLH transcription factors that label distinct RPC lineages. Atoh7^{+ve} RPCs generate early born cell types including RGCs whereas Ascl1^{+ve} RPCs never generate RGCs (Brown et al., 1998; Brzezinski et al., 2011; Brzezinski et al., 2012; Mu et al.,

2005; Wang et al., 2001). Additionally, Cdh6^{+ve} RPCs also mainly generate a particular subtype of RGCs (De la Huerta et al., 2012).

Recent advances in single cell RNA-sequencing technology have revealed some insights on the molecular difference between the fate restricted RPCs and multipotent RPCs. In a pioneering study to assess the changing transcriptomic landscape of mouse retinogenesis from as early as E11 to P14, it was discovered that restricted RPCs vary considerably at the transcriptomic level (Clark et al., 2019). Labelled as 'Neurogenic RPCs', these fate restricted RPCs express all of the factors mentioned above. Cell fate trajectories were computed using Monocle, a software that generates pseudotime plots from scRNA-seq datasets of different temporal stages. This suggested that fate restricted RPCs were derived from multipotent RPCs. Additionally, they cluster in between multipotent RPCs and the differentiated retinal cell types associated with the restricted RPCs. This highlights a key point that restricted RPCs are transitionary cells and part of the multipotent RPC lineage, as previously observed (Hafler et al., 2012). Another study showed using scRNA-seq of Atoh7 labels the population of RPCs in transition to become early cell types including RGCs. In the Atoh7 knockout restricted RPCs, there is an increase in *Neurog2* and *Neurod1* gene expression, two genes important for photoreceptor specification (Wu et al., 2021). Another scRNA-seq dataset, generated from the temporal stages of human fetal retinal development, have shown that these same factors are expressed in early and late human RPCs, that hierarchically precede the fate restricted RPCs (Lu et al., 2020). This suggests that the presence of fate restricted RPCs could be conserved in higher vertebrates and could rely on the same set of genes such as *ATOH7* and *OLIG2*.

1.3.4 Multipotency in RPCs

There have been many factors discovered that bestow multipotency to RPCs. One of the most well studied factors is Pax6, which is required for the specification of the retina and lens placode cells (Ashery-Padan et al., 2000; Collinson et al., 2000; Glaser et al., 1994; Grindley et al., 1995; Walther and Gruss, 1991). Since Pax6 is expressed in the optic vesicle, conditional knockouts were generated that specifically delete Pax6 in RPCs after the retina has been specified. It was shown that Pax6 cKO retinas only produce amacrine cells and Pax6 regulates the expression of bHLH transcription factors such as Atoh7, Neurog2 and Neurod1 (Marquardt et al., 2001). This

suggests that Pax6 allows RPCs to generate the full repertoire of retinal cell types. Additionally, genes involved in the initial induction of the retinal tissue also regulate RPC multipotency. Rax, Vsx2, Sox2, Six3 and Six6 are multipotency factors, part of a highly conserved gene regulatory network (Dhomen et al., 2006; Diacou et al., 2018; Jean et al., 1999; Mathers et al., 1997; Oliver et al., 1995; Taranova et al., 2006). Lhx2 was also discovered as an important regulator of RPC proliferation and maintenance. Lhx2 knockout retinas have decreased RPC due to early cell cycle exit, which leads to the generation of neurons by symmetric divisions (Gordon et al., 2013). Therefore, an intricate genetic network establishes multipotency in RPCs and as detailed above, allow the expression of certain bHLH transcription factors and neurogenic genes that promote particular cell types in an instructive manner.

Notch signaling also plays a key role in maintaining multipotency in RPCs as well as multiple roles in other cell systems including angiogenesis, reviewed in (Kofler et al., 2011). Notch pathway consists of transmembrane receptors, Notch1-4, and ligands Dll1, Dll3, Dll4, Jag1 and Jag2. Trans-interaction between the receptor in one cell and the ligand in the neighboring cell leads to the cleavage of the intracellular domain of the notch receptor, NICD. This activates downstream genes such as *Rbpj*, *Hes1* and *Hes5,* that transcriptionally modulate proliferation in RPCs (Jadhav et al., 2006a; Kechad et al., 2012; Nelson et al., 2007; Riesenberg et al., 2009; Takatsuka et al., 2004; Yaron et al., 2006; Zheng et al., 2009). This induces lateral inhibition in the dividing RPCs to regulate neural determination in the neighboring cells. Notch dependent lateral inhibition in RPCs has also been shown to be well conserved between vertebrate species (Austin et al., 1995; Bao and Cepko, 1997; Dorsky et al., 1995; Henrique et al., 1997; Scheer et al., 2001). Lateral inhibition by Notch signaling only modulates the number of neurons or glia made by a particular RPC. However, it does not impact the competence to generate a cell outside its window of development.

In addition to lateral inhibition, Notch activation is essential for RPCs to respond to Shh signaling. Inactivation of the Notch pathway leads to the reduction of all Gli proteins, the transcriptional components of the Shh pathway, as well as Shh induced proliferation (Ringuette et al., 2016). Additionally, Shh signaling also stabilized the downstream notch component Hes1 in a notch independent manner. Taken together, both pathways help to maintain the proliferation and differentiation in RPCs (Wall et al., 2009).

1.4 Temporal transcription factors of the developing retina

A stochastic model of RPC differentiation has been proposed, in which 'biasing' factors shift the probability to generate one cell type over the other to grant temporal competence. As previously detailed in fly VNC development, tTFs could explain how RPCs gain the competence to generate early-born cell types and late-born cell types during retinogenesis. To uncover these tTFs, homologues of the early tTF in flies, Hunchback, was first assessed as a candidate tTF in the early window of retinogenesis. There are 5 homologues of the Hunchback gene, all belonging to zinc-finger family of transcription factors, Ikzf1, Ikzf2, Ikzf3, Ikzf4 and Ikzf5 (Powell et al., 2019). Many studies have uncovered the role of Ikzf family members in haematopoiesis (Georgopoulos et al., 1992; Hahm et al., 1998; Honma et al., 1999; Kelley et al., 1998; Morgan et al., 1997; Perdomo et al., 2000). Out of the five Ikzf family members, Ikzf1 has been the most well studied.

1.4.1 Ikzf1, a functionally diverse transcription factor

Equipped with a dimerization and DNA-binding domain, Ikzf1 is a versatile modulator of many different cell fates during development, ranging from the neuro-endocrine to hematopoietic system (Allman et al., 2006; Dumortier et al., 2003; Wu et al., 1997). Prominently, Ikzf1 functions in the developing thymus, generating subtypes of $CD4^{+ve}$ T-helper cells and B-cells (Davis, 2011; Kirstetter et al., 2002; Klug et al., 1998; Molnár et al., 1996; Payne et al., 2003; Payne et al., 2001; Quirion et al., 2009; Thomas et al., 2010; Wong et al., 2013). Mutations of Ikzf1 are associated with primary immunodeficiency as well as T-cell and B-cell acute lymphoblastic leukemia (Eskandarian et al., 2019; Kuehn et al., 2016; Yoshida et al., 2017). Ikzf1 is also expressed in several parts of the CNS (Agoston et al., 2007; Ezzat et al., 2006; Gray et al., 2004). Although there is considerable knowledge on how Ikzf1 modulates different immune cell fates, Ikzf1 function in the developing CNS has not been carefully examined, with the exception of a few studies.

1.4.1.1 Ikzf1 as a temporal transcription factor

Ikzf1 was found to be expressed in dividing RPCs during early retinogenesis and progressively decreases in expression during late retinogenesis (Elliott et al., 2008). Ikzf1

expression localized to differentiated early born cell types such as amacrine cells, horizontal cells and RGCs at P2. To assess whether Ikzf1 can suppress RPC differentiation into late born cells, Ikzf1 was misexpressed in late RPCs. Remarkably, Ikzf1 promoted the production of early-born cells, except cones, from late RPCs at the expense of late born cell types, suggesting a shift in the window of temporal competence. It was also shown that Ikzf1$^{-/-}$ retinas have reduced number of all early born cell types, except cones. Therefore, it was concluded that Ikzf1 confers early temporal competence to RPCs during retinogenesis, similar to Hunchback in fly VNC development (Fig. 1.6A). This was the first evidence of a tTF in the developing mammalian CNS.

Interestingly, a similar temporal logic was observed in the developing mouse cortex. It was shown that Ikzf1 is highly expressed in early radial glial and intermediate progenitors in the ventricular zone (VZ) compared to late progenitors (Alsiö et al., 2013). Sustained expression of Ikzf1 in early-stage progenitors led to an increase in deeper layer fates, which are produced during the early window of corticogenesis. This was accompanied by a decrease in superficial layer neurons born later in development, suggesting an extension of temporal competence of early born neurons. A key experiment showed that if dividing cells were labelled by BrdU after sustained expression of Ikzf1, there was an extension of the window of deeper layer neuron production, reminiscent of Hb in fly VNC development. However, Ikzf1 was not sufficient to confer early temporal competence to late radial glial progenitors. This suggests that Ikzf1 alone might not be able to overcome the cellular and epigenetic barriers to shift the temporal stage of the progenitor. Moreover, mice expressing Ikzf1 without exon 7, which codes the DNA-binding domain, showed no defects in superficial and deeper layer neuron numbers. This suggested the possibility of redundancy between the Ikzf family members, most of which are expressed during corticogenesis (Alsiö et al., 2013). Nevertheless, this study demonstrated that Ikzf1 alone can extend the window of early temporal competence in the cortex, similar to the retina.

Despite a major advancement in our understanding of temporal patterning in mammalian central nervous system development, mechanistic insights on how Ikzf1 functions in the developing retina were not explored. Moreover, at the time, it is unclear whether homologues of the rest of the genes in the temporal cascade also function similarly in the developing mouse retina. A promising candidate for late temporal competence was Casz1, the mammalian homologue of the Cas in flies.

1.4.2 Casz1, the late temporal transcription factor

Casz1 is a zinc finger transcription factor first implicated in neurogenesis and heart development (Vacalla and Theil, 2002). In the same study, prominent expression of Casz1 was discovered in developing cardiogenic mesoderm, tubular heart and neural tube at E8. Subsequent studies have detailed the role of Casz1 in cardiac morphogenesis, various cancers, spinal cord development and skeletal muscle differentiation (Christine and Conlon, 2008; Liu et al., 2014b; Liu et al., 2011; Liu et al., 2020b; Monteiro et al., 2016; Virden et al., 2012; Wu et al., 2016). Interestingly, Casz1 was shown to be expressed in a low-early and high-late temporal order in the developing mouse retina but function of Casz1 was not studied (Blackshaw et al., 2004). Therefore, the role of Casz1 in regulating late temporal competence in RPCs was examined in a recent study. It was shown that Casz1 expression in RPCs was first detected at E16 and progressively increased in late RPCs at P0 (Mattar et al., 2015). Since Casz1 expression was low in the early RPCs at E13, Casz1 was overexpressed in early RPCs to assess whether this would lead to generation of late born neurons. As expected, misexpression of two Casz1 isoforms, Casz1v1 and Casz1v2, in early RPCs led to the suppression of early fates and overproduction of all late fates, except Müller glia, from early RPCs. Inversely, Casz1 conditional knockouts (cKO) had decreased rod numbers and an increase in all early fates. Taken together, this suggests that Casz1 is an important regulator of late temporal competence in the developing mouse retina (Fig. 1.6A). Another key observation from the study was that Ikzf1 regulates Casz1 levels during early retinogenesis. Ikzf1 overexpression during early retinogenesis led to a decrease in Casz1 antibody signal. Ikzf1 fused with the activating VP16 peptide, led to an inverse increase in Casz1 antibody signal. This suggested a model, in which Ikzf1 represses Casz1 in the early retina and as the levels of Ikzf1 decrease in RPC, due to a yet unidentified factor, Casz1 is de-repressed, which allows the initiation of the late temporal competence window. Therefore, this study showed that the *Drosophila melanogaster* VNC temporal cascade is partly conserved in the developing mouse retina (Fig. 1.6B).

Follow up studies provided more mechanistic insights on how Casz1 regulates the early to late temporal identity transitions in the developing retina. Through a BioID proteomics screen, it was shown that Casz1 interacts with the nucleosome remodeling and deacetylase (NuRD) complex during development (Mattar et al., 2021). NuRD and polycomb repressor complexes were required

for the function of Casz1 in promoting the rod fate and suppressing the Müller glia fate, the latest-born cell type. This provided epigenetic and mechanistic explanations on how Casz1 regulate late temporal identity in the developing retina. Additionally, in the adult retina, it was shown that Casz1 controls the nuclear organization of the developing rod photoreceptors by repressing nuclear lamins and interacting with polycomb repressor complex proteins (Mattar et al., 2018). Collectively, these studies highlight the role of Casz1 in regulation of chromosomal conformation.

Although there is a partial conservation of the tTFs, there are some retinal cell fates that have not been accounted for. In the Ikzf1 gain and loss of function experiments, cone numbers were not altered (Elliott et al., 2008). On the other hand, Casz1 gain of function experiments do not lead to changes in Müller glia numbers, whereas loss of Casz1 leads to an increase in Müller glia numbers (Mattar et al., 2015). This suggests that other mammalian homologues of the fly temporal cascade might be regulating temporal competence of cones and Müller glia in the developing retina.

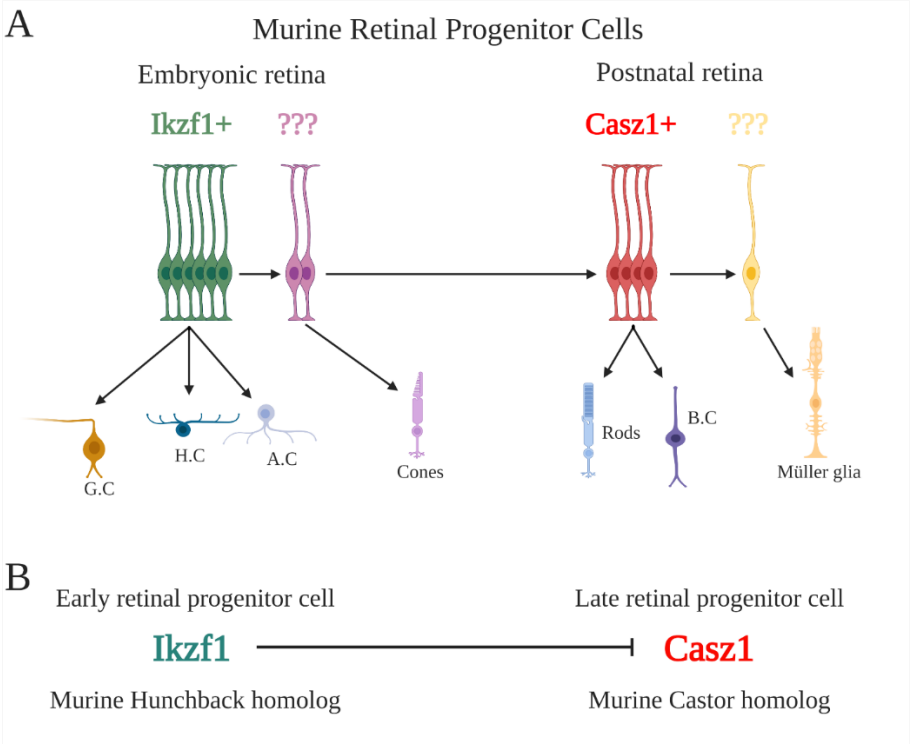

Figure 1.6: Temporal competence in the developing mouse retina. (A) Schematic outlining the current model of temporal competence in the mouse retina. (B) Transcriptional regulation of Casz1 by Ikzf1 similar to the fly temporal competence cascade (Elliott et al., 2008; Mattar et al., 2015). G.C: Ganglion cell. H.C: Horizontal cell. A.C: Amacrine cell. B.C: Bipolar cell. Figure generated by Awais Javed.

1.4.3 Cone development: A colourful affair

In most diurnal retinas, cone photoreceptors are enriched in a region of the macula called the fovea that contains around 200 times more cones than the rest of the retina (Abramov et al., 1982; Hendrickson, 1992, 2016; Hendrickson and Kupfer, 1976; Hendrickson et al., 2016; Hendrickson and Yuodelis, 1984; Mann, 1928; Provis et al., 1998). In many lower vertebrates such as birds, a similar high acuity area (HAA) with high density of cones is present. This makes the avian retina an attractive model to study foveal development, but not necessarily a good model to study temporal competence of cone development. In a study to uncover the molecular mechanism behind HAA formation, it was shown that early spatial patterning by retinoic acid (RA) regulated the HAA in chicks (da Silva and Cepko, 2017). It was hypothesized that RPCs in this region are primed to specifically generate cones, but the temporal order of birth was not altered. This suggests that although spatial cues might increase cone number in a particular region, cones are still born in their temporal window, similar to other retinal cell types. Therefore, a nocturnal animal model such as the mouse is more appropriate to study cone development. Mouse cone numbers are generally even across the adult retina, with a mild increase in cone numbers in the central compared to the peripheral retina as well as slight increase in the dorsal compared to the ventral half of the retina (Jeon et al., 1998). Moreover, it is easier to discern the role of spatial cues with temporal cues in the mouse retina model because such a high acuity or foveal region does not exist. Cones and rods are distributed in a 1:30 ratio across the various regions of the mouse retina, which allows easier examination of cones. Moreover, M-cones are enriched in the ventral retina whereas S-cones are enriched in the dorsal retina. Generally, cones express both opsins in the central retina, which allows experimental focus on the RPC to cone specification step rather than cone subtype differentiation (Ortin-Martinez et al., 2014).

Interesting questions have been raised about the temporal birth order and patterning of both photoreceptors. Are cones and rods derived from the same photoreceptor precursor? What are the molecular mechanisms that ensure the cone and rod numbers are maintained at a 1:30 ratio? How is the gradient of cone subtypes maintained in the developing mouse retina?

1.4.3.1 Transcriptional dominance model of photoreceptor development

In the current model of cone genesis, there is considerable knowledge in how post-mitotic cells divide and generate cones, but not much is known about what kind of factors promote cone production from RPCs. Terminally dividing Olig2^{+ve} neurogenic RPCs generate cones and horizontal cells due to the action of Onecut1 on upregulating the expression of *Thrb* gene, one of the earliest cone markers (Emerson et al., 2013; Hafler et al., 2012). What about multipotent RPCs that continue dividing and generate a self-renewing RPC and another daughter cell? Since only a proportion of cones are generated from Olig2^{+ve} RPCs (Hafler et al., 2012), what factors regulate cone development from multipotent RPCs? The current model in cone development called the transcriptional dominance model has been proposed to explain how photoreceptor development takes place in the post-mitotic precursor. RPCs fated to generate a cone photoreceptor first give rise to a Otx2^{+ve}/Crx^{+ve} generic photoreceptor precursor. Mouse retinas lacking Otx2 and Crx expression, both homeodomain containing proteins, have diminished photoreceptor numbers, whereas Otx2$^{-/-}$ also have reduced bipolar cells (Furukawa et al., 1997; Nishida et al., 2003). Mechanistically, Otx2 transactivates Crx, which then binds to key photoreceptor specification genes (Chen et al., 1997). In addition to Crx, Otx2 also upregulates Blimp1 that represses bipolar fate specification gene, *Vsx2*, in post-mitotic cells fated to become photoreceptors (Brzezinski et al., 2010; Katoh et al., 2010). Blimp1$^{-/-}$ retinas have normal Otx2 expression but overproduced bipolar cells at the expense of rod photoreceptors. This suggests a binary fate choice exists at the level of the post-mitotic cells to ensure the appropriate number of rods and bipolar cells are made (Fig. 1.8). If the Otx2^{+ve}Crx^{+ve} photoreceptor precursor fate decision is committed, these photoreceptor precursors are faced with another binary fate choice to become either a cone precursor or a rod precursor (Fig. 1.7). It has been shown that Nrl, a neural leucine zipper transcription factor, regulates the suppression of the cone fate and promotion of the rod fate (Mears et al., 2001). Nrl knockout retinas have no rods and all photoreceptors become S-cones that exhibited some morphological and gene expression characteristics of rods (Daniele et al., 2005; Montana et al., 2011). Similarly, overexpression of Nrl in the photoreceptor precursors leads to the conversion of all cones into rods highlighting the instructive role of Nrl in promoting the rod fate (Oh et al., 2007). In this model, Nrl is the central rod versus cone cell fate modulator, but the factors that regulate its expression in the early retina remain elusive (Fig, 1.8).

1.4.3.2 Rod specification

According to the transcriptional dominance model, if a photoreceptor precursor is biased to become a rod precursor, Nrl is activated in these precursors by Retinoid-related orphan receptor β, Rorb (Jia et al., 2009; Wang et al., 2014). Rorb$^{-/-}$ exhibited a similar phenotype to Nrl$^{-/-}$, which included the loss of rod fate and gain of cone fate with primitive outer segments, suggesting a secondary role in cones after fate specification. Crx is another the upstream activator of Nrl, that utilizes a homeobox motif at the promoter of Nrl to upregulate its expression (Furukawa et al., 1997). Nrl activates Nr2e3 expression, an orphan nuclear receptor, synergistically with Crx by binding to the promoter Nr2e3 (Oh et al., 2008). Nrl activates rod gene expression including rhodopsin by binding to a consensus binding motif at the promoter of *Rho* gene (Chen et al., 1997; Mitton et al., 2000). In addition to Nrl, Rorb also activates Blimp1, Nr2e3 and Crx with cooperative binding of Otx2 to promote the rod fate (Jia et al., 2009; Wang et al., 2014). Nr2e3 maintains the rod fate and suppresses cone gene expression (Cheng et al., 2006; Cheng et al., 2004a; Oh et al., 2008). This was shown by overexpression of Nr2e3 in the S-cone only Nrl$^{-/-}$ retinas, which led to the repression of S-opsin expression and reversal of some rod nuclear features as well as electroretinogram responses. Since Nr2e3 did not completely rescue the loss of Nrl and the resulting rod-like cells were not similar to normal rods, it was postulated that Nrl has other key targets important for rod differentiation. Indeed, follow up studies revealed Esrrb, Mef2c, Kdm5b and Nono genes required for the maintenance and survival of rods, which are important transcriptional targets of Nrl (Hao et al., 2012; Hao et al., 2011; Onishi et al., 2010; Yadav et al., 2014). Therefore, a transcriptional dominance gene regulatory network is established with Nrl at the center of the binary choice between rods and cones (Fig. 1.7). All photoreceptor precursors become cones if no inducing factors influence the choice (Swaroop et al., 2010).

1.4.3.3 Cone specification

If the photoreceptor precursor becomes a cone precursor as a result of upstream factors, Nrl expression levels are not high enough to promote the rod specification GRN in these precursors (Akimoto et al., 2006; Mears et al., 2001; Oh et al., 2007). Currently, there are no factors discovered that are direct repressors of Nrl in cone precursors. However, the downstream processes after cone specification have been uncovered. Thyroid hormone receptor beta, Thrb2, is expressed

in all cone precursors as it is one of the earliest markers for cone precursors (Ng et al., 2001; Ng et al., 2011; Ng et al., 2009). Thrb2$^{-/-}$ retinas have no M-cones and lack of gradient of S-opsin expression, suggesting that it is required for mature cone gene expression. The total number of cones are not changed in these retinas, suggesting that Thrb2 is not required for cone fate specification. In addition to Thrb2, another early marker expressed in all cone precursors called retinoid X receptor-gamma, Rxrg, also represses the S-opsin expression gradient in cones rather than cone fate, by heterodimerizing with Thrb2 (Roberts et al., 2005). Unlike Thrb2, Rxrg is not required for M-cones as Rxrg$^{-/-}$ retinas have normal M-cone numbers. Therefore, an M-cone versus S-cone fate choice exists in the cone precursor that is dictated by the expression of Thrb2. Additionally, Neurod1 is required for the expression of Thrb2 through an intronic CRM, and opsin genes (Liu et al., 2008). NeuroD1$^{-/-}$ have reduced mRNA levels of *Thrb2* and an identical phenotype to Thrb2$^{-/-}$.

What factors ensure M-opsin and S-opsin expression in arranged in a dorsoventral gradient in the mouse retina? This patterning of opsin gene expression is achieved from fly seven-up homologues and nuclear receptors, Couptf1 and Couptf2, also called Nr2f1 and Nr2f2. Couptf1/2 are expressed in the developing retina in a high-dorsal and low-ventral gradient (Satoh et al., 2009). Moreover, BMPR conditional knockouts have perturbed expression of these receptors and a disruption of the S-opsin gradient, suggesting an upstream regulatory mechanism dependent on BMP. Conversely, Couptf1 cKOs have elevated S-opsin, suggesting that Couptf1 might work in concert with Thrb2 and Rxrg to promote the M-cone fate. Since there was no difference in total cone number, these factors do not affect the cone fate specification, but rather the distribution of sub-types of cones. Rorb collaborates with Crx to bind and upregulate S-opsin expression in the postnatal retina, in addition to its role in rod differentiation (Srinivas et al., 2006). Another retinoid related orphan receptor alpha, Rora, is required for the induction of both M- and S-opsin during maturation of cones (Fujieda et al., 2009). Rora collaborates with Crx to activate the promoter and CRMs of *S-opsin*/*M-opsin* and *Arr3* genes, the latter of which is expressed in all cones and is an important component of phototransduction in cones (Krupnick et al., 1997). Taken together, these data suggest that if no inducing factors are expressed in cone precursors, the default cone subtype is the S-cone fate. This completes the default transcriptional dominance model in which RPCs divide and undergo three levels of binary fate choice decisions. The first one being the decision between a photoreceptor precursor and other cell fates, the second being the one between cones

versus rods and the final being the choice between M-cone versus S-cone (Fig. 1.7). As mentioned previously, although there have been rod promoting factors uncovered that act instructively to promote the rod fate, our understanding on cone promoting factors is poor.

1.4.3.4 Why is understanding the mechanisms behind cone development important?

There has been an increasing need to uncover novel regulators of cone development from RPCs. Retinal degenerative disorders such as Aged-related macular degeneration (AMD) and Stargardt's disease, lead to the initial degeneration of cones and then rods, reviewed in (Jones et al., 2017; Tanna et al., 2017). As humans rely primarily on cones for daylight and color vision, there is a huge interest in the field to find novel methods to replace the degenerated cones. One such method is cell replacement therapies, which entails transplantation of cones from ESC-derived retinal organoids into the retinas of patients with retinal degenerative diseases, reviewed in (Javed and Cayouette, 2017). However, production of cones from ESC-derived retinal organoids is not efficient as there is a temporal limit to produce cones, although many protocol have been used to optimize the production of cones (Brooks et al., 2019; Gonzalez-Cordero et al., 2018; Kaya et al., 2019; Kim et al., 2019; Ovando-Roche et al., 2018; Welby et al., 2017). Moreover, some studies have utilized extrinsic signals such as a Wnt/BMP/TGFβ antagonist COCO, have been successful at generating cone rich hESC-derived retinal sheets (Pan et al., 2020; Zhou et al., 2015). Although promising in its application, it is unclear whether the cones generated are functional.

There have been issues with the transplantation strategies, the most prominent one being the recently uncovered transfer of materials such as GFP from the transplanted donor cells to the host photoreceptors (Decembrini et al., 2017; Ortin-Martinez et al., 2017; Pearson et al., 2016; Santos-Ferreira et al., 2016; Singh et al., 2016). A proposed method to overcome this issue is to transplant cones into an ONL degenerative retina. These retinas do not have photoreceptors, but they have an intact INL and GCL. This could help minimize the instance of material transfer during experimentation procedures (Gasparini et al., 2019). Although promising, the application of this method remains to be fully explored. Nevertheless, there is still a need to discover tTFs for cone development to complement the current methods of generating ESC-derived organoids with enriched and functional cones. Since cones are generated in the early window, could the mammalian homologues of either Kr or Pdm in the fly VNC development play a role in regulating

their temporal competence? Kr has around 17 mouse orthologues, Klf1-17. Some Klf members have been shown to be sufficient for RGC development, although there is a high level of redundancy in their function (Moore et al., 2009; Rocha-Martins et al., 2019). On the other hand, the most similar mouse homologues for Pdm are Pou2f1, Pou2f2 and Pou2f3, all of which have been largely unexplored in the development of CNS. This next section will detail the current knowledge on the Pou2f family of genes.

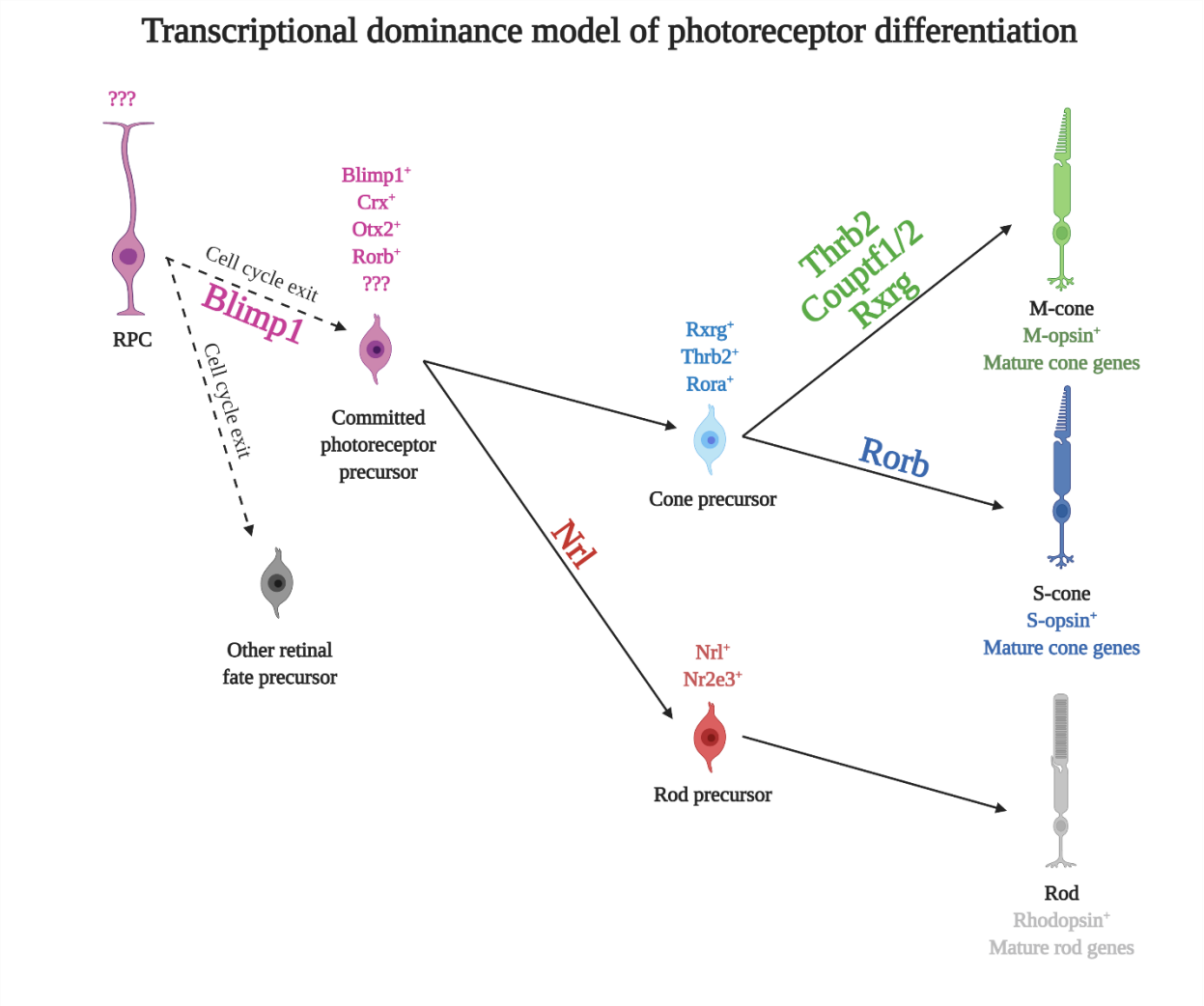

Figure 1.7: Transcriptional dominance model of photoreceptor differentiation. Adapted from (Swaroop et al., 2010). Exit from cell cycle by RPC leads to possibilities of three general cell state transitions in post-mitotic cell fated to become either a rod or cone. Three binary cell fate decisions governed by Blimp1, Nrl and Thrb2 are made by the postmitotic cell to become either M-cone, S-cone, or Rod. Dashed lines indicate cell division whereas solid lines indicate cell state transition possibilities without undergoing cell division. RPC: Retinal progenitor cell.

1.4.4 Pou2f family: POU-erful regulators of chromatin

Pou2f1 and Pou2f2 were first discovered as DNA binding proteins, originally named Otf1 and Otf2 and later classified to Oct1 and Oct2, binding to the DNA motif ATGCAAAT (Gerster and Roeder, 1988; O'Neill et al., 1988; Pruijn et al., 1986). Parallel studies on another set of transcription factors called Nuclear factor I (NF-A2) and III (NF-A1), showed that these two proteins bound a DNA binding motif of TAATGA that also contained overlaps with the Pou2f1/2 DNA binding motif (Gerster and Roeder, 1988). Interestingly, it was later revealed that NF-A1/2 and Pou2f1/2 could be the same proteins as they were functionally identical (Clerc et al., 1988; O'Neill et al., 1988). Subsequent studies uncovered the sequence of the Pou2f proteins, where they were shown to contain a POU (Pit-Oct-Unc) domain that consists of two subdomains. POU-specific subdomain that has binding specificity to two half sites (ATGC-AAAT), and a POU-homeobox (TAATGA) subdomain that is capable of binding distinct motifs in multiple arrangements, explaining the difference in the original identification of the proteins (Herr et al., 1988; Klemm et al., 1994; Stepchenko, 1992; Sturm and Herr, 1988; Suzuki et al., 1993; Verrijzer et al., 1992). Pou2f3 was later shown to be the most divergent of the three Pou2f family of proteins (Yukawa et al., 1996). In addition, Pou2f1 and Pou2f2 have the most sequence similarity to fly *nub/pdm2* (*Pdm*) genes due to their Class II POU DNA binding domain (Billin et al., 1991; Dick et al., 1991; Lloyd and Sakonju, 1991). Pou2f1 and Pou2f2 have been functionally characterized since then, with Pou2f1 being a ubiquitously expressed protein, whereas Pou2f2 functioning in a cell-type specific manner.

1.4.4.1 Octamer binding properties of Pou2f1

Pou2f1 is the only POU-domain containing transcription factor expressed in many tissues in a ubiquitous manner ranging from kidney, pancreas to the CNS, reviewed in (Tantin, 2013; Vazquez-Arreguin and Tantin, 2016). The most well studied role of Pou2f1 is its binding at histone octamers to regulate chromatin conformation (Hori et al., 2002). Pou2f1 can bind to the octamer DNA binding sequences using two main configurations: 1) Palindromic Octamer Related Element or PORE (ATTTGAAATGCAAAT), 2) More palindromic Octamer Related Element or MORE (ATGCATATGCAT) (Reményi et al., 2001; Tomilin et al., 2000; Wang et al., 2000). In PORE, the POU-specific DNA motif is a palindrome, which allows two Pou2f1 proteins to bind in tandem

arrangement in order to modulate transcription. On the other hand, in MORE, one Pou2f1 protein can bind using its POU-specific domain, whereas the other protein binds to the complementary sequence using its POU-homeobox domain (Reményi et al., 2001). Pou2f1 can also differentially regulate chromatin arrangement as a response to oxidative stress by interacting with Lamin B1, the nuclear lamina protein (Kang et al., 2011; Malhas et al., 2009). Many of the MORE binding targets are well conserved in vertebrates including humans, suggesting broad role of Pou2f1 in other species. Taken together these studies highlight the versatility of Pou2f1 in regulating cell fate and chromatin in a wide variety of cell types.

1.4.4.2 Pou2f1 in the CNS

In the vertebrate central nervous system, the role of Pou2f1 has been largely unexplored, except for a few studies. Pou2f1 was shown to be sufficient and necessary for radial glia formation during *Xenopus leavis* CNS development (Kiyota et al., 2008). It was also demonstrated that Pou2f1 expression is regulated by Notch signaling during the formation of radial glia. However, whether Pou2f1 regulates cell fate determination in frog radial glia was not explored. Additionally, another study showed that Pou2f1 and Sox2 are both required for the induction of the optic vesicle at E10 as Pou2f1$^{-/-}$; Sox2$^{+/-}$ embryos had no lens and a disorganised retina (Donner et al., 2007). Importantly, Pou2f1 and Sox2 have combinatorial binding at a Pax6 enhancer region using a tandem POU and Sox binding site. Mutations at the Pou2f1 binding site abolished the activity of the enhancer, suggesting that Pou2f1, along with Sox2, utilizes this binding site to upregulate Pax6 to promote lens morphogenesis. Although the study reported expression of Pou2f1 in the retina at E11, which is the early stage of retinogenesis, the role of Pou2f1 in cell fate determination in the mouse retina was not examined.

1.4.4.3 Pou2f2 in the CNS

Pou2f2 has similar binding properties as Pou2f1 as there is high conservation in the sequence of the POU-domain between the two genes (Clerc et al., 1988; Herr et al., 1988; Ko et al., 1988; Staudt et al., 1988). Pou2f2 is important for B-cell development and disease as biopsies of patients with human follicular and Diffuse large B-cell lymphoma have increased incidence of POU2F2 mutations (Hodson et al., 2016; Li et al., 2014). Pou2f2 is expressed in many parts of the central nervous system (Camós et al., 2014; Hatzopoulos et al., 1990; Latchman et al., 1992;

Lillycrop et al., 1994; Lillycrop and Latchman, 1992; Staudt et al., 1986). The functional role Pou2f2 expression in the central nervous system has been largely understudied, with the exception of a few studies. Pou2f2 was shown to be expressed and required for the migration of the V2 interneuron population in the developing spinal cord (Harris et al., 2019). Interestingly, Pou2f2 neuron specific isoforms were regulated by Onecut factors. Onecut1/2 double knockout led to a change in migration of the Pou2f2^{+ve} V2 interneurons, whereas Pou2f2 knockout spinal cord also had a similar defect in V2 interneuron migration. The loss of Pou2f2 did not lead to a reduction in neuronal numbers, suggesting that Pou2f2 is not required for cell fate determination in the spinal cord. Interestingly, a recent scRNA-seq study found that a core set of transcription factors are temporally expressed in the various regions of the developing neural tube (Sagner et al., 2020). In this study, Onecut family of genes and Pou2f2 were shown to be expressed in the early and mid temporal window of the developing neural tube, respectively. Expression of Pou2f2 was distributed in forebrain, midbrain and hindbrain regions, however, the functional role of Pou2f2 in these regions was not analysed. Finally, a study also uncovered the role of Pou2f2 in mature neurons in the rat brain during ischemia (Camós et al., 2014). Knockdown of Pou2f2 in a transitory cerebral ischemia model led to increase in cytotoxicity of the neurons compared to the control. This suggests that Pou2f2 could also have a protective role in mature neurons, but mechanistic insights are missing. Taken together, although Pou2f2 is expressed in a tissue specific manner in the developing CNS, the role of Pou2f2 in cell fate determination has not been carefully examined.

Pou2f1 and Pou2f2 are excellent tTF candidates due to their role in chromatin regulation and cell fate specification in the immune system. More importantly, the sequence similarity of *Pou2f1/Pou2f2* with *Pdm* genes suggests that these genes could be part of the temporal cascade in the developing mouse retina.

1.4.5 Müller glia development

Müller glia are latest cells to be born from RPCs during late retinal development (Young, 1985b). Interestingly, isolated cultures of rat RPCs revealed that Müller glia are predominantly born from terminally dividing RPCs (Gomes et al., 2011). Currently, the factors confer the RPCs the competence to generate Müller glia are unknown, but some studies have unraveled the role of downstream factors necessary for glial fate commitment. In the current model of retinal

gliogenesis, one of the key events that lead to the switch from neurogenesis to gliogenesis is the upregulation of Notch signaling components in the post-mitotic cells. Overexpression of either activated Notch1, the transmembrane component, or Hes1, the transcriptional component of Notch signaling, leads to an increase in Müller glia numbers from late RPCs at the expense of neuronal fates (Furukawa et al., 2000). Interestingly, activation of Notch signaling in the early RPCs does not promote Müller glia outside their developmental window, but instead promotes proliferation in RPCs. This highlights the importance of the changing temporal landscape of the RPCs conducive to generate Müller glia (Jadhav et al., 2006a). Hes1 and Hes5, the bHLH genes downstream of canonical Notch signaling, have been shown to be required for Müller glia production (Hojo et al., 2000; Takatsuka et al., 2004). In addition to Notch signaling, BMP signaling has also been implicated in promoting Müller glia specification from late RPCs. Interestingly, BMP4 activates Id1 and Id3, two DNA binding inhibitors of bHLH genes, that promote Müller glia differentiation from late RPCs (Ueki et al., 2015). Notch signaling also modulates Id1 and Id3 expression indicating possible crosstalk between these two pathways that could be necessary for Müller glia specification from late RPCs (Mizeracka et al., 2013). Therefore, sustained Notch signaling gene expression is important for the maintenance of the glial cell fate during late retinogenesis. In addition to these signaling events, there are also many transcription factors implicated in Müller glia specification.

1.4.5.1 Transcription factors involved in Müller glia specification

Recent scRNA-seq studies have uncovered Nfi family of transcription factors that are expressed in a low-early and high-late expression pattern in the developing RPCs (Clark et al., 2019). Interestingly, triple of knockouts of Nfia/b/x lead to over-proliferation of RPCs beyond their normal window and a consequential loss of Müller glia and bipolar cells, but not rods. This was also evidenced by reduced expression of RPC maintenance genes such as Pax6, Lhx2, Rax and Vsx2 in triple knockouts of Nfia/b/x, thereby controlling both cell fate specification and proliferative quiescence. In addition to these factors, Lhx2, a LIM-homeodomain transcription factor, has been implicated in regulating Müller glia specification at multiple levels in late RPCs. Expressed in both early and late RPCs, Lhx2 interacts with its co-factor Ldb1 during early retinogenesis to promote wide field amacrine cells and suppress Notch signaling along with gliogenesis (de Melo et al., 2018). Interestingly, during late retinogenesis, Lhx2 switches its

interaction from Ldb1 to Rnf12, that changes the binding profile of Lhx2 and promotes Notch signaling as well as gliogenesis (de Melo et al., 2016a; de Melo et al., 2018; de Melo et al., 2016b). Therefore, a critical balance between Ldb1 or Rnf12 interaction with Lhx2 promotes either neurogenesis or gliogenesis, respectively (Fig. 1.8). Lhx2 is essential for the Notch signaling mediated gliogenesis from late RPCs (de Melo et al., 2016b). Activation of Notch signaling by overexpression of Notch intracellular domain (NICD) in Lhx2 cKO late RPCs did not induce Müller glia specification, as compared to high induction in controls. Similarly, overexpression of Hes5 or Nfia in cKO retinas of Lhx2 did not rescue the loss of Müller glia (de Melo et al., 2016a; de Melo et al., 2016b). In addition to its role in Müller glia specification, Lhx2 is also required for the maintenance of the Müller glia fate in post-mitotic precursors. Temporally regulated knockdown of Lhx2 in post-mitotic precursors fated to become Müller glia leads to the disruption of their apical processes. Therefore, for gliogenesis to take place, Lhx2 is essential in the specification of Müller glia from late RPCs and the post-mitotic commitment of the glial cell fate.

SoxE proteins, Sox8 and Sox9 are also required for Müller glia development. Sox9 is expressed in multipotent RPCs and after differentiation, downregulated in retinal neurons and upregulated in Müller glia (Poche et al., 2008). Sox9 knockout retinas have reduced Müller glia numbers, suggesting a role in fate specification. Another study showed that similar to Sox9, Sox8 is also expressed in dividing RPCs and differentiated Müller glia, the knockdown of which leads to a reduction in Müller glia numbers and compensatory increase in rods (Muto et al., 2009). Activation of Notch signaling by overexpression of NICD led to an increase or inhibition of Notch signaling by γ-secretase DAPT led to a decrease in Sox8/9 gene expression. Therefore, there is evidence of cross-activation of Sox8/9 and Notch signaling during Müller glia specification and glial fate maintenance (Fig. 1.8).

1.4.5.2 Current model of Müller glia specification

According to the above studies, a model is proposed which dictates that as Müller glia are predominantly made from terminally dividing RPCs (Gomes et al., 2011), Lhx2, Nfia/b/x are expressed in these RPCs. As RPCs undergo cell division, Lhx2/Rnf12, Nfia/b/x and Sox9 commits the post-mitotic cell towards the Müller glia fate. Subsequently, the post-mitotic cell expresses various Müller differentiation and Notch signaling genes such as *Hes1*, *Hes5*, *Hesr2*, *Sox9*, *Lhx2*

and *Nfia/b/x*. This maintains the commitment of the glial cell fate in the post-mitotic cell. Additionally, upregulation of the Notch pathway induces Sox8/9 expression in the differentiated Müller glia. Therefore, as a late RPC divides, one of the daughter cells undergoes cell state transitions to become a Müller glia, but there are a few gaps in our understanding of Müller glia specification.

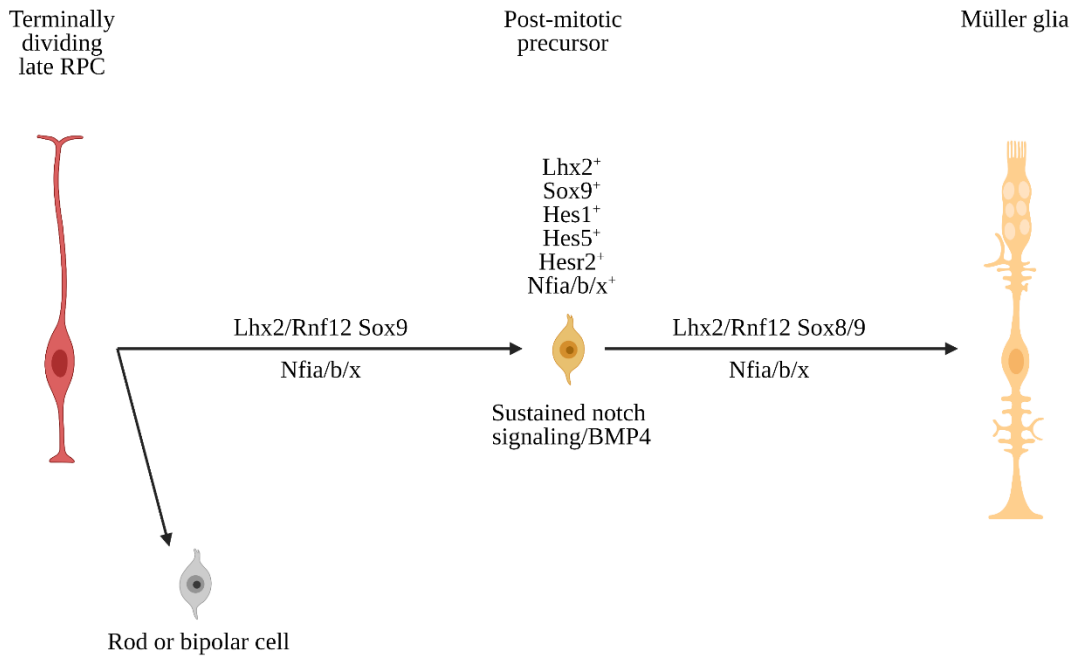

Figure 1.8: Current model of Müller glia development. Terminally dividing RPCs divide to produce a rod/bipolar cell or a post-mitotic cell that undergoes cell state transitions to become a differentiated Müller glia (Gomes et al., 2011). Multiple factors collaborate to commit the precursor towards the Müller glia fate (Clark et al., 2019; de Melo et al., 2016a; de Melo et al., 2018; de Melo et al., 2016b; Furukawa et al., 2000; Hojo et al., 2000; Jadhav et al., 2006a; Jadhav et al., 2006b; Mizeracka et al., 2013; Muto et al., 2009; Poche et al., 2008; Takatsuka et al., 2004; Ueki et al., 2015). Figure generated by Awais Javed.

Late RPCs have a very similar transcriptomic profile to Müller glia (Clark et al., 2019; Roesch et al., 2008). Therefore, it has been difficult to uncover candidate regulators of temporal competence in late RPCs for generating Müller glia. As mentioned previously, other Ikzf family members are expressed during retinal development which makes them interesting candidates for regulating Müller glia competence in the retina (Elliott et al., 2008). In addition to Ikzf1, there is

a distinct temporal expression profile of Ikzf2, Ikzf4 and Ikzf5, whereas Ikzf3 is not detected in the retina. Ikzf2, also known as Helios, is currently being investigated in our lab as a regulator of amacrine development during retinogenesis (unpublished data). Ikzf5, also known as Pegasus, has been investigated and there were no major differences in the cell type compositions of the Ikzf5$^{-/-}$ retinas (unpublished data). Finally, Ikzf4, also known as Eos, is the most promising candidate as Ikzf4 expression is detected during early and late retinogenesis (Elliott et al., 2008).

1.4.6 Ikzf4, Eos: Rising Dawn

'εὖτ᾽ ἀστὴρ ὑπερέσχε φαάντατος, ὅς τε μάλισταἔρχεται ἀγγέλλων φάος Ἠοῦς ἠριγ ενείης'

"That brightest of stars appeared, Eosphoros, that most often heralds the light of early-rising dawn" – Homer. Odyssey XIII.93

Ikzf4 protein is composed of a zinc-finger domain at the C-terminus that can homo- and heterodimerize with other Ikaros family members (Honma et al., 1999). Another zinc-finger domain is present at the N-terminus, which is essential for the DNA binding activity of the protein. Similar to other Ikaros family members, Ikzf4 is expressed in T-lymphocytes, particularly in the regulatory T-cell subtype (Belkaid et al., 2006; Chatila, 2009; Fu et al., 2012; Gokhale et al., 2019; Pan et al., 2009; Rieder et al., 2015; Sharma et al., 2013). Ikzf4 is highly expressed in various parts of the developing and adult mouse central nervous system including the cortex, hippocampus, and spinal cord (Honma et al., 1999). Only one study has assessed the functional role of Ikzf4 in the neuronal context. Ikzf4 was shown to be co-expressed with neuregulin-1 in mature spiral ganglion neurons of the mouse cochlea. It was shown to transcriptionally regulate the expression of PSD-95 (Bao et al., 2004). However, it remains unclear whether Ikzf4 regulates cell fate determination in the developing central nervous system or if Ikzf4 regulates temporal competence, similar to its family member, Ikzf1.

1.5 Objectives and hypothesis

A conserved temporal mechanism enables RPCs to distinguish early and late developmental time in the developing mouse retina. Ikzf1 confers early temporal competence and Casz1 confers late temporal competence to RPCs, thereby partially completing a conserved temporal cascade from flies to mice. As previously mentioned, not all cell fates are accounted for in this cascade which opens the possibility of other tTFs that could modulate RPC temporal identity. The most promising candidates are the homologues of other members of the temporal cascade in flies. These are the two main questions that will be addressed in this thesis: 1) What are the tTFs that confer RPCs the competence to generate cones? 2) What tTFs regulate late RPC temporal identity conducive to Müller glia specification?

In this thesis, I hypothesized that the mammalian homologues of fly *hunchback* and *pdm* genes confer temporal competence to RPCs to generate cones and Müller glia. As mentioned above, Pou2f1 and Pou2f2 are excellent candidate tTFs for the cone fate competence due to their similarity in sequence with Pdm, the mid tTF in the fly VNC temporal cascade (Billin et al., 1991; Dick et al., 1991; Lloyd and Sakonju, 1991). Pou2f1 and Ikzf4 are expressed in the mouse retina during retinogenesis, however, it is unclear whether they are functionally important in cell fate specification from RPCs (Donner et al., 2007; Elliott et al., 2008).

To address these questions and test the hypothesis, I used *ex vivo* and *in vivo* electroporation strategies to misexpress candidate tTFs in RPCs outside their expression windows and assess the effects on retinal cell fate. I also used a combination of CRISPR/Cas9-gRNA mediated indel knockouts, shRNA-mediated knockdowns, Cre-recombinase mediated knockouts and germline knockouts of the candidate tTFs to test their requirement in the production of cones and Müller glia. To assess the molecular mechanism behind their function, I used Chromatin Immunoprecipitation (ChIP) and Cleavage Under Target & Release Under Nuclease (CUT&RUN) to reveal DNA binding targets for the candidate tTFs. Using quantitative PCR, I assessed changes in gene expression for the cone and Müller specification genes associated with the binding sites uncovered by ChIP and CUT&RUN. Finally, I used an *ex vivo* promoter assay in retinal explants to assess the necessity of DNA binding sites important for cone and Müller specification gene expression.

2 Results – Manuscript 1

Pou2f1 and Pou2f2 cooperate to control the timing of cone photoreceptor production in the developing mouse retina

Awais Javed[1,2], Pierre Mattar[1,#], Suying Lu[3], Kamil Kruczek[4,^], Magdalena Kloc[4], Anai Gonzalez-Cordero[4], Rod Bremner[3], Robin R. Ali[4,5] and Michel Cayouette[1,2,6,7,*]

The work presented in the following chapter is reproduced from an article published in Development in 2020, Development 147: dev188730 doi: 10.1242/dev.188730

Author contributions

Conceptualization and experimental design: Awais Javed and Michel Cayouette.

Investigation: Awais Javed performed all experiments in the manuscript except for human fetal retina immunostaining in Fig. 2.1M-Q (performed by Suying Lu), human ESC-derived retinal organoid immunostaining in Fig. S2.2I-J'' (performed by Kamil Kruczek, Magdalena Kloc, Anai Gonzalez-Cordero) and Thrb2 promoter assay design and replicate experiment in Fig. S2.5A-I (performed by Pierre Mattar).

Result analysis: Awais Javed, Pierre Mattar, and Michel Cayouette.

Writing – Original Draft: Awais Javed.

Writing – Review & Editing: Pierre Mattar, Rod Bremner, Robin Ali, and Michel Cayouette.

Resources: Rod Bremner, Robin Ali, and Michel Cayouette.

Supervision: Rod Bremner, Robin Ali, and Michel Cayouette.

Funding Acquisition: Michel Cayouette.

Awais Javed[1,2], Pierre Mattar[1,#], Suying Lu[3], Kamil Kruczek[4,^], Magdalena Kloc[4], Anai Gonzalez-Cordero[4], Rod Bremner[3], Robin R. Ali[4,5] and Michel Cayouette[1,2,6,7, *]

[1]Cellular Neurobiology Research Unit, Institut de recherches cliniques de Montreal (IRCM), Canada.

[2]Molecular Biology Program, Université de Montréal, Canada.

[3]Lunenfeld-Tanenbaum Research Institute, Sinai Health System, Toronto, Canada. Department of Ophthalmology and Vision Science, Department of Lab Medicine and Pathobiology, University of Toronto

[4]UCL Institute of Ophthalmology, London, United Kingdom.

[5] NIHR Biomedical Research Centre at Moorfields Eye Hospital NHS Foundation Trust and UCL Institute of Ophthalmology, London, United Kingdom

[6]Department of Medicine, Université de Montréal, Canada.

[7]Department of Anatomy and Cell Biology; Division of Experimental Medicine, McGill University, Canada.

[#]Current address: Ottawa Hospital Research Institute, Canada

^ Current address: National Eye Institute, Bethesda, USA

Editor: Steve Wilson, University College London, United Kingdom

Received January 23, 2020; Accepted August 19, 2020; **Published September 28, 2020**.

Citation: Javed, A., Mattar, P., Lu, S., Kruczek, K., Kloc, M., Gonzalez-Cordero, A., Bremner, R., Ali, R.R., and Cayouette, M. (2020). Pou2f1 and Pou2f2 cooperate to control the timing of cone photoreceptor production in the developing mouse retina. Development 147.

Competing interests: The authors declare no competing interests.

Funding: This work was funded by grants from the Canadian Institutes of Health Research (FDN-159936), the Foundation Fighting Blindness Canada, the Brain Canada/Kremil Foundations (to M.C. and R.B.), as well as the UK Medical Research Council, the European Research Council and RP Fighting Blindness (to R.A.). A.J. holds a PhD scholarship from Fonds de Recherche du Québec – Santé. M.C. is an Emeritus Scholar from the Fonds de Recherche du Québec – Santé and holds the Gaëtane and Roland Pillenière Chair in Retina Biology.

*corresponding author: michel.cayouette@ircm.qc.ca

Keywords: Retinogenesis, temporal competence, cone photoreceptors, Pou2f1, Pou2f2

2.1 Abstract

In the developing retina, multipotent retinal progenitor cells (RPCs) generate various cell types in a precise chronological order, but how exactly cone photoreceptor production is restricted to early stages remains unclear. Here, we show that the POU-homeodomain factors Pou2f1/Pou2f2, which are homologs of the Drosophila temporal identity factors nub/pdm2, regulate the timely production of cones in the mouse retina. Pou2f1/Pou2f2 are expressed during the period of cone genesis, and forcing sustained expression of either factor in RPCs expands the cone production window, whereas misexpression in late-stage RPCs triggers ectopic cone production at the expense of late-born fates. Conversely, inactivation of Pou2f1/2 decreases cone production. Mechanistically, we report that Pou2f1 induces Pou2f2 expression, which in turn represses the rod-promoting gene Nrl by binding to a POU motif in its promoter. Moreover, Pou2f1/2 transiently promote expression of the cone fate determinant Thrb. These results uncover Pou2f1/2 as regulators of the temporal window for cone genesis and, given their widespread expression in the nervous system, suggest that they might also control temporal patterning in other progenitor populations.

2.2 Introduction

The generation of neuronal diversity is critical to build a functional nervous system. Classical studies have shown that, in some regions of the nervous system, the spatial position of neural progenitors is key to engage transcriptional regulatory networks that induce a particular fate (Jessell, 2000). In other regions, developmental time is used to diversify the progenitor pool (Ebisuya and Briscoe, 2018; Kohwi and Doe, 2013). A particularly striking example of such 'temporal patterning' is observed in the developing vertebrate retina, where the temporal identity of multipotent retinal progenitor cells (RPCs) changes progressively, such that their competence to give rise to different retinal cell types is altered as a function of developmental stage. Ganglion, horizontal, amacrine and cone photoreceptor cells are generally born early, whereas rod, bipolar, and Müller glial cells are generally born late (Carter-Dawson and LaVail, 1979a, b; Rapaport et al., 2004; Turner et al., 1990; Young, 1985a, b). While much is known about the transcriptional networks operating to instruct the generation of various cell fates available to RPCs within a given

temporal window (Bassett and Wallace, 2012), much less is known about how these differentiation programs are activated at the appropriate time to control cell birth order.

Changing environmental signals in the developing retina contribute to alter RPC cell fate potential (Kim et al., 2005; Ma et al., 2007; Ozawa et al., 2007), but these cues act as inhibitory signals for specific cell types rather than as instructive cues, and heterochronic grafting studies have shown that the environment is not sufficient to alter fate output (Belliveau and Cepko, 1999; Cepko, 1999; Watanabe and Raff, 1990). Moreover, the size and composition of clones produced in clonal-density cultures are indistinguishable from that of clones produced in situ and the general order of cell birth is maintained is such cultures (Cayouette et al., 2003; Gomes et al., 2011). Thus, cell intrinsic programs largely appear to control temporal identity transitions in RPCs. But what could these intrinsic factors be? A clue was provided by pioneering studies of Drosophila neuroblasts. In these lineages, the transcription factors hunchback (hb), krüppel (kr), nub/pdm2 (collectively called pdm) and castor (cas) are part of a temporal identity cascade where each factor is necessary and sufficient for the generation of neurons born during the temporal window in which they are expressed (Brody and Odenwald, 2000; Cleary and Doe, 2006; Grosskortenhaus et al., 2005; Grosskortenhaus et al., 2006; Isshiki et al., 2001; Kambadur et al., 1998; Novotny et al., 2002; Pearson and Doe, 2003). This cascade is tightly controlled by feedforward and feedback loops operating to restrict the expression of each temporal factor in its respective expression window (Doe, 2017). More recently, other temporal identity factors have been identified in different lineages of the fly nervous system (Erclik et al., 2017; Li et al., 2013; Suzuki et al., 2013), suggesting that such cascades might represent a general strategy to regulate progenitor competence.

Previously, we showed that mouse Ikzf1 (a.k.a. Ikaros) is orthologous to Drosophila hb and confers early temporal identity in RPCs, allowing production of three of the early born retinal cell types: ganglion, horizontal and amacrine cells (Elliott et al., 2008). Conversely, we showed that mouse Casz1 is orthologous to Drosophila cas and confers mid/late temporal identity in RPCs, allowing the generation of rod photoreceptors and bipolar cells (Mattar et al., 2015). Intriguingly, however, Ikzf1 does not appear to regulate cone photoreceptor production, although these cells are

also produced during early stages of retinogenesis, from around E11.5 to E18.5 (Carter-Dawson and LaVail, 1979b; Rapaport et al., 2004; Turner et al., 1990; Young, 1985a, b). Considering that the Drosophila temporal identity cascade appears to be conserved, at least partially, to regulate temporal patterning in mammalian RPCs, we hypothesized that other homologs of the fly cascade might regulate the timely production of cone photoreceptors.

Here, we show that Pou2f1 and Pou2f2 (originally named Oct-1 and Oct-2), the mammalian homologs of Drosophila nub/pdm2, respectively, regulate the timely production of cone photoreceptors in the mouse retina. This is achieved by the direct repressive action of Pou2f2 on the rod-inducing factor Nrl, providing a rare link between temporal identity factors and downstream regulators of cell fate choice in mammalian CNS development. Importantly, we provide evidence for cross-regulatory mechanisms operating between Pou2f1 and the other temporal identity factors Ikzf1 and Casz1, reinforcing the idea that some aspects of the strategy used to control temporal progression in fly neuroblasts are conserved in mammalian neurogenesis.

2.3 Results

2.3.1 Pou2f1/2 are expressed in early retinal progenitor cells and Pou2f1 expression is maintained in mature cone photoreceptors

We first used BLAST-P to identify Mus musculus proteins presenting high sequence conservation with Drosophila melanogaster Nub/Pdm2 proteins (Altschul et al., 1990). We found that the DNA binding POU-specific domain and POU-homeodomain of Nub/Pdm2 are highly homologous to mouse Pou2f1 and Pou2f2, respectively (Fig. S2.1A), as previously reported for human POU2F1 and POU2F2 (Lloyd and Sakonju, 1991). To study expression of Pou2f1 and Pou2f2 proteins in the developing retina, we first validated antibodies. As it was previously reported that Pou2f1 is expressed in the developing retina at E11.5 (Donner et al., 2007), we asked whether antibodies against Pou2f1 and Pou2f2 recognise the appropriate band size in western blots from E12 retinal extracts. We found that the Pou2f1 antibody recognises two bands around 80kDa, corresponding to the size of two of the isoforms of Pou2f1, whereas the Pou2f2 antibody

recognises two bands at 70 kDa and 65kDa corresponding to the size of the two Pou2f2 isoforms (Fig. S2.1B). To determine whether the antibodies showed any cross-reactivity in immunostaining, we electroporated either CAG:Pou2f1-IRES-GFP or CAG:Pou2f2-IRES-GFP in P0 retinas and stained sections 48 hours later. We found that the anti-Pou2f1 antibody detected overexpressed Pou2f1, but not Pou2f2 and, conversely, the anti-Pou2f2 antibody detected overexpressed Pou2f2 but not Pou2f1 (Fig. S2.1C-F'), indicating that each antibody does not cross react with the other Pou2f protein. Next, we generated shRNAs and gRNAs targeting both Pou2f1 and Pou2f2 and electroporated P0 retinal explants with CAG:GFP, CAG:Pou2f1-IRES-GFP or CAG:Pou2f2-IRES-GFP along with the respective gRNA or shRNA vector (Fig. S2.1G), and stained the retina three days later with the antibodies against Pou2f1 or Pou2f2. We found a considerable decrease in immunostaining signal in both cases (Fig. S2.1H-S"). Furthermore, the shRNA vectors significantly decreased the levels of Pou2f1 and Pou2f2 proteins detected by western blot after co-expression in HEK293 cells (Fig. S2.1T-V). Together, these results show that the Pou2f1 and Pou2f2 antibodies recognize the right antigen and at the same time validate the targeting efficiency of our gRNAs and shRNAs.

Using these validated reagents, we first studied the spatiotemporal expression pattern of Pou2f1 and Pou2f2 in the developing mouse retina. We found Pou2f1 and Pou2f2 positive (Pou2f1/2^{+ve}) cells of the retinal progenitor layer (RPL) that co-labelled with proliferating cell markers Ki67 or EdU from E11.5 to E15.5, indicating expression in RPCs. Starting from E15.5, however, the number of Pou2f1/2^{+ve} RPCs declined (Fig. 2.1A-F") and only a few RPCs expressing Pou2f1 at low levels and virtually no RPCs expressing Pou2f2 by P0 were found (Fig. S2.2A-B'). We observed Pou2f1/Pou2f2 co-labelling of in the majority of cells at E11 (Fig. S2.2C), consistent with recently published RNA-Seq datasets (Fig. S2.2D) (Clark et al., 2019) (Aldiri et al., 2017; Hoshino et al., 2017). This demonstrates that Pou2f1 and Pou2f2 are expressed in mitotic RPCs during the period of cone genesis, but not in RPCs generating late-born cell types.

At E15.5, some Pou2f1^{+ve} cells co-labelled with Rxrg, which label cone photoreceptors on the apical-most region of the retina, whereas others co-labelled with Vsx2, a marker for RPCs at this stage, suggesting Pou2f1 expression in both cones and dividing RPCs (Fig. S2.2E). By E17.5

and onwards, Pou2f1 was expressed primarily in Rxrg^{+ve}, Lim-1^{+ve} (horizontal cell marker) and Brn3b^{+ve} (ganglion cell marker) cells (Fig. 2.1G-L', Fig. S2.2F-G"). Consistent with this data, when we analysed expression of Pou2f1 in a published RNA-seq dataset of sorted cone photoreceptors, we found high expression of Pou2f1 mRNA (Daum et al., 2017). These data suggest that Pou2f1 expression is maintained in mature cone, horizontal and ganglion cells.

The antibodies against Pou2f2 and Rxrg were both raised in rabbits, precluding double-stainings. We therefore used the Chrnb4-eGFP mouse line, which expresses GFP specifically in cones and ganglion cells, to assess Pou2f expression in these cells at E14.5 (Decembrini et al., 2017; Siegert et al., 2009). Some apically-located cells co-labelled with Pou2f2 and GFP and were negative for Brn3b, consistent with expression in a subset of cones, while other Pou2f2^{+ve} cells were co-labelled with Brn3b, indicating expression in RGCs (Fig. S2.2H).

Next, we asked whether POU2F1/2 are also expressed in the developing human retina. Our POU2F2 antibodies did not produce a signal in human retinas. However, the POU2F1-specific antibody stained cells in the progenitor layer that lacked OTX2 and BRN3B, while others expressed OTX2 or BRN3B at fetal week (FW) 12 (Fig. 2.1M), suggesting expression in RPCs, RGCs and differentiating photoreceptors. From FW15 to FW19, POU2F1 labelling in the progenitor layer decreased, but was maintained in cells found at the apical side of the outer nuclear layer (ONL) in the macula region, where cones reside, and co-labelled with OTX2 (Fig. 2.1N), a marker of photoreceptors in this layer. Some POU2F1^{+ve} cells also co-labelled with L/M-OPSIN and ONECUT2, a cone and horizontal cell marker, respectively (Fig. 2.1M"'-Q"'). To further characterize the expression of POU2F1 in human retinal tissue, we generated human embryonic stem cell-derived retinal organoids using a previously-published protocol (Gonzalez-Cordero et al., 2017). As observed in human fetal retinas, we found that POU2F1 was expressed in proliferating KI67^{+ve} progenitors in early-stage organoids (Fig. S2.2I), whereas its expression decreased in the progenitor layer at later stages, but remained in differentiated cones at 24 weeks, as determined by co-staining with S-OPSIN, L/M-OPSIN, and ARRESTIN (Fig. S2.2J). Thus, POU2F1 is expressed in early- but not late-stage RPCs and is maintained in mature cone photoreceptors in the human retina, similar to what we observed in the mouse retina.

2.3.2 Sustained Pou2f1/2 expression expands cone production outside the normal developmental window

As expression of Pou2f1 and Pou2f2 in RPC is lost when cone production is over, we wanted to investigate whether their sustained expression could extend the period of cone production. We electroporated CAG:GFP, CAG:Pou2f1-IRES-GFP or CAG:Pou2f2-IRES-GFP vectors in E14 retinal explants, and assessed the percentage of cones produced by co-staining with GFP and cone markers 19 days later (Fig. 2.2A). Interestingly, we found an increase in the proportion of GFP^{+ve} cells that co-expressed Rxrg and S-opsin after Pou2f1 or Pou2f2 expression (Fig. 2.2B-G). These additional cones might have arisen from an increased production during the normal temporal window of cone genesis or from an extension of this window into later stages. To distinguish between these possibilities, we added EdU to the culture medium 5 days after electroporation of Pou2f1 or Pou2f2, when cone production is normally over, and analyzed the explants 14 days later (Fig. 2.2H). While virtually no S-$opsin^{+ve}$/EdU^{+ve}/GFP^{+ve} cells were detected in controls (1/455 cells counted), as expected, we found a significant fraction of these cells after Pou2f1 or Pou2f2 overexpression (Fig. 2.2I-M). Moreover, we did not observe an increase in the total number of EdU^{+ve}/GFP^{+ve} cells, suggesting that misexpression of Pou2f1 or Pou2f2 does not affect the proliferative potential of early RPCs (Fig. S2.3A). These results suggest that sustained expression of Pou2f1 and Pou2f2 in RPCs extends the period of cone production.

2.3.3 Ectopic expression of Pou2f1 or Pou2f2 in late-stage retinal progenitors induces cone production at the expense of late-born fates

Post-natal murine RPCs have normally lost the competence to generate cones. To determine whether Pou2f1/2 is sufficient to confer competence to generate cones in late-stage RPCs, we first infected P0 retinal explants with retroviral vectors expressing Venus, Pou2f1-IRES-Venus, or Pou2f2-IRES-Venus and analyzed cell type composition and clone size 14 days later (Fig. 2.3A). Retroviral-mediated expression of Pou2f1 at P0 increased the production of $Rxrg^{+ve}$/S-$opsin^{+ve}$, PNA^{+ve}/S-$opsin^{+ve}$, and $Rxrg^{+ve}$/$Otx2^{+ve}$ cells in the photoreceptor layer (Fig. 2.3B-E", Fig. S2.3A-E'). Pou2f2, in contrast, induced the production of $Rxrg^{+ve}$ cells located in the

photoreceptor layer, but these cells did not express mature cone markers like S-opsin (Fig. 2.3B”-E”). Since Rxrg is also expressed in ganglion cells, we wondered whether the Rxrg^{+ve} cells observed after Pou2f2 expression might be ganglion cells mis-localised in the photoreceptor layer. However, the Rxrg^{+ve} cells in the photoreceptor layer observed after expression of Pou2f2 were co-labelled with Otx2, which labels photoreceptors in this layer, and never stained for the RGC marker Brn3b (Fig. S2.3B’’-E’’’), excluding this possibility. Pou2f2 also induced the production of a small number of horizontal cells, another early-born cell type (Fig. 2.3F, Fig. S2.3F-H’). Interestingly, both Pou2f1 and Pou2f2 promoted Rxrg^{+ve} cells at the expense of late-born cell types (rods, bipolars, Müllers), without changing the distribution of clone size (Fig. 2.3F-G), suggesting that Pou2f1/2 do not trigger cone production by altering proliferation or cell death.

We next assessed if Pou2f1 and Pou2f2 could promote cone production *in vivo*. We electroporated mouse retinas at P0 with GFP, Pou2f1-IRES-GFP, or Pou2f2-IRES-GFP. Two weeks later, the retinas were stained for GFP, Rxrg, and S-opsin. While GFP-transfected RPCs did not generate cones at this stage, as expected, misexpression of either Pou2f1 or Pou2f2 substantially increased the proportion of Rxrg^{+ve} cells located in the photoreceptor layer (Fig. 2.3H, Fig. S2.3I-L”). The Rxrg^{+ve} cells induced by Pou2f1 also expressed S-opsin, whereas those induced by Pou2f2 did not (Fig. S2.3I”-L”), as observed in retinal explants (see Fig. 2.3B-G). Interestingly, Pou2f1 misexpression did not promote M-opsin-expressing cells (data not shown). Together, these results indicate that ectopic expression of Pou2f1 in P0 RPCs is sufficient to trigger the production of S-cones, whereas Pou2f2 induces the production of immature cones.

Interestingly, co-electroporation of Pou2f1 and Pou2f2 does not elicit an additive effect in the number of cones produced by P0 RPCs (Fig. 2.3H), suggesting that Pou2f1/2 might function in the same genetic pathway. Consistently, we found that Pou2f1 significantly increases Pou2f2 transcript levels 9 hours after electroporation, whereas Pou2f2 has no effect on Pou2f1 transcripts (Fig. 2.3I). Moreover, when we electroporated Pou2f1 in P0 retinal explants and stained for Pou2f2 3 days later, we found that Pou2f1 increases Pou2f2 levels in some GFP^{+ve} cells, whereas co-electroporating Pou2f1 with a Pou2f1 gRNA and Cas9 abrogates this effect (Fig. 2.3J-M’). These results suggest that Pou2f1 upregulates Pou2f2 expression. To test the functional hierarchy of the

Pou2f1→ Pou2f2 cascade in cone production, we co-electroporated P0 retinas with Pou2f1 while knocking-down Pou2f2 with an shRNA, or vice versa, and assessed cone production 14 days later. Whereas Pou2f1 increased cone numbers when co-expressed with a control shRNA, as predicted, it was unable to do so when Pou2f2 was knocked down (Fig. 2.3N). In contrast, Pou2f2 was equally able to promote cones in presence or absence of Pou2f1. Together, these results support a model in which Pou2f1 requires Pou2f2 to promote the cone fate.

2.3.4 Pou2f1/2 are required for cone cell fate specification in the developing retina.

To ask whether Pou2f1 and Pou2f2 are required for cone production, we first knocked down their expression using shRNA and CRISPR/Cas9 gRNA in E14 retinal explants, a stage when cones are normally produced. Three weeks later, we determined the proportion of electroporated cells that became cones by counting the proportion of $GFP^{+ve}/Rxrg^{+ve}$ cells in the photoreceptor layer. With both approaches, we found a significant decrease in the proportion of cones produced (Fig. S2.4A-C). Given that shRNAs were delivered using retroviral vectors, we were also able to determine the effect of Pou2f1/2 knockdown on other retinal fates and clone size. We found that the loss of cones is compensated by an increase in late-born rod production after Pou2f2 knockdown, while Pou2f1 knockdown does not significantly affect other fates, most likely because the decrease in cone production is less than with Pou2f2 knockdown (Fig. S2.4B). Both Pou2f1 and Pou2f2 knockdown did not affect clone size distribution (Fig. S2.4C). Finally, Cre electroporation in $Pou2f2^{fl/fl}$ retinal explants at E13 also significantly reduced the generation of cones (Fig. S2.4D). These results suggest that Pou2f1 and Pou2f2 are required for cone photoreceptor development.

Next, we sought to determine whether Pou2f1/2 are required for cone production *in vivo*. Since our data suggests that Pou2f2 lies downstream of Pou2f1 and is required for the cone-inducing activity of Pou2f1, we decided to focus our analysis on Pou2f2. As $Pou2f2^{-/-}$ mice die shortly after birth (Konig et al., 1995), we generated conditional knockouts (cKO) by crossing $Pou2f2^{fl/fl}$ mice (Hodson et al., 2016) with two different Cre driver lines: the alpha-Pax6-Cre line, which drives Cre expression in peripheral RPCs from E10 onwards (Marquardt et al., 2001), and

the Chx10-Cre^{ERT2} line (RIKEN Bioresource Centre RRID: IMSR_RBRC06574), which allows tamoxifen-inducible activation of Cre. When we stained the peripheral retina of aPax6-Cre^{+};Pou2f2$^{fl/fl}$ (aPax6Cre-Pou2f2 cKO) with the Pou2f2 antibody, we observed a reduction in immunostaining signal specifically in Cre^{+ve} cells at E12 (Fig. S2.4E-G') and in RGCs at P14 (Fig. S2.4H-J'). To assess the recombination efficiency in the Chx10-Cre^{ERT2} mice, we crossed them with Rosa26-tdT reporter mice, injected tamoxifen at E11.5, and assessed tdT expression at E13.5. As expected, we found robust recombination throughout the retina (Fig. S2.4K-M'). Next, we stained retinas from Chx10-Cre^{ERT2}; Pou2f2$^{fl/fl}$ (Chx10Cre-Pou2f2 cKOs) for Pou2f2 and observed a reduction in immunostaining signal in the GCL at E17.5 (Fig. S2.4N-P'). These results provide additional evidence for the specificity of the Pou2f2 antibody and validate both conditional knockout approaches.

Next, we stained retinal sections from P14 aPax6Cre-Pou2f2 cKO and control mice for markers of various retinal cell types. We found that deletion of Pou2f2 leads to a decrease in cone photoreceptors and horizontal cells, as determined by counting Rxrg, PNA, Arr3, Cnga3 and Lim-1 expressing cells (Fig. 2.4A-F). We did not observe any significant change in the number of amacrines (Pax6), bipolars (Chx10), ganglion cells (Brn3b), or Müllers (Sox2) produced in these retinas (Fig. 2.4F). We also observed a decrease in Arr3 staining in flat-mounts of temporal regions of P14 cKO retinas (Fig. 2.4G-G"). Finally, we observed a similar decrease in cone numbers (Rxrg^{+ve} in the photoreceptor layer) and a compensatory increase in rod numbers (Nrl^{+ve} cells) in the Chx10Cre-Pou2f2 cKO retinas compared to controls at E17.5 (Fig. 2.4H-J). Collectively, these experiments demonstrate that Pou2f2 is required, at least partially, for the production of cone and horizontal cells in the developing retina.

2.3.5 Ikzf1 induces Pou2f1, which in turn represses Casz1

We next investigated whether Pou2f1/2 might be part of a temporal identity cascade controlled by cross-regulatory mechanisms, similar to that observed in Drosophila, where hb activates kr, which then activates pdm to ensure temporal identity progression in neuroblasts (Doe, 2017). We first hypothesized that Ikzf1 might induce Pou2f1/2 expression in mouse RPCs, as they are expressed at the same stages. To test this idea, we transfected E14 retinal explants with vectors

expressing GFP, Ikzf1-IRES-GFP, or Ikzf1-VP16-IRES-GFP. After 10 hours, a time point when the majority of GFP^{+ve} cells are still RPCs, we sorted the GFP^{+ve} cells and isolated total RNA for RT-qPCR (Fig. 2.5A). We found that Ikzf1 and Ikzf1-VP16 induced or repressed Pou2f1/2, respectively (Fig. 2.5B-C). Interestingly, we found that Ikzf1 has no effect on Pou2f1 expression in P0 retinal explants (Fig. 2.5D-E), suggesting that Ikzf1 promotes Pou2f1 expression in early but not late RPCs.

In a previous study, we reported that Ikzf1 represses Casz1 expression, likely via an indirect mechanism (Mattar et al., 2015). Therefore, we hypothesized that Pou2f1 might function as an intermediate factor downstream of Ikzf1 to repress Casz1. Consistently, we found that ectopic Pou2f1 expression at P0, during the window of Casz1 expression, decreases the levels of *Casz1* transcripts (Fig. 2.5F-G). In contrast, Pou2f2 did not significantly alter expression of Casz1. Together, these results suggest that Pou2f1 is part of a cross-regulatory temporal identity cascade together with Ikzf1 and Casz1.

2.3.6 Pou2f2 binds to the Nrl promoter and represses its activity

How could Pou2f1/2 induce the cone photoreceptor cell fate? In Olig2^{+ve} early RPCs, Onecut1 and Otx2 bind to a cis-regulatory module (CRM) of the Thrb gene (active in dividing RPCs) and promote cone and horizontal cell production (Emerson et al., 2013). This CRM was cloned from the chick genome, but it remains unclear whether an equivalent CRM exists in the mouse. As this CRM is located at the downstream promoter of the chick Thrb gene, we cloned the equivalent mouse region (Thrb-PR2::GFP) as well as the upstream promoter sequence of the mouse Thrb gene (Thrb-PR1::GFP) (Fig. S2.5A). When we electroporated GFP constructs driven by these CRMs in E13 retinal explants, we found that they are active in cones, similar to what was observed with the chick sequences (Fig. S2.5B-C) (Emerson et al., 2013). To test whether Pou2f1 or Pou2f2 might regulate any of the Thrb CRMs, we co-electroporated P0 retinal explants with CAG:mCherry to label all electroporated cells and an empty CAG vector, CAG:Pou2f1, or CAG:Pou2f2, and either ThrbPR1:GFP or ThrbPR2:GFP, and analysed GFP expression 24 hours later (Fig. S2.5D-I). Interestingly, we found that Pou2f1 and Pou2f2 induce ThrbPR1:GFP activity but not ThrbPR2:GFP. Moreover, ThrbPR1:GFP is active as soon as mCherry expression turns on,

and the GFP expression disappears 72hours after electroporation, suggesting transient activity of the CRM in the electroporated cells (data not shown). These data suggest that Pou2f1 and Pou2f2 operate in parallel with Onecut1, acting transiently at a distinct CRM of Thrb to promote the cone fate. Another role for Thrb2 has been shown at later stages during cone differentiation to promote the M-cone subtype (Applebury et al., 2007; Ng et al., 2001; Ng et al., 2009). Therefore, we tested whether Pou2f1 and Pou2f2 could promote *Thrb2* mRNA expression in a stage-dependent manner. We electroporated P0 retinal explants with CAG:GFP, CAG:Pou2f1-IRES-GFP or CAG:Pou2f2-IRES-GFP, sorted the GFP^{+ve} cells 6 or 14 days later and assessed *Thrb2* mRNA levels. Consistent with the promoter assays described above, we found that both Pou2f1 and Pou2f2 increased *Thrb2* expression at 6 days (Fig. S2.5J). In contrast, both Pou2f1 and Pou2f2 had no effect on Thrb levels at 14 days. On the other hand, when we assessed *Thrb2* mRNA levels in adult aPax6-Cre Pou2f2 cKOs, we observed no change in expression, suggesting that Pou2f2 is sufficient but not required for Thrb2 expression (Fig. S2.5K). Finally, although POU-binding motifs were present in this CRM of Thrb, when we conducted chromatin immunoprecipitation (ChIP) in E14 mouse retinas to assess binding of Pou2f2 at this region, we did not observe significant enrichment (Fig. S2.5L-M). These results suggest that Pou2f1 and Pou2f2 transiently regulate Thrb2 levels to promote cone specification, but likely via an indirect mechanism.

An additional pathway known to regulate the rod to cone fate decision involves the transcription factor Nrl, which activates the nuclear receptor Nr2e3 in photoreceptor precursors to promote rod photoreceptor gene expression (Mears et al., 2001; Oh et al., 2008). In Nrl KO mice, rods are not produced and all photoreceptor precursors turn into S-cone-like cells (Mears et al., 2001). These results suggest a model in which downregulation of Nrl is important for the generation of cones, but direct repressors of Nrl remain unknown. Interestingly, we noticed that the Nrl promoter region, which was previously characterized (Kautzmann et al., 2011), contains a POU binding motif. This prompted us to postulate that Pou2f1/2 might repress Nrl expression. To test this hypothesis, we transfected P0 retinal explants with either GFP, Pou2f1-IRES-GFP or Pou2f2-IRES-GFP, sorted the GFP^{+ve} cells 20 hours later and analyzed transcript levels by RT-qPCR. Remarkably, we found that Pou2f2 significantly reduces the levels of *Nrl* and *Nr2e3*, whereas Pou2f1 had no effect (Fig. 2.6A), most likely because 20 hours is not long enough for

Pou2f1 to trigger sufficient Pou2f2 expression to detect changes in Nrl and Nr2e3 expression. Consistent with this idea, Pou2f1 decreased Nrl transcript 6 days after transfection (Fig. 2.6B). Pou2f2 overexpression also reduced the number of cells staining for Nrl in the photoreceptor layer (Fig. 2.6C-E), supporting the RT-qPCR data. These results suggest that Pou2f2 functions as a negative regulator of Nrl.

We thus sought to determine whether Pou2f2 could repress the Nrl promoter. To do this, we co-electroporated GFP, Pou2f1-IRES-GFP, or Pou2f2-IRES-GFP, together with an pNrl:dsRed reporter construct (Akimoto et al., 2006; Matsuda and Cepko, 2007) in retinal explants and studied dsRed expression two days later (Fig. 2.6F). As expected, the pNrl:dsRed reporter was robustly activated when co-electroporated with the control construct, but not when co-electroporated with Pou2f1 or Pou2f2 (Fig. 2.6G-I"). Importantly, when we mutated the POU-specific binding motif in the pNrl:dsRed reporter, Pou2f1 and Pou2f2 no longer repressed dsRed expression (Fig. 2.6J-L"). Given that Pou2f1 was unable to reduce Nrl transcripts 20 hours after expression (Fig. 2.6B), we hypothesized that its repressive action on the Nrl promoter activity was likely mediated via upregulation of Pou2f2. If this were the case, we predicted that Pou2f2, but not Pou2f1, would bind the Nrl promoter. Consistently, ChIP-qPCR from E14 retinas detected significant enrichment of Pou2f2 at the POU-specific binding region of the Nrl promoter, whereas it was not detected in a control intronic region (Fig. 2.6M-N). In contrast, we failed to detect any enrichment at the same region after Pou2f1 ChIP (Fig. 2.6M-N). These results indicate that Pou2f2 represses Nrl expression by binding the POU motif in the Nrl promoter.

2.3.7 Pou2f2 functions in postmitotic photoreceptor precursors to promote the cone fate

We next wanted to determine whether Pou2f2 functions in RPCs or in postmitotic photoreceptor precursors to induce the cone fate. To address this question, we used the wild-type and mutated Nrl promoter (mpNrl) to drive expression of Pou2f1 or Pou2f2 in photoreceptor precursors (Fig. 2.6O). We first validated these vectors by co-electroporating them with GFP in retinal explants at P0 and staining for Pou2f1 and Pou2f2 three and 14 days later. We found that Pou2f1 and Pou2f2 were weakly expressed from the wild-type Nrl promoter (Fig. S2.6A-G"), most

likely due to the negative feedback of Pou2f2 on the promoter, whereas they were robustly expressed when using mpNrl (Fig. S2.6H-N").

We next stained the explants for Rxrg to assess whether overexpressing Pou2f1 or Pou2f2 in post-mitotic photoreceptor precursors was sufficient to drive cone production. Whereas mpNrl:Pou2f2 induced Rxrg^{+ve} cells in the photoreceptor layer, mpNrl:Pou2f1 was much less efficient at doing so (Fig. 2.6P-S). As control, we found that the wildtype pNrl:Pou2f1 and pNrl:Pou2f2 did not yield any Rxrg^{+ve} cells (Fig. S2.6F-F"). We speculate that the weak activity of the mpNrl:Pou2f1 construct on cone production is due to activation of Pou2f2 (Fig. 2.3G). These results indicate that expression of Pou2f2 in post-mitotic photoreceptor precursors is sufficient to promote the cone fate.

2.4 Discussion

There has been considerable work done to understand how neural progenitor cells generate neuronal diversity in the developing central nervous system. However, not much is known about how temporal identity is encoded in progenitors to initiate the correct transcriptional code producing the appropriate cell types for a given developmental stage. In this study, we provide evidence that Pou2f1 endows RPCs with the competence to generate cone photoreceptors by promoting expression of Pou2f2, which then induces Thrb and represses Nrl to favor the cone fate. We also provide evidence that Pou2f1 lies in a temporal cascade reminiscent of that observed in Drosophila neuroblasts. Ikzf1 contributes to Pou2f1 upregulation, which in turn represses the late-stage temporal factor Casz1, thereby ensuring that RPCs do not switch prematurely to a late temporal identity and allowing production of cones within the early developmental window (Fig. 2.7).

2.4.1 Encoding temporal identity vs. promoting cone fate

Multiple lines of evidence support a model in which Pou2f1 confers RPCs competence to generate cones during early retinogenesis, whereas Pou2f2 functions primarily as a classical cone fate determinant in photoreceptor precursors. First, although normal P0 RPCs are unable to

generate cones, Pou2f1 is sufficient to drive production of mature cones in this context, whereas Pou2f2 is not. Thus, Pou2f1 appears able to fully open the temporal identity window in RPCs to generate cones. Subsequently, once the window of cone development is open, Pou2f2 can repress Nrl and promote cone photoreceptor specification. Consistently, expression of Pou2f1 using the Nrl promoter fails to induce a high number of cones, whereas mpNrl-Pou2f2 efficiently induces cones. Second, although the early temporal identity factor Ikzf1 induces the expression of Pou2f1 and Pou2f2, only Pou2f1 regulates the expression of the mid/late-stage temporal factor Casz1. Thus, Pou2f1 appears to be integrated into the temporal cascade. Whether Ikzf1 regulates Pou2f1 and Pou2f2 directly will need further investigation, but genomic regions upstream of the transcriptional start site of Pou2f1 and Pou2f2 contain multiple Ikzf 'GGGAA' consensus sequence, suggesting possible binding. Third, Pou2f2 directly binds and represses the rod determinant Nrl, which is restricted to post-mitotic photoreceptor precursors (Mears et al., 2001; Oh et al., 2007). Together with our finding that Pou2f2 is able to induce the cone fate when expressed from the Nrl promoter, this is further evidence that Pou2f2 primarily regulates cell fate decisions in postmitotic precursor cells, rather than acting in RPCs to control temporal identity. Importantly, however, we cannot rule out an additional role for Pou2f2 in dividing RPCs. Indeed, we show that Pou2f2 is expressed in early RPCs, and its overexpression not only promotes cone production, but horizontal cells as well, which is consistent with a role in RPCs.

2.4.2 Integrating Pou2f1/2 in the current view of cone genesis

There are currently two non-mutually exclusive pathways by which cone photoreceptors are thought to be generated. In one model, postmitotic photoreceptor precursors default to the cone fate, unless Nrl is induced, which in turn activates Nr2e3 to promote the rod fate (Mears et al., 2001; Oh et al., 2008). In another model, RPCs expressing Olig2 are pre-programmed to generate cones or horizontal cells at their last division (Emerson et al., 2013; Hafler et al., 2012). How do Pou2f1/2 fit into these models?

As Pou2f1 and Pou2f2 are co-expressed in RPCs, we posit that Pou2f1 induces Pou2f2 expression prior to cell cycle exit, which may lead to sufficient levels of Pou2f2 expression in postmitotic precursors to repress Nrl. Such transient and possibly weak expression might have

been difficult to detect by scRNA-seq (Clark et al., 2019). Clearly, however, Pou2f2 is also expressed in RPCs, as shown by the widespread immunostaining observed at E11.5 and as reported in scRNA-Seq data (Fig. 2.1D-F) (Clark et al., 2019). As mentioned above, whether Pou2f2 is functionally relevant in RPCs will need further investigation, but it may have a role to control Olig2 progenitor fate decisions. RNA-seq analysis of Onecut1/2 double knockout retina reveals a 2-fold increase in Pou2f2 mRNA levels at E14 (Sapkota et al., 2014), suggesting that Onecut1/2 might negatively regulate Pou2f2 expression. Similar observations were recently made in the developing spinal cord, where Onecut factors, although not required for the production of V2 interneurons, repress Pou2f2 to regulate the distribution of V2 interneurons (Harris et al., 2019). A possibility is that Pou2f2 and Onecut1/2 constitute two complementary branches of cone development. Pou2f1 might compete with Onecut1/2 for the activation or repression of Pou2f2, respectively, in Olig2^{+ve} RPCs. When Pou2f1 activity is dominant, Pou2f2 would be upregulated and progenitors would take on the horizontal fate via unknown targets of Pou2f2 and the cone fate via repression of Nrl in postmitotic photoreceptor precursors. In contrast, when Onecut1 activity is dominant, Pou2f2 would be repressed, leading cells into the Onecut1 pathway to produce cones or horizontal cells. This model could explain why inactivation of Pou2f2 (this study) or Onecut1/2 (Sapkota et al., 2014) only reduces cone production by about 25%. Consistent with this idea, out of the two CRMs of Thrb that are active in cones, Pou2f2 activates one of the elements and Onecut1 activates the other (Fig. S2.6D-F) (Emerson et al., 2013). Since Pou2f2 and Onecut1/2 could potentially regulate different CRMs of Thrb, it will be interesting to assess whether Pou2f2 is expressed in Olig2^{+ve} RPCs and inactivate both Onecut1/2 and Pou2f2 in the retina to see if this would lead to a more important decrease in cones and horizontal cells.

2.4.3 Pou2f1/2 as negative regulators of Nrl

A long-standing question in the field has been how exactly Nrl expression is repressed in some photoreceptor precursors. Positive regulators of Nrl such as Crx, Otx2 and RORβ have been identified (Montana et al., 2011), but negative regulators have remained elusive. Montana et al. hypothesized that a “repressor X” could down-regulate Nrl in photoreceptor precursors, to restrict expression to rod precursors. Although Onecut1 acts genetically upstream of Nrl and eventually leads to its downregulation, this effect is likely indirect (Emerson et al., 2013). While multiple studies have analysed the regulatory regions of Nrl to uncover a direct repressor (Kautzmann et

al., 2011; Montana et al., 2011; Zelinger et al., 2017), the identity of such repressors remained elusive. Our work now identifies Pou2f2 as one of the potential direct repressors of Nrl in the developing mammalian retina. We provide evidence that Pou2f2 functions by binding a POU binding motif located 55bp upstream of the transcription start site of Nrl.

2.4.4 Potential role for Pou2f1/2 as temporal identity factors outside the retina

The functional role of Pou2f1 and Pou2f2 has been extensively characterised in the immune system and embryonic stem cells, but the role of Pou2f1 and Pou2f2 in the developing CNS is poorly studied. However, Pou2f1 and Pou2f2 are highly expressed in different regions of the CNS (He et al., 1989; Luchina et al., 2003; Schonemann et al., 1998; Treacy and Rosenfeld, 1992). One study found that Pou2f1 is required for the development of radial glia in Xenopus hindbrain and is modulated by Notch signalling (Kiyota et al., 2008). Whether Pou2f1 regulates radial glia development in mammals remains to be investigated, but the results reported here support this possibility. On the other hand, Pou2f2 is expressed in the diencephalon, mesencephalon, rhombencephalon during embryogenesis as well as suprachiasmatic and medial mammillary nuclei in the adult hypothalamus (Treacy and Rosenfeld, 1992). Since the global Pou2f2 mutants die at birth, it will interesting to specifically delete Pou2f2 in these regions to assess a potential role in neurogenesis (Konig et al., 1995). Finally, since there is a high overlap of expression between Pou2f1 and Pou2f2 in the developing CNS (He et al., 1989; Treacy and Rosenfeld, 1992), it is possible that the same Pou2f1/Pou2f2 cascade operates in the specification of the neurons in other parts of the CNS.

2.4.5 Conclusions

Understanding how the cone photoreceptor cell fate is specified is critical to the development of cell replacement therapies for various retinal degenerative diseases. In this study, we add to the general knowledge of cone specification mechanisms by identifying Pou2f1 and Pou2f2 as previously unknown players in cone photoreceptor development. Our data also helps to elucidate how Nrl expression is negatively regulated during retinal development to ensure the correct balance of rod/cone production.

2.5 Figures and legends

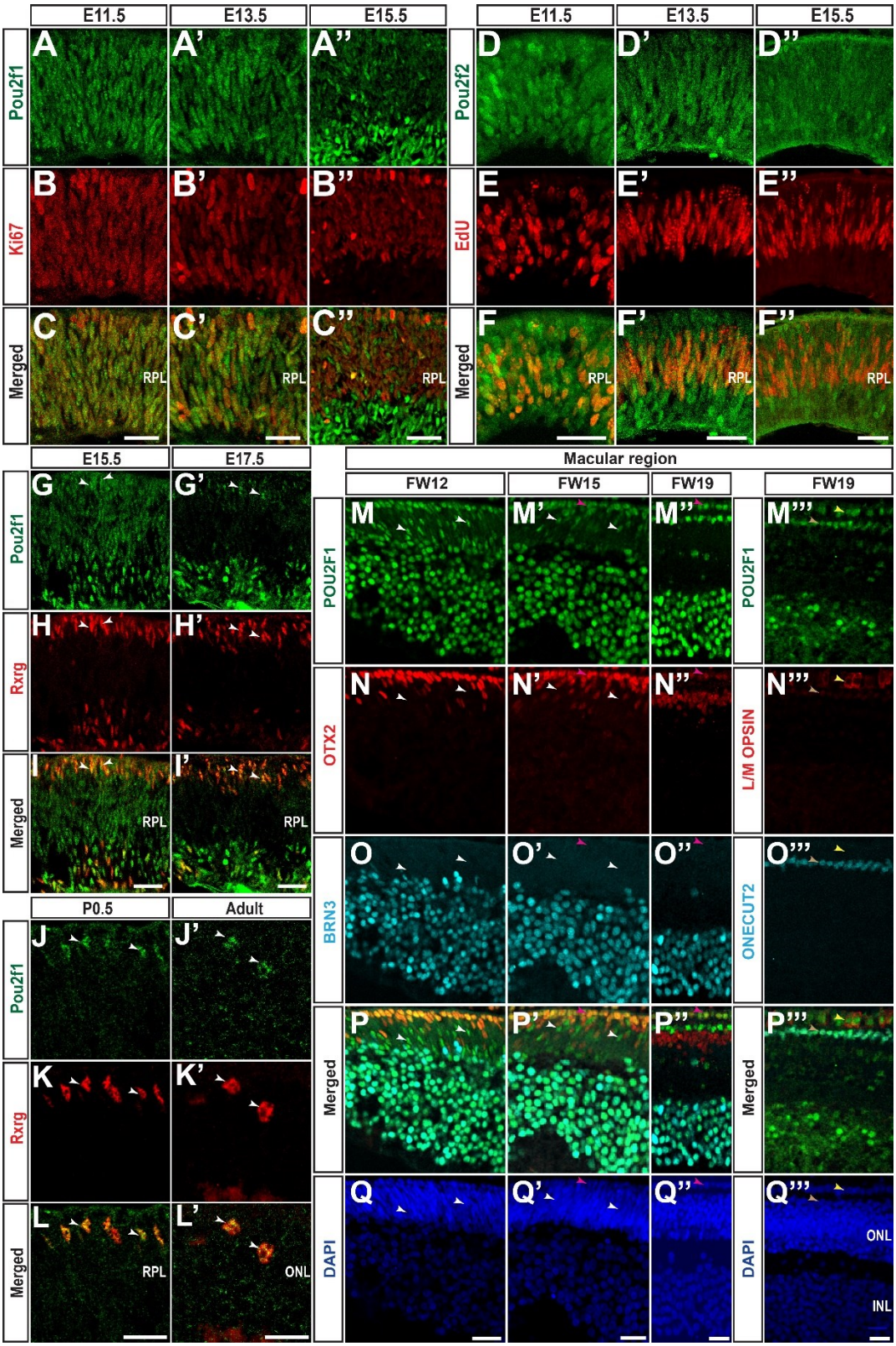

Figure 2.1. Pou2f1 and Pou2f2 expression in developing mouse and human retinas. (A-F'') Co-immunostaining for Pou2f1 or Pou2f2, the proliferation marker Ki67 or EdU (injected 1 hour before sacrifice) in the mouse retina at different stages, as indicated. (G-L') Co-immunostaining for Pou2f1 (green) and the cone marker Rxrg (red) at different stages of mouse retinogenesis. Arrows indicate cone photoreceptors expressing Pou2f1. (M-Q''') Co-immunostaining for POU2F1, OTX2, L/M OPSIN, BRN3, ONECUT2 and DAPI on human retinal sections at fetal week (FW) 12, 15, and 19. White arrows indicate OTX2-BRN3- cells expressing POU2F1, Magenta arrows indicate $OTX2^{+ve}BRN3^{-ve}$ cells expressing POU2F1. Yellow and brown arrows indicate L/M $OPSIN^{+ve}$ or $ONECUT2^{+ve}$ cells expressing POU2F1 respectively. RPL: Retinal progenitor layer. ONL: Outer nuclear layer. INL: Inner nuclear layer. Scale bars = 20µm (A-I"), 10µm (J-Q''').

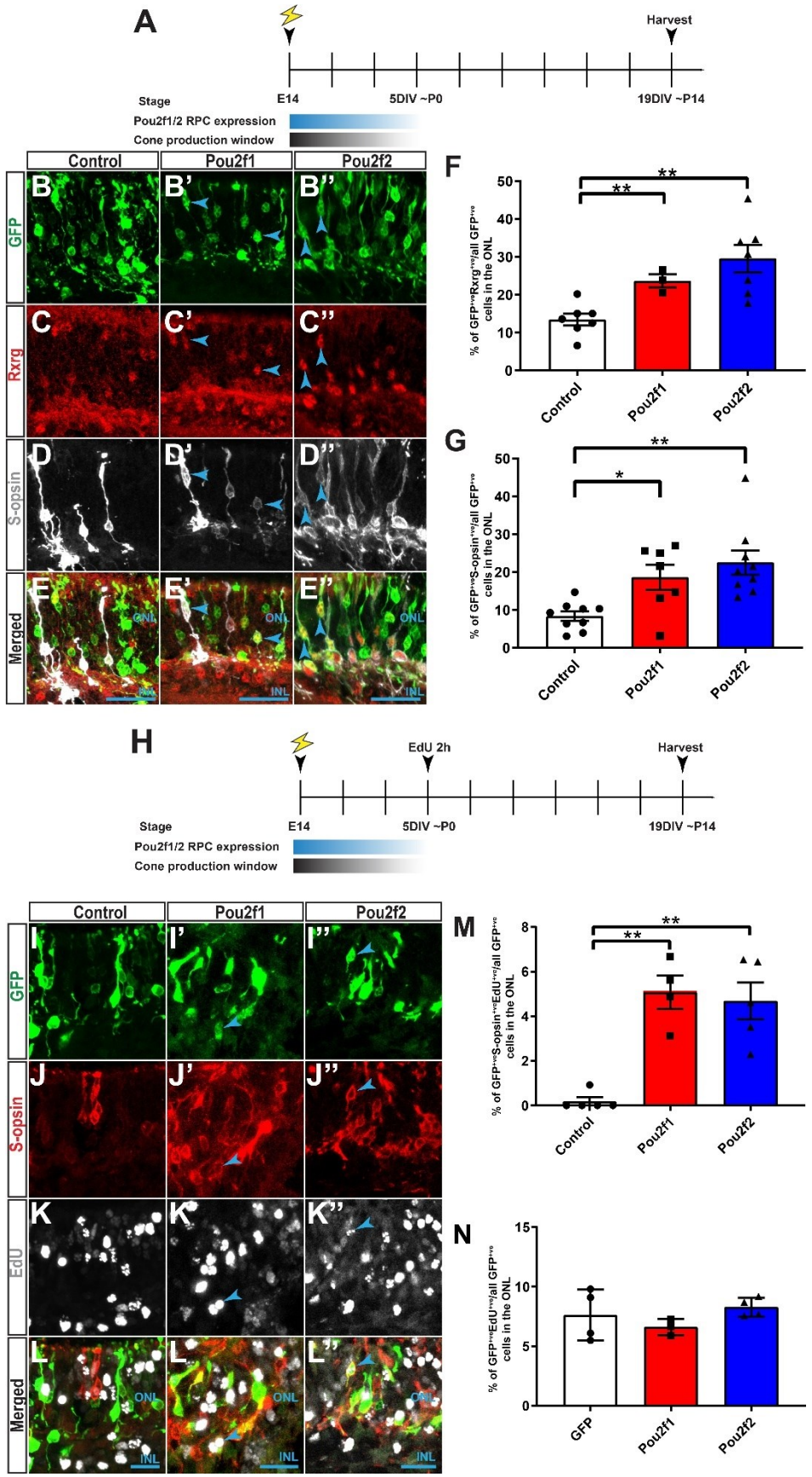
A
Harvest
Stage
E14
5DIV ~P0
19DIV ~P14
Pou2f1/2 RPC expression
Cone production window
Control
Pou2f1
Pou2f2
GFP
Rxrg
S-opsin
Merged
ONL
INL
F
G
H
EdU 2h
M
N
GFP

Figure 2.2. Continuous Pou2f1/2 expression prolongs the cone production window. (A) Schematic representation of the experimental paradigm for results shown in B-G. (B-E") Z-stack projection of ex-vivo electroporated cells with a GFP control vector (B), Pou2f1-IRES-GFP (B') or Pou2f2-IRES-GFP (B") stained for the cone photoreceptor markers Rxrg and S-opsin. Arrows point to GFP^{+ve} cells expressing both Rxrg and S-opsin. (F-G) Quantification of GFP^{+ve} cells expressing Rxrg (Control: n=7, Pou2f1: n=3, Pou2f2: n=7) (F) or S-opsin (Control: n=9, Pou2f1: n=7, Pou2f2: n=9) (G) 19 days after ex-vivo electroporations at E14. (H) Schematic representation of the experimental paradigm for results shown in I-M. (I-L") Z-stack projection of the ONL region of retinal explants electroporated with control GFP (n=4) (I), Pou2f1-IRES-GFP (n=3) (I') or Pou2f2-IRES-GFP (n=4) (I") and stained for EdU and S-opsin. Arrows point to GFP^{+ve}S-opsin^{+ve} cells. (M) Quantification of the number of $GFP^{+ve}EdU^{+ve}$ cells expressing S-opsin in each electroporated condition, as indicated. (N) Quantification of all $EdU^{+ve}GFP^{+ve}$ cells in explants analyzed in (M). *$p<0.05$, **$p<0.01$, ***$p<0.001$. Statistics: One-way ANOVA with Dunnett. Graphs show mean±s.e.m. ONL: Outer nuclear layer. Scale bars: 20µm (B-E'''), 10µm (I-L").

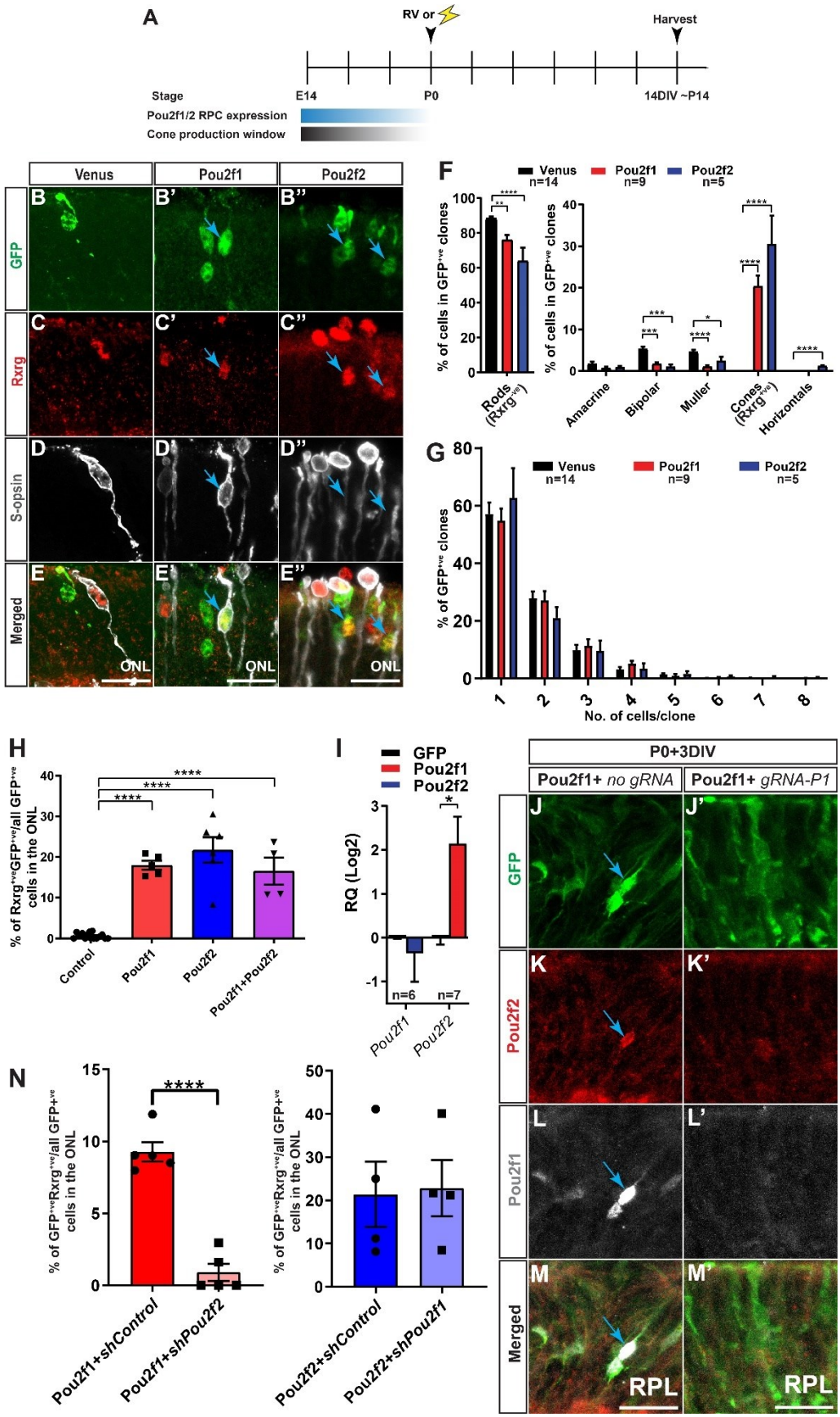
A
RV or
Harvest
Stage
E14
P0
14DIV ~P14
Pou2f1/2 RPC expression
Cone production window
Venus
Pou2f1
Pou2f2
GFP
Rxrg
S-opsin
Merged
ONL
F
Venus n=14
Pou2f1 n=9
Pou2f2 n=5
% of cells in GFP+ve clones
Rods (Rxrg+ve)
Amacrine
Bipolar
Muller
Cones (Rxrg+ve)
Horizontals
G
% of GFP+ve clones
No. of cells/clone
H
% of Rxrg+ve GFP+ve/all GFP+ve cells in the ONL
Control
Pou2f1
Pou2f2
Pou2f1+Pou2f2
I
GFP
Pou2f1
Pou2f2
RQ (Log2)
n=6
n=7
N
% of GFP+ve Rxrg+ve/all GFP+ve cells in the ONL
Pou2f1+shControl
Pou2f1+shPou2f2
Pou2f2+shControl
Pou2f2+shPou2f1
P0+3DIV
Pou2f1+ no gRNA
Pou2f1+ gRNA-P1
J
J'
K
K'
L
L'
M
M'
RPL

Figure 2.3. Pou2f1/2 are sufficient to induce cone production in mid/late-stage mouse retina. (A) Schematic representation of the experimental paradigm for results shown in B-G. (B-E") Z-stack projection of retrovirally infected cells with Venus control (B), Pou2f1-IRES-GFP (B'), and Pou2f2-IRES-GFP (B") stained for Rxrg and S-opsin as cone markers. Arrows point to $GFP^{+ve}Rxrg^{+ve}$ cells. (F-G) Retroviral clonal analysis of Control (1206 clones counted), Pou2f1 (639 clones counted), or Pou2f2 (376 clones counted) misexpression in mid-late stage retinas. n values indicated in the graph. (F) Cell type analysis of GFP^{+ve} cells found in the clones. Cones were counted using Rxrg as a marker, whereas the other cell types were quantified based on morphology and laminar positioning in the retina. (G) Average size distribution of the clones presented in (F). (H) Quantification of GFP^{+ve} cells expressing Rxrg in the ONL following *in vivo* electroporation of GFP (n=15), Pou2f1 (n=5), Pou2f2 (n=6), or Pou2f1+Pou2f2 (n=4). (I) RT-qPCR analysis of *Pou2f1* and *Pou2f2* expression from sorted GFP^{+ve} cells 9 hours after electroporation at P0 in retinal explants of either control GFP, Pou2f1-IRES-GFP or Pou2f2-IRES-GFP. n values indicated in the graph. (J-M') Retinal explant electroporated at P0 with Pou2f1-IRES-GFP with no *gRNA* (J) or *gRNA-Pou2f1* (J'), cultured for 3 DIV, and stained for Pou2f2 (K-K') or Pou2f1(L-L'). (N) Quantification of the number of $GFP^{+ve}Rxrg^{+ve}$ cells after Pou2f1 misexpression with either shControl-GFP (n=5) or shPou2f2-GFP (n=5) and vice versa (Pou2f2+shControl: n=4, Pou2f2+shPou2f1: n=4) in P0 retinal explants. *$p<0.05$, **$p<0.01$, ***$p<0.001$, ****$p<0.0001$. Statistics: (F, H) One-way ANOVA with Dunnett. (I) Mann-Whitney test. (G) Two-way ANOVA with Dunnett. (N) Two tailed unpaired t test. Graphs show mean±s.e.m. DIV: Days in-vitro. RQ: Relative quantitation. RPL: Retinal progenitor layer. ONL: Outer nuclear layer. Scale bars: 20µm (B-E'', J-M').

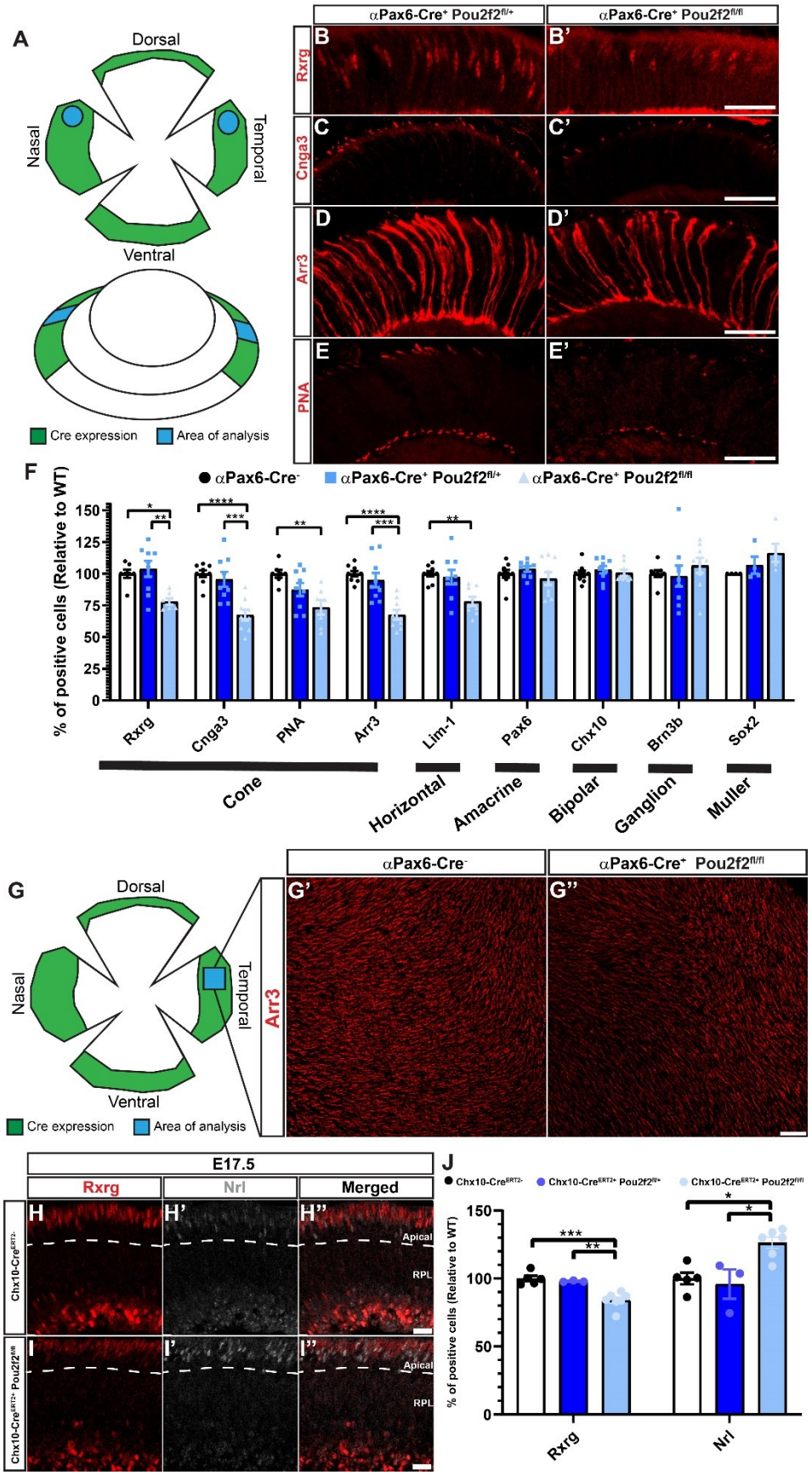
A
Dorsal
Nasal
Temporal
Ventral
Cre expression
Area of analysis
αPax6-Cre+ Pou2f2fl/+
αPax6-Cre+ Pou2f2fl/fl
Rxrg
Cnga3
Arr3
PNA
B
B'
C
C'
D
D'
E
E'
F
αPax6-Cre-
αPax6-Cre+ Pou2f2fl/+
αPax6-Cre+ Pou2f2fl/fl
% of positive cells (Relative to WT)
Rxrg
Cnga3
PNA
Arr3
Lim-1
Pax6
Chx10
Brn3b
Sox2
Cone
Horizontal
Amacrine
Bipolar
Ganglion
Muller
G
αPax6-Cre-
αPax6-Cre+ Pou2f2fl/fl
G'
G''
E17.5
Rxrg
Nrl
Merged
H
H'
H''
I
I'
I''
Apical
RPL
J
Chx10-CreERT2-
Chx10-CreERT2+ Pou2f2fl/+
Chx10-CreERT2+ Pou2f2fl/fl
% of positive cells (Relative to WT)
Rxrg
Nrl

Figure 2.4: Pou2f2 is required for cone development in the developing mouse retina. (A) Diagram showing area of analysis. (B-E') Immunostaining of Rxrg (B), Cnga3 (C), Arr3 (D), and PNA (E) in either αPax6-Cre^{+} Pou2f2$^{fl/+}$ (B-E) or αPax6-Cre^{+} Pou2f2$^{fl/fl}$ (B'-E') mouse retinas at P14. (F) Quantification of retinal cell types using various markers (αPax6-Cre^{+}: Cnga3, Arr3, Lim-1, Pax6, Chx10: n=9, Brn3b: n=8, Rxrg, PNA: n=7, Sox2: n=4; αPax6-Cre^{+} Pou2f2$^{fl/+}$: Cnga3, Arr3, Lim-1, Pax6, Chx10, Brn3b, Rxrg, PNA: n=9, Sox2: n=4; αPax6-Cre^{+} Pou2f2$^{fl/fl}$: Cnga3, Arr3, Lim-1, Pax6, Chx10, Brn3b: n=9, Rxrg, PNA: n=7, Sox2: n=5). (G-G") Flatmount area of analysis and flatmount image of P14 retinas of either αPax6-Cre^{-} (G') or αPax6-Cre^{+} Pou2f2$^{fl/fl}$ (G"). (H-I") Immunostaining of Rxrg (H-I) or Nrl (H'-I') in either Chx10-Cre^{ERT2-} (H-H') or Chx10-Cre^{ERT2+} Pou2f2$^{fl/fl}$ mouse retinas at E17.5. (J) Quantification of percentage of Rxrg^{+ve} (Chx10-Cre^{ERT2-}: n=5, Chx10-Cre^{ERT2+} Pou2f2$^{fl/+}$: n=3, Chx10-Cre^{ERT2+} Pou2f2$^{fl/fl}$: n=7) and Nrl^{+ve} (Chx10-Cre^{ERT2-}: n=5, Chx10-Cre^{ERT2+} Pou2f2$^{fl/+}$: n=3, Chx10-Cre^{ERT2+} Pou2f2$^{fl/fl}$: n=6) cells relative to the WT. *$p<0.05$, **$p<0.01$, ***$p<0.001$, ****$p<0.0001$. Statistics: (E, J) One-way ANOVA with Tukey (E). Graphs show mean±s.e.m. Scale bars: 20µm (B-E'), 100µm (G'-G''), 10µm (H-I").

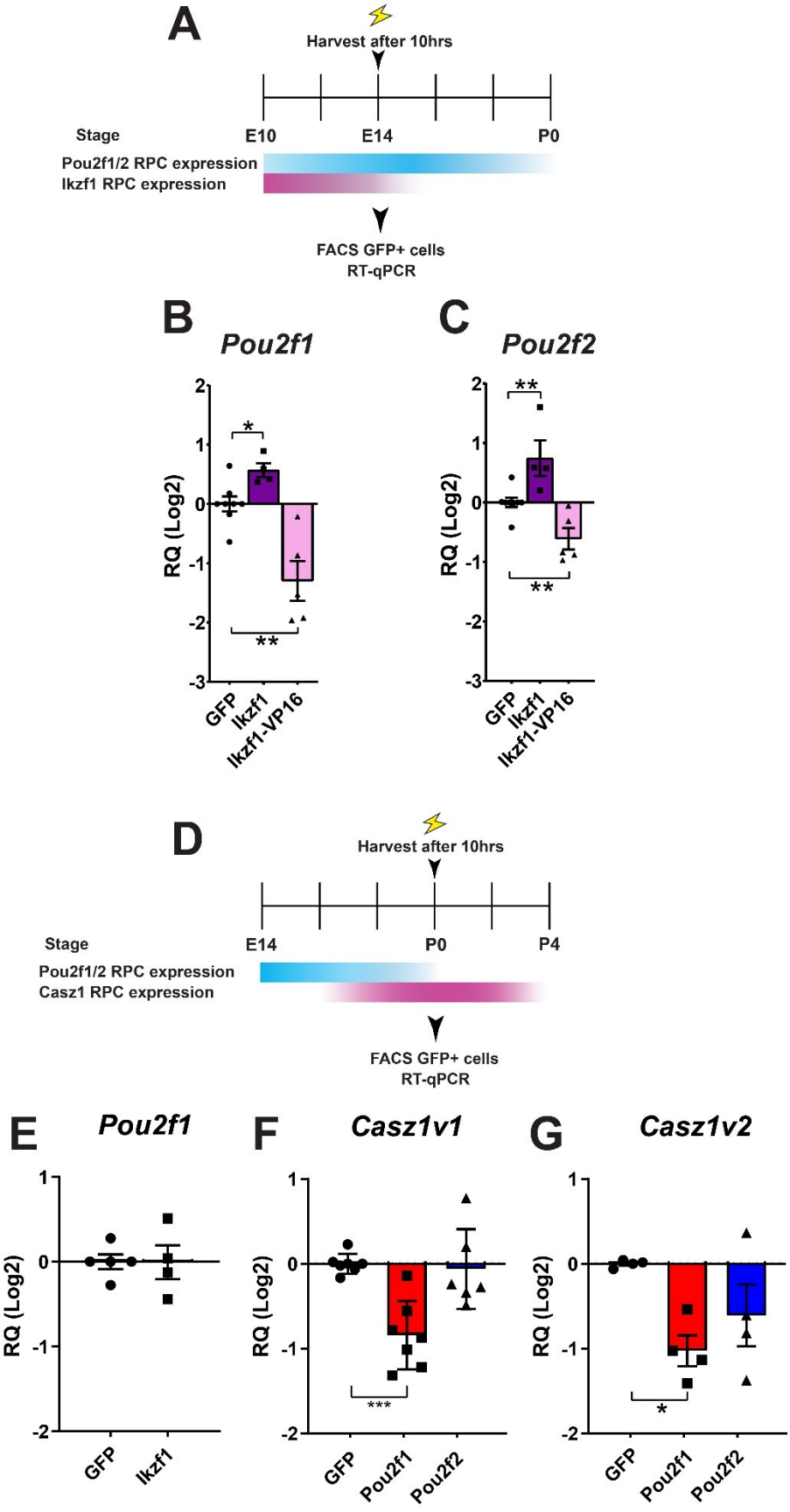
A
Harvest after 10hrs
Stage
E10
E14
P0
Pou2f1/2 RPC expression
Ikzf1 RPC expression
FACS GFP+ cells
RT-qPCR
B
Pou2f1
C
Pou2f2
RQ (Log2)
GFP
Ikzf1
Ikzf1-VP16
D
Harvest after 10hrs
Stage
E14
P0
P4
Pou2f1/2 RPC expression
Casz1 RPC expression
FACS GFP+ cells
RT-qPCR
E
Pou2f1
F
Casz1v1
G
Casz1v2
RQ (Log2)
GFP
Ikzf1
Pou2f1
Pou2f2

Figure 2.5. Ikzf1 induces Pou2f1 expression, and Pou2f1 represses Casz1. (A) Schematic representation of the experimental paradigm for results shown in B and C. (B-C) RT-qPCR analysis of *Pou2f1* and *Pou2f2* from GFP^{+ve} sorted cells after electroporation at E14 of either control GFP (*Pou2f1*: n=8, *Pou2f2*: n=8), Ikzf1-IRES-GFP (*Pou2f1*: n=4, *Pou2f2*: n=4), or Ikzf1:VP16-IRES-GFP (*Pou2f1*: n=5, *Pou2f2*: n=5). (D) Schematic representation of the experimental paradigm for results shown in E-G. (E) RT-qPCR analysis of *Pou2f1* from GFP^{+ve} sorted cells after electroporation at P0 of either control GFP (n=5) or Ikzf1-IRES-GFP (n=4). (F-G) RT-qPCR analysis of the two isoforms of Casz1 (Casz1v1 and Casz1v2) after electroporation of either control GFP (*Casz1v1*: n=7, Casz1v2: n=4), Pou2f1-IRES-GFP (*Casz1v1*: n=7, Casz1v2: n=4) or Pou2f2-IRES-GFP (*Casz1v1*: n=6, Casz1v2: n=4) at P0. *$p<0.05$, **$p<0.01$, ***$p<0.001$. Statistics: Mann-Whitney test. Graphs represent mean±s.e.m. RQ: Relative quantitation.

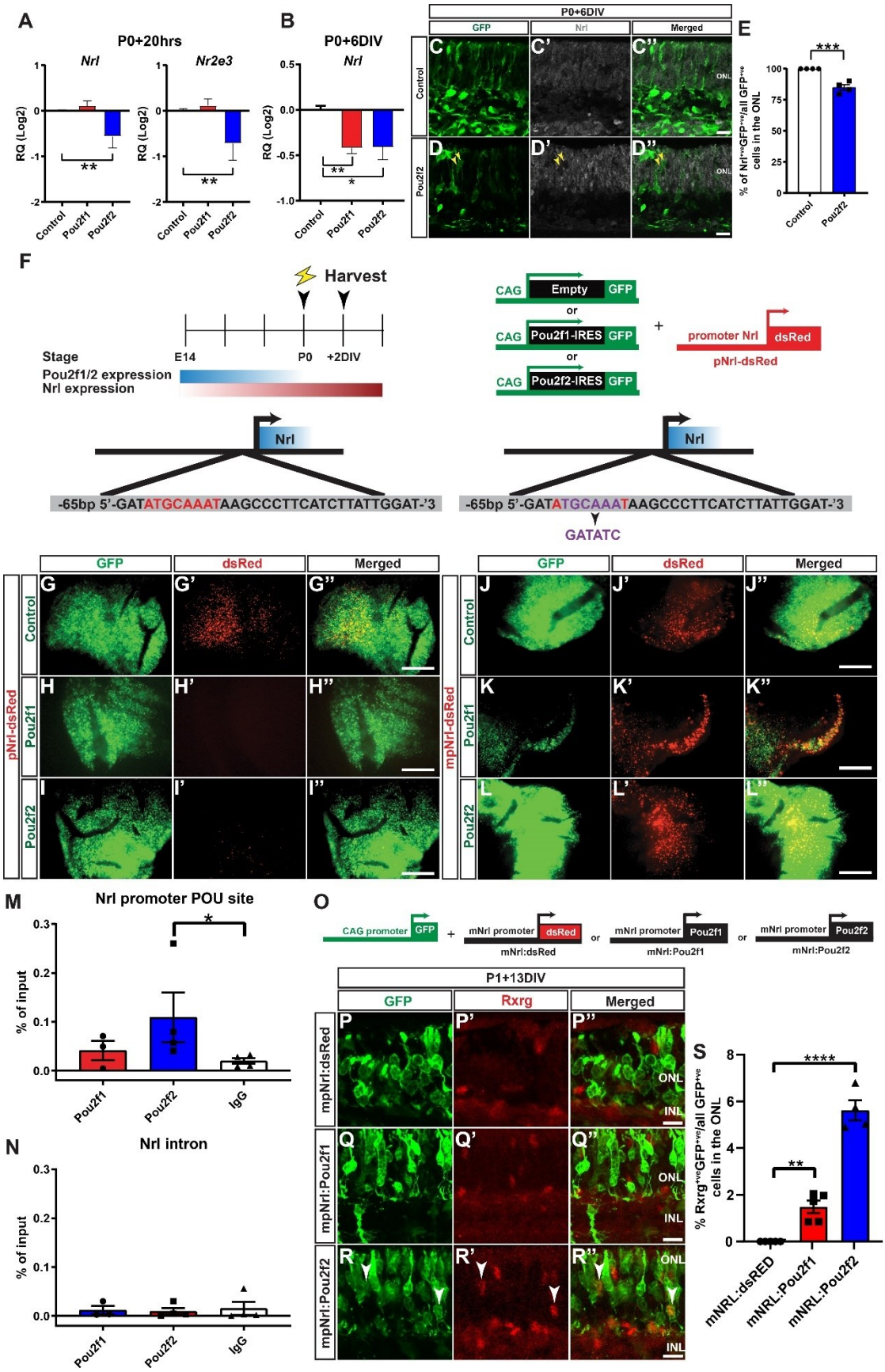
A
P0+20hrs
Nrl
Nr2e3
RQ (Log2)
Control
Pou2f1
Pou2f2
B
P0+6DIV
Nrl
P0+6DIV
GFP
Nrl
Merged
Control
Pou2f2
ONL
E
% of Nrl+veGFP+ve/all GFP+ve cells in the ONL
F
Harvest
Stage
E14
P0
+2DIV
Pou2f1/2 expression
Nrl expression
CAG
Empty
GFP
or
Pou2f1-IRES
Pou2f2-IRES
promoter Nrl
dsRed
pNrl-dsRed
Nrl
-65bp 5'-GATATGCAAATAAGCCCTTCATCTTATTGGAT-'3
GATATC
pNrl-dsRed
mpNrl-dsRed
M
Nrl promoter POU site
% of input
IgG
N
Nrl intron
O
CAG promoter
mNrl promoter
mNrl:dsRed
mNrl:Pou2f1
mNrl:Pou2f2
P1+13DIV
Rxrg
mpNrl:dsRed
mpNrl:Pou2f1
mpNrl:Pou2f2
INL
S
% Rxrg+veGFP+ve/all GFP+ve cells in the ONL
mNRL:dsRED
mNRL:Pou2f1
mNRL:Pou2f2

Figure 2.6. Pou2f2 binds to the promoter of Nrl and negatively regulates its expression. (A) RT-qPCR analysis of *Nrl* and *Nr2e3* mRNA expression following electroporation of control GFP (n=6), Pou2f1-IRES-GFP (n=6), or Pou2f2-IRES-GFP (n=6). (B) RT-qPCR analysis of *Nrl* from GFP^{+ve} sorted cells 6 days after electroporation at P0 of either control GFP, Pou2f1-IRES-GFP, or Pou2f2-IRES-GFP (n=5). (C-D'') Images of P0 retinal explants electroporated with either control GFP (C-C'') or Pou2f2-IRES-GFP (D-D'') and immunostained with Nrl. Yellow arrow show GFP^{+ve} cells lacking Nrl. (E) Quantification of $GFP^{+ve}Nrl^{+ve}$ cells and $GFP^{+ve}Rxrg^{+ve}Nrl^{-ve}$ cells in the ONL (n=4). (F) RT-qPCR of retinas from P14-P27 αPax6-Cre^{-} (n=4), αPax6-Cre^{+} $Pou2f2^{fl/+}$ (n=3), or αPax6-Cre^{+} $Pou2f2^{fl/fl}$ (n=4) animals using primers specific for *Nrl*. (G) Schematic representation of the experiments shown in H-M". Retinal explants were co-electroporated with vectors expressing GFP alone, Pou2f1-IRES-GFP or Pou2f2-IRES-GFP with either control pNrl:dsRed or POU-motif mutated pNrl:dsRed (mpNrl:dsRed). (H-M") Photomicrographs of retinal flatmounts showing reduced dsRed signal after expression of Pou2f1 (I') or Pou2f2 (J'). (K-M") Photomicrographs of retinal flatmounts showing loss of repression on the Nrl promoter activity when Pou2f1 (L') or Pou2f2 (M') are co-electroporated with the mpNrl-dsRed. (N-O) Chromatin immunoprecipitation (ChIP) of Pou2f1 (n=3), Pou2f2 (n=4) or control IgG (n=4) followed by quantitative PCR (qPCR) for the *Nrl* promoter region containing the POU-binding site, compared to an intronic control region. (P) Schematic representation of the experimental paradigm for results shown in (Q-S). (Q-S") Retinal explants electroporated at P1 with either mpNrl-dsRed (Q-Q"), mpNrl-Pou2f1 (R-R"), or mpNrl-Pou2f2 (S-S") along with CAG:GFP, cultured for 13 DIV, and immunostained for Rxrg to quantify cones in the ONL. (T) Quantification of GFP^{+ve} cells expressing Rxrg in the ONL (pNrl-dsRed: n=5, pNrl-Pou2f1: n=5, pNrl-Pou2f2: n=4). *$p<0.05$, **$p<0.01$, ****<p.0.0001. Statistics: (A, B, F, N, O) Mann-Whitney test, (E) Two tailed unpaired t test, (T) One-way ANOVA with Dunnett. Graphs represent mean±s.e.m. ONL: Outer nuclear layer, INL: Inner nuclear layer, RQ: Relative Quantitation. Scale bars: 10µm (C-D'', Q-S''), Scale bars: 50µm (H-M").

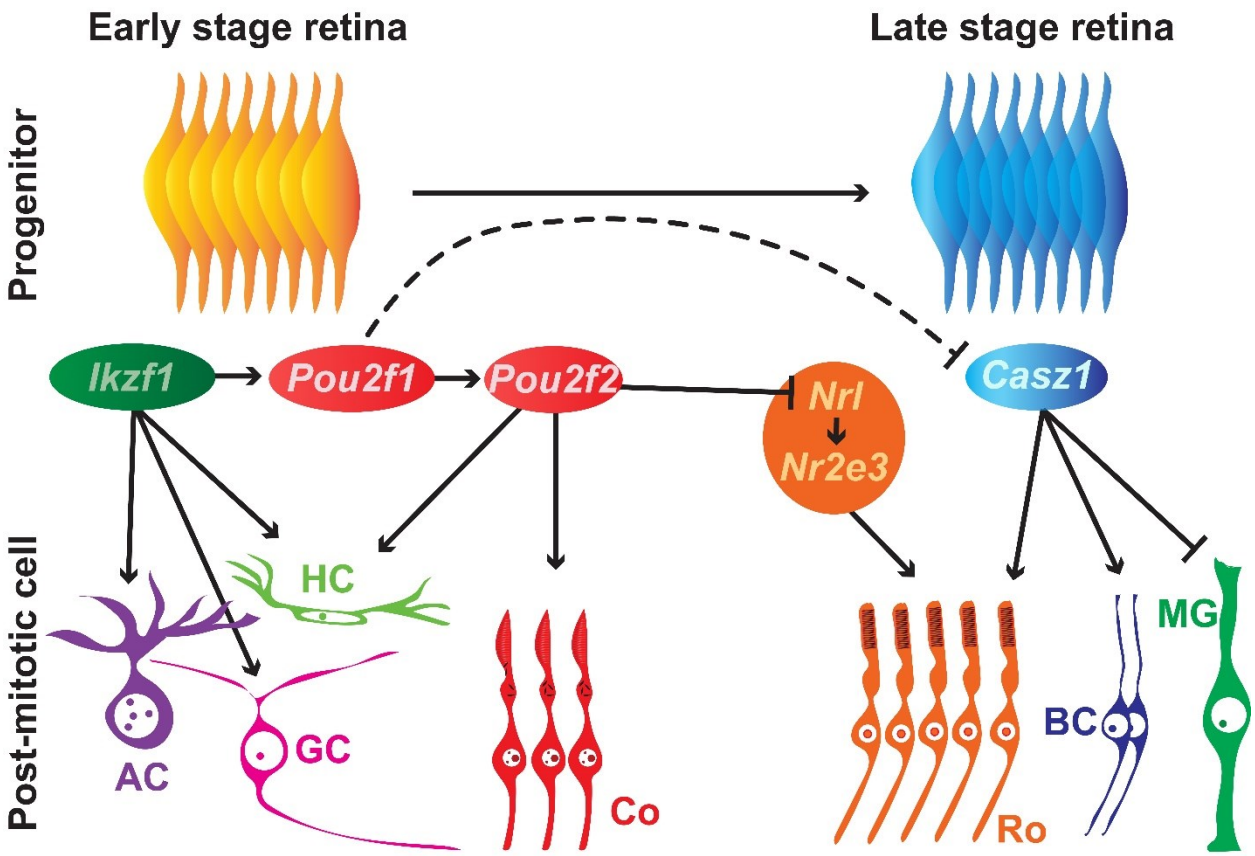

Figure 2.7. Model of temporal control of cone production during retinal development. In RPCs, Ikzf1 sets up the early temporal window for horizontal, amacrine and ganglion cell production, and upregulates Pou2f1 expression, which in turn sets up the temporal window for cone production by preventing expression of the mid/late temporal factor Casz1. Pou2f1 initiates expression of Pou2f2, which binds and represses Nrl to induce the cone fate.

2.6 Supplementary figures and legends

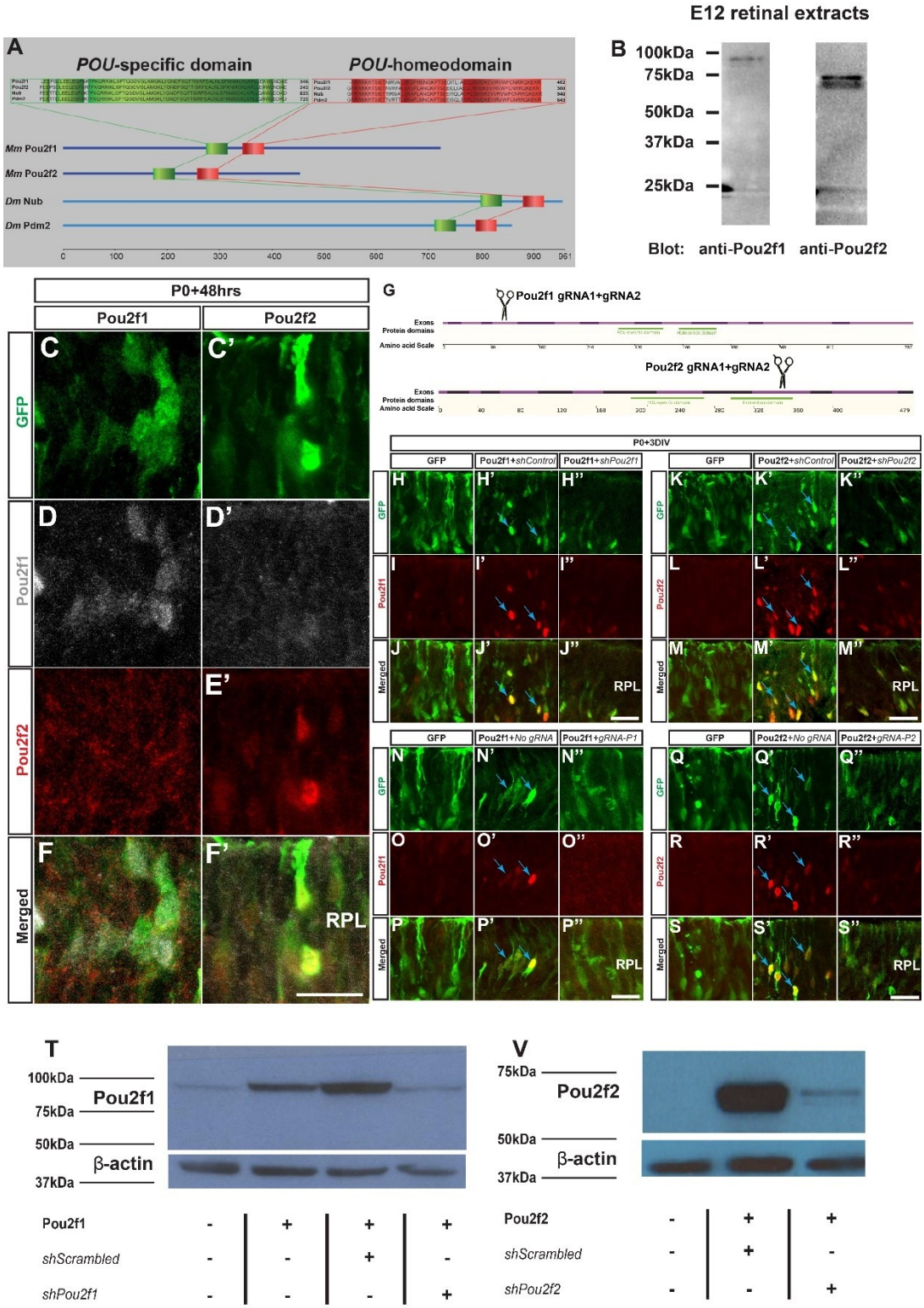

Figure S2.1: Validation of specific antibodies, shRNA knockdown and CRISPR/Cas9 knockout of Pou2f1/2. (A) Multiple sequence alignment of Drosophila Pdm proteins against mammalian Pou2f1 and Pou2f2 proteins using BLAST-p (Altschul et al., 1990). (B) Western blot of E12 retinal extracts blotted with anti-Pou2f1 and anti-Pou2f2 antibodies. (C-F') Retinal explants electroporated at P0 with Pou2f1-IRES-GFP or Pou2f2-IRES-GFP, cultured for 48hrs, and stained for Pou2f2 (D-D') or Pou2f1 (E-E'). (G) CRISPR-Cas9 gRNA design for Pou2f1 and Pou2f2. (H-M") Retinal explants electroporated at P0 with control GFP (H-M), Pou2f1/Pou2f2 with sh*Control* (H'-M'), or Pou2f1/Pou2f2 with sh*Pou2f1/*sh*Pou2f2* (H''-M''), cultured for 3 days ex-vivo, and stained for Pou2f1 (I-I") or Pou2f2 (L-L"). (N-S") Retinal explants electroporated at P0 with control GFP (N-S), Pou2f1/Pou2f2 with no *gRNA* (N'-S'), or Pou2f1/Pou2f2 with *gRNA-Pou2f1/gRNA-Pou2f2* (N"-S"), cultured for 3 days ex-vivo, and stained for Pou2f1 (O-O") or Pou2f2 (R-R"). (T) Western blot of HEK293T cell lysates either untransfected (-) or transfected (+) with Pou2f1-IRES-GFP alone, Pou2f1-IRES-GFP with shScrambled, or Pou2f1-IRES-GFP with shPou2f1, and blotted using anti-Pou2f1/2 and anti-β-actin antibodies. (V) Western blot of HEK293T cell lysates either un-transfected or transfected with Pou2f2-IRES-GFP with shScrambled or Pou2f2-IRES-GFP with shPou2f2 and blotted using anti-Pou2f1/2 and anti-β-actin antibodies. Scale bars: 10µm.

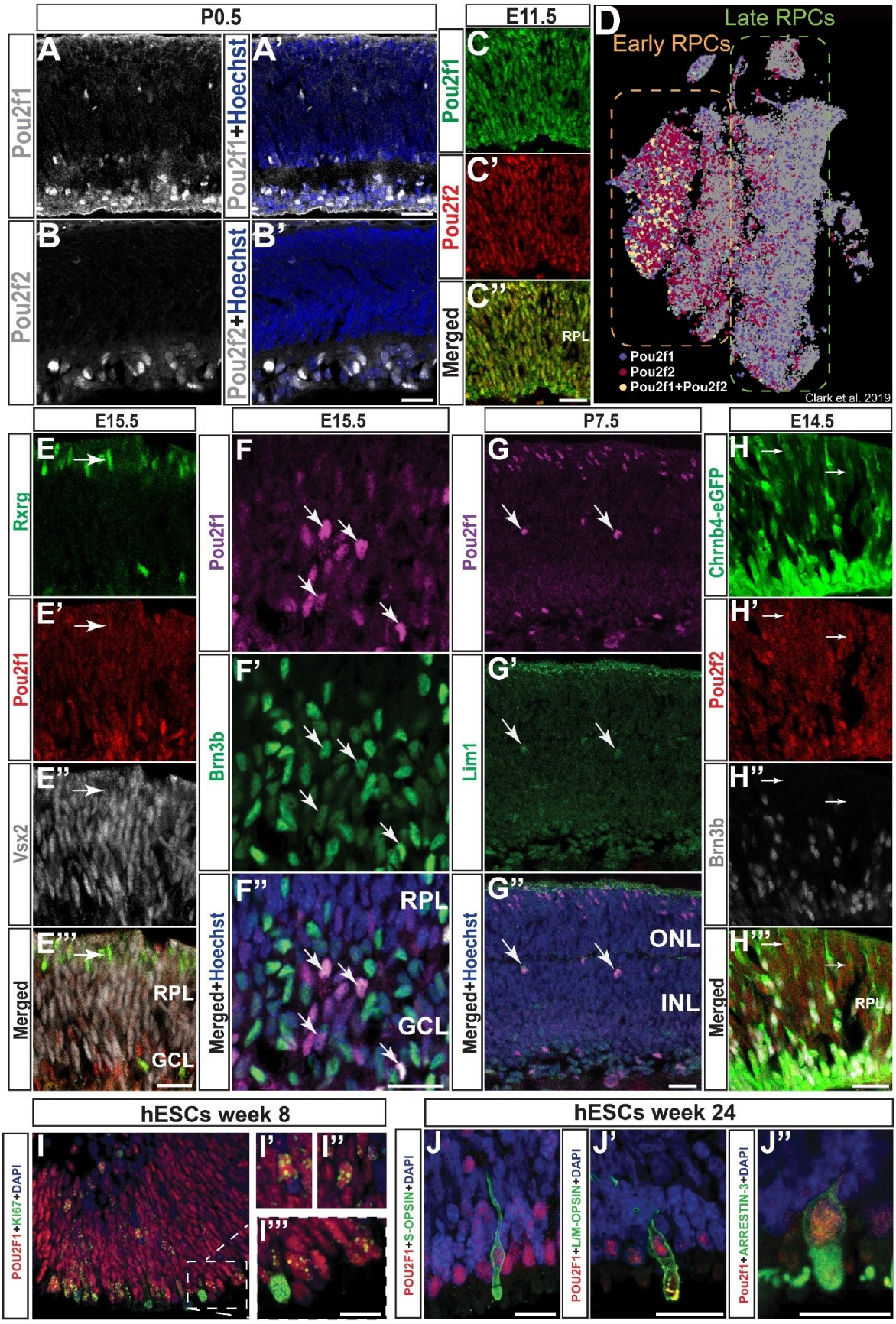
P0.5
E11.5
Pou2f1
Pou2f1+Hoechst
Pou2f2
Pou2f2+Hoechst
Merged
RPL
Late RPCs
Early RPCs
Pou2f1
Pou2f2
Pou2f1+Pou2f2
Clark et al. 2019
E15.5
E15.5
P7.5
E14.5
Rxrg
Vsx2
Brn3b
Lim1
Chrnb4-eGFP
Merged+Hoechst
GCL
ONL
INL
hESCs week 8
hESCs week 24
POU2F1+Ki67+DAPI
POU2F1+S-OPSIN+DAPI
POU2F1+L/M-OPSIN+DAPI
Pou2f1+ARRESTIN-3+DAPI

Figure S2.2: Spatiotemporal expression of Pou2f1 and Pou2f2. (A-B') Immunostaining for Pou2f1 (A) or Pou2f2 (B) in P0.5 mouse retina. (C-C") Immunostaining for Pou2f1 (C) and Pou2f2 (C') in E11.5 mouse retina. (D) scRNA-seq dataset of the developing mouse retina sorted for early and late RPCs. (E-E''') Co-immunostaining of Pou2f1, Rxrg, and Vsx2 in E15.5 mouse retina. Arrows point to Pou2f1^{+ve}Rxrg^{+ve}Chx10^{-ve} cells. (F-G") Immunostaining for Pou2f1, Brn3b or Lim-1 and Hoechst in the mouse retina at E15.5 (F-F") and P7.5 (G-G"). Arrows point to Pou2f1/2^{+ve}Brn3b^{+ve} (F-F") or Pou2f1/2^{+ve}Lim-1^{+ve} (G-G") cells. (H-H''') Co-immustaining of Pou2f2 (H') and Brn3b (H") in Chrnb4-eGFP mouse retina at E14.5. (I-J") Co-immunostaining for POU2F1 and KI67 (I-I''') or S-OPSIN, L/M OPSIN, and ARRESTIN-3 (J-J") in human embryonic stem cell-derived retinal organoids at week 8 or 24, respectively. RPL: Retinal progenitor layer. ONL: Outer nuclear layer. INL: Inner nuclear layer. Scale bars = 20µm (A-C", E-H'''), 10µm (M-N"), 5µm (J-J").

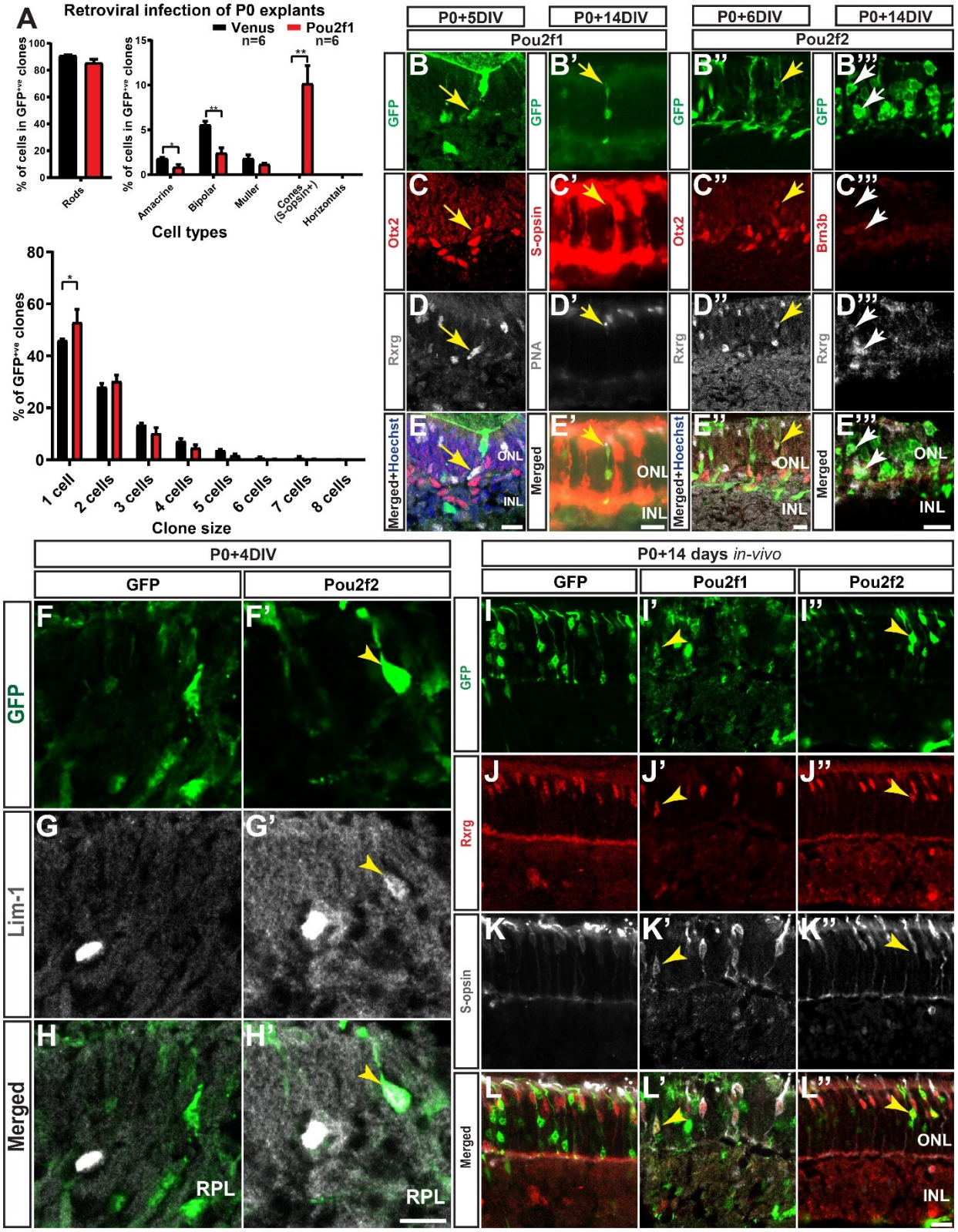
A
Retroviral infection of P0 explants
Venus n=6
Pou2f1 n=6
% of cells in GFP+ve clones
Rods
Amacrine
Bipolar
Muller
Cones (S-opsin+)
Horizontals
Cell types
% of GFP+ve clones
1 cell
2 cells
3 cells
4 cells
5 cells
6 cells
7 cells
8 cells
Clone size
P0+5DIV
P0+14DIV
Pou2f1
P0+6DIV
P0+14DIV
Pou2f2
GFP
Otx2
S-opsin
Brn3b
Rxrg
PNA
Merged+Hoechst
Merged
ONL
INL
P0+4DIV
GFP
Pou2f2
Lim-1
RPL
P0+14 days in-vivo
Pou2f1

Figure S2.3: Cone and horizontal cell markers expression after Pou2f1/2 expression in P0 retinal explants. (A) Retinal explants infected with Pou2f1-IRES-Venus at P0, cultured for 14 days, and stained for S-opsin (A') and PNA (A"). (B) Retroviral clonal analysis of Control Venus (1469 clones counted) or Pou2f1 (1055 clones counted) misexpression in mid-late stage retinas. Cell type analysis of GFP^{+ve} cells found in the clones. Cones were counted using S-opsin as a marker, whereas the other cell types were quantified based on morphology and laminar positioning in the retina. Average size distribution of the clones. n values indicated in the graph. (B-E"') Retinal explants either infected with Pou2f1-IRES-Venus (B-B'), cultured for 5 DIV (B) and 14 DIV (B') and stained for Otx2 (C), Rxrg (D), S-opsin (C') or PNA (D') or electroporated with Pou2f2-IRES-GFP (B''-B'''), cultured for 6 DIV (B") and 14 DIV (B''') and stained for Otx2 (C''), Brn3b (C'''), or Rxrg (D"-D'''). Yellow arrows point to co-labelled cells and white arrows point to $GFP^{+ve}Rxrg^{+ve}$ cells lacking Brn3b immunostaining. (F-H') Retinal explants electroporated at P0 with control GFP (F) or Pou2f2-IRES-GFP (F'), cultured for 4 days, and stained for the horizontal cell marker Lim1 (G-G'). Yellow arrowheads point to $GFP^{+ve}Lim\text{-}1^{+ve}$ cells. (I-L") Z-stack projection of electroporated cells with GFP control (I), Pou2f1-IRES-GFP (I'), and Pou2f2-IRES-GFP (I") stained for Rxrg and S-opsin as cone photoreceptor markers. Arrows point to $GFP^{+ve}Rxrg^{+ve}$ cells. ONL: Outer nuclear layer. RPL: Retinal progenitor layer. DIV: Days in-vitro. *$p<0.05$, **$p<0.01$. Statistics: (B) One-way ANOVA with Dunnett for cell types and Two-way ANOVA with Dunnett for clone sizes. Scale bars: 10 µm (B-E''', F-L").

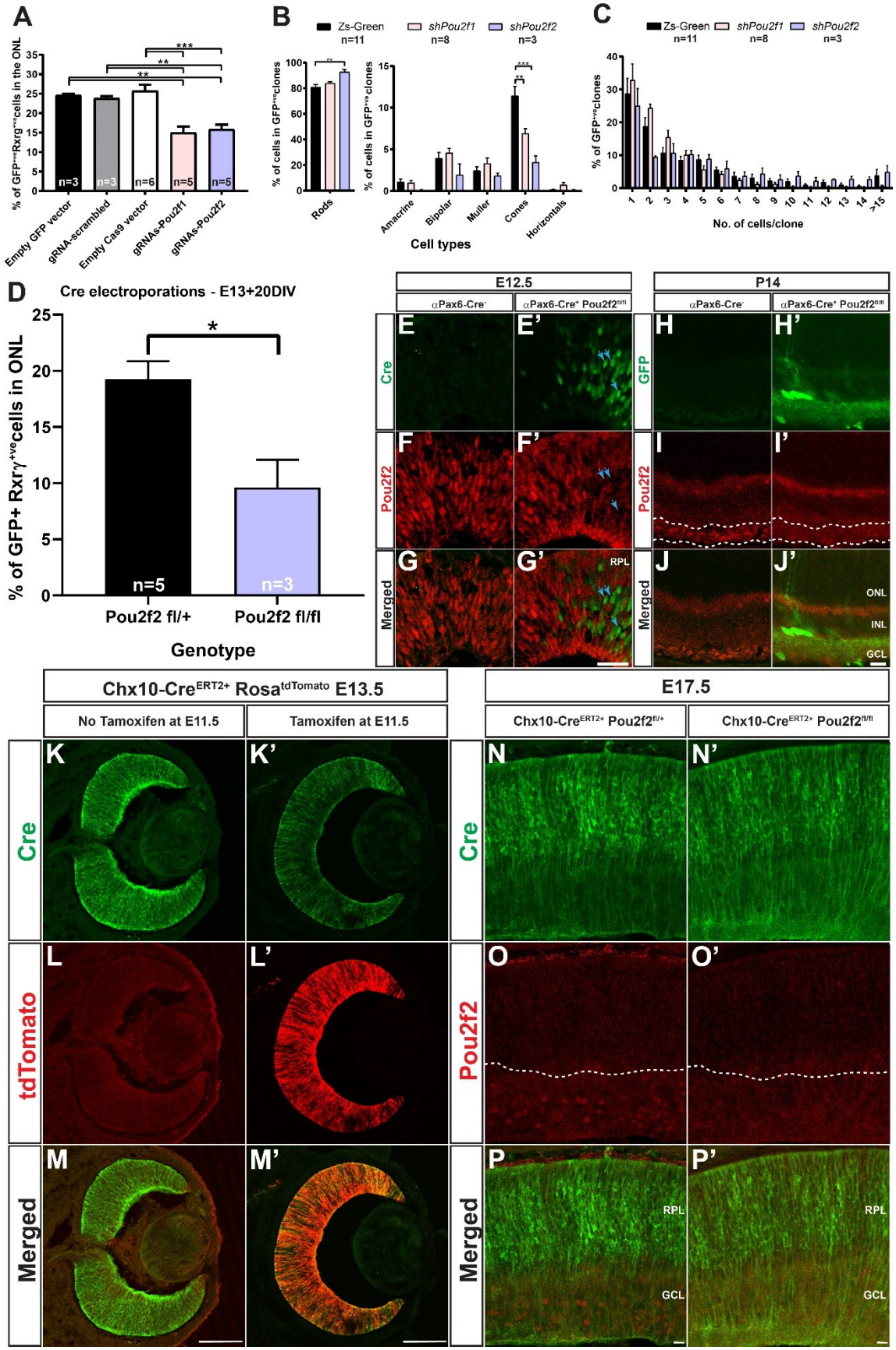
A
% of GFP+ve Rxrg+ve cells in the ONL
n=3
n=3
n=6
n=5
n=5
Empty GFP vector
gRNA-scrambled
Empty Cas9 vector
gRNAs-Pou2f1
gRNAs-Pou2f2
B
Zs-Green n=11
shPou2f1 n=8
shPou2f2 n=3
% of cells in GFP+ve clones
Rods
Amacrine
Bipolar
Muller
Cones
Horizontals
Cell types
C
Zs-Green n=11
shPou2f1 n=8
shPou2f2 n=3
% of GFP+ve clones
No. of cells/clone
D
Cre electroporations - E13+20DIV
% of GFP+ Rxrγ+ve cells in ONL
n=5
n=3
Pou2f2 fl/+
Pou2f2 fl/fl
Genotype
E12.5
αPax6-Cre-
αPax6-Cre+ Pou2f2fl/fl
P14
αPax6-Cre-
αPax6-Cre+ Pou2f2fl/fl
Cre
Pou2f2
Merged
GFP
RPL
ONL
INL
GCL
Chx10-CreERT2+ RosatdTomato E13.5
No Tamoxifen at E11.5
Tamoxifen at E11.5
E17.5
Chx10-CreERT2+ Pou2f2fl/+
Chx10-CreERT2+ Pou2f2fl/fl
Cre
tdTomato
Pou2f2
Merged
RPL
GCL

Figure S2.4: shRNA knockdown, CRISPR/Cas9 knockout and validation of Pou2f2 cKOs. (A) Quantification of the number of $GFP^{+ve}Rxrg^{+ve}$ cells in the outer nuclear layer (ONL) following electroporation of E14 retinal explants with either empty GFP, CRISPR-Cas9-scrambled gRNA with GFP, empty CRISPR-Cas9 with GFP, CRISPR-Cas9-gRNA Pou2f1 with GFP, or CRISPR-Cas9-gRNA Pou2f2 with GFP. (B) Clonal analysis 19 days after infection of E14 retinal explants with retroviral vectors expressing an empty shRNA vector (790 clones counted), or shRNAs for Pou2f1 (619 clones counted) or Pou2f2 (197 clones counted). Cones were counted using Rxrg as a marker whereas other cells were quantified based on morphology and laminar positioning in the retina. (C) Average size distribution of the clones presented in (B). (D) Quantification of the number of $GFP^{+ve}Rxrg^{+ve}$ cells in the ONL following electroporation of retinal explants from E13 $Pou2f2^{fl/+}$ or $Pou2f2^{fl/fl}$ mice with CAG:Cre and cultured for 20 DIV. (E-G') Co-immunostaining of Pou2f2 and Cre in E12.5 αPax6-Cre^{-} (E) or αPax6-Cre^{+} $Pou2f2^{fl/fl}$ (E') mouse retina. Blue arrows show Cre^{+ve} cells lacking Pou2f2 expression. (H-J') Immunostaining of Pou2f2 in P14 retina of αPax6-Cre cKO. Dashed boxes highlight the GCL. (K-M') Immunostaining of Cre and TdTomato in Chx10-Cre^{ERT2+} Rosa26.$tdT^{+/-}$ E13.5 retinas treated without tamoxifen (K) or with tamoxifen (K') at E11.5. (N-P') Co-immunostaining of Cre and Pou2f2 in E17.5 retina of Chx10-Cre cKO. Dashed line highlights the GCL. n values indicated in the graphs. *$p<0.05$, **$p<0.05$, ***$p<0.05$. Statistics: (A, D) Two tailed unpaired t test, (B) One-way ANOVA with Dunnett, (C) Two-way ANOVA with Dunnett. Graphs represent mean±s.e.m. RPL: Retinal progenitor layer, ONL: Outer nuclear layer, INL: Inner nuclear layer, GCL: Ganglion cell layer. Scale bar: 20µm (E-J'), 100µm (K-M'), 10µm (N-P').

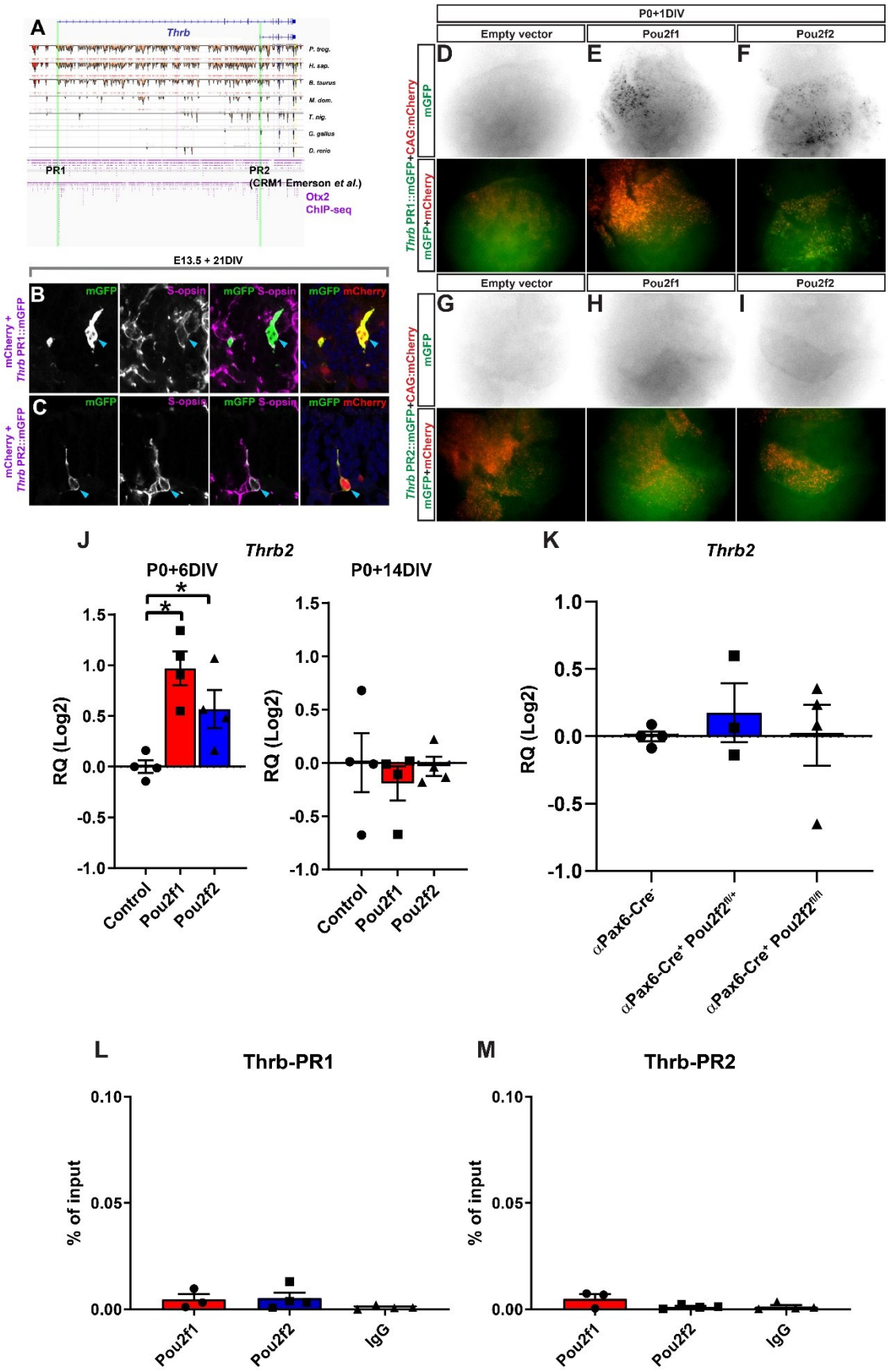
A
Thrb
P. trog.
H. sap.
B. taurus
M. dom.
T. nig.
G. gallus
D. rerio
PR1
PR2
(CRM1 Emerson et al.)
Otx2
ChIP-seq
E13.5 + 21DIV
B
C
mGFP
S-opsin
mGFP S-opsin
mGFP mCherry
mCherry + Thrb PR1::mGFP
mCherry + Thrb PR2::mGFP
P0+1DIV
Empty vector
Pou2f1
Pou2f2
D
E
F
G
H
I
Thrb PR1::mGFP+CAG:mCherry
Thrb PR2::mGFP+CAG:mCherry
mGFP
mGFP+mCherry
J
Thrb2
P0+6DIV
P0+14DIV
RQ (Log2)
Control
Pou2f1
Pou2f2
K
Thrb2
αPax6-Cre-
αPax6-Cre+ Pou2f2fl/+
αPax6-Cre+ Pou2f2fl/fl
L
Thrb-PR1
% of input
IgG
M
Thrb-PR2

Figure S2.5: Pou2f1 and Pou2f2 indirectly activate a cis regulatory module of *thrb* active in cones. (A) Sequence alignment of *thrb* gene for different species showing conservation of the cis-regulatory modules (CRM) PR1 and PR2. (B-C) E13 retinal explants co-transfected with *thrbPR1:GFP* (B) or *thrbPR2:GFP* (C) and mCherry, cultured for 21 days, and stained for the cone marker S-opsin. Green arrows point to $GFP^{+ve}mCherry^{+ve}S\text{-}opsin^{+ve}$ cells. (D-I) Photomicrographs of retinal flatmounts electroporated with either control (D, G), Pou2f1 (E, H), or Pou2f2 (F, I) along with either *thrbPR1:GFP* (D-F) or *thrbPR2:GFP* (G-I) and mCherry as a electroporation control at P0 and cultured for one day. (J) RT-qPCR analysis of *Thrb2* from GFP^{+ve} sorted cells 6 days or 14 days after electroporation at P0 of either control GFP (n=4), Pou2f1-IRES-GFP (n=4), or Pou2f2-IRES-GFP (n=4). (K) RT-qPCR analysis *Thrb2* in retinas from P14-P27 αPax6-Cre^{-} (n=4), αPax6-Cre^{+} $Pou2f2^{fl/+}$ (n=3), or αPax6-Cre^{+} $Pou2f2^{fl/fl}$ (n=4) animals. (L-M) Chromatin immunoprecipitation (ChIP) of control IgG (n=4), Pou2f1 (n=3), or Pou2f2 (n=4) followed by quantitative PCR (qPCR) for the *Thrb* promoter region 1 and 2. Statistics: Mann-Whitney test. Graphs represent mean±s.e.m. *$p<0.05$. ONL: Outer nuclear layer. DIV: Days in-vitro. Scale bars: 5µm (B-C), 50µm (D-I).

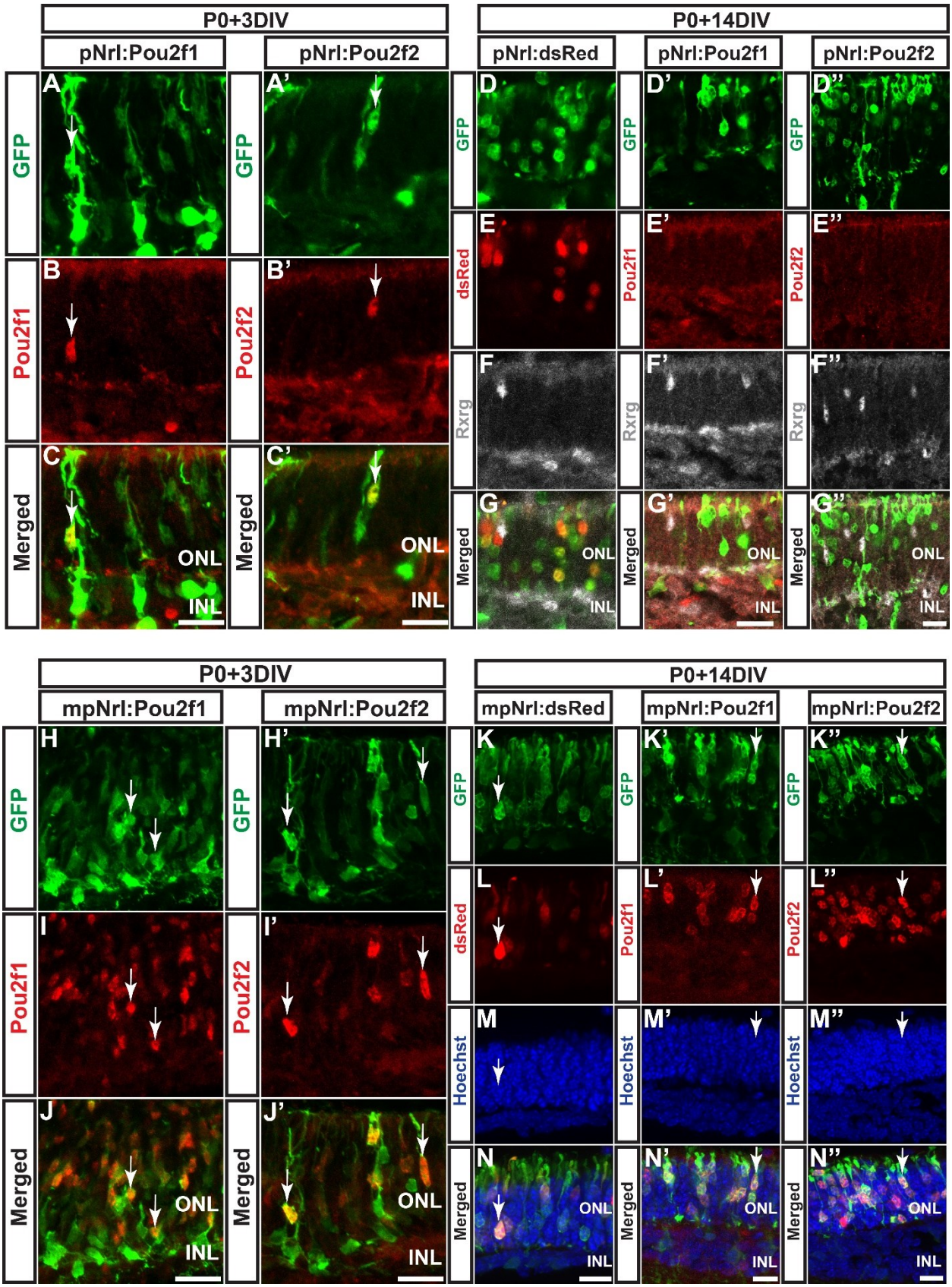
P0+3DIV
pNrl:Pou2f1
pNrl:Pou2f2
P0+14DIV
pNrl:dsRed
pNrl:Pou2f1
pNrl:Pou2f2
GFP
Pou2f1
Pou2f2
dsRed
Rxrg
Merged
ONL
INL
P0+3DIV
mpNrl:Pou2f1
mpNrl:Pou2f2
P0+14DIV
mpNrl:dsRed
mpNrl:Pou2f1
mpNrl:Pou2f2
Hoechst

Figure S2.6: Validation of wildtype and mutated pNrl-Pou2f1/2 vectors. (A-N”) Retinal explants electroporated at P0 with either pNrl-Pou2f1/2 (A-G”) or pmNrl-Pou2f1/2 (H-N”) along with CAG:GFP, cultured for 3DIV (A-C’, H-J’) or 14DIV (D-G”, K-N”), and stained for Pou2f1 (B, E’, I, L’) or Pou2f2 (B’, E”, I’, L”), Rxrg (F-F”) or Hoechst (M-M”). ONL: Outer nuclear layer. INL: Inner nuclear layer. DIV: Days in-vitro. Scale bars: 10 µm (A-N”).

2.7 Supplementary tables

Table S2.1: Manuscript 1 - Sequences of primers and oligos.

mRNA primers				
No.		pF (5'>3')	pR (5'>3')	References
1	Pou2f1	AACACGACACAGACCACCTC	TAGCAGCAAGACTGGCGTT	This paper
2	Pou2f2	CACCACCAACAGCACAAACC	GGGGTTCAGGCCCGACAAG	This paper
3	Gapdh	TGCAGTGGCAAAGTGGAGAT	ACTGTGCCGTTGAATTTGCC	Ouimette et al. 2010.
4	Casz1v1	CTTCGGGAACTGCAAGTACG	GTTGATGTGGTCCAAGCAGTG	This paper
5	Casz1v2	TCGCAGAGTTACACTGGCTG	GGATCCCAACGGATCACTGG	This paper
6	Nr2e3	AAGCTCCTGTGTGACATGTTCAA	AAGCTCCTGTGTGACATGTTCAA	This paper
7	Nrl	CGAGCAGTGCACATCTCAGTTC	AACTGGAGGGCTGGGTTACC	This paper
ChIP primers				
1	Nrl-OCT	TCTTTCACTGGCTTCTGAGTCC	CTGAGATCATCTGTGGTCCTCG	This paper
2	Nrl-intron	CGGTGGTGTACCGAGAGACT	GCCCAACTCCTACACTGACTC	This paper
3	Thrb-PR1	GACGCGGCGGGATTAACTTT	CCTGCCAAGTTACCAGAGCG	This paper
4	Thrb-PR2	GTTGTCAACCATAAGGGCAGTA	AAAGGTGCCTATTATGCTGGGG	This paper
gRNA sequences				
1	Scrambled	GCACTACCAGAGCTAACTCA		Ruan et al. 2017.
2	Pou2f1 gRNA A	GCTGACTGCACTGAAGGCGGC		This paper
3	Pou2f1 gRNA B	GCCGCCTTCAGTGCAGTCAGC		This paper
4	Pou2f2 gRNA A	GCCGGTTGCAGAACCAGACG		This paper
5	Pou2f2 gRNA B	GACGCATCAACCCTTGCAGTG		This paper

shRNA oligos				
1	Negative control shRNA	GATCCGGTGAAATTGAGGTCACGCCTTCAAGAGAGGCGTGACCTCAATTTCACCTTTTTTAGATCT	AGATCTAAAAAAGGTGAAATTGAGGTCACGCCTCTCTTGAAGGCGTGACCTCAATTTCACCGGATC	Chan et al. 2006.
2	Pou2f1	CCAGCACAGTTTATCATCTTTCAAGAGAAGATGATAAACTGTGCTGGTTTTTTAAGCTTGAATT	AATTCAAGCTTAAAAAACCAGCACAGTTTATCATCTTCTCTTGAAAGATGATAAACTGTGCTGG	This paper
3	Pou2f2	gatccGCGCCAAATCTATTCCAGCTTTCAAGAGAAGCTGGAATAGATTTGGCGTTTTTTAAGCTTg	aattcAAGCTTAAAAAACGCCAAATCTATTCCAGCTTCTCTTGAAAGCTGGAATAGATTTGGCGCg	This paper
Thrb promoter sequences				
1	PR1	CTGGGTCATCTGGAACAGCACAC mm9 genomic coordinates : chr14:18492293-18492315	CGCCCACCCTGCCAAGTTACC mm9 genomic coordinates : chr14:18493538-18493558	This paper
2	PR2	GGAACAGATCAGAACTCAGGACTC mm9 genomic coordinates : chr14:18813644-18813667	GCAGAGAAGCCAGTAACACTCAC mm9 genomic coordinates : chr14:18814966-18814988	This paper
Infusion HD sequences				
1	mNRL-dsRED	GATGATATCAAGCCCTTCATCTTATTGG	TCATTGGCCTGGGGCGCTTGATATCATC	This paper
2	Nrl-Pou2f1	CCCGGGATCCACCGGATGCTGGACTGCAGT	CTGAGGAGTGCGGCCTTACTGTGCCTTGGA	This paper
3	Nrl-Pou2f2	CCCGGGATCCACCGGatggttcattccagc	CTGAGGAGTGCGGCCtcaaggctggtaagg	This paper

Table S2.2: Manuscript 1 - Materials

REAGENT or	SOURCE	IDENTIFIER	APPLICATION
Primary antibodies			
Arrestin-3	Novus	NBP1-37003	IF 1:500
Arrestin-3	Millipore Sigma	AB15282	IF 1:500
Brn3b	Santa Cruz	SC-6026	IF 1:500
β-actin	Sigma-Aldrich	A5441	WB 1:2000
Cnga3	Alomone Labs	APC-060	IF 1:500
Vsx2/Chx10	Exalpha	X1180P	IF 1:500
Cre	Synaptic Systems	257 004	IF 1:2000
GFP	Abcam	ab13970	IF 1:2000
Mouse control IgG Isotope	Fischer Scientific	31903	ChIP 5ug
Ki-67	Fischer Scientific	9106S 901H	IF 1:100
Ki-67	BD Biosciences	550609	IF 1:100
Lim1/2	DSHB	4F2	IF 1:50
Nrl	R&D systems	AF2945	IF 1:200
Onecut2	R&D systems	AF6294	IF 1:200
Otx2	R&D systems	AF1979	IF 1:500
OTX2	Abcam	AB114138	IF 1:500
PNA-647	Molecular Probes	L-32460	IF 1:1000
Pax6	Milipore Sigma	AB2237	IF 1:100
Pou2f1	Sigma-Aldrich	clone 1E12	IF 1:100 WB 1:1000
Pou2f1	Santa Cruz	12F11 X	ChIP 5ug
Pou2f2	Santa Cruz	SC-233 (Discontinued)	IF 1:500 WB 1:1000
Pou2f2	Santa Cruz	F5 X	ChIP 5ug
Rxrg	Abcam	ab15518	IF 1:100
S-opsin	Santa Cruz	N-20	IF 1:1000
S-opsin	Millipore/Merck	AB5407	IF 1:1000
L/M OPSIN	Milipore/Merck	AB5405	IF 1:500
Secondary antibodies			
AF-488 Donkey anti-Chicken	Jackson ImmunoResearch	AB_2340375	IF 1:1000
AF-488 Donkey anti-Mouse	Jackson ImmunoResearch	2.7.1.1 **AB_2340846**	IF 1:1000
AF-488 Donkey anti-Guinea Pig	Jackson ImmunoResearch	2.7.1.2 **AB_2340472**	IF 1:1000
AF-555 Donkey anti-Rabbit	Jackson ImmunoResearch	2.7.1.3 **AB_2313584**	IF 1:1000
AF-647 Donkey anti-Goat	Jackson ImmunoResearch	2.7.1.4 **AB_2340436**	IF 1:1000

AF-647 Donkey anti-Mouse	Jackson ImmunoResearch	2.7.1.5 **AB_2340863**	IF 1:1000
AF-647 Donkey anti-Sheep	Jackson ImmunoResearch	2.7.1.6 **AB_2340751**	IF 1:1000
Goat anti-Mouse HRP	Jackson ImmunoResearch	2.7.1.7 **AB_10015289**	WB 1:10000
Goat anti-Rabbit HRP	Jackson ImmunoResearch	2.7.1.8 **AB_2307391**	WB 1:10000
Bacterial and Virus Strains			
Subcloning Efficiency™ DH5α™ Competent Cells	Fischer Scientific	18265017	
Biological Samples			
Chrnb4-eGFP mouse retinas	(Siegert et al., 2009)	N/A	
Chemicals, Peptides, and Recombinant Proteins			
FGF	Fisher Scientific	E6	
Taurine	Sigma Aldrich	T4871	
GSK-3 inhibitor	Tocris Bioscience	CHIR99021	
MEK inhibitor	Tebu-bio	PD032590101	
Retinoic Acid	Fisher Scientific	R2625	
Papain	Worthington	LS003124	
Critical Commercial Assays			
RNeasy Microkit	Qiagen	74004	
Superscript VILO Master Mix	Fisher Scientific	11755050	
SYBR Green Master mix	Fisher Scientific	A25742	
Dynabeads Protein G	Fisher Scientific	10003D	
In-Fusion HD Cloning plus	Takara	638920	
Click-iT™ EdU Alexa Fluor™ 647	Fisher Scientific	C10340	
Experimental Models: Cell Lines			
Phoenix-AMPHO	ATCC	CRL-3213	
Experimental Models: Organisms/Strains			
CD1	Charles Rivers	Cat#022	
Pou2f2$^{fl/fl}$	Jackson	029132	
α-Pax6 promoter::Cre	(Marquardt et al., 2001)	N/A	

Chx10 promoter ::Cre^{ERT2}	RIKEN – Depositor : Takahashi Furukawa (Osaka Bioscience institute)	RBRC06574
Oligonucleotides		
For qPCR primers, see Supplementary Table 1	This paper	N/A
For shRNA sequences, see Supplementary Table 1	This paper	N/A
For gRNA sequences, see Supplementary Table 1	This paper	N/A
For ChIP primers, see Supplementary Table 1	This paper	N/A
For Infusion HD sequences, see Supplementary Table 1	This paper	N/A
Recombinant DNA		
cDNA Pou2f1	DNASU	FLH265709.01X
cDNA Pou2f2	The I.M.A.G.E. Consortium (Lennon et al., 1996)	IMAGE:40046289
pCAG-mGFP	Addgene (Matsuda and Cepko, 2007)	14757
pCAG-Cre	Addgene (Matsuda and Cepko, 2007)	13775
pCAG-Otx2	(Mattar et al., 2008)	N/A
pCLE-venus	Addgene (Gaiano et al., 2000)	17703
pSIREN-RetroQ-ZsGreen	Clontech	632455
pX330-U6-Chimeric_BB-CBh-hSpCas9	Addgene (Cong et al., 2013)	42230
pCIG2-IRES-GFP	(Hand et al., 2005)	N/A
pNrl-dsRed	Addgene (Matsuda and Cepko, 2007)	13764
Software		
Prism 8	Graphpad	https://www.graphpad.com/scientific-software/prism/

Volocity software 6	Improvision	http://www.perkinelmer.com/lab-solutions/resources/docs/BRO_VolocityBrochure_PerkinElmer.pdf;
ZEN software	Zeiss Microscope	https://www.zeiss.com/microscopy/int/products/microscope-software/zen.html
Adobe Illustrator CC 2019	Adobe	http://www.adobe.com/products/illustrator.html
Adobe Photoshop CC 2019	Adobe	https://www.adobe.com/products/photoshop.html
Adobe Acrobat Pro DC 2019	Adobe	https://acrobat.adobe.com/us/en/acrobat.html
Quant-Studio Real Time PCR software	Fisher Scientific	https://www.thermofisher.com/ca/en/home/life-science/pcr/real-time-pcr/real-time-pcr-instruments/quantstudio-3-5-real-time-pcr-system.html
Office 365	Microsoft	https://www.office.com/
Bioturing Browser	Bioturing	https://blog.bioturing.com/2019/06/18/bioturing-browser-making-published-single-cell-data-really-accessible/
Other		
DMEM+Glutamax	Thermofisher	10569010
Penicillin/Streptomycin	Thermofisher	15140148
Fetal Bovine Serum	Wisent Bioproducts	080-150

2.9 Materials and methods

Animals

All experiments in this study was done in accordance with the Canadian Council on Animal guidelines and United Kingdom Animals (Scientific Procedure) Act of 1986 and Policies on the Use of Animals and Humans in Neuroscience Research guidelines. Pregnant Pou2f2$^{fl/fl}$ females raised in the C57BL/6J background (Mus musculus) were sacrificed at E13.5 and retinas from embryos were extracted for pCAG:Cre electroporation and ex-vivo retinal explant culture, αPax6-Cre^{+} Pou2f2$^{fl/fl}$ mice were P14 at the time of cell count analysis. The Chx10-Cre^{ERT2} mouse line was generated by Dr. Takahisa Furukawa (Osaka Univ.) and provided by the RIKEN BRC through the National Bio-Resource Project of the MEXT/AMED, Japan (RIKEN Bioresource RRID: IMSR_RBRC06574). Chx10-Cre^{ERT2+} Pou2f2$^{fl/fl}$ pregnant females were injected with tamoxifen at E11.5 and sacrificed at E17.5 for cell count analysis. Chx10-Cre^{ERT2+} Rosa^{tdTomato} were injected with tamoxifen at E11.5 and sacrificed at E13.5. All the rest of the mouse experiments in this study were carried out on WT CD1 mice (Mus musculus, Charles Rivers).

Tissue collection and immunofluorescence

Mouse embryos were collected from timed pregnant females with the day of vaginal plug considered as 0.5 day (E0.5). Embryos were collected from the pregnant females at E11.5, E13.5, E15.5, E17.5, whereas eyes were collected at P0.5 and Adult stages. The decapitated heads from embryos and eyes from postnatal pups were fixed for 15mins or 5mins, respectively, in 4% PFA/PBS followed by immersion in 20% Sucrose/PBS for 2 hours. Eyes were then embedded in OCT, frozen in liquid nitrogen, and sectioned at 25µm using a cryostat.

For immunofluorescence, retinal sections were blocked and permeabilized with the blocking solution (3% BSA in 1XPBS with 0.5% Triton X-100) for 1 hour. Primary antibodies diluted in blocking solution were then applied on the sections overnight at room temperature (RT). Sections were then washed three times for 5 mins with PBS and incubated with the appropriate secondary antibodies diluted in PBS (Invitrogen, 1:1000) for 1hour at RT. After three 5 mins PBS

wash, sections were incubated in Hoechst/PBS (Invitrogen, 33342, 1: 20,000) for 5 mins. at RT. Slides were washed once in PBS for 5 mins and cover-slipped with Mowiol (Calbiochem). List of primary antibodies can be found in the Table S2.

Retroviral constructs preparation and retinal explant culture

The retroviral constructs were prepared and purified as previously outlined (Cayouette et al., 2003). Retinal explants were prepared and cultured as previously described (Cayouette et al., 2001). Retroviral infections were done after placing the retinal explants in CO_2 incubator at 37ºC 1-hour after dissection. In ex-vivo electroporations and retroviral infections, left and right retinas from the same animal was separated to ensure control and experimental conditions were electroporated between different animals. The clones generated by the retroviral infection were analysed using morphology, positioning and cell type markers such as Rxrg and S-opsin, as previously described (Elliott et al., 2008).

Western blot

Protein extraction and immunoblotting was done as previously described in (Ramamurthy et al., 2014). The secondary antibody used was HRP-conjugated goat anti-mouse or HRP-conjugated goat anti-rabbit (1:10,000, Jackson immunoresearch).

In vivo electroporation

P0 eyes were injected sub-retinally with 3µg of DNA suspended in 1µl water containing 0.5% fast green and electroporated with 5 pulses at 50V, 50ms as previously described (de Melo and Blackshaw, 2011). The mice were sacrificed 14 days or more after the electroporation and the retinas were dissected, fixed, and sectioned as stated above.

CRISPR-Cas9 gRNA generation

CRISPR-Cas9 gRNAs targeting Pou2f1 and Pou2f2 were generated and cloned into pX330-U6-Chimeric_BB-CBh-hSpCas9 vector as described (Cong et al., 2013; Ruan et al., 2017; Wang et al., 2014). gRNA sequences used for CRISPR/Cas9 indel knockouts are listed in the Table S1.

Plasmids

Pou2f1 and Pou2f2 cDNA were cloned into a pCIG2-IRES-GFP and pCLE-Venus backbone vector using appropriate restriction sites (Gaiano et al., 2000; Hand et al., 2005; Lennon et al., 1996). shRNA sequences listed in Table S1 were cloned into pSIREN-retroQ-ZsGreen (Chan et al., 2006). pmNrl-dsRed, pNrl-Pou2f1, pmNrl-Pou2f1, pNrl-Pou2f2, and pmNrl-Pou2f2 were generated by Infusion HD Plus cloning kit using primers listed in Table S1. ThrbPR1:GFP and ThrbPR2:GFP sequences were generated by amplifying the promoter regions of the long and short isoform of thrb using PCR primers listed in Table S1. PCR products were then cloned into CAG:mGFP in place of the CAG promoter (Matsuda and Cepko, 2007).

EdU labelling assay

5µM EdU was added in the culture medium for 2 hours at specified time points, depending on the experiment (see text). Click-iT™ EdU Alexa Fluor™ 647 imaging kit was used to label the cells that incorporated EdU.

Chromatin Immunoprecipitation

ChIP was performed using ~50 E14 retinas per biological replicate (at least three biological replicates were done for each ChIP condition). Retinas were dissected and fixed for 10mins with 1% Formaldehyde. 125mM Glycine/PBS was used to quench the Formaldehyde for 10mins. Buffer A (0.25% Triton, 10 mM Tris pH8, 10 mM EDTA, 0.5 mM EGTA, protease inhibitors) was added to the samples and incubated for 10mins. The samples were then incubated for 30mins

in Buffer B (200 mM NaCl, 10 mM Tris pH8, 1 mM EDTA, 0.5 mM EGTA, protease inhibitors). The nuclei were sonicated to obtain fragments of 400bp average length. Immunoprecipitation of the sonicated chromatin was done with either mouse IgG (Invitrogen, 02-6502), Pou2f1 (Santa Cruz, cat. no. 12F11 X) or Pou2f2 (Santa Cruz, cat. no. F-5 X) whereas 10% of the chromatin was used as input. Dynabeads Protein G (Thermofisher scientific, 10003D) were used to collect immunoprecipitated material and Qiagen PCR purification kit (28104) was used to isolate DNA fragments after washing and de-crosslinking. qPCR was used to amplify regions of interest using specific primers. Complete primer list is detailed in Table S1.

RNA isolation and Quantitative PCR

Retinal explants and cKO eyes were dissociated with 100 units of papain (Worthington, LS003124). A MoFlo (Beckman Coulter) cell sorter was used to isolate GFP^{+ve} cells from the electroporated and dissociated retinal explants at various time points. Replicates with more than 1000 GFP^{+ve} cells sorted were included in the study. Collected cells were placed directly into Qiagen Buffer RLT plus and RNeasy microkit (Qiagen, 74004) was used to isolate RNA from the cells, as instructed by the manufacturer's protocol but with an additional 2mins of vortex in Buffer RLT. Isolated RNA was reverse transcribed using Superscript VILO Master Mix (Thermofisher Scientific, 11755050). cDNA was amplified by quantitative PCR using SYBR Green Master mix (Thermofisher Scientific, A25742). The detailed primer list can be found in Table S1 (Emerson et al., 2013; Ouimette et al., 2010). All primers used in this study were validated with a standard curve dilution of cDNA before the experiments were conducted.

Statistical and Quantitative analysis

Two-tailed unpaired student's t-test, one-way ANOVA with Tukey and Dunnett, two-way ANOVA with Tukey, and Mann-Whitney tests were conducted in this study, as indicated in Figure legends. All quantifications shown are mean±s.e.m. n represents number of biological replicates. In retroviral clonal analysis, all samples with less than 70 GFP^{+ve} clones counted were pooled to generate a single n. In the E14 and P0 retinal explants cultures, samples with disorganised retinal layers were discarded and only retinal explants with organised layers were analysed. Retinal

explants with low number of cells counted were pooled to generate one biological replicate. All experiments were repeated at least 3 times. All retinal sections were oriented according to standard conventions with apical side of the retina at the top of the image. All samples met the power testing criteria of at least n=3 with prespecified effect size of a 20% difference with default power value of 0.8 and a significance p-value of 0.05.

αPax6-Cre^{+} Pou2f2$^{fl/fl}$ were analysed as follows. 2 sections spanning the naso-dorsal and temporo-dorsal regions of the distal most retina around 200µm apart from each other, were analysed per marker per animal (4 sections per antibody per animal for Lim-1). The same region was counted between different animals, sectioned at the same time with the same orientation with the control conditions on the same slide. Cells positive for the respective markers were counted in a 200µm segment on the section. Retinas with poor antibody staining were excluded from the study. The raw counts were then averaged and compared to the WT from the same experiment. n is equal to biological repeats. The investigator was blinded to the genotype for cell counts, and counts for the Pax6 cKO were validated by another blinded lab member who analysed the images taken by the primary investigator. Sections with poor antibody immunostainings were omitted from the study.

Chx10-Cre^{ERT2} Pou2f2$^{fl/fl}$ pregnant females were injected with 3ul/g tamoxifen at E11.5 and sacrificed at E17.5. The embryos were decapitated, and heads were fixed with 4%PFA for 15min and 1hour depending on the antibody used whereas the tails were used for genotyping. Heads were oriented similarly, and each mutant was embedded in OCT and subsequently cryo-sectioned with a control condition. Counts of Rxrg and Nrl were done on two 200µm segments from the temporal and nasal portion each of the peripheral retina, averaged and normalized over the control. The investigator was blinded from the outcome of the genotyping results during the acquisition of the images and assessing the counts of each genotype. Sections with poor antibody immunostainings were omitted from the study.

Human ESC maintenance and retinal differentiation culture

The human embryonic stem cell line (H9 from Wicell) was maintained as previously described (Gonzalez-Cordero et al., 2017). For retinal organoid differentiation human ES cells were maintained until 90-95% confluent, then media without FGF (E6, Thermo Fisher) was added to the cultures for two days (D1 and 2 of differentiation) followed by a neural induction period (up to 7 weeks) in proneural induction media (Advanced DMEM/F12, MEM non-essential amino acids, N2 Supplement, 100mM Glutamine and Pen/Strep). Lightly pigmented islands of retinal pigmented epithelium (RPE) appeared as early as week 3 in culture. Optic vesicles were formed from within the RPE region between weeks 4 and 7. During this period, neuroretinal vesicles were manually excised with 21G needles and kept individually in low binding 96 well plates in retinal differentiation media (DMEM, F12, Pen/Strep and B27 without retinoic acid). At 6 weeks of differentiation, retinal differentiation medium was supplemented with 10% FBS, 100uM taurine (Sigma, T4871) and 2mM glutamax and at 10 weeks 1uM retinoic acid (RA) was added. For long-term cultures, vesicles were transferred to low binding 24 well plates (5 vesicles/well) at 10 weeks. At 12 weeks of differentiation, in addition to B27 and other factors described above, media was supplemented with 1% N2 and the RA concentration was reduced to 0.5uM. Maintenance cultures of hPSCs were feed daily and differentiation cultures were feed every 2 days.

2.10 Acknowledgements

We thank Christine Jolicoeur, Jessica Barthe, Marie-Claude Lavallée, Caroline Dube, Androne Constantin, Odile Neyret-Djossou, Éric Massicotte, Philip St-Onge and Julie Lord for animal and technical assistance. We also thank Pedro Dos Santos Franca for blind quantification of cone numbers in cKO mice and members of the Cayouette lab for their support. We also thank Dr. Rachel Pearson for providing Chrnb4-eGFP mouse retinas.

2.11 Conflict of interest

The authors declare no conflict of interest.

2.12 Temporal transcription factor gene regulatory network

During our examination of Pou2f1 and Pou2f2 as candidate regulators of cone temporal competence in the developing mouse retina, another tTF was discovered. Foxn4, a winged helix/forkhead box transcription factor, has been previously implicated in cell fate specification in the spinal cord as well as regulation of alveologenesis in the lung (Boije et al., 2013; Chi et al., 2008; Li et al., 2005; Li et al., 2010; Li and Xiang, 2011; Misra et al., 2014). In the retina, Foxn4 was previously shown to be expressed during the early temporal competence window and required for the horizontal and amacrine fate specification as well as RPC differentiation (Boije et al., 2008; Islam et al., 2013; Kunzevitzky et al., 2011; Li et al., 2004; Luo et al., 2012). Although it could promote amacrine fate outside its competence window, it was never tested as a potential tTF.

Foxn4 was shown to be important for the mid window of temporal competence state in RPCs (Liu et al., 2020a). Knockout retinas of Foxn4 had increased RGC and decreased cone numbers during early retinogenesis, in addition to amacrine and horizontals cells previously identified (Li et al., 2004). Overexpression of Foxn4 in early RPCs led to a reduction of RGC numbers and an increase in horizontal cell and cone numbers. Interestingly, microarray and RNA-seq analysis of Foxn4 KO and WT retinas revealed downregulation of genes associated with amacrine cell, horizontal cell and photoreceptor specification. On the other hand, there was an increase in genes associated with RGC development, suggesting that Foxn4 represses genes associated with RGC development. There were also dynamic changes observed in photoreceptor gene expression in Foxn4 KO compared to WT retinas. At E14, halfway through the early retinogenesis window, Foxn4 KO retinas had a drastic decrease in photoreceptor differentiation genes, which recovered by E16, and increased by P0. Therefore, Foxn4 regulates photoreceptor gene expression dynamically as retinal development progress. As germline Foxn4 knockout mice die at birth, the effect of Foxn4 deletion in the adult retina could not be assessed. Therefore, in the same study, a retina specific conditional knockout of Foxn4 was generated. Foxn4 cKO adult retinas had impaired photoreceptor synaptogenesis with bipolar cells and exhibited retinal degeneration due to thinning of retinal layers. These results demonstrated that important roles of Foxn4 during retinal development and in the adult retina.

Is there cross regulation between Foxn4 and other tTFs? Remarkably, Foxn4 represses Ikzf1 when overexpressed during early retinogenesis (Liu et al., 2020a). In the Foxn4 knockout retinas, *Ikzf1* mRNA expression is elevated in Foxn4 knockout retinas compared to WT control retinas at E16. Interestingly, there was no difference in *Ikzf1* mRNA expression between Foxn4 knockout and WT retinas at E14 and P0. This suggests that Foxn4 could be regulating Ikzf1 expression at a specific temporal stage. On the other hand, *Casz1* mRNA expression was increased by Foxn4 overexpression and decreased in E16 and P0 Foxn4 KO retinas. This regulation is reminiscent of the fly VNC temporal cascade, where a tTF represses the preceding gene and activates the succeeding gene (Fig.1.4C). As our study was published in parallel to Foxn4, the regulatory relationship between Pou2f1 and Foxn4 was not assessed.

The results presented in chapter 2 and this study provided major insights into how temporal identity could be transcriptionally regulated in RPCs. These results also suggest that only assessing the mammalian homologues of tTFs in fly VNC nerve cord development might be too limited to explain the complex temporal competence GRN. Evidence supporting this are the loss of function experiments of the currently discovered tTFs. The knockout or knockdown of Ikzf1, Casz1, Foxn4 Pou2f1/Pou2f2 does not lead to a complete loss of the cell fate associated with these genes. This is in direct contrast of the fly VNC NBs where deletion of any of the tTFs leads to a complete loss of the neuron associated with the tTF. Therefore, a gene regulatory network model of temporal competence could explain how these tTFs cross-regulate each other. This could also explain why there is an overlap in cell fate regulation between these tTF, such as the one between Foxn4 and Pou2f1 for the cone fate or Foxn4 and Ikzf1 for the amacrine fate.

Nonetheless, the one cell fate not accounted for so far in these studies have been Müller glia. As mentioned previously, Ikzf4 is a promising candidate for regulation of Müller glia temporal competence in late RPCs. In the next chapter of this thesis, the role of Ikzf4 in controlling Müller glia fate is assessed.

3 Results – Manuscript 2

Ikzf4 regulates cone development during early and Müller glia development during late mouse retinogenesis

Awais Javed[1,2], Allie Cui[1] and Michel Cayouette[1,2,3,4,*]

In preparation

Author contributions

Conceptualization and experimental design: Awais Javed and Michel Cayouette.

Investigation: Awais Javed performed all experiments in the manuscript, except biological replicate quantifications in Fig. 3.3D-G (performed by Allie Cui).

Result analysis: Awais Javed, Allie Cui, and Michel Cayouette.

Writing – Original Draft: Awais Javed.

Writing – Review & Editing: Michel Cayouette.

Resources: Michel Cayouette.

Supervision: Michel Cayouette.

Funding Acquisition: Michel Cayouette.

Awais Javed[1,2], Allie Cui[1] and Michel Cayouette[1,2,3,4,*]

[1]Cellular Neurobiology Research Unit, Institut de recherches cliniques de Montreal (IRCM), Canada.
[2]Molecular Biology Program, Université de Montréal, Canada.
[3]Department of Medicine, Université de Montréal, Canada.
[4]Department of Anatomy and Cell Biology; Division of Experimental Medicine, McGill University, Canada.
[*]corresponding author: michel.cayouette@ircm.qc.ca

Competing interests: The authors declare no competing interests.

Funding: This work was funded by grants from the Canadian Institutes of Health Research (FDN-159936) and Fighting Blindness Canada (to M.C.), the Brain Canada/Kremil Foundations (to M.C.). A.J. holds a Ph.D. scholarship from Fonds de Recherche du Québec – Santé. M.C. is an Emeritus Scholar from the Fonds de Recherche du Québec – Santé and holds the Gaëtane and Roland Pillenière Chair in Retina Biology from the IRCM Foundation.
*corresponding author: michel.cayouette@ircm.qc.ca

Keywords: Retinogenesis, temporal competence, cone photoreceptors, Müller glia, Ikzf4

3.1 Abstract

Transcription factors expressed in a temporally restricted manner have been extensively studied in neural development. How widely expressed transcription factors modulate their binding activity over time to change cell fate identity remains largely unclear. Here we show that Ikzf4, a zinc finger transcription factor expressed throughout retinal development, regulates cone development during early stages of retinogenesis and Müller glia development during late stages. We used CUT&RUN sequencing to show that Ikzf4 alters its DNA binding profile over time, binding to the cone-promoting factors Pou2f1/2 early and to Müller glia differentiation genes late during retinal development. Finally, we found two critical binding Ikzf sites at the Hes1 promoter that allow Ikzf4 to maintain the expression of Hes1 in differentiated cells and induce Müller glia cell fate commitment. These results uncover a novel role for Ikzf4 in CNS development and provide mechanistic insights on how widely expressed transcription factors change their DNA binding activity to impact cell fate identity.

3.2 Introduction

Generation of cell diversity in the central nervous system is a highly controlled and regulated process. Neural progenitors alter their potential to generate specific neurons and glia through spatial and temporal patterning cues (Florio and Huttner, 2014; Jessell, 2000; Stiles and Jernigan, 2010). In CNS development of invertebrates, timely expression of certain transcription factors is necessary to allow neural progenitors to progress forward in time (Brody and Odenwald, 2000; Cleary and Doe, 2006; Erclik et al., 2017; Grosskortenhaus et al., 2005; Grosskortenhaus et al., 2006; Isshiki et al., 2001; Kambadur et al., 1998; Li et al., 2013; Novotny et al., 2002; Pearson and Doe, 2003). As the neural progenitor divides, changes in the chromatin landscapes ensure that specific neurons are produced in their respective windows of development (Sen et al., 2019). A vertebrate example of such a system with restricted and timely generation of neurons is the developing mouse retina. Seven broad cell types are formed in an overlapping but sequential manner from retinal progenitor cells (RPCs) (Turner and Cepko, 1987). Retinal ganglion cells (RGCs), amacrine cells, cone photoreceptors and horizontal cells are born during embryonic window of retinogenesis. Rod photoreceptors and bipolar cells are primarily born during postnatal

stage of retinogenesis (Carter-Dawson and LaVail, 1979a, b; Rapaport et al., 2004; Turner et al., 1990; Young, 1985a, b). A neurogenesis to gliogenesis switch, driven by Notch signaling, occurs in the terminally dividing RPCs during the last phase of post-natal retinogenesis to produce Müller glia, the resident glial cell type of the retina (Furukawa et al., 2000; Gomes et al., 2011; Jadhav et al., 2006a; Jadhav et al., 2006b). However, the factors that guide the transition from neurogenesis into gliogenesis in RPCs remain elusive.

Lhx2 has been shown to regulate the balance between neurogenesis and gliogenesis. Lhx2 interacts with Ldb1 early retinogenesis to promote amacrine cell specification. During late retinogenesis, Lhx2 interacts with Rnf12 promote Müller glia specification (de Melo et al., 2016a; de Melo et al., 2018; de Melo et al., 2012; de Melo et al., 2016b; Zibetti et al., 2019). In addition to Müller glia specification, Lhx2 is also necessary for Notch dependent Müller glia differentiation (de Melo et al., 2016a). Additionally, SoxE genes, *Sox8* and *Sox9,* have also been shown to be required for Müller glia development (Muto et al., 2009; Poche et al., 2008). However, upstream regulators of these genes are currently unknown.

Recent advances in scRNA-seq technology have demonstrated key transcriptomic changes during early and late retinogenesis. Nfi family of transcription factors have been shown to have a 'low-early' and 'high-late' expression profile in RPCs and are required for the specification of Müller glia and bipolar cells (Clark et al., 2019). In addition to their role in Müller glia and bipolar cell development, triple knockout retinas of Nfia/b/x also have reduced expression of RPC multipotency genes such as Pax6, Lhx2, Rax and Vsx2. However, it is unclear what factors orchestrate the expression of *Nfia/b/x* genes in post-natal RPCs and committed glial precursors.

We have previously shown that Ikzf1 confers temporal competence to RPCs to generate all early-born cell types, except cones (Elliott et al., 2008). Casz1 confers late temporal competence to RPCs to generate rods and bipolar cells, but not Müller glia (Mattar et al., 2015) . Moreover, Pou2f1 regulates RPC competence to generate cones, thereby partially completing a temporal competence cascade, similar to the cascade observed in the fruit fly CNS development (Brody and Odenwald, 2000; Cleary and Doe, 2006; Grosskortenhaus et al., 2005; Grosskortenhaus et al.,

2006; Isshiki et al., 2001; Javed et al., 2020; Kambadur et al., 1998; Novotny et al., 2002; Pearson and Doe, 2003). Foxn4 is another temporal transcription factor (tTF), controlling a specific mid-late window of early temporal competence to generate amacrine cells, horizontal cells, cones and rods (Liu et al., 2020a). This suggests the possibility of other yet undiscovered temporal factors that could work together to form a complete temporal competence gene regulatory network (Liu et al., 2020a). There are five members of Ikaros family of transcription factor, four of which are expressed in the retina and homologous to the Drosophila *Hunchback* gene. Therefore, we wondered whether other Ikaros family members also take part in the regulating RPC competence during retinogenesis (Georgopoulos et al., 1992; Hahm et al., 1998; Honma et al., 1999; John et al., 2009; Kelley et al., 1998; Morgan et al., 1997; Perdomo et al., 2000; Powell et al., 2019).

Here we show that Ikzf4, along with Ikzf1, is required for cone development during early retinogenesis. In addition, Ikzf4 is also required for Müller glia development during late retinogenesis. We also show that Ikzf4 binds to the genomic regions around *Pou2f1/Pou2f2* gene bodies and promotes their expression. During post-natal retinogenesis, Ikzf4 binds to several Notch signaling and Müller glia differentiation genes. Finally, we show that Ikzf4 binds to two 'GGAA' sites in the Hes1 promoter to upregulate its expression. We provide evidence of dynamic properties of Ikzf4 binding during early and late retinogenesis that leads to cell fate regulation in a cell context dependent and temporal manner.

3.3 Results

3.3.1 Ikzf4 is expressed in retinal progenitor cells during early and late retinogenesis

We first studied the spatiotemporal expression of Ikzf4 in the mouse retina during retinogenesis. To validate our Ikzf4 antibody, we electroporated CAG:GFP or CAG:Ikzf4-IRES-GFP vectors in E17 retinas. After culturing the retinal explants for 2 days in vitro (DIV), we sectioned and immunostained using an anti-Ikzf4 antibody. As expected, we found that the Ikzf4

antibody recognizes the overexpressed Ikzf4 protein (Fig. S3.1A-C'). Moreover, we also immunostained Ikzf4$^{+/+}$ and Ikzf4$^{-/-}$ (RIKEN Bioresource RRID: IMSR_RBRC06808) retinas at E12, E15 and P9. We found that Ikzf4 is expressed in all retinal cells at E12 and E15, whereas its expression is more cell type specific at P9 (Fig. S3.1D-G). As expected, Ikzf4 is undetected in the Ikzf4-/- retinas, thereby validating both the Ikzf4$^{-/-}$ mutant and antibody (Fig. S3.1D-H'). We next assessed whether Ikzf4 is expressed in RPCs. We found that most Ikzf4^{+ve} cells co-labelled with proliferative cell marker Ki67 during embryonic and post-natal retinogenesis (Fig. 3.1A-F"). At P2, we observed only some Ki67^{+ve} cells co-labelling with Ikzf4 (Fig. 3.1F-F''). We next compared our immunostaining data of Ikzf4 with published scRNA-seq datasets to see if there is a similar temporal profile for *Ikzf4* and *IKZF4* mRNA expression in the developing mouse and human fetal retinas, respectively (Clark et al., 2019; Lu et al., 2020). Focusing on RPCs, we generated UMAP plots by sub-setting the RPC populations from various developmental stages of the mouse and human retina. We found that *Ikzf4*/*IKZF4* mRNA is expressed in early and late RPCs (Fig. S3.1I-J). At P5 in mice and HGW17 in humans, *Ikzf4* was detected at lower expression levels and in fewer RPCs (Fig. S3.1I-J). In addition to the RPCs, we found expression of *Ikzf4/IKZF4* in all differentiated retinal cell types of the mouse and human retina (Fig. S3.2A-B). This suggests that Ikzf4 is expressed in the mouse and human retina throughout development, albeit at reduced levels during later stages.

To assess the expression of Ikzf4 in differentiated cell types, we used specific antibodies to label retinal cell types at P7. We detected expression of Ikzf4 in Lim1/2^{+ve} horizontal cells, Brn3a^{+ve} RGCs, Pax6^{+ve} amacrine cells and S-opsin^{+ve} cone photoreceptors (Fig. 3.1G-H'''). We could also detect weak immunosignal of Ikzf4 antibody staining in S-opsin^{-ve} cells in the ONL, indicating expression in rod photoreceptors (H'-H'''), similar to Ikzf4/IKZF4 expression in published scRNA-seq datasets (Clark et al., 2019; Lu et al., 2020) (Fig. S3.2A-B). We also found Ikzf4 expression in Nfia/b^{+ve}Chx10^{-ve} Müller glia and Chx10^{+ve} bipolar cells (Fig. S3.1H-H'''). Taken together, these data suggest that Ikzf4 is expressed in both early- and late-born cell types of the mouse retina with dynamic expression levels.

3.3.2 Overexpression of Ikzf4 in late-stage retinal progenitors promotes immature cone and Müller glia production

Next, we investigated the functional role of Ikzf4 in the developing retina. Since we observed higher expression of Ikzf4 mRNA and protein in early RPCs, we postulated that Ikzf4 might have a role in promoting early born retinal cell types. We infected P0 retinal explants with retroviral vectors expressing Venus or Ikzf4-IRES-Venus and cultured the infected retinal explants for 14 DIV. Since a retrovirus sparsely infects individual RPCs, clonal composition of a single RPC can be determined. We used Rxrg staining to label cones, Nrl to label rods, and cell morphology to identify other cell types. We found a higher proportion of Venus^{+ve}Rxrg^{+ve}Nrl^{-ve} cells Ikzf4-IRES-Venus infected clones compared to control Venus infections, located in the ONL. This suggests that Ikzf4 might be sufficient to promote cone photoreceptors outside their window of development (Fig. 3.2A-D'). Moreover, we also observed an increase in Müller glia as demonstrated by their radial morphology spanning across the retina (Fig. 3.2E). The increase in cones and Müller glia was compensated by a decrease in rods (Fig. 3.2F). When we assessed the number of cells per clone, we also found that Ikzf4 increases the number of small clones (Fig. 3.2G). Finally, we also found that most 1 and 2 cell clones contain either cones or Müller glia compared to mostly rods in control Venus (Fig. S3.3A-B). This suggests that Ikzf4 is sufficient to promote cones and Müller glia when expressed in late RPCs at the expense of rods.

We next assessed whether Ikzf4 overexpression generates immature photoreceptors with both cone and rod markers. To increase the number of cells for analysis and test our retroviral lineage tracing results with another method, we electroporated retinal explants with either CAG:GFP or CAG:Ikzf4-IRES-GFP at P0. 14 days later, when we analyzed the GFP^{+ve} cells, we found a similar induction of Rxrg^{+ve} cells in the ONL following electroporation of CAG:Ikzf4-IRES-GFP vector as compared to the control CAG:GFP (Fig. S3.3C-F). We also found that Ikzf4 overexpression leads to a reduction of GFP^{+ve} cells expressing Nr2e3, a rod differentiation gene, in the ONL (Fig. S3.3G-J). Additionally, these GFP^{+ve} cells also co-labelled with Crx/Otx2, which are markers for photoreceptors in the ONL and bipolar cells in the INL (Fig. S3.3G-J'). To assess whether Ikzf4 represses Nrl and Nr2e3 during photoreceptor differentiation, we electroporated either CAG:GFP or CAG:Ikzf4-IRES-GFP in P0 retinas. After culturing the retinal explants for 6 DIV,

we sorted the GFP^{+ve} cells to extract mRNA and perform RT-qPCR quantitation. We found that that Ikzf4 represses *Nrl* and *Nr2e3* as well as promotes *Rxrg* mRNA expression during photoreceptor differentiation (Fig. 3.2H). To assess whether Ikzf4 overexpression leads to a repression of Nrl protein *in vivo*, we electroporated either CAG:GFP or CAG:Ikzf4-IRES-GFP in P0 retinas and after 14 days, immunostained the electroporated retinas with Nrl. We found a drastic reduction of GFP^{+ve}Nrl^{+ve} cells in Ikzf4 overexpression as compared to control GFP, suggesting that Ikzf4 inhibits the rod cell fate by repressing rod differentiation factors (Fig. 3.2I-L).

We next assessed whether Ikzf4 promotes mature or immature cones. We electroporated retinal explants with either CAG:GFP or CAG:Ikzf4-IRES-GFP at P0. After 14 days, we immunostained the retinal explant sections with late cone markers. We were not able to observe any late cone markers such as S-opsin, M-opsin or PNA co-labelling with GFP^{+ve}Rxrg^{+ve} cells. This suggests that these might either be immature cones or mis-localized RGCs, which also express Rxrg (Javed et al., 2020) (Fig. S3.3K'-N'). To rule out the latter possibility, we co-immunostained the sections of Ikzf4-IRES-GFP electroporated retinas with RGC markers, Brn3a and Brn3b, to co-label with GFP^{+ve}Rxrg^{+ve} cells. We found that Ikzf4 overexpression induces Rxrg^{+ve} cells that do not express Brn3a and Brn3b, suggesting that Ikzf4 likely promotes immature cones rather than RGCs (Fig. S3.3O-R').

We next validated Müller glia production using specific markers *in vivo* and *ex vivo*. We electroporated P0 retinas with CAG:Ikzf4-IRES-GFP and harvested the retinas or retinal explants after 14 days. We found GFP^{+ve}Sox2^{+ve} cells in the INL when Ikzf4 was overexpressed *in vivo*, similar to what was observed *ex vivo* (Fig. S3.3S'-S''). Moreover, we also observed GFP^{+ve}Hes1^{+ve}Chx10^{-ve} and GFP^{+ve}Lhx2^{+ve}Nfia/b^{+ve} cells in the INL when we electroporated retinas explants with Ikzf4-IRES-GFP. These results suggest that Ikzf4 promotes Müller glia that express multiple glial markers (Fig. S3.3T-W').

We next assessed whether Ikzf4 promotes smaller clones by inducing early cell cycle exit or the reduction in clone size is due to apoptosis of the electroporated cells. To assess whether

Ikzf4 promotes early cell cycle exit, we electroporated CAG:GFP or CAG:Ikzf4-IRES-GFP vectors in P0 retinas. After culturing the retinal explants for 2 days, we added EdU in the media for 2hours to label cells undergoing S-phase. We observed a significant decrease in $EdU^{+ve}GFP^{+ve}$ when we overexpressed Ikzf4 as compared to the GFP control, suggesting that Ikzf4 promotes early cell cycle exit (Fig. 3.2M-P). Additionally, we next immunostained the retinal explants with Cleaved Caspase-3, which labels cells undergoing programmed cell death. We found no major difference between the GFP and Ikzf4-IRES-GFP electroporated conditions, suggesting that Ikzf4 overexpression does not promote smaller RPC clones due to apoptosis of electroporated cells (Fig. S3.3X-Z').

3.3.3 Ikzf4 is required for Müller glia development

We next assessed the role of Ikzf4 in cone and Müller glia specification in the developing retina. We analyzed retinas of $Ikzf4^{+/+}$, $Ikzf4^{+/-}$, and $Ikzf4^{-/-}$ mice to quantify cell types using specific markers at P10, a stage at which retinogenesis is mostly complete. We observed a reduction in $Sox2^{+ve}$ and $Lhx2^{+ve}$ cells in the INL of $Ikzf4^{-/-}$ retinas compared to $Ikzf4^{+/+}$ and $Ikzf4^{+/-}$ retinas (Fig. 3.3A-C). This suggests that Ikzf4 is required for Müller glia specification (Fig. 3.3A-C). Additionally, we did not observe any difference in the numbers of RGCs ($Brn3a^{+ve}$), amacrine cells ($Pax6^{+ve}$), horizontal cells ($Lim1^{+ve}$) or bipolar cells ($Otx2^{+ve}$) between the three conditions. Surprisingly, when we quantified the number of $Rxrg^{+ve}$ cells in the ONL, we also did not observe a difference between $Ikzf4^{+/+}$ and $Ikzf4^{-/-}$ retinas (Fig. 3.3C). This suggest that, although Ikzf4 can promote immature cone production, Ikzf4 by itself is not required for cone development.

3.3.4 Ikzf1 and Ikzf4 are required for cone development

We have previously shown that Ikzf1 confers early temporal competence to RPCs to generate all early born cell types except cones (Elliott et al., 2008). Since Ikzf1 and Ikzf4 are expressed in the same cells as early as E11 (Fig. S3.4A-D), we wondered whether there is redundancy in function between Ikzf1 and Ikzf4 for cone development. Therefore, we generated double knockout mice for Ikzf1 and Ikzf4 to assess the effect on cone production. Interestingly, $Ikzf1^{-/-}Ikzf4^{+/-}$ and $Ikzf1^{-/-}Ikzf4^{-/-}$ embryos were paler and exhibited a reduced fetal liver size

compared to Ikzf1$^{+/-}$Ikzf4$^{-/-}$ and Ikzf1$^{+/-}$Ikzf4$^{+/-}$ embryos (Fig. S3.4E-H). Moreover, we also observed postnatal death of the Ikzf1$^{-/-}$Ikzf4$^{+/-}$ and Ikzf1$^{-/-}$Ikzf4$^{-/-}$ mice. Therefore, we focused our analyses at the embryonic stages and quantified cone numbers using Rxrg at E15, when cone genesis is at its peak. We found a significant reduction in cone numbers only when both Ikzf1 and Ikzf4 were deleted, suggesting that Ikzf1 and Ikzf4 are both required for cone development (Fig. 3.3D-F). Since Ikzf1$^{-/-}$ have fewer RGCs compared to the controls (Elliott et al., 2008), we wondered whether there could be a compounding decrease in RGC numbers in Ikzf1$^{-/-}$Ikzf4$^{-/-}$ retinas. Interestingly, we did not observe a significant difference between Ikzf1$^{-/-}$ Ikzf4$^{+/-}$ and Ikzf1$^{-/-}$ Ikzf4$^{-/-}$ retinas suggesting that Ikzf4 is dispensable for RGC development, similar to what was observed in the P10 mice (Fig. 3.3C, G). Taken together, our data shows that Ikzf1 and Ikzf4 cooperate to regulate cone development.

3.3.5 Ikzf4 binds to promoters of notch signaling genes and upregulates Müller glia genes during retinogenesis

We next assessed whether Ikzf4 regulates an early born and a late born cell fate by changing its DNA binding profiles. Therefore, we performed Ikzf4 CUT&RUN assays on E14 and P0 retinas. We observed that Ikzf4 has a higher proportion of promoter bound peaks at E14 compared to P0 (Fig. S3.5A). Moreover, the promoter bound peaks are also dispersed away from the transcription start site (TSS) at P0 (Fig. S3.5B). These results highlight general changes in Ikzf4 binding profile between early and late retinogenesis. We further validated Ikzf4 binding peaks by performing HOMER to discover transcription factor motifs present in the dataset. We found that the canonical Ikzf binding motif 'GGAA' or the complementary sequence is present in ~45-55% of the target sites. This suggests that Ikzf4 binds the DNA using the canonical Ikzf motif in the developing retina (Fig. S3.5C). We next computed the overlap of binding peaks between E14 and P0 stages. We found that out of the ~2500 peaks at each stage, only 1010 peaks are shared between the two stages (Fig. 3.4A). To link the genes associated with the binding peaks, we performed gene ontology (GO) classification on the peaks using GREAT and annotated the top 5 GO biological processes. We found multiple binding peaks around Notch signaling genes such as *Hes1*, *Hes5* and *Dll1* in E14 exclusive, P0 exclusive and common shared peaks.

We previously showed that Ikzf1 upregulates Pou2f1, which activates *Pou2f2* and represses *Casz1* expression to promote cone development (Javed et al., 2020). Since Ikzf1 and Ikzf4 together contribute to cone development, we wondered whether Ikzf4 might also upregulate *Pou2f1* and repress *Casz1* expression. Interestingly, we found that Ikzf4 binds to the promoter and an intergenic region of *Pou2f1* gene (Fig. S3.5D). Additionally, we also observed binding at a region 20kbp upstream of the promoter of *Pou2f2* gene with open chromatin at E14, scored as a Pou2f2 associated peak by GREAT (Fig. S3.5D). To test the functional relevance of Ikzf4 binding at these genomic regions, we electroporated P0 retinas with either CAG:GFP or CAG:Ikzf4-IRES-GFP and sorted the GFP+ cells 18hours later to extract mRNA and perform RT-qPCR. We found that Ikzf4 upregulates mRNA levels of both *Pou2f1* and *Pou2f2*. In addition, there is no significant change in the expression of other tTFs, *Casz1v1* and *Casz1v2* or *Foxn4* (Fig. S3.5E) (Liu et al., 2020a; Mattar et al., 2015). This suggests that Ikzf4 could be promoting cone development by binding and upregulating Pou2f1 and Pou2f2, but without modulating tTFs during early retinogenesis. Interestingly, when we electroporated Ikzf4-IRES-GFP with either shControl or shPou2f2, we found a significant decrease in the number of $GFP^{+ve}Rxrg^{+ve}$ cells in the ONL. This suggests that Ikzf4, similar to Pou2f1, requires Pou2f2 to promote cone development (Fig. S3.3F-H).

We next focused our analyses on Ikzf4 P0 CUT&RUN to uncover the mechanism of Müller glia specification. Complementary to the Notch signaling genes, we assessed the binding of Ikzf4 at the regions around the genes enriched in the Müller glia cluster in scRNA-seq dataset at P14 (Clark et al., 2019). We found Ikzf4 binding peaks at the top 8 genes enriched in the Müller glia cluster (Fig. S3.5I). This suggests that Ikzf4 might be regulating expression of these genes to specify Müller glia cell fate (Fig. S3.5I). However, since late RPCs and Muller glia have similar transcriptomes (Roesch et al., 2008), these genes are also expressed in RPCs. Therefore, we focused the rest of our analysis on genes that have been shown to be required for Müller glia development. We found Ikzf4 binding at genomic regions around *Sox8*, *Sox9*, *Lhx2*, *Rnf12*, and *Nfia/b/x* gene bodies (Fig. 3.4B) (Clark et al., 2019; de Melo et al., 2018; de Melo et al., 2016b; Muto et al., 2009; Poche et al., 2008; Zibetti et al., 2019). We then assessed whether Ikzf4 also regulates mRNA levels of these genes by electroporating P0 retinas with either CAG:GFP or

CAG:Ikzf4-IRES-GFP. We sorted the electroporated cells 18 or 72 hours later to extract mRNA and perform RT-qPCR. We found that 18hours post-electroporation, Ikzf4 promotes expression of *Sox8* and *Sox9* but we observe no change in the mRNA expression levels of *Lhx2*, *Rnf12*, *Nfia/b/x, Ldb1* or negative control *beta-actin* compared to GFP (Fig. 3.4C). Interestingly, 72hours after electroporation, we observe an increase in *Lhx2*, *Rnf12*, *Nfib/x*, suggesting sequential change in expression of Müller glia genes (Fig. 3.4D). Moreover, to validate our qPCR results, we electroporated P0 retinas with the same vectors and fixed the retinal explants after 72hours to immunostain with the Nfia/b antibody. Interestingly, we found a significant increase in the number of GFP^{+ve} cells expressing Nfia/b (Fig. 3.4C-H). This suggests that Ikzf4 promotes Müller glia specification by binding and upregulating glia differentiation genes.

3.3.6 Ikzf4 binds to the promoter of Hes1 at the 'GGAA' motif to upregulates its expression

From our CUT&RUN data, we noticed that the Hes1 and Hes5 promoters are strongly enriched with Ikzf4 binding, both early and late during retinogenesis. It was previously shown that Hes1 expression oscillates during the various stages of RPC differentiation (Shimojo et al., 2008). Interestingly, Hes1 expression decreases when the RPCs exit the cell cycle and is repressed in cells fated to become neurons (Furukawa et al., 2000). On the other hand, Hes1 expression is maintained in post-mitotic cells fated to become Müller glia. To uncover the mechanism and dynamics of Ikzf4 binding at the Hes1 and Hes5 promoter, we first performed a time course assay to assess the dynamics of the Hes1 and Hes5 promoter activity by co-electroporating the pHes1-dsRed or pHes5-dsRed vector with either CAG:GFP or CAG:Ikzf4-IRES-GFP in P0 retinas. We tracked the same electroporation patch to assess the dynamics of dsRed expression overtime. We observed that Ikzf4 promotes the activity of the Hes1 promoter compared to the control GFP at 48 and 72 hours (Fig. S3.6A-D''). Interestingly, 6 days after electroporation, Ikzf4 maintained higher expression of dsRed, whereas expression of dsRed was reduced in the control GFP condition (Fig. S3.6E-F''). We did not observe similar dynamics in dsRed expression for the Hes5 promoter at 48hours or 6DIV after Ikzf4 electroporation compared to the GFP control (G-J''). This suggests that Ikzf4 maintains Hes1, but not Hes5, promoter activity.

Next, we evaluated whether Ikzf4 alters the activity of the Hes1 promoter specifically in the retina or if it is a general mechanism that requires direct binding of Ikzf4 regardless of the cellular context. We transfected HEK293T cells with CAG:GFP or CAG:Ikzf4-IRES-GFP with pHes1-dsRed and imaged dsRed expression 24 hours post-transfection. We could not detect a change in the dsRed activity between Ikzf4 and GFP control conditions. This suggests that Ikzf4 regulation of the Hes1 promoter is likely retinal cell context dependent (Fig. S3.6K-L'').

We next assessed whether the increase in the Hes1 promoter activity also leads to an increase in expression of Hes1. To test this, we electroporated P0 retinas with either CAG:GFP or CAG:Ikzf4-IRES-GFP and after 44 hours of retinal explant culture, analyzed the number of GFP^{+ve} cells expressing Hes1. As expected, we observed an increase in the number of $GFP^{+ve}Hes1^{+ve}$ cells when we overexpressed Ikzf4 compared to the control GFP condition. These results suggest that Ikzf4 overexpression leads to an increase in the number of cells expressing Hes1 (Fig. 3.5A-C).

We next sought to identify the Ikzf4 binding sites required for the regulation of the Hes1 promoter. When we analyzed the region that contains the Ikzf4 binding at the Hes1 promoter, we found three 'GGAA' Ikzf binding motifs (Fig. 3.5D). Therefore, we mutated each of the 'GGAA' motifs to assess the effect on the activity of the Hes1 promoter with or without Ikzf4. We electroporated either CAG:GFP or CAG:Ikzf4-IRES-GFP with either WT or the mutated Hes1 promoter vectors (Fig. 3.5E). When we mutated site 1 (mut1), 2 (mut2) or 3 (mut3) and electroporated with CAG:GFP, we observed a reduction in dsRed signal compared to the unmutated vector (Fig. 3.5F-Q'). However, this was rescued by overexpression of Ikzf4, albeit mildly for mutation site 2 (Fig. 3.5F'-Q'). This suggests that these sites alone are not required for Ikzf4 binding but could be required for the activity of the Hes1 promoter itself (Fig. 3.5F-Q'). Interestingly, when we mutated site 2 (mut2) or 3 (mut3) together, we found that Ikzf4 is no longer able to activate the Hes1 promoter (Fig. 3.5R-T'). Taken together, these results suggest that Ikzf4 binding at two 'GGAA' sites is required for the sustained expression of Hes1 in post-mitotic cells, leading to Müller glia differentiation.

3.4 Discussion

Neural diversity in the central nervous system is generated by a combination of spatial and temporal factors working in concert to establish the intricate structure of neurons and glia found in the CNS. Previously, many studies have established candidate regulators of cell fate in neural progenitors based on temporal differences in their expression or regional localization. However, there are many factors expressed throughout early and late neurodevelopment, in neural progenitors and post-mitotic cells alike, that have not been examined as thoroughly. In this study, we show that a zinc-finger transcription factor, Ikzf4, modulates its binding activity in a temporal manner to generate cone photoreceptor early and Müller glia late during retinogenesis. We also found that Ikzf1 and Ikzf4 regulate cone development together. Ikzf4 binds to the promoter of Pou2f1 and an upstream region of Pou2f2 to upregulate their expression and promote the cone fate. We show that Ikzf4 binds to downstream Notch signaling and genes involved in Müller glia development. Finally, we propose a mechanism in which Ikzf4 induces sustained expression of Hes1 in post-mitotic cells to promote gliogenesis, which requires two 'GGAA' Ikzf binding sites. Taken together, this study demonstrates Ikzf4 as a novel regulator of cone development early and Müller glia development late (Fig. 3.6).

3.4.1 Ikzf4 as a novel regulator of cone development

Single knockout retinas of Ikzf1 and Ikzf4 have normal cone numbers (Fig. 3.3C) (Elliott et al., 2008). On the other hand, Ikzf1 and Ikzf4 double knockouts have reduced cone numbers. This suggests that there could be a compensatory mechanism between the two genes. Which of two factors is the primary factor involved in cone development? If Ikzf4 compensates for Ikzf1 function, then Ikzf1 could the primary factor that promotes cone development. If this is true, then Ikzf4 could also compensate for the loss of Ikzf1 function in promoting other early cell fates such as RGCs. However, Ikzf1/Ikzf4 double knockout retinas do not have a pronounced reduction in RGC numbers compared to single Ikzf1 knockout retinas (Fig. 3.3G). This suggests that Ikzf4 is dispensable for RGC development, which is one of the functions of Ikzf1. On the other hand, Ikzf1 could compensate for Ikzf4 function to promote cone development. In this case, Ikzf4 would be the primary factor that has the potential to specify the cone fate. This is likely because Ikzf1 cannot activate Pou2f1/Pou2f2 expression in late RPCs that can no longer generate cones (Javed et al.,

2020). On the other hand, Ikzf4 can activate Pou2f1/Pou2f2 expression and promote cone production in late RPCs, outside their temporal window of development. This suggests that Ikzf1 lacks the ability to fully re-open the cone production window after it is closed. In contrast, Ikzf4 is able to overcome this barrier and could be the primary cone promoting factor. Whether Ikzf1 has similar DNA binding targets as Ikzf4 during early retinogenesis remains to be fully explored.

Our data suggests that Ikzf4 could either be a tTF for cone fate specification upstream to Pou2f1 or it could be utilizing a general notch signaling program along with Pou2f1/Pou2f2 to initiate cone genesis. We observe an increase in Rxrg^{+ve} cells when Ikzf4 is overexpressed in late RPCs, thereby opening the window of cone genesis. This provides some evidence to the role of Ikzf4 as tTF. However, Ikzf4 does not promote mature cone gene expression such as Arr3, S-opsin or M-opsin from late RPCs, unlike Pou2f1 that can promote mature cones when overexpressed in late RPCs (Javed et al., 2020). This suggests that Ikzf4 is able to promote cone genesis but likely requires additional factors to produce mature cones outside their window of development. Ikzf4 also promotes early cell cycle exit to promote cone specification, which is uncharacteristic of some tTFs such as Ikzf1, Pou2f1 and Casz1, but not Foxn4 (Elliott et al., 2008; Javed et al., 2020; Li et al., 2004; Mattar et al., 2015). Moreover, Ikzf4 does not regulate the expression of other tTFs, except Pou2f1. Nonetheless, our results show that Ikzf4 is an important part of the gene regulatory network that allows RPCs to generate cones.

3.4.2 Ikzf4 as a regulator of notch signaling during late retinogenesis.

The current model of gliogenesis in the retina proposes that terminally dividing RPCs in the late-stage retina give rise to post-mitotic cells that maintain the expression of Notch signaling genes to promote Müller glia (de Melo et al., 2018; de Melo et al., 2016b; Gomes et al., 2011; Jadhav et al., 2006a; Nelson et al., 2011). In the RPCs, a balance between Lhx2 interacts with Ldb1 to promote neurogenesis and with Rnf12 to promote Notch-dependent gliogenesis (de Melo et al., 2018; de Melo et al., 2016b). Additionally, Lhx2 dynamically alters its DNA binding profile early and late during retinogenesis in order to switch from promoting neurogenesis to gliogenesis, similar to what we observe with Ikzf4 (Zibetti et al., 2019). Sox8/9 induce sustained Notch signaling in post-mitotic cells to ensure the commitment to the glial cell fate (Poche et al., 2008).

Moreover, activation of Notch signaling in post-mitotic cells also regulates Sox8/9 expression in Müller glia (Muto et al., 2009). Where does Ikzf4 fit in the above proposed model of gliogenesis? We propose that high Ikzf4 expression induces early cell cycle exit in late RPCs. Subsequently, Ikzf4 induces Sox8/9 and Hes1 expression in a subset of post-mitotic cells committed to the glial cell fate. Sox8/9^{+ve} precursors undergo sustained Notch signaling by the action of Ikzf4, which activates downstream genes to ensure the glial cell fate commitment is maintained. This is evidenced by the increase in the number of Hes1^{+ve} cells 2 days and increased mRNA levels of *Lhx2*, *Nfia/b/x* and *Sox8/9* 3 days following electroporation of Ikzf4. Previously published RNA-seq dataset of Lhx2 cKO and Nfia/b/x cKOs also provides evidence for this model as there is no significant change in Ikzf4 mRNA between the WT and cKO of Lhx2 or Nfia/b/x. This suggests that Ikzf4 could be upstream to these factors in the gliogenesis gene regulatory network (Clark et al., 2019; de Melo et al., 2016b). Future experiments aimed at characterizing the epistatic relationship between these factors would shed light on precisely how these factors contribute to gliogenesis.

Ikzf4 binds to regions close to the gene bodies of many Notch signaling genes and our data shows that Ikzf4 can bind to multiple sites at the promoter of Hes1 and upregulate its expression. Although we observed a change in binding profiles of Ikzf4 from early to late stages of retinal development, binding peaks close to Notch signaling genes were shared between the two stages. We did, however, observe additional binding peaks close to many Notch signaling genes that were exclusively present at P0. This suggests that Ikzf4 regulation of Notch signaling is more prominent role later rather than earlier in retinal development. Interestingly, it has been recently reported that Hes1 deletion in the early retina leads to a reduction in cone numbers without a change in other cell types, similar to what we observe in the Ikzf1/Ikzf4 double knockout retinas (Bosze et al., 2020). It is possible that Ikzf4 activates Hes1 in a non-canonical Notch signaling manner, in addition to promoting Pou2f1/Pou2f2 expression. This could partially explain the weaker representation of Ikzf4 binding peaks close to Notch signaling genes during early retinal development.

3.4.3 Broader role of Ikzf4 in encoding cell fate specification

Previous studies have elucidated the role of Ikzf4 in the immune system. Most notably, Ikzf4 function in T-cell differentiation varies considerably depending on $CD4^+$ T-cell subtype. This further highlights the dynamic role of Ikzf4's function based on the temporal and cellular context within similar cell classes (Liu et al., 2014a; Pan et al., 2009; Powell et al., 2019; Read et al., 2017; Rieder et al., 2015; Sekiya et al., 2015; Sharma et al., 2013). Interestingly, widespread expression of Ikzf4 has been reported in different organs including the CNS (Perdomo et al., 2000). One study has detailed the role of Ikzf4 in regulating expression of PSD-95 in adult cochlear afferent neurons (Bao et al., 2004). However, the function of Ikzf4 in the developing CNS remains elusive. Since there is also widespread expression of other Ikaros family members in the developing CNS, it is likely that other Ikaros family members can compensate for one another. Future studies on conditional knockouts of combination of Ikzf genes would be interesting to unravel the precise role of each Ikaros family member in other parts of the developing CNS.

3.4.4 Conclusions

Dynamic DNA binding and functional properties of widely expressed transcription factors in the developing CNS are poorly understood. In this study, we show that Ikzf4 utilizes a variety of DNA binding sites to control cone produciton during early and Müller glia production during late retinogenesis. Our results highlight a novel role of Ikzf4 in neuronal and glial specification in the developing CNS. These results provide mechanistic insights on how widely expressed transcription factors in neural progenitors alter cell fate specification in a temporal manner.

3.5 Figures and legends

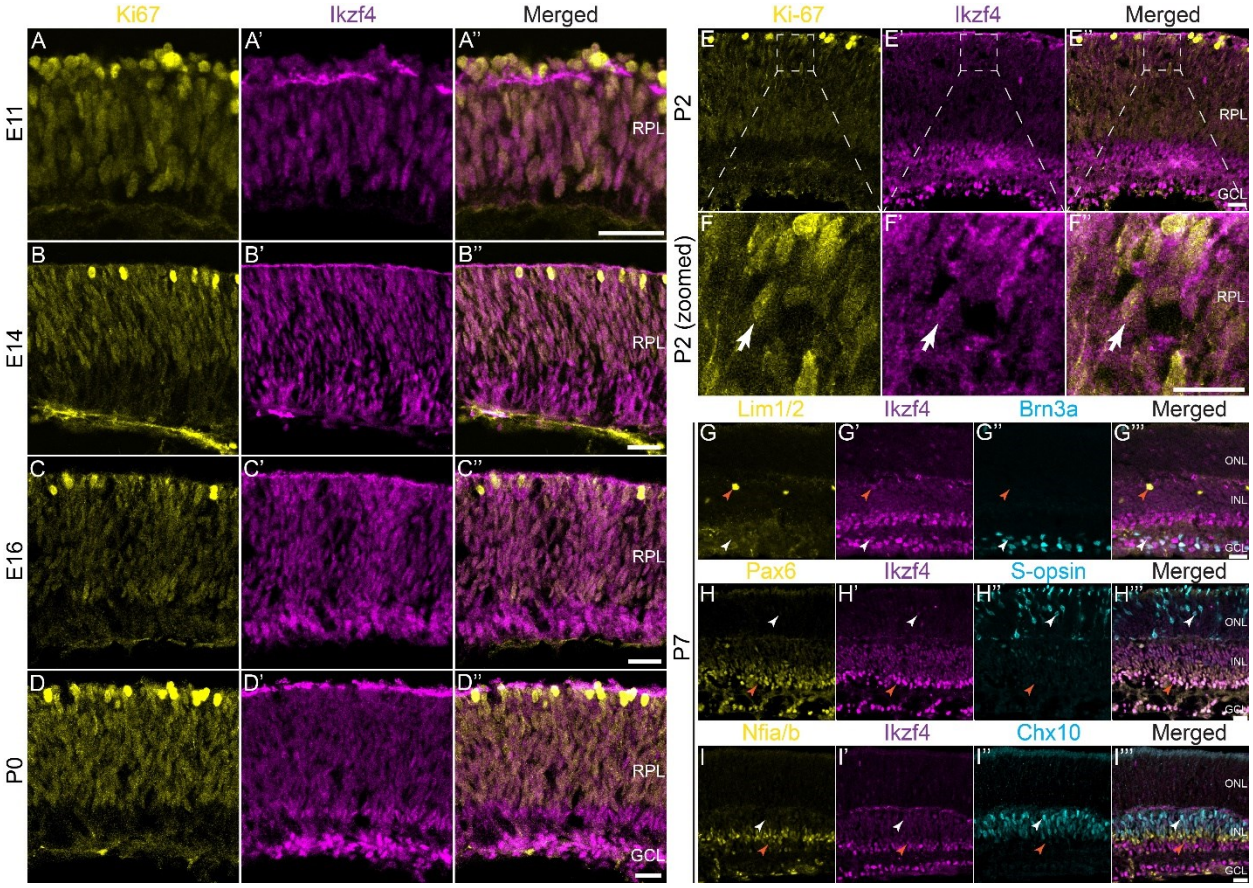

Figure 3.1: Ikzf4 is expressed during early and late retinogenesis. (A-E") Co-immunostaining of Ki67 (yellow) with Ikzf4 (magenta) at various stages of mouse retinal development. (F-F") Zoomed-in images of (E-E"), arrows show co-expression of Ki67 (yellow) and Ikzf4 (magenta) in some cells. (G-I''') Examples of P7 mouse retinas co-immunostained with Lim1/2 (G), Brn3a (G''), Pax6 (H), S-opsin (H''), Nfia/b (I) and Chx10 (I''). Orange arrows indicate Lim1/2^{+ve}Ikzf4^{+ve} (G-G'''), Pax6^{+ve}Ikzf4^{+ve}(H-H''') and Nfia/b^{+ve}Chx10^{-ve}Ikzf4^{+ve} (I-I'''). White arrows indicate Brn3a^{+ve}Ikzf4^{+ve} (G-G'''), S-opsin^{+ve}Ikzf4^{+ve}(H-H''') and Nfia/b^{-ve}Chx10^{+ve}Ikzf4^{+ve} (I-I'''). RPL: Retinal progenitor layer. ONL: Outer nuclear layer. INL: Inner nuclear layer. GCL: Ganglion cell layer. Scale bars: 20µm (A-E''), 10µm (F-I''').

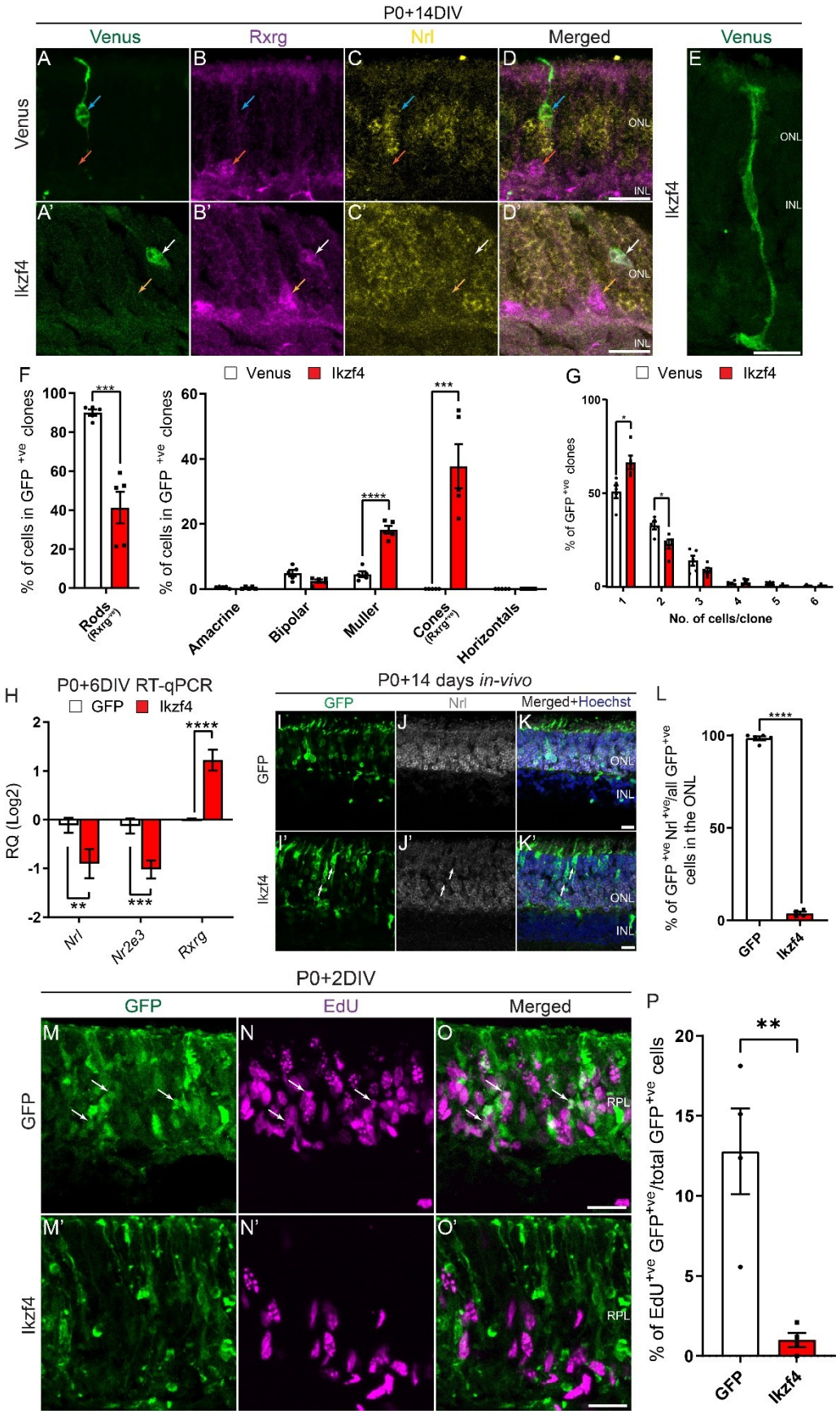
P0+14DIV
Venus
Rxrg
Nrl
Merged
Venus
Ikzf4
ONL
INL
F
Venus
Ikzf4
% of cells in GFP +ve clones
Rods (Rxrg+ve)
Amacrine
Bipolar
Muller
Cones (Rxrg+ve)
Horizontals
G
% of GFP +ve clones
No. of cells/clone
H
P0+6DIV RT-qPCR
GFP
Ikzf4
RQ (Log2)
Nrl
Nr2e3
Rxrg
P0+14 days in-vivo
GFP
Nrl
Merged+Hoechst
L
% of GFP +ve Nrl +ve/all GFP+ve cells in the ONL
P0+2DIV
EdU
RPL
P
% of EdU+ve GFP+ve/total GFP+ve cells

Figure 3.2: Ikzf4 promotes cones and Müller glia fate specification from late-stage RPCs. (A-D) Examples of retroviral infections of Venus (A-D) and Ikzf4-IRES-Venus (A'-D') co-immunostained with Rxrg (B-B') and Nrl (C-C') as cone and rods markers, respectively. (E) Example of Müller glia generated by Ikzf4 retroviral infection. (F-G) Retroviral clonal analysis of Venus control (469 clones counted) and Ikzf4-IRES-Venus (388 clones counted) overexpression in late-stage retinas (n=5). (F) Quantifications for cell type analysis was based on morphology and laminar positioning of the cell bodies in the retina. Cones ($Rxrg^{+ve}$) and rods ($Rxrg^{-ve}$) were counted in the ONL based on Rxrg expression. (G) Quantifications on the number of cells per clone presented in (F). (H) RT-qPCR analysis of *Nrl*, *Nr2e3* and *Rxrg* expression from sorted GFP^{+ve} cells 6 days after electroporation of P0 retinal explants with either GFP (n=5) or Ikzf4-IRES-GFP (n=5). (I-L) Examples of *in vivo* electroporations of either GFP (n=4) or Ikzf4-IRES-GFP (n=4) at P0 retinas and immunostained for Nrl (J-J') 14 days after electroporation. (L) Quantification of the number of $GFP^{+ve}Nrl^{+ve}$ cells presented in (I-K'). (M-P) Examples of P0 retinal explants electroporations of either GFP (n=4) or Ikzf4-IRES-GFP (n=4) with 30µM EdU added to the medium 2 days later. Retinal explants were immunostained with EdU after fixation. (P) Quantifications of the number of $EdU^{+ve}GFP^{+ve}$ cells presented in (M-O'). *$p<0.05$, **$p<0.01$, ***$p<0.001$, ****$p<0.0001$. Statistics: Two-tailed unpaired t-test (F-G, L, P), Mann-Whitney test (H). RPL: Retinal progenitor layer. ONL: Outer nuclear layer. INL: Inner nuclear layer. RQ: Relative quantitation. Scale bars: 10µm (A-E, I-K', M-O').

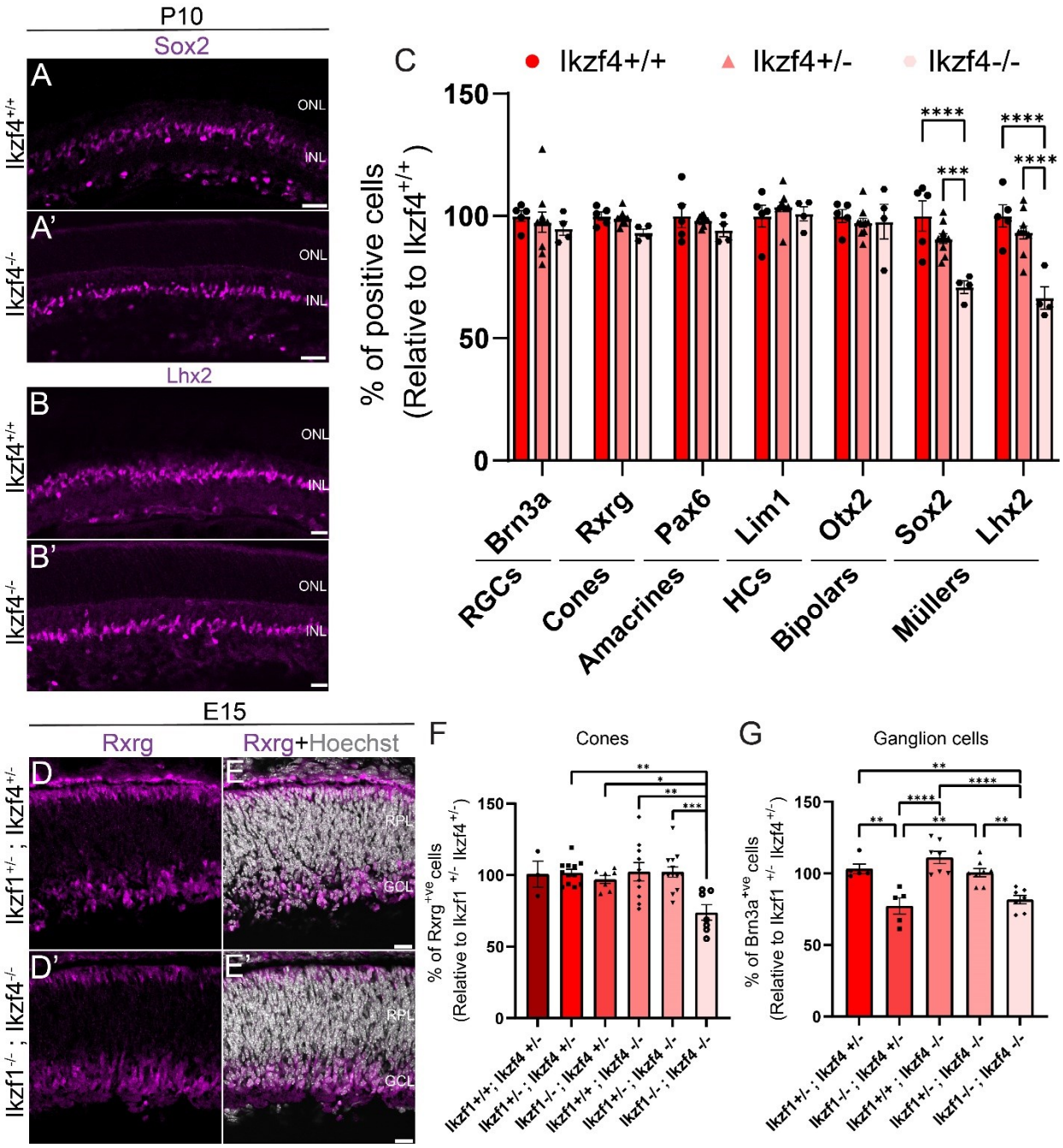
P10
Sox2
A
ONL
INL
Ikzf4+/+
A'
Ikzf4-/-
Lhx2
B
B'
C
Ikzf4+/+
Ikzf4+/-
Ikzf4-/-
% of positive cells
(Relative to Ikzf4+/+)
150
100
50
0
****
***
Brn3a
Rxrg
Pax6
Lim1
Otx2
Sox2
Lhx2
RGCs
Cones
Amacrines
HCs
Bipolars
Müllers
E15
Rxrg
Rxrg+Hoechst
D
E
RPL
GCL
Ikzf1+/- ; Ikzf4+/-
D'
E'
Ikzf1-/- ; Ikzf4-/-
F
Cones
% of Rxrg+ve cells
(Relative to Ikzf1 +/- Ikzf4+/-)
Ikzf1+/+; Ikzf4 +/-
Ikzf1+/- ; Ikzf4 +/-
Ikzf1-/- ; Ikzf4 +/-
Ikzf1+/+ ; Ikzf4 -/-
Ikzf1+/- ; Ikzf4 -/-
Ikzf1-/- ; Ikzf4 -/-
G
Ganglion cells
% of Brn3a+ve cells
(Relative to Ikzf1 +/- Ikzf4+/-)

Figure 3.3: Ikzf4 is required for cone fate during early retinogenesis and Müller glia during late retinogenesis. (A-C) Examples of Sox2 (A-A') and Lhx2 (B-B') immunostaining in either Ikzf4$^{+/+}$ (A-B) or Ikzf4$^{-/-}$ (A'-B') mouse retinas at P10. (C) Quantifications of various retinal cell types using specific markers in either Ikzf4$^{+/+}$ (n=5), Ikzf4$^{+/-}$ (n=7) or Ikzf4$^{-/-}$ (n=4) mouse retinas. (D-E') Examples of Rxrg (D-D') immunostaining in either Ikzf1$^{+/-}$Ikzf4$^{+/-}$(D-E) or Ikzf1$^{-/-}$Ikzf4$^{-/-}$ (D'-E') mouse retinas at E15. (F) Quantifications of Rxrg^{+ve} cells in either Ikzf1$^{+/+}$Ikzf4$^{+/-}$(n=3), Ikzf1$^{+/-}$Ikzf4$^{+/-}$(n=12), Ikzf1$^{-/-}$Ikzf4$^{+/-}$(n=7), Ikzf1$^{+/+}$Ikzf4$^{-/-}$(n=10), Ikzf1$^{+/-}$Ikzf4$^{+/-}$(n=13) or Ikzf1$^{-/-}$ Ikzf4$^{-/-}$(n=7) mouse retinas. (G) Quantifications of Brn3a^{+ve} cells in either Ikzf1$^{+/-}$Ikzf4$^{+/-}$(n=5), Ikzf1$^{-/-}$Ikzf4$^{+/-}$(n=5), Ikzf1$^{+/+}$Ikzf4$^{-/-}$(n=7), Ikzf1$^{+/-}$Ikzf4$^{+/-}$(n=8) or Ikzf1$^{-/-}$Ikzf4$^{-/-}$(n=7) mouse retinas. *$p<0.05$, **$p<0.01$, ***$p<0.001$, ****$p<0.0001$. Statistics: One-way ANOVA with Tukey correction (C, F-G). RPL: Retinal progenitor layer. ONL: Outer nuclear layer. INL: Inner nuclear layer. GCL: Ganglion cell layer. Scale bars: 10µm (A-B', D-E').

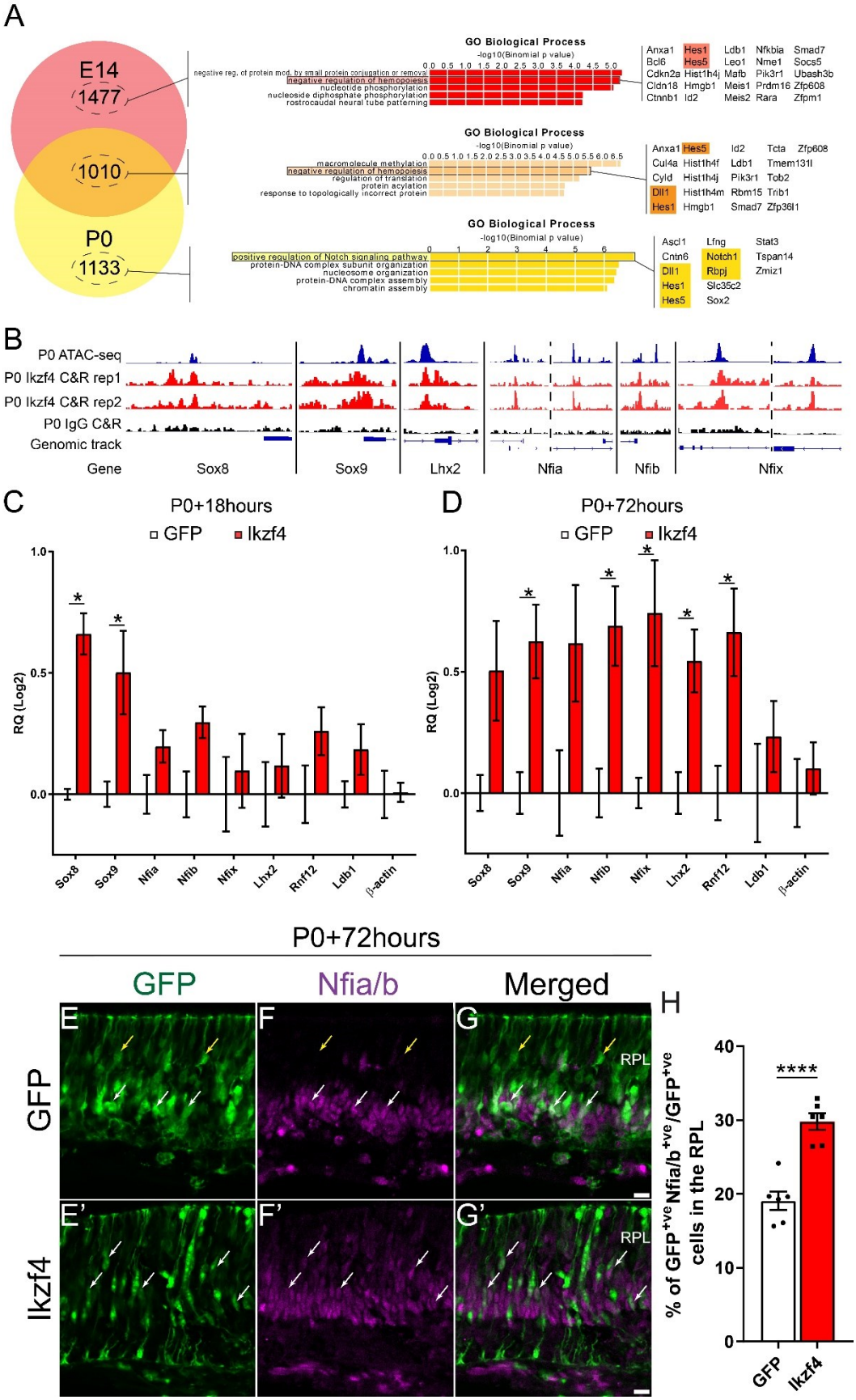
A
E14
1477
1010
P0
1133
GO Biological Process
-log10(Binomial p value)
negative reg. of protein mod. by small protein conjugation or removal
negative regulation of hemopoiesis
nucleotide phosphorylation
nucleoside diphosphate phosphorylation
rostrocaudal neural tube patterning
Anxa1 Hes1 Ldb1 Nfkbia Smad7
Bcl6 Hes5 Leo1 Nme1 Socs5
Cdkn2a Hist1h4j Mafb Pik3r1 Ubash3b
Cldn18 Hmgb1 Meis1 Prdm16 Zfp608
Ctnnb1 Id2 Meis2 Rara Zfpm1
GO Biological Process
-log10(Binomial p value)
macromolecule methylation
negative regulation of hemopoiesis
regulation of translation
protein acylation
response to topologically incorrect protein
Anxa1 Hes5 Id2 Tcta Zfp608
Cul4a Hist1h4f Ldb1 Tmem131l
Cyld Hist1h4j Pik3r1 Tob2
Dll1 Hist1h4m Rbm15 Trib1
Hes1 Hmgb1 Smad7 Zfp36l1
GO Biological Process
-log10(Binomial p value)
positive regulation of Notch signaling pathway
protein-DNA complex subunit organization
nucleosome organization
protein-DNA complex assembly
chromatin assembly
Ascl1 Lfng Stat3
Cntn6 Notch1 Tspan14
Dll1 Rbpj Zmiz1
Hes1 Slc35c2
Hes5 Sox2
B
P0 ATAC-seq
P0 Ikzf4 C&R rep1
P0 Ikzf4 C&R rep2
P0 IgG C&R
Genomic track
Gene
Sox8
Sox9
Lhx2
Nfia
Nfib
Nfix
C
P0+18hours
GFP
Ikzf4
RQ (Log2)
Sox8
Sox9
Nfia
Nfib
Nfix
Lhx2
Rnf12
Ldb1
β-actin
D
P0+72hours
GFP
Ikzf4
RQ (Log2)
Sox8
Sox9
Nfia
Nfib
Nfix
Lhx2
Rnf12
Ldb1
β-actin
P0+72hours
GFP
Nfia/b
Merged
E
F
G
RPL
GFP
E'
F'
G'
RPL
Ikzf4
H
% of GFP+ve Nfia/b+ve/GFP+ve cells in the RPL
****
GFP
Ikzf4

Figure 3.4: Ikzf4 binds to regions close to notch signaling and Müller specification genes during retinogenesis. (A) Venn diagram representing the overlap of the number of Ikzf4 CUT&RUN binding peaks between E14 and P0. Gene Ontology classification of the genes in proximity of Ikzf4 binding peaks. GO terms and associated notch signaling genes in the list are highlighted and displayed on the right. (B) Genomic peaks of P0 ATAC-seq (Aldiri et al., 2017), P0 Ikzf4 CUT&RUN replicate 1, P0 Ikzf4 CUT&RUN replicate 2, P0 IgG CUT&RUN at genomic tracks of Nfia family members. (C-D) RT-qPCR analysis of Müller specification gene expression from sorted GFP^{+ve} cells either 18 (C) or 72hours (D) after electroporation of P0 retinas with either GFP (n=5) or Ikzf4-IRES-GFP (n=5). (E-G') Examples of GFP or Ikzf4-IRES-GFP electroporations at P0 and immunostained for Nfia/b 72 hours later. (H) Quantifications of $GFP^{+ve}Nfia/b^{+ve}$ cells 72 hours after GFP (n=6) or Ikzf4-IRES-GFP (n=6) electroporation in P0 retinas. *$p<0.05$, ****$p<0.0001$. Statistics: Mann-Whitney test (C). Two-tailed unpaired t-test (G). RPL: Retinal progenitor layer. RQ: Relative quantitation. Scale bars: 10µm (D-F').

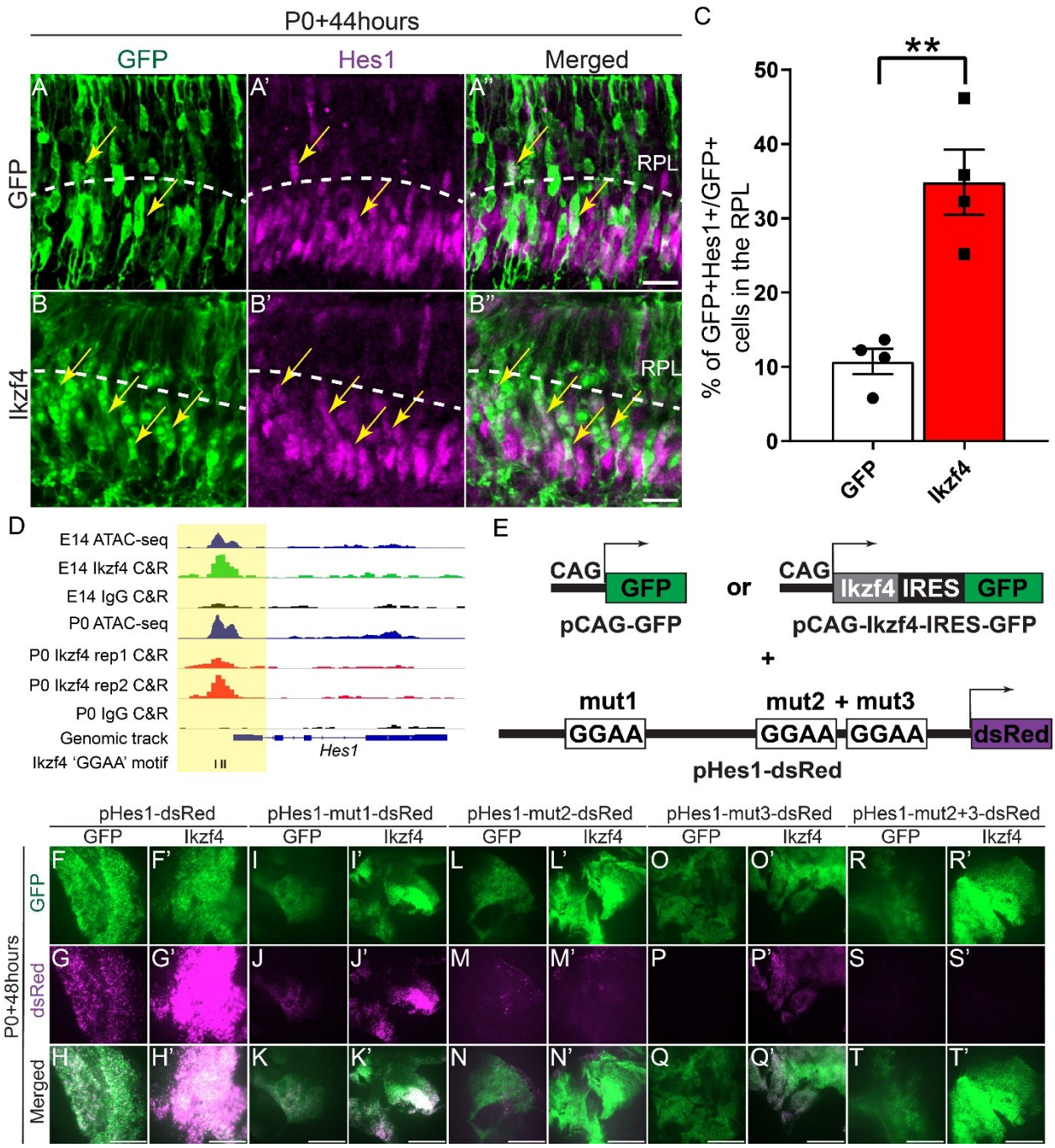
P0+44hours
GFP
Hes1
Merged
A
A'
A''
B
B'
B''
RPL
Ikzf4
C
**
% of GFP+Hes1+/GFP+ cells in the RPL
0
10
20
30
40
50
GFP
Ikzf4
D
E14 ATAC-seq
E14 Ikzf4 C&R
E14 IgG C&R
P0 ATAC-seq
P0 Ikzf4 rep1 C&R
P0 Ikzf4 rep2 C&R
P0 IgG C&R
Genomic track
Ikzf4 'GGAA' motif
Hes1
E
CAG
GFP
pCAG-GFP
or
CAG
Ikzf4
IRES
GFP
pCAG-Ikzf4-IRES-GFP
+
mut1
GGAA
mut2 + mut3
GGAA
GGAA
dsRed
pHes1-dsRed
pHes1-dsRed
pHes1-mut1-dsRed
pHes1-mut2-dsRed
pHes1-mut3-dsRed
pHes1-mut2+3-dsRed
GFP
Ikzf4
P0+48hours
GFP
dsRed
Merged
F
F'
I
I'
L
L'
O
O'
R
R'
G
G'
J
J'
M
M'
P
P'
S
S'
H
H'
K
K'
N
N'
Q
Q'
T
T'

Figure 3.5: Ikzf4 binds and upregulates promoter of Hes1 and its expression. (A) Examples of GFP or Ikzf4-IRES-GFP electroporated P0 retinas and immunostained with Hes1 44 hours later. Yellow arrows indicate $GFP^{+ve}Hes1^{+ve}$ cells in the RPL. (C) Quantification of $GFP^{+ve}Hes1^{+ve}$ cells in the RPL at P0+44 hours after electroporation with either GFP (n=4), or Ikzf4-IRES-GFP (n=4). (D) Genomic peaks of E14 ATAC-seq in (blue) (Aldiri et al., 2017), E14 Ikzf4 CUT&RUN (green), E14 IgG CUT&RUN (black), P0 ATAC-seq (blue) (Aldiri et al., 2017), P0 Ikzf4 CUT&RUN replicate 1 (red), P0 Ikzf4 CUT&RUN replicate 2 (red) and P0 IgG CUT&RUN (black) at Hes1 promoter. Ikzf4 motif 'GGAA' are denoted as black bars. Yellow highlighted area is 500bp around the promoter region of Hes1. (E) Schematic representation of experiment shown in (F-T'). Retinal explants were co-electroporated with either pCAG-GFP or pCAG-Ikzf4-IRES-GFP along with vectors expressing dsRed under the control of either WT Hes promoter (pHes1-dsRed), Hes1 promoter with mutation at first 'GGAA' site (mut1), second 'GGAA' site (mut2), third 'GGAA' (mut3) site and second and third GGAA mutations together (mut2+mut3). (F-T') Photomicrographs of retinal flatmounts showing increase in dsRed expression when Ikzf4-IRES-GFP is co-electroporated with either pHes1-dsRed (F'-H'), pHes1-mut1-dsRed (I'-K'), pHes1-mut2-dsRed (L'-N'), pHes1-mut3-dsRed (O'-Q') but not with pHes1-mut2+3-dsRed (R'-T') compared to the control GFP (F-G, I-K, L-N, O-Q, R-T). Statistics: Two tailed unpaired t-test (C). **$p<0.01$. RPL: Retinal progenitor layer. Scale bars: 10µm (A-B"), 250µm (F-T').

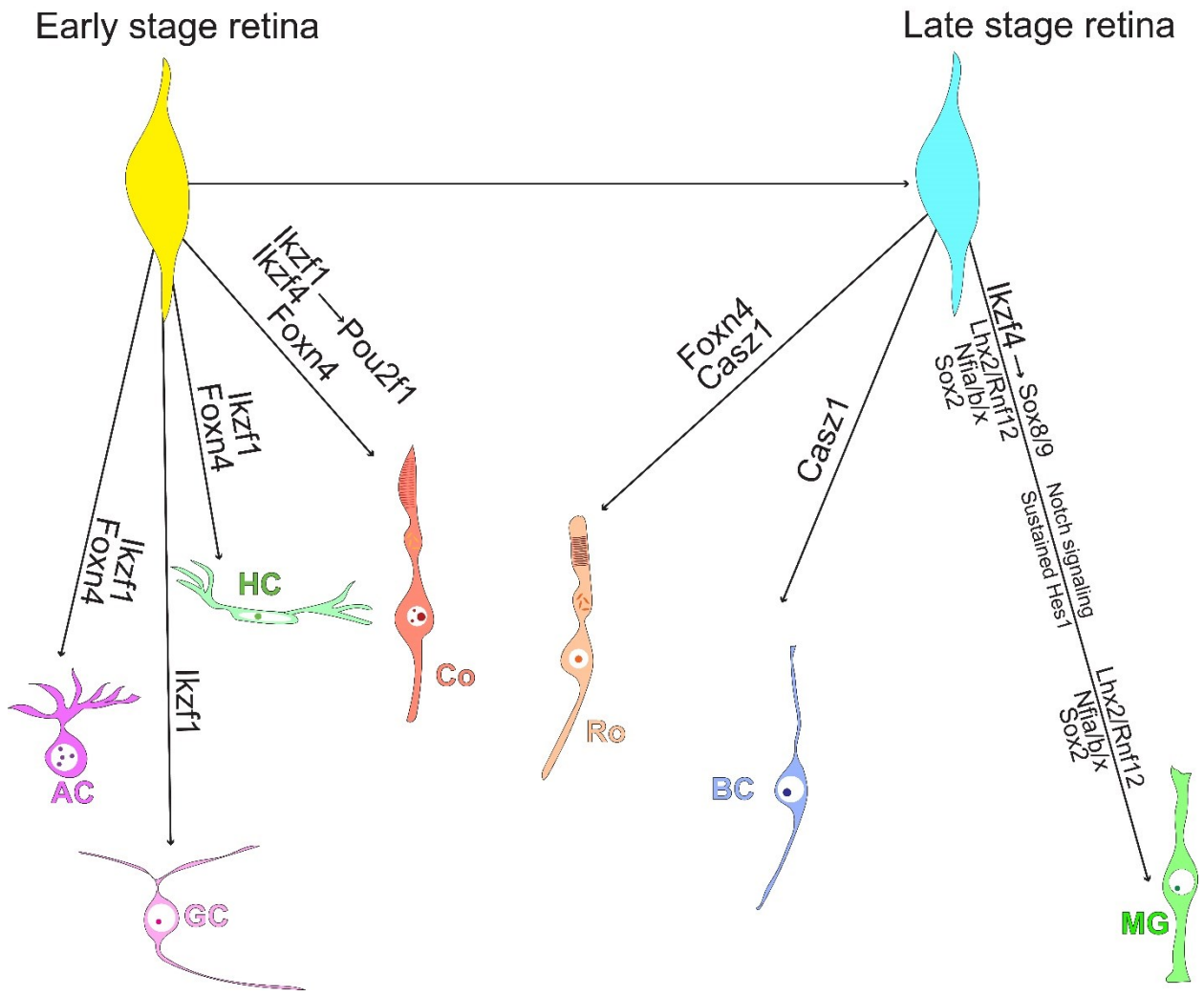

Figure 3.6: Model of cell fate determination in RPCs during mouse retinogenesis. In early RPCs, Ikzf4 functions redundantly with Ikzf1 as a regulator of temporal identity gene Pou2f1 and its downstream factor Pou2f2. In late RPCs, Ikzf4 acts as a classical fate determinant by binding and upregulating expression of Müller specification genes as well as instigating the maintenance of notch signaling to ensure the Müller glia fate commitment.

3.6 Supplementary figures and legends

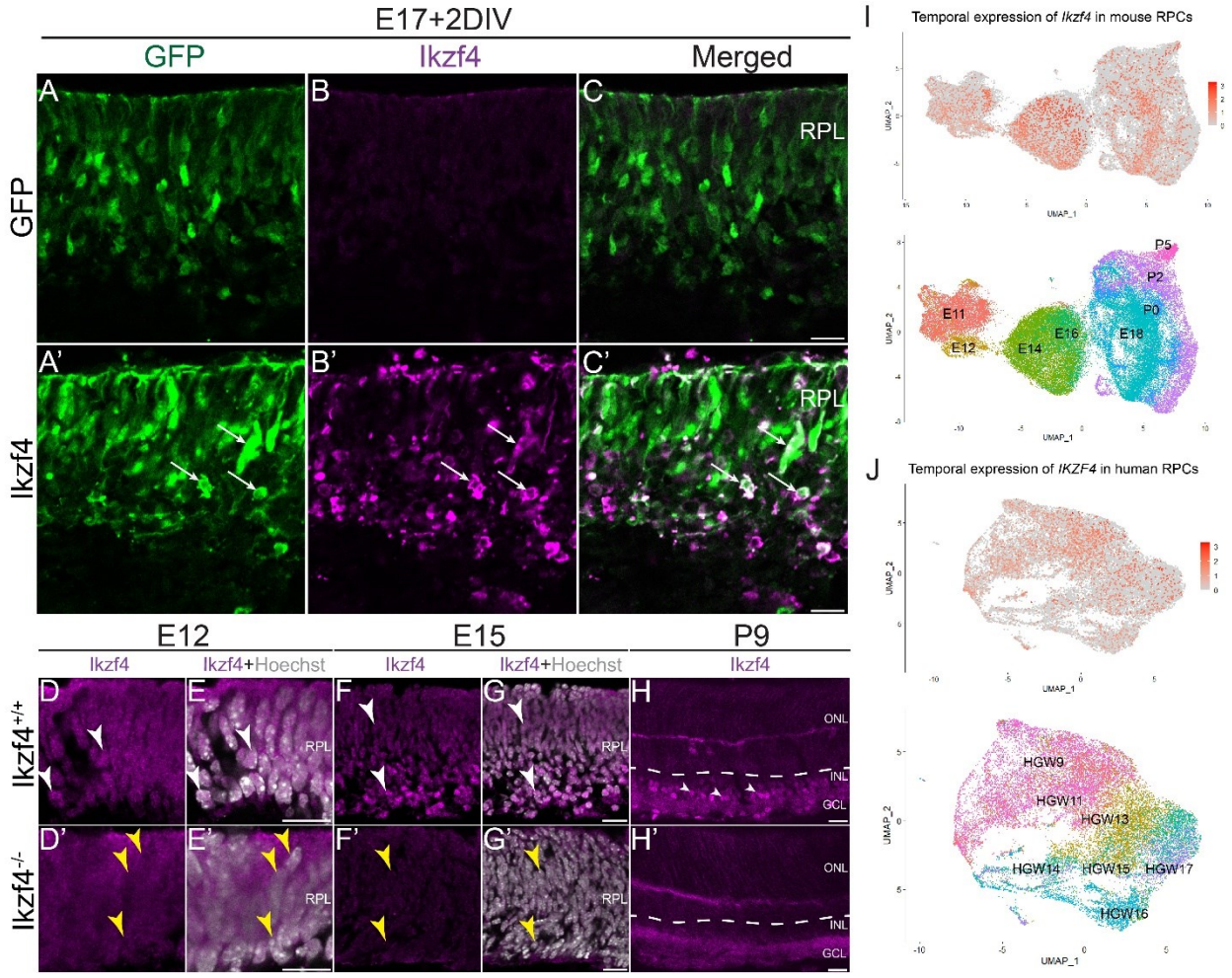

Figure S3.1: Specificity of Ikzf4 antibody and scRNA-seq re-analysis of human and mouse RPCs. (A-C') Examples of electroporation of either GFP (A-C) or Ikzf4-IRES-GFP (A'-C') in E17 retinas and immunostained with Ikzf4 antibody 2 days later. White arrows indicate $GFP^{+ve}Ikzf4^{+ve}$ cells. (D-H') Validation of the Ikzf4 antibody in $Ikzf4^{+/+}$ retinas (D-H) compared to $Ikzf4^{-/-}$ retinas (D'-H') at E12 (D-E'), E15 (F-G') and P9 (H-H'). White arrows show $Ikzf4^{+ve}$ cells with nuclear immunostaining and yellow arrow indicate absence of nuclear immunostaining. (I-J) Re-analysis of previously published Single cell RNA-seq datasets from mouse (Clark et al. 2019) and human fetal (Lu et al. 2020) retinas. RPL: Retinal progenitor layer. ONL: Outer nuclear layer. INL: Inner nuclear layer. GCL: Ganglion cell layer. Scale bars: 10µm (A-H').

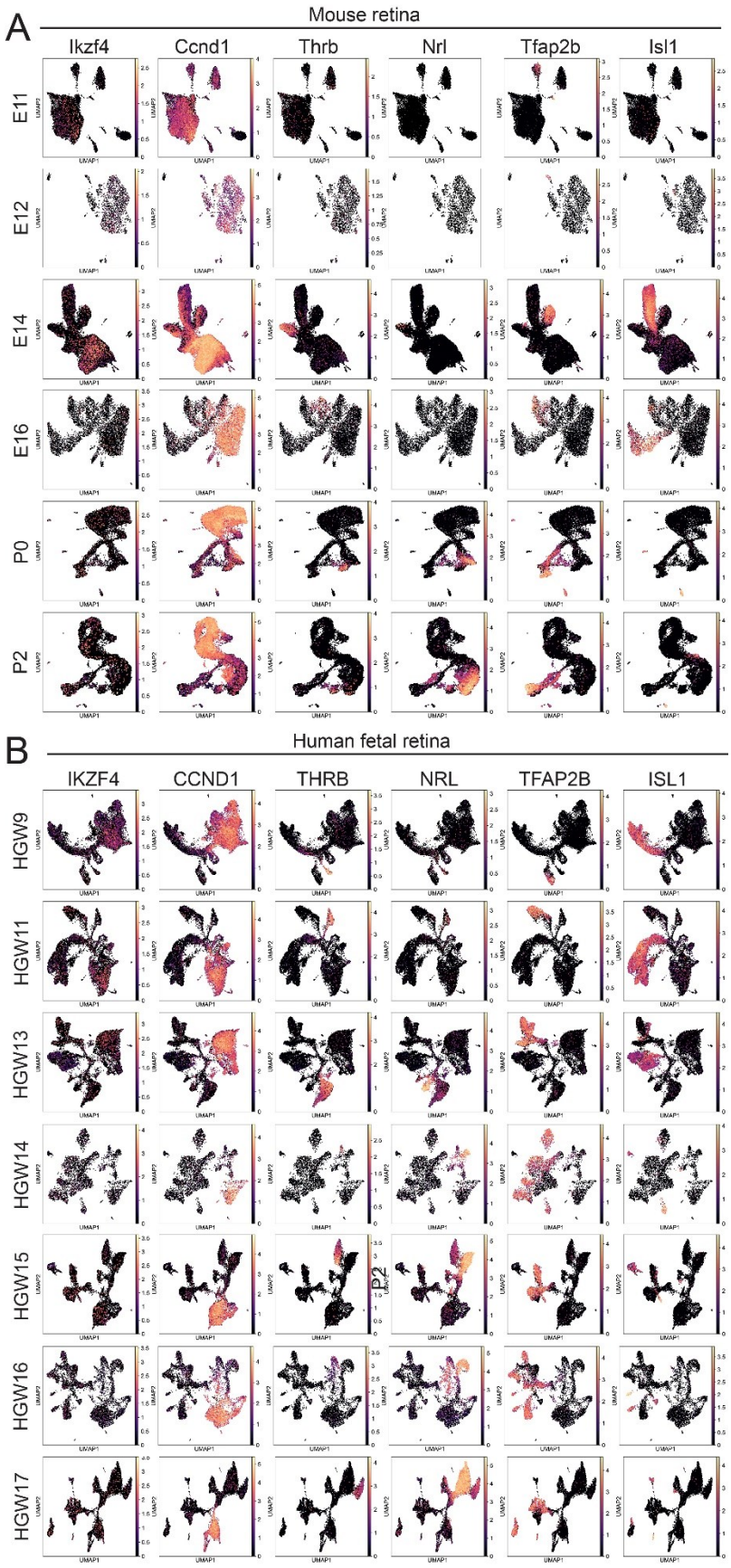
A
Mouse retina
Ikzf4
Ccnd1
Thrb
Nrl
Tfap2b
Isl1
E11
E12
E14
E16
P0
P2
B
Human fetal retina
IKZF4
CCND1
THRB
NRL
TFAP2B
ISL1
HGW9
HGW11
HGW13
HGW14
HGW15
HGW16
HGW17
UMAP1
UMAP2

Figure S3.2: Ikzf4 is expressed in the early and late retina during mouse and human retinogenesis. (A) *Ikzf4* mRNA expression during early to late mouse retinogenesis in RPCs (Ccnd1), cones (Thrb), rods (Nrl), amacrines and horizontal cells (Tfap2b) and RGCs (Isl1). (B) *IKZF4* mRNA expression during early to late human fetal retinogenesis in RPCs (CCND1), cones (THRB), rods (NRL), amacrines and horizontal cells (TFAP2B) and RGCs (ISL1).

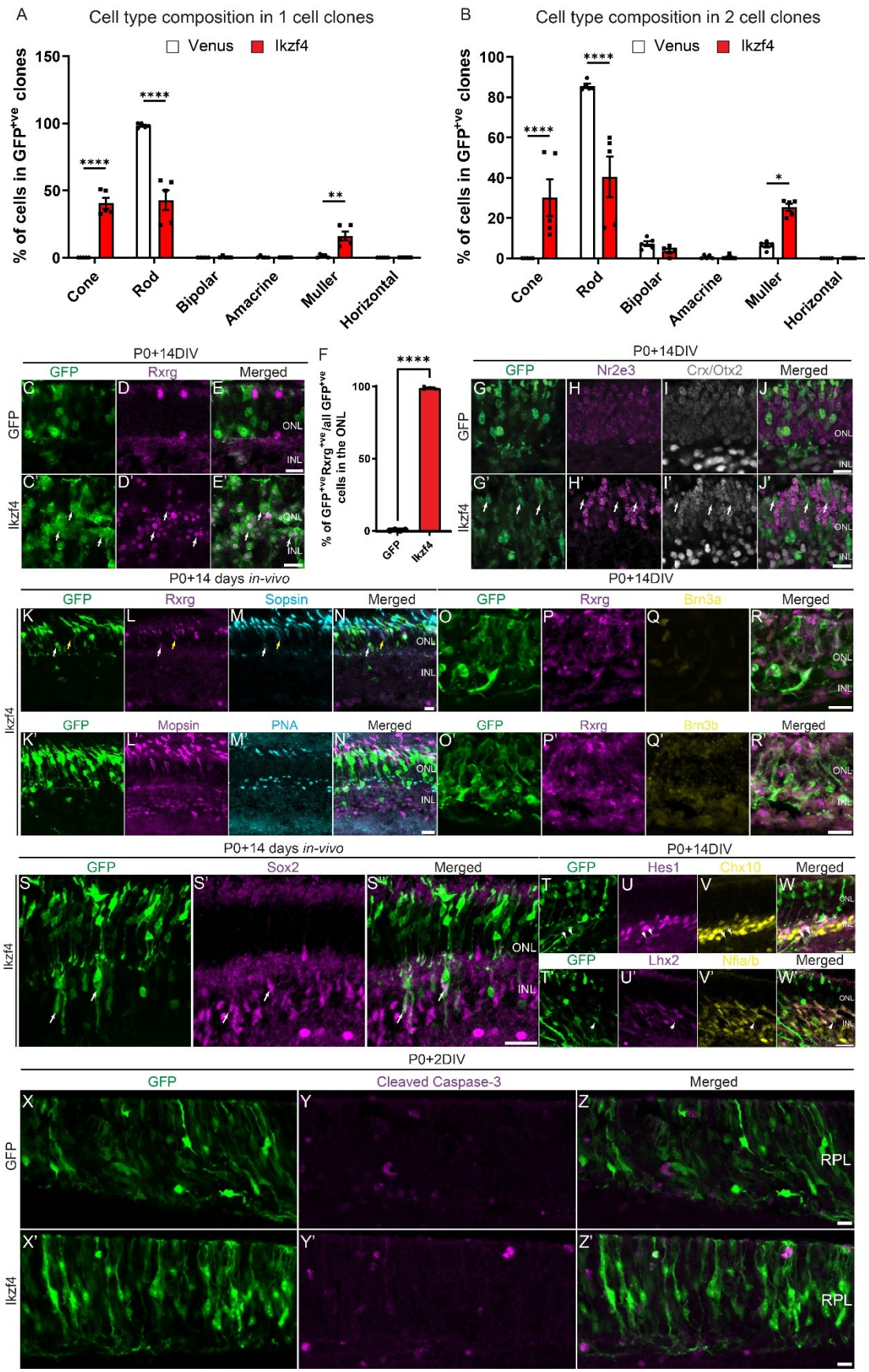
A
Cell type composition in 1 cell clones
Venus
Ikzf4
% of cells in GFP+ve clones
Cone
Rod
Bipolar
Amacrine
Muller
Horizontal
B
Cell type composition in 2 cell clones
F
% of GFP+ve Rxrg+ve/all GFP+ve cells in the ONL
P0+14DIV
P0+14 days in-vivo
P0+2DIV
GFP
Rxrg
Merged
Nr2e3
Crx/Otx2
Sopsin
Brn3a
Mopsin
PNA
Brn3b
Sox2
Hes1
Chx10
Lhx2
Nfia/b
Cleaved Caspase-3
ONL
INL
RPL

Figure S3.3: Ikzf4 promotes cones and Müller glia from late RPCs by inducing early cell cycle exit rather than apoptosis. (A-B) Retroviral clonal analysis of Venus or Ikzf4 as shown in (Fig. 3.2A-G) focusing on cell type composition of 1 cell (A) or 2 cell (B) clones. (C-J') Examples of retinal explants electroporated at P0 with either GFP (C-E) or Ikzf4-IRES-GFP (C'-E') and immunostained with Rxrg (D-D') 14 days later. White arrows denote electroporated cells expressing Rxrg (F) Quantification of retinal explants electroporated with either GFP (n=4) or Ikzf4-IRES-GFP (n=4). (G-J') Examples of retinal explants electroporated at P0 with either GFP (G-J) or Ikzf4-IRES-GFP (G'-J') and immunostained with Nr2e3 (H-H') or Crx/Otx2 (I-I') after 14 days of culture. White arrows represent electroporated cells without Nr2e3 and with Crx/Otx2 expression. (K-N') Examples of *in vivo* electroporations at P0 with Ikzf4-IRES-GFP (K-N') and immunostained 14 days later with Rxrg (L), S-opsin (M), M-opsin (L') or PNA (M'). White arrows denote $GFP^{+ve}Rxrg^{+ve}S\text{-}opsin^{-ve}$ cells whereas yellow arrow represent endogenous non-eletroporated $Rxrg^{+ve}S\text{-}opsin^{+ve}$ cones. (O-R') Examples of Ikzf4-IRES-GFP (O-R') electroporations of retinal explants at P0 and co-immunostained Rxrg (P-P') with either Brn3a (Q) or Brn3b (Q'). (S-S'') Examples of *in vivo* electroporation of P0 retinas with Ikzf4-IRES-GFP (S-S'') and immunostained with Sox2 (S') 14 days later. (T-W') Examples of retinal explants electroporated at P0 with Ikzf4-IRES-GFP (T-W') and immunostained with Hes1 (U), Chx10 (V), Lhx2 (U') or Nfia/b (V'). White arrows represent either $Hes1^{+ve}Chx10^{-ve}$ cells (T-W) or $Lhx2^{+ve}Nfia/b^{+ve}$ cells (T'-W'). (X-Z') Examples of retinal explants electroporated at P0 with either GFP (X-Z) or Ikzf4-IRES-GFP (X'-Z') and immunostained with Cleaved Caspase-3 (Y-Y') 2 days later. *$p<0.05$, **$p<0.01$, ****$p<0.0001$. Statistics: Two tailed unpaired t-test (A-B, F). ONL: Outer nuclear layer. INL: Inner nuclear layer. RPL: Retinal progenitor layer. Scale bars: 10µm (C-E', G-R', T-W'), 20µm (S-S'').

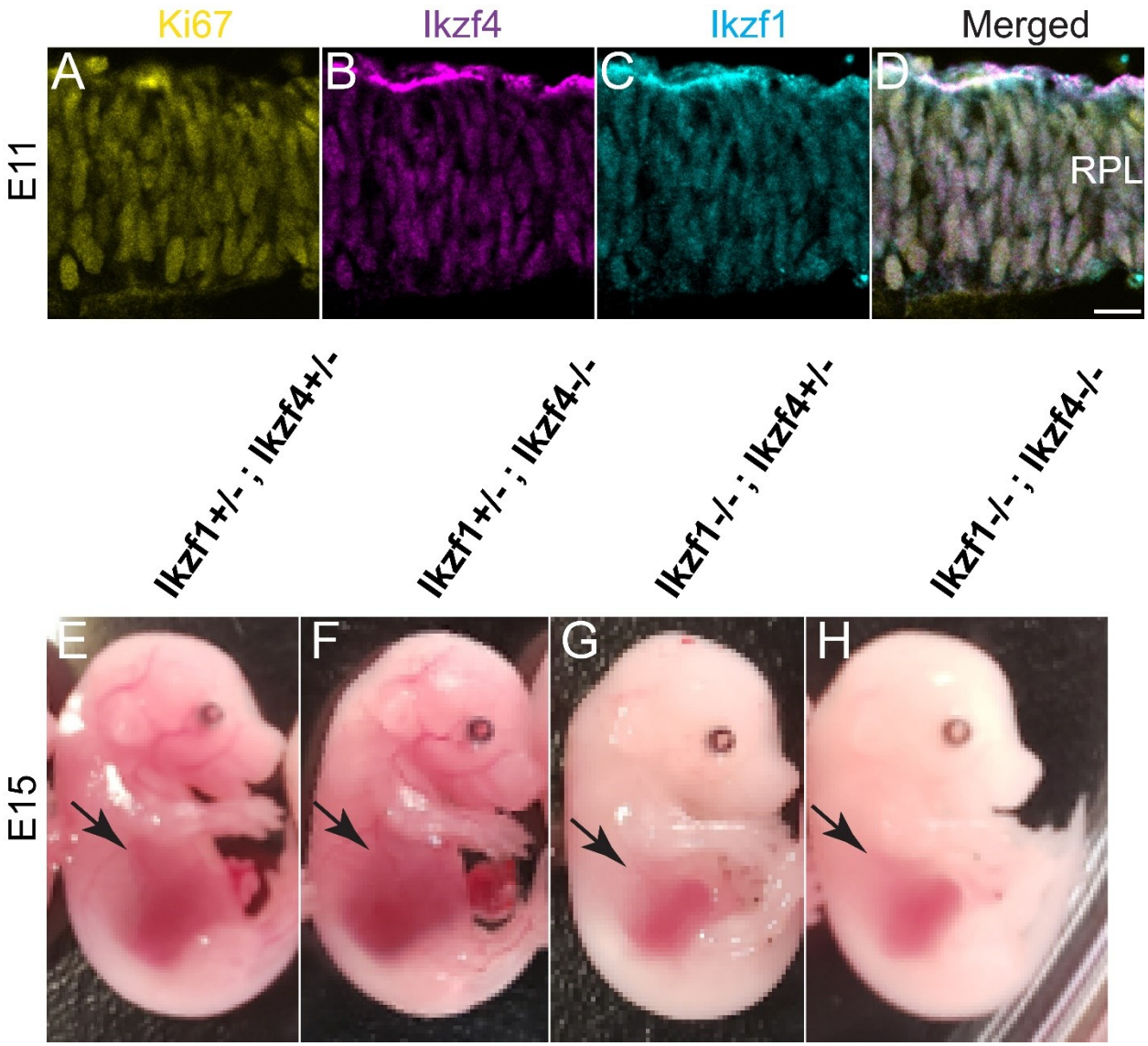

Figure S3.4: Ikzf1 and Ikzf4 are expressed in the same cells during early retinogenesis and redundantly required for fetal liver size. (A-D) Co-immunostaining of Ki67 (A), Ikzf4 (B), Ikzf1 (C) in E11 retinas. (E-H) Examples of E15 embryos with genotypes, Ikzf1$^{+/-}$;Ikzf4$^{+/-}$ (E), Ikzf1$^{+/-}$;Ikzf4$^{-/-}$ (F), Ikzf1$^{-/-}$;Ikzf4$^{+/-}$(G) or Ikzf1$^{-/-}$;Ikzf4$^{-/-}$ (H). Black arrows denote the fetal liver. RPL: Retinal progenitor layer. Scale bars: 10μm.

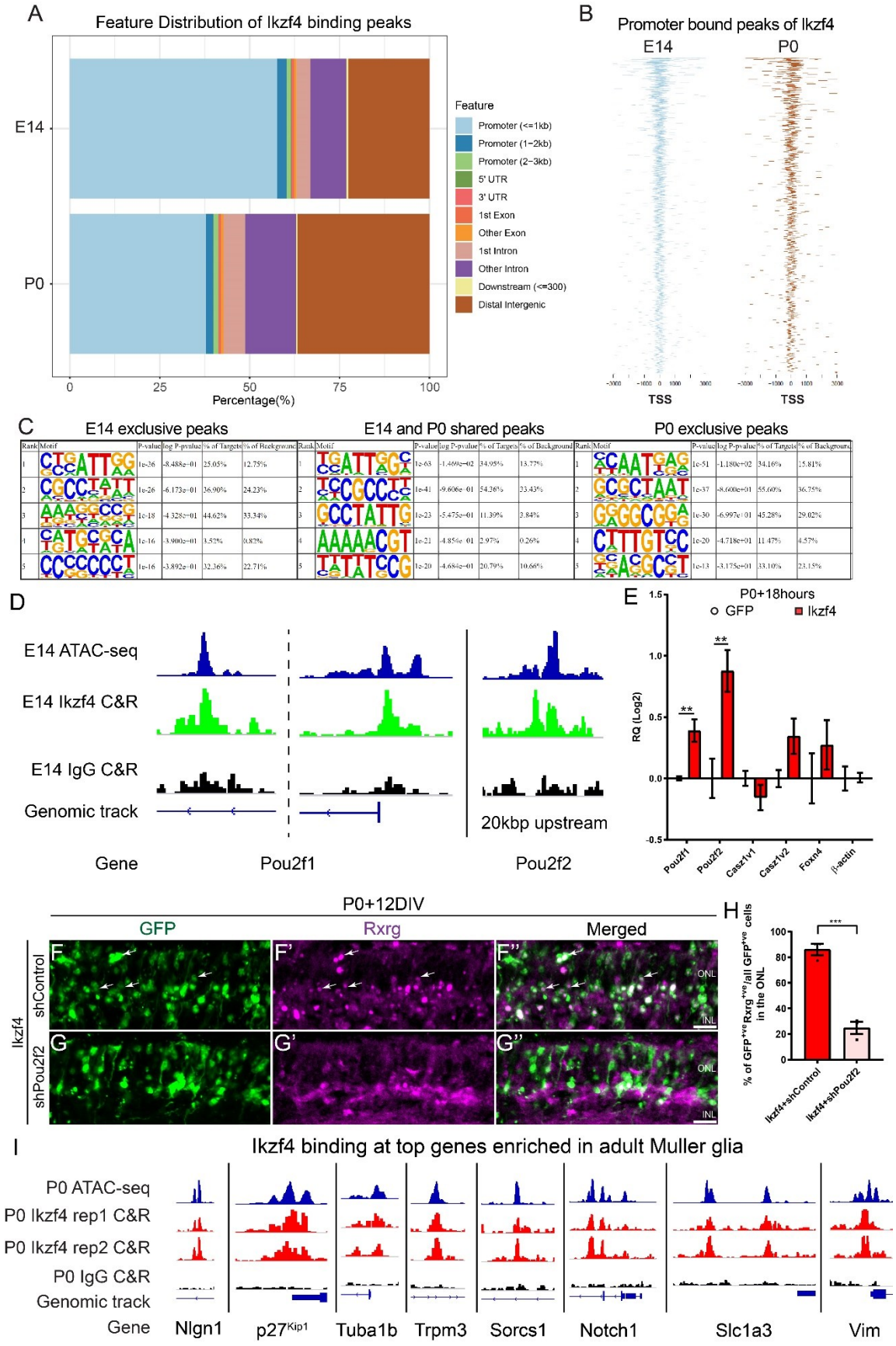
A
Feature Distribution of Ikzf4 binding peaks
E14
P0
Feature
Promoter (<=1kb)
Promoter (1~2kb)
Promoter (2~3kb)
5' UTR
3' UTR
1st Exon
Other Exon
1st Intron
Other Intron
Downstream (<=300)
Distal Intergenic
0
25
50
75
100
Percentage(%)
B
Promoter bound peaks of Ikzf4
E14
P0
TSS
TSS
C
E14 exclusive peaks
E14 and P0 shared peaks
P0 exclusive peaks
D
E14 ATAC-seq
E14 Ikzf4 C&R
E14 IgG C&R
Genomic track
Gene
Pou2f1
Pou2f2
20kbp upstream
E
P0+18hours
GFP
Ikzf4
RQ (Log2)
Pou2f1
Pou2f2
Casz1v1
Casz1v2
Foxn4
β-actin
P0+12DIV
GFP
Rxrg
Merged
Ikzf4
shControl
shPou2f2
F
F'
F''
G
G'
G''
ONL
INL
H
% of GFP+ve Rxrg+ve/all GFP+ve cells in the ONL
Ikzf4+shControl
Ikzf4+shPou2f2
I
Ikzf4 binding at top genes enriched in adult Muller glia
P0 ATAC-seq
P0 Ikzf4 rep1 C&R
P0 Ikzf4 rep2 C&R
P0 IgG C&R
Genomic track
Gene
Nlgn1
p27Kip1
Tuba1b
Trpm3
Sorcs1
Notch1
Slc1a3
Vim

Figure S3.5: Ikzf4 binds and upregulates Pou2f1/2 during retinal development and Müller glia specification genes during late retinogenesis. (A-B) ChIP-seeker genomic annotation of the Ikzf4 CUT&RUN peaks at E14 and P0 across the entire genome (A) or at promoters (B). (C) HOMER analysis of Ikzf4 CUT&RUN peaks exclusively present at E14, both E14 and P0, or exclusively present at P0. (D) Genomic tracks of ATAC-seq at E14 in blue (Aldiri et al. 2017), Ikzf4 CUT&RUN at E14 in green, IgG Control CUT&RUN at E14 in black at genomic location of promoter or intronic region of Pou2f1, or 20kbp upstream from the Pou2f2 promoter. (E) RT-qPCR analysis of *Pou2f1*, *Pou2f2*, *Casz1v1*, *Casz1v2*, *Foxn4* or *β-actin* from sorted GFP^{+ve} cells 18hours after electroporation of P0 retinal explants with either GFP (n=5) or Ikzf4 (n=5). (F-G'') Examples of retinal explants electroporated at P0 with Ikzf4-IRES-GFP and either shControl (n=3) or shPou2f2 (n=3) and immunostained for Rxrg. White arrows indicate $GFP^{+ve}Rxrg^{+ve}$ cells in the ONL. (H) Quantification of $GFP^{+ve}Rxrg^{+ve}$ cells in the ONL as shown in (F-G''). (I) Genomic tracks of ATAC-seq at P0 in blue (Aldiri et al. 2017), two replicates of Ikzf4 CUT&RUN at P0 in red, or IgG Control CUT&RUN at P0 in black at genomic location of Müller glia genes enriched in scRNA-seq dataset of P14 mouse retinas (Clark et al. 2019). Statistics: Mann-Whitney test (E), Two-tailed unpaired t-test (H). TSS: Transcription start site. RQ: Relative quantitation. Kbp: Kilo base pair. ONL: Outer nuclear layer. INL: Inner nuclear layer. Scale bars: 10µm.

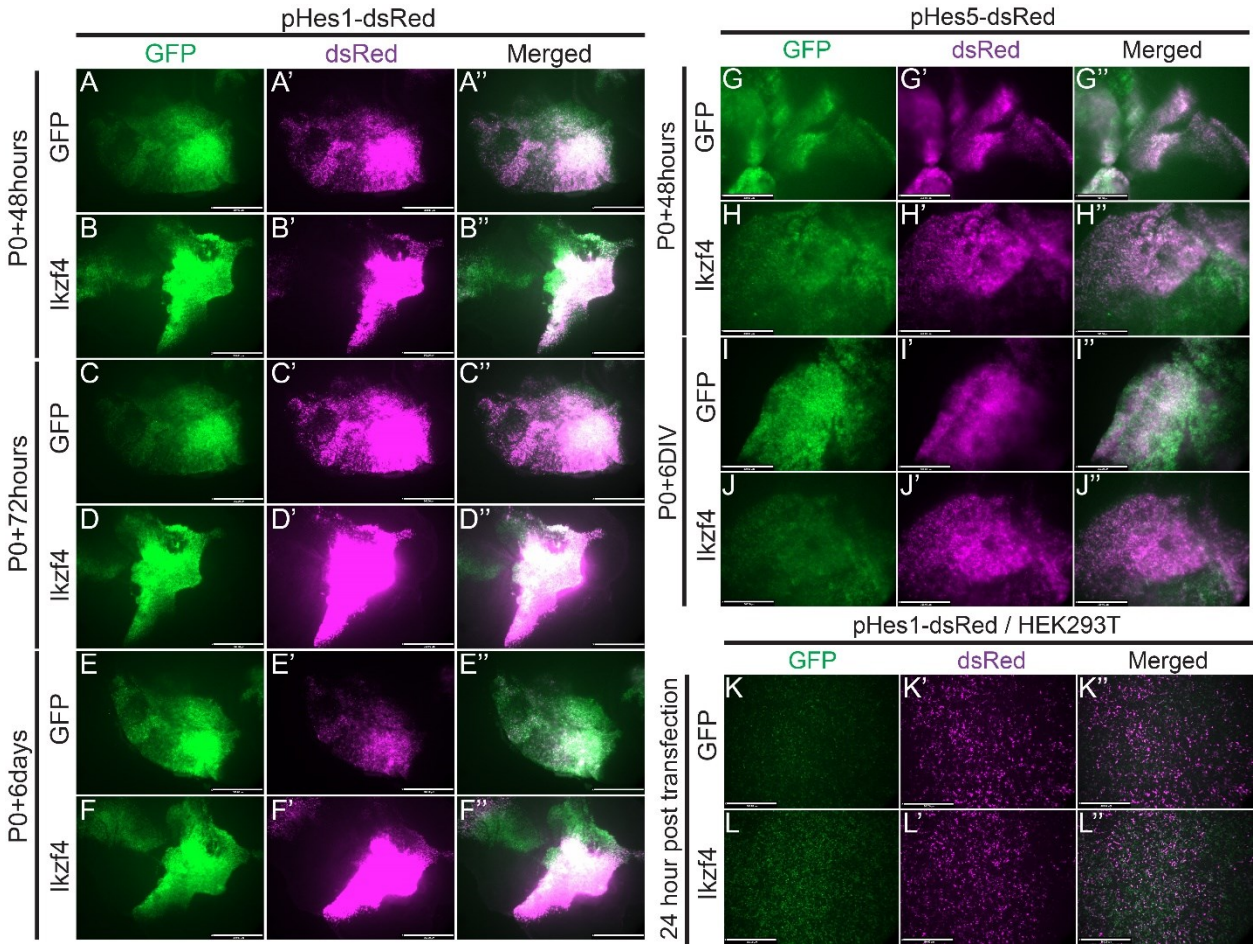

Figure S3.6: Ikzf4 maintains Hes1 expression in post-mitotic cells during late retinogenesis. (A-J'') Photomicrographs of retinal explants co-electroporated at P0 with Hes1-dsRed or Hes5-dsRed and either GFP (A-A'', C-C'', E-E'', G-G'', I-I'') or Ikzf4-IRES-GFP (B-B'', D-D'', F-F'', H-H'', J-J'') followed by imaging after either 48hours (A-B'', G-H''), 72hours (C-D''), or 6 days (E-F'', I-J''). (K-L'') Photomicrographs of HEK293T cells transfected with Hes1-dsRed and either GFP (K-K'') or Ikzf4-IRES-GFP (L-L'') imaged 24hours post-transfection. Scale bars: 360µm (A-L'').

3.7 Supplementary tables

Table S3.1: Manuscript 2 - Sequences of primers and oligos

mRNA primers				
No.		pF (5'>3')	pR (5'>3')	References
1	β-actin	TGATGGTGGGAATGGGTCAGAA	TCCATGTCGTCCCAGTTGGTAA	
2	Foxn4	AATGATCAGAAGCTCGGGGC	CAGGACAGCGACTGAAGGTC	This paper
3	Gapdh	TGCAGTGGCAAAGTGGAGAT	ACTGTGCCGTTGAATTTGCC	Ouimette et al. 2010
4	Ldb1	TTCTGCTTGGAGGATGGACC	ATGCTTCGGAAGTAGCGTGG	This paper
5	Lhx2	GGCAAGATCTCTGACCGCTA	TGCTGAAGCAGGTGAGTTCC	This paper
6	Nfia	GCATAGGGTGACAGCAACCA	ACCTAAACTGCCTTGGTCGG	This paper
7	Nfib	CTCATGAAGTCCCCGCACTG	CTCCTGCACGTAGTATGCCAA	This paper
8	Nfix	AGCTTTCATCCCCGCTAAGG	TTGTAATGTCCTCGCGGCTC	This paper
9	Nr2e3	AAGCTCCTGTGTGACATGTTCAA	AAGCTCCTGTGTGACATGTTCAA	Javed et al. 2020
10	Nrl	CGAGCAGTGCACATCTCAGTTC	AACTGGAGGGCTGGGTTACC	Javed et al. 2020
11	Pou2f1	AACACGACACAGACCACCTC	TAGCAGCAAGACTGGCGTT	Javed et al. 2020
12	Pou2f2	CACCACCAACAGCACAAACC	GGGGTTCAGGCCCGACAAG	Javed et al. 2020
13	Rnf12	AATGGATCGCTTGGATCGGG	GTACTTTCACCTGGGGTGCC	This paper
14	Rxrg	CCTCAATGCTCTTGGCTCTC	AGCTGCTGACACTGTTGACC	This paper
15	Sox8	CGAGCAATGGAAGCAAGCAA	CTGAGCTCGGAGATGTCCAC	This paper
16	Sox9	CAAAACCGACGTGCAAGCTG	TCAGTTCACCGATGTCCACG	This paper
Infusion HD sequences				
1	Hes1-mut1-dsRed	CCGCGTGTCTGATATCCCCATTGGCTGAAA	TTTCAGCCAATGGGGATATCAGACACGCGG	This paper

2	Hes1-mut2-dsRed	AAAGTTACTGTGATATCAAAGTTTGGGAA	TTCCCAAACTTTGATATCACAGTAACTTT	This paper
3	Hes1-mut3-dsRed	TGGGAAAGAAAGTTTGATATCTTTCACACGAGC	GCTCGTGTGAAAGATATCAAACTTTCTTTCCCA	This paper
4	Hes1-mut2+3-dsRed	GAAAGTTACTGTGATATCGAAAGTTTGATATCTTTCACACGAGCC	GGCTCGTGTGAAAGATATCAAACTTTCGATATCACAGTAACTTTC	This paper
shRNA sequences				
1	shPou2f2	gatccGCGCCAAATCTATTCCAGCTTTCAAGAGAAGCTGGAATAGATTTGGCGTTTTTTAAGCTTg	aattcAAGCTTAAAAAACGCCAAATCTATTCCAGCTTCTCTTGAAAGCTGGAATAGATTTGGCGCg	Javed et al. 2020

Table S3.2: Manuscript 2 - Materials

REAGENT	SOURCE	IDENTIFIER	APPLICATION
Primary antibodies			
Brn3a	Synaptic Systems	411004	IF 1:2000
Brn3b	Santa Cruz	SC-6026	IF 1:500
Chx10	Exalpha	X1180P	IF 1:500
Crx/Otx2	R&D systems	AF1979	IF 1:500
GFP	Abcam	ab13970	IF 1:2000
Hes1	Cell Signaling Technology	11988S	IF 1 :500
Ikzf1	Santa Cruz	M-20 (sc-9859)	IF 1 :100
Ikzf4	Millipore Sigma	ABE1331	IF 1:100, C&R 2ug
Ki-67	BD Biosciences	550609	IF 1:100
Lhx2	Fischer Scientific	PA5-78287	IF 1 :200
Lim1/2	DSHB	4F2	IF 1:50
M-opsin	Millipore Sigma	AB5405	IF 1 :200
Nfia/b	DSHB	2C6	IF 1 :500
Nrl	R&D systems	AF2945	IF 1:200
Nr2e3	Chemicon	Discontinued	IF 1 :200
PNA-647	Molecular Probes	L-32460	IF 1:1000
Pax6	DSHB	AB_528427	IF 1 :100
Pax6	Millipore Sigma	AB2237	IF 1:100
Rabbit control IgG Isotope	Fischer Scientific	02-6102	C&R 2ug
Rxrg	Abcam	AB15518	IF 1 :200
S-opsin	Santa Cruz	N-20	IF 1:1000
Sox2	Abcam	AB97959	IF 1 :200
Secondary antibodies			
AF-488 Donkey anti-Chicken	Jackson ImmunoResearch	AB_2340375	IF 1:1000
AF-488 Donkey anti-Mouse	Jackson ImmunoResearch	3.7.1.1 **AB_2340846**	IF 1:1000
AF-488 Donkey anti-Guinea Pig	Jackson ImmunoResearch	3.7.1.2 **AB_2340472**	IF 1:1000
AF-555 Donkey anti-Rabbit	Jackson ImmunoResearch	3.7.1.3 **AB_2313584**	IF 1:1000
AF-647 Donkey anti-Goat	Jackson ImmunoResearch	3.7.1.4 **AB_2340436**	IF 1:1000
AF-647 Donkey anti-Mouse	Jackson ImmunoResearch	3.7.1.5 **AB_2340863**	IF 1:1000

AF-647 Donkey anti-Sheep	Jackson ImmunoResearch	3.7.1.6 **AB_2340751**	IF 1:1000
Bacterial and Virus Strains			
Subcloning Efficiency™ DH5α™ Competent Cells	Fischer Scientific	18265017	
Chemicals, Peptides, and Recombinant Proteins			
Papain	Worthington	LS003124	
Critical Commercial Assays			
RNeasy Microkit	Qiagen	74004	
Superscript VILO Master Mix	Fisher Scientific	11755050	
SYBR Green Master mix	Fisher Scientific	A25742	
Dynabeads Protein G	Fisher Scientific	10003D	
In-Fusion HD Cloning plus	Takara	638920	
Click-iT™ EdU Alexa Fluor™ 647	Fisher Scientific	C10340	
Experimental Models: Cell Lines			
Phoenix-AMPHO	ATCC	CRL-3213	
Experimental Models: Organisms/Strains			
CD1	Charles Rivers	Cat#022	
Ikzf1$^{-/-}$	Wang et al. 1996	N/A	
Ikzf4$^{-/-}$	International Mouse Phenotyping Consortium and RIKEN Bioresource	RBRC06808	
Oligonucleotides			
For qPCR primers, see Table S1	This paper	N/A	
For Infusion HD sequences, see Table S1	This paper	N/A	
Recombinant DNA			
pCIG2-Ikzf1-IRES-GFP	Mattar et al. 2015	N/A	
pCIG2-Ikzf4-IRES-GFP	This paper	N/A	
pCLE-venus	Addgene Gaiano et al. 2000	17703	
pCLE-Ikzf4-IRES-venus	This paper	N/A	
pCIG2-IRES-GFP	Hand et al. 2005	N/A	
pHes1-dsRed	Addgene Matsuda and Cepko. 2007	13767	
pSIREN-RetroQ-ZsGreen	Clontech	632455	
Software			

Prism 8	Graphpad	https://www.graphpad.com/scientific-software/prism/
Volocity software 6	Improvision	http://www.perkinelmer.com/lab-solutions/resources/docs/BRO_VolocityBrochure_PerkinElmer.pdf;
ZEN software	Zeiss Microscope	https://www.zeiss.com/microscopy/int/products/microscope-software/zen.html
Adobe Illustrator CC 2020	Adobe	http://www.adobe.com/products/illustrator.html
Adobe Photoshop CC 2020	Adobe	https://www.adobe.com/products/photoshop.html
Adobe Acrobat Pro DC 2020	Adobe	https://acrobat.adobe.com/us/en/acrobat.html
Quant-Studio Real Time PCR software	Fisher Scientific	https://www.thermofisher.com/ca/en/home/life-science/pcr/real-time-pcr/real-time-pcr-instruments/quantstudio-3-5-real-time-pcr-system.html
Office 365	Microsoft	https://www.office.com/
Cellranger (4.0)	10x Genomics	https://support.10xgenomics.com/single-cell-gene-expression/software/overview/welcome
RStudio (1.3.1056)	Rstudio	https://rstudio.com/
R (4.0.2)	The R Project for Statistical Computing	https://www.r-project.org/
Seurat (3.2.1)	Butler et al. 2018	https://satijalab.org/seurat/
Spyder (4.1.4)	Spyder IDE	https://www.spyder-ide.org/
Python (3.8.3)	Python programming language	https://www.python.org/
Scanpy (2.1.0)	Wolf et al. 2018	https://scanpy.readthedocs.io/en/stable/index.html
Velocyto.py (0.17)	La Manno et al. 2018	http://velocyto.org/velocyto.py/index.html

Galaxy platform	Afgan et al. 2016	https://usegalaxy.org/
Bowtie2 (2.3.4.3)	Langmead and Salzberg et al. 2012	http://bowtie-bio.sourceforge.net/bowtie2/index.shtml
MACS2 (2.1.1.20160309.6)	Feng et al. 2012	https://github.com/taoliu/MACS/releases
Bedtools (2.28.0)	Quinlan and Hall. 2010	https://bedtools.readthedocs.io/en/latest/content/bedtools-suite.html
Deeptools2 (3.3.2.0.0)	Ramirez et al. 2016	https://deeptools.readthedocs.io/en/develop/
Integrative Genomics Viewer (IGV) (2.8.13)	Broad Institute	http://software.broadinstitute.org/software/igv/
Other		
DMEM+Glutamax	Thermofisher	10569010
Penicillin/Streptomycin	Thermofisher	15140148
Fetal Bovine Serum	Wisent Bioproducts	080-150

3.8 Materials and methods

Animals

All experiments were done in accordance with the Canadian Council on Animal guidelines. Ikzf1 (Wang et al., 1996) and Ikzf4 (International Mouse Phenotyping Consortium and RIKEN Bioresource RRID: IMSR_RBRC06808) knockout mice were raised in the C57BL/6J background (Mus musculus). All other mouse experiments were performed on WT CD1 mice (Mus musculus, Charles River Laboratories).

Retroviral constructs preparation and retinal explant culture

Retroviruses were designed, produced and concentrated as previously described (Cayouette et al., 2003). Retinal explants were cultured as previously outlined (Cayouette et al., 2001). Retroviral infections of retinal explants and analyses of the retroviral clones were done as previously stated (Javed et al., 2020). Eyes were harvested from the mice 14 days or more after electroporation as required for the experiment and processed for immunostaining.

Plasmid and mutation cloning

Ikzf1 and Ikzf4 cDNA were cloned into a pCIG2-IRES-GFP and pCLE-venus vector using restriction sites previously outlined (Gaiano et al., 2000; Hand et al., 2005). pHes1-dsRed vector was mutated with Infusion HD Cloning Plus kit from Takara using primers listed in Table S2 (Matsuda and Cepko, 2007).

In vivo electroporation

P0 or P1 eyes were injected with DNA plasmid at 3ug/ul concentration containing 0.5% fast green and electroporated as previously described (de Melo and Blackshaw, 2011).

RNA isolation and Quantitative PCR

RNA extraction and qPCR quantitation were performed as previously described (Javed et al., 2020). Primers used are listed in Table S1.

Tissue collection and immunofluorescence

Age of mouse embryos was calculated from pregnant females with the day of vaginal plug considered as day 0 (E0) and collected at E11, E14, E15, E16, E17, P0, P2 for spatiotemporal analyses. For Ikzf1 and Ikzf4 immunostaining, the retinas were dissected and fixed for 2mins in 4%PFA/PBS followed by immersion in 20% Sucrose/PBS for 1hour. Retinas were then embedded in OCT, frozen in liquid nitrogen, sectioned at 25µm using a cryostat and immunostained on the same day. For all other antibodies, the decapitated heads from embryos or eyes from postnatal pups were fixed for 15mins in 4%PFA/PBS and immersed in 20% Sucrose/PBS for 2 hours.

Immunofluorescence was performed as previously described (Javed et al., 2020). List of primary antibodies can be found in Table S2.

EdU labelling assay

30µM of EdU was added to the culture medium for 2hours before collection and fixation. Click-iT™ EdU Alexa Fluor™ 647 was used to label cells that incorporated EdU.

Statistical and Quantitative analyses

Statistical tests were performed for each experiment in this study as indicated in the Figure legends. All quantifications in the bar graphs of this study are represented as mean±s.e.m whereas n number and individual values on the graphs represent biological repeats. Statistics for the retroviral clonal analyses were performed as previously outlined (Pounds and Dyer, 2008). Retinal explants containing disorganised layers and poor immunostainings were discarded and analyses was limited to the organised regions of the retinal explants. All experiments were repeated at least three times.

Ikzf4 knockouts were analysed as follows: Two sections of P10 central retinas oriented temporo-nasally were examined with quantifications of 200µm (Pax6), 400µm (Otx2, Sox2, and

Lhx2 staining in the INL, Rxrg in the ONL) and 800µm (Brn3a and Lim-1) length of the imaged section. The investigator was blinded to the genotype of animals. An ImageJ analysis macro was written to count cell automatically in a section. Analyse particles was used after defining a region of interest and setting threshold for each antibody to auto-count cell numbers of Pax6^{+ve}, Otx2^{+ve}, Sox2^{+ve}, Lhx2^{+ve} and Brn3a^{+ve} cells whereas Rxrg^{+ve} and Lim-1^{+ve} were manually counted.

Ikzf1/4 double knockouts were analysed as follows: Three sections of E15 central retinas in embryonic heads oriented dorso-ventrally were analysed with quantification of 200µm for Rxrg^{+ve} cells and 400µm for Brn3a^{+ve} cells. Rxrg^{+ve} cell were manually counted due to background signal whereas Brn3a^{+ve} cells were counted using the ImageJ analysis macro as described above. Cell number quantifications were performed by blinding the investigators to the genotype of the animals.

CUT&RUN assays

CUT&RUN was performed as previously described (Skene et al., 2018), with a few added modifications. The entire procedure was done in 200µl PCR tubes. 0.01% digitonin concentration was used and pAG-MNase digestion was performed for 30min on ice.

Libraries were prepared with the KAPA DNA HyperPrep Kit (Roche 07962363001 - KK8504). This protocol includes an End-Repair/A-tailing step and an adapter ligation step followed by a PCR amplification (enrichment) of ligated fragments. The adapters used for ligation were IDT for Illumina TruSeq UD Indexes (Illumina - 20022371). The final enriched product (library, after PCR) was purified using KAPA purification beads (Roche 07983298001 - KK8002) and a dual-SPRI size selection was performed (with KAPA beads) to select fragments between 180-500 bp. Libraries were then quantified using a Nanodrop microvolume spectrophotometer (ng/□l) and quality was assessed using the Agilent High Sensitivity DNA Kit (Agilent -5067-4626) on a Bioanalyzer 2100. The libraries were then quantified by q-PCR to obtain their nanomolar (nM) concentration. Libraries were diluted, pooled equimolar and sequenced in pair end 50 cycles (PE50) on a S1 flowcell (Illumina - 20012863) of the Illumina NovaSeq 6000 System.

Bioinformatics analyses

scRNA-seq analyses of previously published datasets was performed as follows. Fastq raw reads were aligned and counted to generate matrices for each individual stage from Mouse retina atlas (GEO: GSE118614) (Clark et al., 2019) and Human fetal retina atlas (GEO: GSE116106, GSE122970, GSE138002) (Lu et al., 2020) using Cellranger 4.0 (10x Genomics). Velocyto (La Manno et al., 2018) with run10x function was used on cellranger output folders to generate .loom files for each individual stages. Seurat (Butler et al., 2018) was used to analyse the mouse and human retina. loom files and subset RPC clusters for Ikzf4/IKZF4 expression analyses using markers previously described (Clark et al., 2019; Lu et al., 2020). Scanpy (Wolf et al., 2018) was used to analyse the same .loom files and generate Ikzf4/IKZF4 expression UMAPs along with cell type markers (Fig. S3.2).

CUT&RUN analyses were performed by aligning the raw fastq reads with the mouse mm9 genome using default parameters of bowtie2 on Galaxy platform (Afgan et al., 2016; Langmead and Salzberg, 2012). Bam files generated for Ikzf4 and IgG CUT&RUN at each stage were used to call peaks using 0.5 FDR parameter on MACS2 (Feng et al., 2012). Bedtools was used to find overlapping peaks between the two stage (Quinlan and Hall, 2010). Bigwig files were generated using deeptools2 (Ramirez et al., 2016). Integrative Genomics Viewer (IGV) was used to visualize bigwig files.

Information on each software version is listed in Table S2.

Data availability

Processed MACS2 peaks and bigwig files are available on GEO accession number: XXXXXXX.

3.9 Acknowledgements

We thank Christine Jolicoeur, Jessica Barthe, Androne Constantin, Odile Neyret-Djossou, Éric Massicotte and Julie Lord for animal and technical assistance. We thank Aurelie Huang-Sung and Dr. Nicole Francis for providing the pAG-MNase for the CUT&RUN experiments. We also thank all members of the Cayouette lab for their comments and support.

3.10 Conflict of interest

The authors declare no conflict of interest.

4 General discussion

The developing CNS requires a stereotypic and controlled temporal order of birth for neurons and glia to ensure the appropriate circuitry is established. This is important not only for the correct migration of neurons and glia in their respective layers, but also for axonal projections and connections with their appropriate targets. As detailed in this thesis, the CNS undergoes development by two key mechanisms, spatial patterning and temporal patterning. The critical components of spatial patterning in vertebrates are well understood and there is significant understanding on how it influences the type of neurons and glia generated. However, even after decades of research on invertebrates, temporal patterning in vertebrates is a poorly understood phenomenon.

This thesis has provided some key insights on how neural progenitors could be utilizing a transcriptional cascade that forms a complex gene regulatory network to establish temporal competence. In chapter 2, Pou2f1 was discovered as a novel tTF that regulates temporal competence in early RPCs to generate cones. In addition, Pou2f2 was demonstrated as an important regulator of cone differentiation in post-mitotic cells. In chapter 3, it was demonstrated that Ikzf4 cooperated with Ikzf1 to establish the window conducive to cone development in early RPCs. Ikzf4 also regulated Müller glia specification from late RPCs. Mechanistic evidence showed that Ikzf4 could be employing tTF Pou2f1 early to promote cones and Notch signaling genes late to promote Müller glia fate.

From a fundamental and discovery science perspective, these results help us identify key regulators of cone and Müller glia development. As suggested by the expression profiling of these factors in developing human fetal retinas, this also proposes possibility of conservation of function of these tTFs in higher vertebrates. The insights on the temporally controlled function of Ikzf4 in the mouse retina advances our understanding on the function o widely expressed transcription factors. From a translational and therapeutic perspective, these results could have many potential applications in cell replacement therapies using ESC-derived retinal organoids and *in vivo* regeneration of retina using Müller glia.

4.1 Fundamental science perspectives

From a strictly fundamental and discovery science perspective, Pou2f1/Pou2f2 as critical regulators of cone development fill many gaps in the current model of transcriptional dominance. Additionally, Ikzf4, along with Ikzf1, regulating Pou2f1 in early and Müller specification in late retinogenesis explains discrepancies in the literature. In addition to the points discussed above in chapter 2 and 3, there are still many unanswered questions and future directions.

4.1.1 Genome wide targets of Pou2f1/2

One critical question is how Pou2f1 functions in RPCs to promote cone development in addition to its role in upregulating Pou2f2. The binding targets of Pou2f1 in early RPCs are unknown. ChIP-seq or CUT&RUN assays at the genome wide level would uncover novel candidate tTFs that might be regulated by Pou2f1 to favor the cone fate. This data coupled with RNA-sequencing of Pou2f1$^{-/-}$ early RPCs would help identify additional candidate tTFs and direct targets of Pou2f1.

In chapter 2, one Pou2f2 binding site involved in regulating the expression of *Nrl* gene was uncovered, but other targets of Pou2f2 remain elusive. Moreover, Pou2f2 is widely expressed in early RPCs but our data suggests its specific role in post-mitotic precursors. By utilizing novel methods that can uncover DNA binding targets of transcription factors at single cell level such as single cell CUT&TAG (Wu et al., 2020), the RPC specific and post-mitotic cell specific binding targets of Pou2f2 could be revealed in the same assay. This could potentially identify novel CRMs that are involved in cone development and possibly conserved in higher vertebrates such as humans. Another future direction would be to uncover the role of Pou2f2 in horizontal cell production. Pou2f2 cKO retinas have reduced number of horizontal cells, suggesting that Pou2f2 could be regulating the horizontal cell fate in the early RPCs (Fig. 2.4F). However, the mechanism remains unexplored. Single cell RNA-sequencing of Pou2f2 KO retinas would help unveil global changes in transcriptomic profiles of RPCs and post-mitotic cells. This could uncover how Pou2f2 modulates the gene regulatory network behind cone and horizontal development.

4.1.2 Pou2f1/2 as possible chromatin regulators in the mouse retina

Interestingly, the Pou2f2 binding site important for the regulation of the Nrl promoter is the octamer binding motif ATGCAAAT, as detailed in chapter 1. This raises the possibility of Pou2f2 could also be modulating chromatin conformation by binding to histone octamers, in addition to its role in direct transcriptional modulation of gene expression. As Pou2f1 also possesses octamer binding properties, it would be interesting to assess whether Pou2f1 utilizes the Jmjd1 and NuRD complexes as previously described in the regulation of *Il2* gene expression during memory T-cell development (Shakya et al., 2015; Shakya et al., 2011). These epigenetic modifiers have been implicated in retinal development before, most relevantly, the NuRD complex being important for the role of Casz1 in conferring RPC competence for rod development (Mattar et al., 2021). Therefore, assessing the epigenetic role of Pou2f1/2 could provide key mechanistic insights on how these proteins function in the retina and how temporal competence could be established epigenetically. Single cell ATAC-seq on Pou2f1/2 knockout retinas would uncover novel regions associated with temporal competence in early RPCs and would be an important advance in the field.

4.1.3 How do Pou2f1/Pou2f2 and Ikzf4 fit into the competence model with Foxn4?

As the study on Foxn4 was published in parallel to the results in chapter 2, questions remain on how Foxn4 and Pou2f1 confer cone competence together in RPCs. Although Foxn4 promotes cones outside their window of development, mature cone markers were not analyzed (Liu et al., 2020a). Foxn4 cKO retinas have normal number of cones compared to controls before the onset of retinal degeneration. This suggests that either another factor compensates for Foxn4 in cone production or Foxn4 only partially confers cone competence to RPCs. From the results in chapter 3, Ikzf4 might also be providing partial competence for cone development to RPCs. This suggests that Ikzf4 is also an important part of the GRN conducive for cone production, but the combined role of these factors remains to be tested.

A possible model to explain their combined role would be the establishment of a GRN of cone competence. Multipotent RPCs stochastically upregulate the GRN conducive to generate cones by expressing higher levels of tTFs such as Foxn4, Pou2f1 and Ikzf4. This would lead to

activation of downstream cues such as Pou2f2, which represses Nrl and promotes the cone fate. Testing this model by generating combination of knockout mice for these would help uncover the requirement of these factors in cone competence. If there is a subtractive decrease in cone numbers in the double or triple KO retinas compared to single knockouts, this would suggest that all genes are part of a complete cone competence GRN. The deletion of one factor merely shifts the bias towards non-cone fates slightly whereas the rest of the cone tTFs in the GRN help achieve partial competence for cone production in early RPCs.

It is unclear whether Ikzf4 promotes Müller glia competence to late RPCs as the overexpression of Ikzf4 was performed in the late retinogenesis window when Müller glia are normally made. However, it is clear from the results in chapter 3 that Ikzf4 maintains the expression of Müller differentiation genes in post-mitotic precursors (Fig. 3.4C-D). Future studies aimed at characterizing the precise role of Ikzf4 in RPCs and post-mitotic precursors using scRNA-seq of Ikzf4$^{-/-}$ retinas would help provide major insights into Müller glia development.

4.1.4 RPC lineage and tTF competence windows

Foxn4 was shown to dynamically regulate Ikzf1 and Casz1 from early to late retinogenesis, however, it was not shown whether this occurs in RPCs or differentiated cells (Liu et al., 2020a). Nonetheless, this raises the possibility of tTFs dynamically regulating other tTFs. Now that there is increasing evidence of a set of tTFs, the dynamic expression profiling of these factors in live RPCs would be essential to correctly uncover the exact relationship between tTFs. Developing tools such as CRMs of either Ikzf1, Ikzf4, Pou2f1, Foxn4 and Casz1 active in RPCs would be greatly beneficial in performing time-lapse experiments in *ex vivo* retinal explants cultures to track the expression of these tTFs in real time. This would provide insights on how the expression of these factors dynamically change overtime as early RPCs transition into late RPCs. Additionally, employing novel cell lineage tracking methods such as CellTagging, which allows simultaneous lineage and cell identity indexing by single cell RNA-seq, would reveal novel insights on how tTF generate specific cell types (Kong et al., 2020). Using CellTagging in the developing mouse retina could help identify gene regulatory networks dynamically altered in the RPCs depending on what type of cell fate is present in the lineage.

4.1.5 tTFs in other parts of the central nervous system

All the tTFs discovered in the mouse retina have widespread expression in various part of the developing CNS (Gouge et al., 2001; Honma et al., 1999; Latchman et al., 1992; Liu et al., 1995). A promising future direction would be to uncover whether the same tTFs also regulate neural progenitor temporal identity in other parts of the CNS. More importantly, it would be interesting to assess whether the same tTFs are also conserved in their function in higher vertebrates such as humans and whether tTFs cross regulate each other. The advances in the human ESC-derived brain organoid technology has opened new avenues for human CNS development research, reviewed in (Chiaradia and Lancaster, 2020). It would be interesting to functionally assess whether tTFs are also required for temporal identity in human neural progenitors.

4.1.6 Bioinformatics analysis of GRN of temporal competence

scRNA-seq has revolutionized molecular biology research. The immense amount of data generated by scRNA-seq provides a unique opportunity to probe whether similar tTF codes are hidden between different scRNA-seq datasets depending on the CNS region. Recently, scRNA-seq studies have generated cross-compared datasets between various species and uncovered many conserved aspects of development (Hoang et al., 2020; Liu et al., 2021; Ray et al., 2018). A promising endeavor would be designing a bioinformatic tool that can efficiently cross compare scRNA-seq datasets to look for similar transcriptomic signatures conserved between various parts of the CNS, specifically in neural progenitors of the same species. This would also help unravel the GRN responsible for temporal identity and help uncover a broader range of candidates for examination. An approach similar to the one proposed above was used to uncover tTF codes in neural tube development by comparison of forebrain, midbrain, and hindbrain tissue. Pou2f2 was found to be one of the key transcription factors expressed in post-mitotic neurons made during the mid-temporal window in all three tissues (Sagner et al., 2020). Although no functional assays were performed, this study demonstrates that precise candidates tTFs can be uncovered for other parts of the CNS by analyzing the wealth of data already available. The main caveat being that these codes are uncovered by restricted gene expression of tTFs. However, as demonstrated in chapter 3, there is a possibility that some important candidate tTFs would be missed with this approach due to their widespread temporal expression. Nonetheless, the results shown in this thesis and work

done on other tTFs provide a preliminary template on which these bioinformatics tools could be tested on. Although the transcriptomic signatures are only part of the full portrait of the mechanism behind temporal competence, it would provide important insights on how temporal competence is established in RPCs and beyond.

4.2 Therapeutic perspectives

Retinal degeneration is one of the leading causes of blindness worldwide, some of which trigger death of photoreceptors, reviewed in (Javed and Cayouette, 2017). As detailed in chapter 1, many strategies have been proposed to replenish degenerated cones as the disease progresses. Uncovering novel temporal identity factors for cone development provides novel tools to promote cone production from several sources.

4.2.1 Cell replacement therapies

Although efficient integration of donor cones into host retinas remains the largest hurdle in cell replacement therapies, promoting efficient and mature cone production from ESC-derived retinal organoids and sheets also remains difficult. The results presented in this thesis highlight Pou2f1 and Pou2f2 as novel factors that can extend the window of cone development beyond their limits. Pou2f1 in particular, can re-open the window of cone production when overexpressed at the late retinogenesis stage. Interestingly, the results presented in chapter 2 also provide a promoter specific tool for promoting cones from post-mitotic precursors. Utilizing overexpression of Pou2f2 fused to the mutated Nrl promoter would allow post-mitotic conversion of rods into cones, which could also be used for efficient cone production. As the cones promoted by Pou2f2 from post-mitotic cells do not express late markers, this would have to be supplemented with additional factors. Nonetheless, this provides additional tools to the field to design new approaches for efficient cone production. Another caveat to utilizing Pou2f1/2 as a cone inducing factor is whether these cones are functional as this remains to be tested. Thorough profiling of cones generated from ESC-derived retinal organoids and sheet would be important to overcome this issue. Therefore, the results in this thesis propose the combined use of tTFs along with extrinsic cues to maximize the production of cones in ESC-derived retinal organoids and sheets. Future studies would also

have to focus on assessing whether the human homologues of POU2F1 and POU2F2 can promote cone production in human ESC-derived retinal organoids.

Transplantation into degenerated retinas has been proposed as the next step to counter material transfer observed in host cells incoming from the transplanted donor cells, as discussed in chapter 1 (Gasparini et al., 2019; Ortin-Martinez et al., 2017; Pearson et al., 2016; Santos-Ferreira et al., 2016). As rods provide trophic support to cones and are important for their survival (Aït-Ali et al., 2015), this poses new challenges for the design of cell replacement therapies. As Pou2f1 and Pou2f2 promote photoreceptor production at the expense of all other fates, it provides an opportunity to design photoreceptor-rich cultures that can be used for transplantation. From the results presented above, following overexpression of Pou2f1 and Pou2f2 in late RPCs, the cone rod ratio of the photoreceptors produced was 1:4 (Fig. 2.3A-G). This is a considerable increase compared to the endogenous 1:30 cone rod ratio present in mice (Jeon et al., 1998). A foreseeable caveat is the possibility of the rods formed by Pou2f1 and Pou2f2 overexpression exhibiting immature properties as this remains to be tested. Nonetheless, these results propose new methods for the field to overcome some of the current challenges in cell replacement therapies.

4.2.2 *In vivo* reprogramming

Lower vertebrates such as zebrafish have the unique ability to regenerate their retinas using an endogenous source of Müller glia that undergo proliferation upon injury, reviewed in (Lahne et al., 2020). Mammals such as mice and primates cannot regenerate their retinas naturally through Müller glia. However, studies have shown that RGC, bipolar cell and rod production is achievable by targeted overexpression of key factors in the mammalian Müller glia (Jorstad et al., 2017; Jorstad et al., 2020; Xiao et al., 2019; Yao et al., 2018). Regeneration of cones following degeneration or injury has not been efficiently demonstrated so far. Interestingly, cross-species comparison between zebrafish, chick and mouse retinas revealed the presence of a dedicated GRN in murine Müller glia that represses reprogramming (Hoang et al., 2020). This GRN contains many Notch signaling and Nfi family of genes, which are direct targets of Ikzf4, as presented in chapter 3. As Ikzf4 maintains the glial cell fate, it is possible it also ensures that murine Müller glia do not undergo reprogramming. It would be interesting to test whether Ikzf4$^{-/-}$ Müller glia are able to reprogram into retinal cell types following injury. Additionally, as Ikzf1 and Ikzf4 can both

promote Pou2f1/Pou2f2 expression, it would be interesting to assess whether their co-expression could also promote *in vivo* reprogramming of Müller glia into cones.

Since Pou2f1 and Pou2f2 can efficiently promote cone production from late RPCs that have a similar transcriptome to Müller glia (Blackshaw et al., 2004; Clark et al., 2019; Roesch et al., 2008; Trimarchi et al., 2008), they could be candidates for promoting Müller glia reprogramming into cones. This would allow *in vivo* replenishment of cones in retinas affected by degeneration. Taken together, the results presented in this thesis reveal novel tools for *in vivo* reprogramming of Müller glia into cones.

In retinitis pigmentosa, inheritance of a mutation of key phototransduction genes leads to aberrant function of rods, causing degeneration, reviewed in (Ferrari et al., 2011). Therefore, reprogramming Müller glia into rods would not be beneficial as the inherited mutation would manifest in rod degeneration after reprogramming. Therefore, an alternative approach has to be designed to overcome this issue. As Nrl is upstream to most of the known mutated genes in retinitis pigmentosa, multiple studies demonstrated efficient knocked down of Nrl genetically or via Adeno Associated Virus (AAV) CRISPR-Cas9 prevented retinal degeneration in retinitis pigmentosa mouse models (Montana et al., 2013; Yu et al., 2017). Genetic ablation of genes using AAV-CRISPR/Cas9 poses challenges such as off-target effects and poor efficiency of loss of function. Therefore, natural repressors of Nrl could be utilized to efficiently reprogram adult rods into either cone-like cells or cones to circumvent retinal degeneration caused by aberrant rod gene function. This thesis proposes possible candidate repressors of Nrl in Pou2f1, Pou2f2 and Ikzf4. Ikzf4 overexpression in late RPCs leads to a robust repression of Nrl (Fig. 3.2I-L). Whether Ikzf4 can also repress Nrl in adult rods remains to be tested. Pou2f2, although not as efficient in repressing Nrl as Ikzf4, can promote cone-like cells from post-mitotic precursors. Whether Pou2f2 can also execute the same function from adult rods, remains to be tested. Nonetheless, these results provide novel tools to improve the current designs of *in vivo* reprogramming.

4.3 Concluding remarks

Temporal patterning in the CNS is a poorly understood phenomenon in vertebrates. Previous studies in invertebrates have provided clues on how this mechanism could be set up but

our current understanding is very limited. The work presented in this thesis uncovers novel temporal transcription factors that modulate the competence of neural progenitors to generate specific cells at a particular time. Mouse retina was used as a model to understand how these tTFs function during retinogenesis. This thesis provides evidence of partial conservation of homologues of fly ventral nerve cord neuroblast tTFs functioning in the mammalian retina. This work also provided insights on the diversity and complexity of temporal transcription factors that govern cell fate specification during retinal development. This thesis provides fundamental insights on CNS development that could employ the same tTFs to promote cell fate specification in other parts of the CNS. Finally, this work provides foundational roles of tTFs that can provide novel ways to design efficient and functional therapeutic strategies in the future.

Bibliography

Abramov, I., Gordon, J., Hendrickson, A., Hainline, L., Dobson, V., and LaBossiere, E. (1982). The retina of the newborn human infant. Science *217*, 265-267.

Afgan, E., Baker, D., van den Beek, M., Blankenberg, D., Bouvier, D., Cech, M., Chilton, J., Clements, D., Coraor, N., Eberhard, C.*, et al.* (2016). The Galaxy platform for accessible, reproducible and collaborative biomedical analyses: 2016 update. Nucleic Acids Res *44*, W3-W10.

Agoston, D.V., Szemes, M., Dobi, A., Palkovits, M., Georgopoulos, K., Gyorgy, A., and Ring, M.A. (2007). Ikaros is expressed in developing striatal neurons and involved in enkephalinergic differentiation. J Neurochem *102*, 1805-1816.

Aït-Ali, N., Fridlich, R., Millet-Puel, G., Clérin, E., Delalande, F., Jaillard, C., Blond, F., Perrocheau, L., Reichman, S., Byrne, Leah C.*, et al.* (2015). Rod-Derived Cone Viability Factor Promotes Cone Survival by Stimulating Aerobic Glycolysis. Cell *161*, 817-832.

Akimoto, M., Cheng, H., Zhu, D., Brzezinski, J.A., Khanna, R., Filippova, E., Oh, E.C., Jing, Y., Linares, J.L., Brooks, M.*, et al.* (2006). Targeting of GFP to newborn rods by Nrl promoter and temporal expression profiling of flow-sorted photoreceptors. Proc Natl Acad Sci U S A *103*, 3890-3895.

Aldiri, I., Xu, B., Wang, L., Chen, X., Hiler, D., Griffiths, L., Valentine, M., Shirinifard, A., Thiagarajan, S., Sablauer, A.*, et al.* (2017). The Dynamic Epigenetic Landscape of the Retina During Development, Reprogramming, and Tumorigenesis. Neuron *94*, 550-568 e510.

Allman, D., Dalod, M., Asselin-Paturel, C., Delale, T., Robbins, S.H., Trinchieri, G., Biron, C.A., Kastner, P., and Chan, S. (2006). Ikaros is required for plasmacytoid dendritic cell differentiation. Blood *108*, 4025-4034.

Alsiö, J.M., Tarchini, B., Cayouette, M., and Livesey, F.J. (2013). Ikaros promotes early-born neuronal fates in the cerebral cortex. Proc Natl Acad Sci U S A *110*, E716-725.

Altschul, S.F., Gish, W., Miller, W., Myers, E.W., and Lipman, D.J. (1990). Basic local alignment search tool. J Mol Biol *215*, 403-410.

Altshuler, D., and Cepko, C. (1992). A temporally regulated, diffusible activity is required for rod photoreceptor development in vitro. Development *114*, 947-957.

Altshuler, D., Lo Turco, J.J., Rush, J., and Cepko, C. (1993). Taurine promotes the differentiation of a vertebrate retinal cell type in vitro. Development *119*, 1317-1328.

Applebury, M.L., Farhangfar, F., Glosmann, M., Hashimoto, K., Kage, K., Robbins, J.T., Shibusawa, N., Wondisford, F.E., and Zhang, H. (2007). Transient expression of thyroid hormone nuclear receptor TRbeta2 sets S opsin patterning during cone photoreceptor genesis. Dev Dyn *236*, 1203-1212.

Araujo, H., and Bier, E. (2000). sog and dpp exert opposing maternal functions to modify toll signaling and pattern the dorsoventral axis of the Drosophila embryo. Development *127*, 3631-3644.

Ashery-Padan, R., Marquardt, T., Zhou, X., and Gruss, P. (2000). Pax6 activity in the lens primordium is required for lens formation and for correct placement of a single retina in the eye. Genes Dev *14*, 2701-2711.

Austin, C.P., Feldman, D.E., Ida, J.A., Jr., and Cepko, C.L. (1995). Vertebrate retinal ganglion cells are selected from competent progenitors by the action of Notch. Development *121*, 3637-3650.

Bao, J., Lin, H., Ouyang, Y., Lei, D., Osman, A., Kim, T.W., Mei, L., Dai, P., Ohlemiller, K.K., and Ambron, R.T. (2004). Activity-dependent transcription regulation of PSD-95 by neuregulin-1 and Eos. Nat Neurosci *7*, 1250-1258.

Bao, Z.Z., and Cepko, C.L. (1997). The expression and function of Notch pathway genes in the developing rat eye. J Neurosci *17*, 1425-1434.

Bassett, E.A., and Wallace, V.A. (2012). Cell fate determination in the vertebrate retina. Trends Neurosci *35*, 565-573.

Baumgardt, M., Karlsson, D., Salmani, B.Y., Bivik, C., MacDonald, R.B., Gunnar, E., and Thor, S. (2014). Global programmed switch in neural daughter cell proliferation mode triggered by a temporal gene cascade. Dev Cell *30*, 192-208.

Baumgardt, M., Karlsson, D., Terriente, J., Díaz-Benjumea, F.J., and Thor, S. (2009). Neuronal subtype specification within a lineage by opposing temporal feed-forward loops. Cell *139*, 969-982.

Belanger, M.C., Robert, B., and Cayouette, M. (2017). Msx1-Positive Progenitors in the Retinal Ciliary Margin Give Rise to Both Neural and Non-neural Progenies in Mammals. Dev Cell *40*, 137-150.

Belkaid, Y., Blank, R.B., and Suffia, I. (2006). Natural regulatory T cells and parasites: a common quest for host homeostasis. Immunol Rev *212*, 287-300.

Belliveau, M.J., and Cepko, C.L. (1999). Extrinsic and intrinsic factors control the genesis of amacrine and cone cells in the rat retina. Development *126*, 555-566.

Belliveau, M.J., Young, T.L., and Cepko, C.L. (2000). Late retinal progenitor cells show intrinsic limitations in the production of cell types and the kinetics of opsin synthesis. J Neurosci *20*, 2247-2254.

Bello, B.C., Izergina, N., Caussinus, E., and Reichert, H. (2008). Amplification of neural stem cell proliferation by intermediate progenitor cells in Drosophila brain development. Neural Dev *3*, 5.

Benito-Sipos, J., Estacio-Gomez, A., Moris-Sanz, M., Baumgardt, M., Thor, S., and Diaz-Benjumea, F.J. (2010). A genetic cascade involving klumpfuss, nab and castor specifies the abdominal leucokinergic neurons in the Drosophila CNS. Development *137*, 3327-3336.

Bermingham, N.A., Hassan, B.A., Wang, V.Y., Fernandez, M., Banfi, S., Bellen, H.J., Fritzsch, B., and Zoghbi, H.Y. (2001). Proprioceptor pathway development is dependent on Math1. Neuron *30*, 411-422.

Berry, M., and Rogers, A.W. (1965). The migration of neuroblasts in the developing cerebral cortex. J Anat *99*, 691-709.

Betschinger, J., Mechtler, K., and Knoblich, J.A. (2006). Asymmetric segregation of the tumor suppressor brat regulates self-renewal in Drosophila neural stem cells. Cell *124*, 1241-1253.

Bhat, K.M., and Schedl, P. (1997). Establishment of stem cell identity in the Drosophila germline. Dev Dyn *210*, 371-382.

Biehs, B., Francois, V., and Bier, E. (1996). The Drosophila short gastrulation gene prevents Dpp from autoactivating and suppressing neurogenesis in the neuroectoderm. Genes Dev *10*, 2922-2934.

Billin, A.N., Cockerill, K.A., and Poole, S.J. (1991). Isolation of a family of Drosophila POU domain genes expressed in early development. Mech Dev *34*, 75-84.

Blackshaw, S., Harpavat, S., Trimarchi, J., Cai, L., Huang, H., Kuo, W.P., Weber, G., Lee, K., Fraioli, R.E., Cho, S.H.*, et al.* (2004). Genomic analysis of mouse retinal development. PLoS Biol *2*, E247.

Boije, H., Edqvist, P.H., and Hallböök, F. (2008). Temporal and spatial expression of transcription factors FoxN4, Ptf1a, Prox1, Isl1 and Lim1 mRNA in the developing chick retina. Gene Expr Patterns *8*, 117-123.

Boije, H., Shirazi Fard, S., Ring, H., and Hallböök, F. (2013). Forkheadbox N4 (FoxN4) triggers context-dependent differentiation in the developing chick retina and neural tube. Differentiation *85*, 11-19.

Boone, J.Q., and Doe, C.Q. (2008). Identification of Drosophila type II neuroblast lineages containing transit amplifying ganglion mother cells. Dev Neurobiol *68*, 1185-1195.

Bossing, T., Udolph, G., Doe, C.Q., and Technau, G.M. (1996). The embryonic central nervous system lineages of Drosophila melanogaster. I. Neuroblast lineages derived from the ventral half of the neuroectoderm. Dev Biol *179*, 41-64.

Bosze, B., Moon, M.S., Kageyama, R., and Brown, N.L. (2020). Simultaneous Requirements for Hes1 in Retinal Neurogenesis and Optic Cup-Stalk Boundary Maintenance. J Neurosci *40*, 1501-1513.

Bowman, S.K., Rolland, V., Betschinger, J., Kinsey, K.A., Emery, G., and Knoblich, J.A. (2008). The tumor suppressors Brat and Numb regulate transit-amplifying neuroblast lineages in Drosophila. Dev Cell *14*, 535-546.

Briscoe, J., Pierani, A., Jessell, T.M., and Ericson, J. (2000). A homeodomain protein code specifies progenitor cell identity and neuronal fate in the ventral neural tube. Cell *101*, 435-445.

Broadus, J., Skeath, J.B., Spana, E.P., Bossing, T., Technau, G., and Doe, C.Q. (1995). New neuroblast markers and the origin of the aCC/pCC neurons in the Drosophila central nervous system. Mech Dev *53*, 393-402.

Brody, T., and Odenwald, W.F. (2000). Programmed transformations in neuroblast gene expression during Drosophila CNS lineage development. Dev Biol *226*, 34-44.

Brooks, M.J., Chen, H.Y., Kelley, R.A., Mondal, A.K., Nagashima, K., De Val, N., Li, T., Chaitankar, V., and Swaroop, A. (2019). Improved Retinal Organoid Differentiation by Modulating Signaling Pathways Revealed by Comparative Transcriptome Analyses with Development In Vivo. Stem Cell Reports *13*, 891-905.

Brown, N.L., Kanekar, S., Vetter, M.L., Tucker, P.K., Gemza, D.L., and Glaser, T. (1998). Math5 encodes a murine basic helix-loop-helix transcription factor expressed during early stages of retinal neurogenesis. Development *125*, 4821-4833.

Brzezinski, J.A.t., Kim, E.J., Johnson, J.E., and Reh, T.A. (2011). Ascl1 expression defines a subpopulation of lineage-restricted progenitors in the mammalian retina. Development *138*, 3519-3531.

Brzezinski, J.A.t., Lamba, D.A., and Reh, T.A. (2010). Blimp1 controls photoreceptor versus bipolar cell fate choice during retinal development. Development *137*, 619-629.

Brzezinski, J.A.t., Prasov, L., and Glaser, T. (2012). Math5 defines the ganglion cell competence state in a subpopulation of retinal progenitor cells exiting the cell cycle. Dev Biol *365*, 395-413.

Burrill, J.D., Moran, L., Goulding, M.D., and Saueressig, H. (1997). PAX2 is expressed in multiple spinal cord interneurons, including a population of EN1+ interneurons that require PAX6 for their development. Development *124*, 4493-4503.

Butler, A., Hoffman, P., Smibert, P., Papalexi, E., and Satija, R. (2018). Integrating single-cell transcriptomic data across different conditions, technologies, and species. Nat Biotechnol *36*, 411-420.

Camós, S., Gubern, C., Sobrado, M., Rodríguez, R., Romera, V.G., Moro, M., Lizasoain, I., Serena, J., Mallolas, J., and Castellanos, M. (2014). Oct-2 transcription factor binding activity and expression up-regulation in rat cerebral ischaemia is associated with a diminution of neuronal damage in vitro. Neuromolecular Med *16*, 332-349.

Carl, M., Loosli, F., and Wittbrodt, J. (2002). Six3 inactivation reveals its essential role for the formation and patterning of the vertebrate eye. Development *129*, 4057-4063.

Carter-Dawson, L.D., and LaVail, M.M. (1979a). Rods and cones in the mouse retina. I. Structural analysis using light and electron microscopy. J Comp Neurol *188*, 245-262.

Carter-Dawson, L.D., and LaVail, M.M. (1979b). Rods and cones in the mouse retina. II. Autoradiographic analysis of cell generation using tritiated thymidine. J Comp Neurol *188*, 263-272.

Cayouette, M., Barres, B.A., and Raff, M. (2003). Importance of intrinsic mechanisms in cell fate decisions in the developing rat retina. Neuron *40*, 897-904.

Cayouette, M., Whitmore, A.V., Jeffery, G., and Raff, M. (2001). Asymmetric segregation of Numb in retinal development and the influence of the pigmented epithelium. J Neurosci *21*, 5643-5651.

Cepko, C.L. (1999). The roles of intrinsic and extrinsic cues and bHLH genes in the determination of retinal cell fates. Curr Opin Neurobiol *9*, 37-46.

Chamberlain, C.E., Jeong, J., Guo, C., Allen, B.L., and McMahon, A.P. (2008). Notochord-derived Shh concentrates in close association with the apically positioned basal body in neural target cells and forms a dynamic gradient during neural patterning. Development *135*, 1097-1106.

Chan, J.R., Jolicoeur, C., Yamauchi, J., Elliott, J., Fawcett, J.P., Ng, B.K., and Cayouette, M. (2006). The polarity protein Par-3 directly interacts with p75NTR to regulate myelination. Science *314*, 832-836.

Chang, J.C., Meredith, D.M., Mayer, P.R., Borromeo, M.D., Lai, H.C., Ou, Y.H., and Johnson, J.E. (2013). Prdm13 mediates the balance of inhibitory and excitatory neurons in somatosensory circuits. Dev Cell *25*, 182-195.

Chatila, T.A. (2009). Regulatory T cells: key players in tolerance and autoimmunity. Endocrinol Metab Clin North Am *38*, 265-272, vii.

Chen, S., Wang, Q.L., Nie, Z., Sun, H., Lennon, G., Copeland, N.G., Gilbert, D.J., Jenkins, N.A., and Zack, D.J. (1997). Crx, a novel Otx-like paired-homeodomain protein, binds to and transactivates photoreceptor cell-specific genes. Neuron *19*, 1017-1030.

Cheng, H., Aleman, T.S., Cideciyan, A.V., Khanna, R., Jacobson, S.G., and Swaroop, A. (2006). In vivo function of the orphan nuclear receptor NR2E3 in establishing photoreceptor identity during mammalian retinal development. Hum Mol Genet *15*, 2588-2602.

Cheng, H., Khanna, H., Oh, E.C., Hicks, D., Mitton, K.P., and Swaroop, A. (2004a). Photoreceptor-specific nuclear receptor NR2E3 functions as a transcriptional activator in rod photoreceptors. Hum Mol Genet *13*, 1563-1575.

Cheng, L., Arata, A., Mizuguchi, R., Qian, Y., Karunaratne, A., Gray, P.A., Arata, S., Shirasawa, S., Bouchard, M., Luo, P.*, et al.* (2004b). Tlx3 and Tlx1 are post-mitotic selector genes determining glutamatergic over GABAergic cell fates. Nat Neurosci *7*, 510-517.

Chi, N.C., Shaw, R.M., De Val, S., Kang, G., Jan, L.Y., Black, B.L., and Stainier, D.Y. (2008). Foxn4 directly regulates tbx2b expression and atrioventricular canal formation. Genes Dev *22*, 734-739.

Chiaradia, I., and Lancaster, M.A. (2020). Brain organoids for the study of human neurobiology at the interface of in vitro and in vivo. Nature Neuroscience *23*, 1496-1508.

Chow, R.L., Altmann, C.R., Lang, R.A., and Hemmati-Brivanlou, A. (1999). Pax6 induces ectopic eyes in a vertebrate. Development *126*, 4213-4222.

Christine, K.S., and Conlon, F.L. (2008). Vertebrate CASTOR is required for differentiation of cardiac precursor cells at the ventral midline. Dev Cell *14*, 616-623.

Chu-LaGraff, Q., and Doe, C.Q. (1993). Neuroblast specification and formation regulated by wingless in the Drosophila CNS. Science *261*, 1594-1597.

Clark, B.S., Stein-O'Brien, G.L., Shiau, F., Cannon, G.H., Davis-Marcisak, E., Sherman, T., Santiago, C.P., Hoang, T.V., Rajaii, F., James-Esposito, R.E*., et al.* (2019). Single-Cell RNA-Seq Analysis of Retinal Development Identifies NFI Factors as Regulating Mitotic Exit and Late-Born Cell Specification. Neuron *102*, 1111-1126 e1115.

Cleary, M.D., and Doe, C.Q. (2006). Regulation of neuroblast competence: multiple temporal identity factors specify distinct neuronal fates within a single early competence window. Genes Dev *20*, 429-434.

Clerc, R.G., Corcoran, L.M., LeBowitz, J.H., Baltimore, D., and Sharp, P.A. (1988). The B-cell-specific Oct-2 protein contains POU box- and homeo box-type domains. Genes Dev *2*, 1570-1581.

Collinson, J.M., Hill, R.E., and West, J.D. (2000). Different roles for Pax6 in the optic vesicle and facial epithelium mediate early morphogenesis of the murine eye. Development *127*, 945-956.

Cong, L., Ran, F.A., Cox, D., Lin, S., Barretto, R., Habib, N., Hsu, P.D., Wu, X., Jiang, W., Marraffini, L.A*., et al.* (2013). Multiplex genome engineering using CRISPR/Cas systems. Science *339*, 819-823.

da Silva, S., and Cepko, C.L. (2017). Fgf8 Expression and Degradation of Retinoic Acid Are Required for Patterning a High-Acuity Area in the Retina. Dev Cell *42*, 68-81.e66.

Daniele, L.L., Lillo, C., Lyubarsky, A.L., Nikonov, S.S., Philp, N., Mears, A.J., Swaroop, A., Williams, D.S., and Pugh, E.N., Jr. (2005). Cone-like morphological, molecular, and electrophysiological features of the photoreceptors of the Nrl knockout mouse. Invest Ophthalmol Vis Sci *46*, 2156-2167.

Daum, J.M., Keles, O., Holwerda, S.J., Kohler, H., Rijli, F.M., Stadler, M., and Roska, B. (2017). The formation of the light-sensing compartment of cone photoreceptors coincides with a transcriptional switch. Elife *6*.

Davis, K.L. (2011). Ikaros: master of hematopoiesis, agent of leukemia. Ther Adv Hematol *2*, 359-368.

De la Huerta, I., Kim, I.J., Voinescu, P.E., and Sanes, J.R. (2012). Direction-selective retinal ganglion cells arise from molecularly specified multipotential progenitors. Proc Natl Acad Sci U S A *109*, 17663-17668.

de Melo, J., and Blackshaw, S. (2011). In vivo electroporation of developing mouse retina. J Vis Exp.

de Melo, J., Clark, B.S., and Blackshaw, S. (2016a). Multiple intrinsic factors act in concert with Lhx2 to direct retinal gliogenesis. Sci Rep *6*, 32757.

de Melo, J., Clark, B.S., Venkataraman, A., Shiau, F., Zibetti, C., and Blackshaw, S. (2018). Ldb1- and Rnf12-dependent regulation of Lhx2 controls the relative balance between neurogenesis and gliogenesis in the retina. Development *145*.

de Melo, J., Miki, K., Rattner, A., Smallwood, P., Zibetti, C., Hirokawa, K., Monuki, E.S., Campochiaro, P.A., and Blackshaw, S. (2012). Injury-independent induction of reactive gliosis in retina by loss of function of the LIM homeodomain transcription factor Lhx2. Proc Natl Acad Sci U S A *109*, 4657-4662.

de Melo, J., Zibetti, C., Clark, B.S., Hwang, W., Miranda-Angulo, A.L., Qian, J., and Blackshaw, S. (2016b). Lhx2 Is an Essential Factor for Retinal Gliogenesis and Notch Signaling. J Neurosci *36*, 2391-2405.

Debrulle, S., Baudouin, C., Hidalgo-Figueroa, M., Pelosi, B., Francius, C., Rucchin, V., Ronellenfitch, K., Chow, R.L., Tissir, F., Lee, S.K.*, et al.* (2020). Vsx1 and Chx10 paralogs sequentially secure V2 interneuron identity during spinal cord development. Cell Mol Life Sci *77*, 4117-4131.

Decembrini, S., Martin, C., Sennlaub, F., Chemtob, S., Biel, M., Samardzija, M., Moulin, A., Behar-Cohen, F., and Arsenijevic, Y. (2017). Cone Genesis Tracing by the Chrnb4-EGFP Mouse Line: Evidences of Cellular Material Fusion after Cone Precursor Transplantation. Mol Ther *25*, 634-653.

Dhomen, N.S., Balaggan, K.S., Pearson, R.A., Bainbridge, J.W., Levine, E.M., Ali, R.R., and Sowden, J.C. (2006). Absence of chx10 causes neural progenitors to persist in the adult retina. Invest Ophthalmol Vis Sci *47*, 386-396.

Diacou, R., Zhao, Y., Zheng, D., Cvekl, A., and Liu, W. (2018). Six3 and Six6 Are Jointly Required for the Maintenance of Multipotent Retinal Progenitors through Both Positive and Negative Regulation. Cell Rep *25*, 2510-2523 e2514.

Dick, T., Yang, X.H., Yeo, S.L., and Chia, W. (1991). Two closely linked Drosophila POU domain genes are expressed in neuroblasts and sensory elements. Proc Natl Acad Sci U S A *88*, 7645-7649.

Doe, C.Q. (2017). Temporal Patterning in the Drosophila CNS. Annu Rev Cell Dev Biol *33*, 219-240.

Donner, A.L., Episkopou, V., and Maas, R.L. (2007). Sox2 and Pou2f1 interact to control lens and olfactory placode development. Dev Biol *303*, 784-799.

Dorsky, R.I., Rapaport, D.H., and Harris, W.A. (1995). Xotch inhibits cell differentiation in the Xenopus retina. Neuron *14*, 487-496.

Dumortier, A., Kirstetter, P., Kastner, P., and Chan, S. (2003). Ikaros regulates neutrophil differentiation. Blood *101*, 2219-2226.

Ebisuya, M., and Briscoe, J. (2018). What does time mean in development? Development *145*.

Echelard, Y., Epstein, D.J., St-Jacques, B., Shen, L., Mohler, J., McMahon, J.A., and McMahon, A.P. (1993). Sonic hedgehog, a member of a family of putative signaling molecules, is implicated in the regulation of CNS polarity. Cell *75*, 1417-1430.

Egger, B., Chell, J.M., and Brand, A.H. (2008). Insights into neural stem cell biology from flies. Philos Trans R Soc Lond B Biol Sci *363*, 39-56.

Elliott, J., Jolicoeur, C., Ramamurthy, V., and Cayouette, M. (2008). Ikaros confers early temporal competence to mouse retinal progenitor cells. Neuron *60*, 26-39.

Emerson, M.M., Surzenko, N., Goetz, J.J., Trimarchi, J., and Cepko, C.L. (2013). Otx2 and Onecut1 promote the fates of cone photoreceptors and horizontal cells and repress rod photoreceptors. Dev Cell *26*, 59-72.

Erclik, T., Li, X., Courgeon, M., Bertet, C., Chen, Z., Baumert, R., Ng, J., Koo, C., Arain, U., Behnia, R.*, et al.* (2017). Integration of temporal and spatial patterning generates neural diversity. Nature *541*, 365-370.

Ericson, J., Rashbass, P., Schedl, A., Brenner-Morton, S., Kawakami, A., van Heyningen, V., Jessell, T.M., and Briscoe, J. (1997). Pax6 controls progenitor cell identity and neuronal fate in response to graded Shh signaling. Cell *90*, 169-180.

Eskandarian, Z., Fliegauf, M., Bulashevska, A., Proietti, M., Hague, R., Smulski, C.R., Schubert, D., Warnatz, K., and Grimbacher, B. (2019). Assessing the Functional Relevance of

Variants in the IKAROS Family Zinc Finger Protein 1 (IKZF1) in a Cohort of Patients With Primary Immunodeficiency. Front Immunol *10*, 568.

Ezzat, S., Mader, R., Fischer, S., Yu, S., Ackerley, C., and Asa, S.L. (2006). An essential role for the hematopoietic transcription factor Ikaros in hypothalamic–pituitary-mediated somatic growth. *103*, 2214-2219.

Ezzeddine, Z.D., Yang, X., DeChiara, T., Yancopoulos, G., and Cepko, C.L. (1997). Postmitotic cells fated to become rod photoreceptors can be respecified by CNTF treatment of the retina. Development *124*, 1055-1067.

Fan, C.M., Kuwana, E., Bulfone, A., Fletcher, C.F., Copeland, N.G., Jenkins, N.A., Crews, S., Martinez, S., Puelles, L., Rubenstein, J.L.*, et al.* (1996). Expression patterns of two murine homologs of Drosophila single-minded suggest possible roles in embryonic patterning and in the pathogenesis of Down syndrome. Mol Cell Neurosci *7*, 1-16.

Fekete, D.M., Perez-Miguelsanz, J., Ryder, E.F., and Cepko, C.L. (1994). Clonal analysis in the chicken retina reveals tangential dispersion of clonally related cells. Dev Biol *166*, 666-682.

Feng, J., Liu, T., Qin, B., Zhang, Y., and Liu, X.S. (2012). Identifying ChIP-seq enrichment using MACS. Nat Protoc *7*, 1728-1740.

Ferda Percin, E., Ploder, L.A., Yu, J.J., Arici, K., Horsford, D.J., Rutherford, A., Bapat, B., Cox, D.W., Duncan, A.M., Kalnins, V.I.*, et al.* (2000). Human microphthalmia associated with mutations in the retinal homeobox gene CHX10. Nat Genet *25*, 397-401.

Ferrari, S., Di Iorio, E., Barbaro, V., Ponzin, D., Sorrentino, F.S., and Parmeggiani, F. (2011). Retinitis pigmentosa: genes and disease mechanisms. Curr Genomics *12*, 238-249.

Fischer, A.J., Bosse, J.L., and El-Hodiri, H.M. (2013). The ciliary marginal zone (CMZ) in development and regeneration of the vertebrate eye. Exp Eye Res *116*, 199-204.

Florio, M., and Huttner, W.B. (2014). Neural progenitors, neurogenesis and the evolution of the neocortex. Development *141*, 2182-2194.

Francius, C., Harris, A., Rucchin, V., Hendricks, T.J., Stam, F.J., Barber, M., Kurek, D., Grosveld, F.G., Pierani, A., Goulding, M.*, et al.* (2013). Identification of multiple subsets of ventral interneurons and differential distribution along the rostrocaudal axis of the developing spinal cord. PLoS One *8*, e70325.

Francius, C., Ravassard, P., Hidalgo-Figueroa, M., Mallet, J., Clotman, F., and Nardelli, J. (2015). Genetic dissection of Gata2 selective functions during specification of V2 interneurons in the developing spinal cord. Dev Neurobiol *75*, 721-737.

Fu, W., Ergun, A., Lu, T., Hill, J.A., Haxhinasto, S., Fassett, M.S., Gazit, R., Adoro, S., Glimcher, L., Chan, S.*, et al.* (2012). A multiply redundant genetic switch 'locks in' the transcriptional signature of regulatory T cells. Nat Immunol *13*, 972-980.

Fujieda, H., Bremner, R., Mears, A.J., and Sasaki, H. (2009). Retinoic acid receptor-related orphan receptor alpha regulates a subset of cone genes during mouse retinal development. J Neurochem *108*, 91-101.

Furukawa, T., Morrow, E.M., and Cepko, C.L. (1997). Crx, a novel otx-like homeobox gene, shows photoreceptor-specific expression and regulates photoreceptor differentiation. Cell *91*, 531-541.

Furukawa, T., Mukherjee, S., Bao, Z.Z., Morrow, E.M., and Cepko, C.L. (2000). rax, Hes1, and notch1 promote the formation of Muller glia by postnatal retinal progenitor cells. Neuron *26*, 383-394.

Gaiano, N., Nye, J.S., and Fishell, G. (2000). Radial glial identity is promoted by Notch1 signaling in the murine forebrain. Neuron *26*, 395-404.

Gallardo, M.E., Lopez-Rios, J., Fernaud-Espinosa, I., Granadino, B., Sanz, R., Ramos, C., Ayuso, C., Seller, M.J., Brunner, H.G., Bovolenta, P.*, et al.* (1999). Genomic cloning and characterization of the human homeobox gene SIX6 reveals a cluster of SIX genes in chromosome 14 and associates SIX6 hemizygosity with bilateral anophthalmia and pituitary anomalies. Genomics *61*, 82-91.

Gallardo, M.E., Rodriguez De Cordoba, S., Schneider, A.S., Dwyer, M.A., Ayuso, C., and Bovolenta, P. (2004). Analysis of the developmental SIX6 homeobox gene in patients with anophthalmia/microphthalmia. Am J Med Genet A *129A*, 92-94.

Gasparini, S.J., Llonch, S., Borsch, O., and Ader, M. (2019). Transplantation of photoreceptors into the degenerative retina: Current state and future perspectives. Progress in retinal and eye research *69*, 1-37.

Georgopoulos, K., Moore, D.D., and Derfler, B. (1992). Ikaros, an early lymphoid-specific transcription factor and a putative mediator for T cell commitment. Science *258*, 808-812.

Gerster, T., and Roeder, R.G. (1988). A herpesvirus trans-activating protein interacts with transcription factor OTF-1 and other cellular proteins. Proc Natl Acad Sci U S A *85*, 6347-6351.

Glaser, T., Jepeal, L., Edwards, J.G., Young, S.R., Favor, J., and Maas, R.L. (1994). PAX6 gene dosage effect in a family with congenital cataracts, aniridia, anophthalmia and central nervous system defects. Nat Genet *7*, 463-471.

Glasgow, S.M., Henke, R.M., Macdonald, R.J., Wright, C.V., and Johnson, J.E. (2005). Ptf1a determines GABAergic over glutamatergic neuronal cell fate in the spinal cord dorsal horn. Development *132*, 5461-5469.

Gokhale, A.S., Gangaplara, A., Lopez-Occasio, M., Thornton, A.M., and Shevach, E.M. (2019). Selective deletion of Eos (Ikzf4) in T-regulatory cells leads to loss of suppressive function and development of systemic autoimmunity. J Autoimmun *105*, 102300.

Gomes, F.L., Zhang, G., Carbonell, F., Correa, J.A., Harris, W.A., Simons, B.D., and Cayouette, M. (2011). Reconstruction of rat retinal progenitor cell lineages in vitro reveals a surprising degree of stochasticity in cell fate decisions. Development *138*, 227-235.

Gonzalez-Cordero, A., Goh, D., Kruczek, K., Naeem, A., Fernando, M., Kleine Holthaus, S.M., Takaaki, M., Blackford, S.J.I., Kloc, M., Agundez, L.*, et al.* (2018). Assessment of AAV Vector Tropisms for Mouse and Human Pluripotent Stem Cell-Derived RPE and Photoreceptor Cells. Hum Gene Ther.

Gonzalez-Cordero, A., Kruczek, K., Naeem, A., Fernando, M., Kloc, M., Ribeiro, J., Goh, D., Duran, Y., Blackford, S.J.I., Abelleira-Hervas, L.*, et al.* (2017). Recapitulation of Human Retinal Development from Human Pluripotent Stem Cells Generates Transplantable Populations of Cone Photoreceptors. Stem Cell Reports *9*, 820-837.

Gordon, P.J., Yun, S., Clark, A.M., Monuki, E.S., Murtaugh, L.C., and Levine, E.M. (2013). Lhx2 balances progenitor maintenance with neurogenic output and promotes competence state progression in the developing retina. J Neurosci *33*, 12197-12207.

Gouge, A., Holt, J., Hardy, A.P., Sowden, J.C., and Smith, H.K. (2001). Foxn4 – a new member of the forkhead gene family is expressed in the retina. Mechanisms of Development *107*, 203-206.

Gowan, K., Helms, A.W., Hunsaker, T.L., Collisson, T., Ebert, P.J., Odom, R., and Johnson, J.E. (2001). Crossinhibitory activities of Ngn1 and Math1 allow specification of distinct dorsal interneurons. Neuron *31*, 219-232.

Gray, P.A., Fu, H., Luo, P., Zhao, Q., Yu, J., Ferrari, A., Tenzen, T., Yuk, D.I., Tsung, E.F., Cai, Z.*, et al.* (2004). Mouse brain organization revealed through direct genome-scale TF expression analysis. Science *306*, 2255-2257.

Grindley, J.C., Davidson, D.R., and Hill, R.E. (1995). The role of Pax-6 in eye and nasal development. Development *121*, 1433-1442.

Grosskortenhaus, R., Pearson, B.J., Marusich, A., and Doe, C.Q. (2005). Regulation of temporal identity transitions in Drosophila neuroblasts. Dev Cell *8*, 193-202.

Grosskortenhaus, R., Robinson, K.J., and Doe, C.Q. (2006). Pdm and Castor specify late-born motor neuron identity in the NB7-1 lineage. Genes Dev *20*, 2618-2627.

Hafler, B.P., Surzenko, N., Beier, K.T., Punzo, C., Trimarchi, J.M., Kong, J.H., and Cepko, C.L. (2012). Transcription factor Olig2 defines subpopulations of retinal progenitor cells biased toward specific cell fates. Proc Natl Acad Sci U S A *109*, 7882-7887.

Hahm, K., Cobb, B.S., McCarty, A.S., Brown, K.E., Klug, C.A., Lee, R., Akashi, K., Weissman, I.L., Fisher, A.G., and Smale, S.T. (1998). Helios, a T cell-restricted Ikaros family member that quantitatively associates with Ikaros at centromeric heterochromatin. Genes Dev *12*, 782-796.

Hand, R., Bortone, D., Mattar, P., Nguyen, L., Heng, J.I., Guerrier, S., Boutt, E., Peters, E., Barnes, A.P., Parras, C.*, et al.* (2005). Phosphorylation of Neurogenin2 specifies the migration properties and the dendritic morphology of pyramidal neurons in the neocortex. Neuron *48*, 45-62.

Hao, H., Kim, D.S., Klocke, B., Johnson, K.R., Cui, K., Gotoh, N., Zang, C., Gregorski, J., Gieser, L., Peng, W.*, et al.* (2012). Transcriptional regulation of rod photoreceptor homeostasis revealed by in vivo NRL targetome analysis. PLoS Genet *8*, e1002649.

Hao, H., Tummala, P., Guzman, E., Mali, R.S., Gregorski, J., Swaroop, A., and Mitton, K.P. (2011). The transcription factor neural retina leucine zipper (NRL) controls photoreceptor-specific expression of myocyte enhancer factor Mef2c from an alternative promoter. J Biol Chem *286*, 34893-34902.

Harland, R. (2000). Neural induction. Curr Opin Genet Dev *10*, 357-362.

Harris, A., Masgutova, G., Collin, A., Toch, M., Hidalgo-Figueroa, M., Jacob, B., Corcoran, L.M., Francius, C., and Clotman, F. (2019). Onecut Factors and Pou2f2 Regulate the

Distribution of V2 Interneurons in the Mouse Developing Spinal Cord. Front Cell Neurosci *13*, 184.

Hartenstein, V., Younossi-Hartenstein, A., and Lekven, A. (1994). Delamination and division in the Drosophila neurectoderm: spatiotemporal pattern, cytoskeletal dynamics, and common control by neurogenic and segment polarity genes. Dev Biol *165*, 480-499.

Hatzopoulos, A.K., Stoykova, A.S., Erselius, J.R., Goulding, M., Neuman, T., and Gruss, P. (1990). Structure and expression of the mouse Oct2a and Oct2b, two differentially spliced products of the same gene. *109*, 349-362.

He, J., Zhang, G., Almeida, Alexandra D., Cayouette, M., Simons, Benjamin D., and Harris, William A. (2012). How Variable Clones Build an Invariant Retina. Neuron *75*, 786-798.

He, X., Treacy, M.N., Simmons, D.M., Ingraham, H.A., Swanson, L.W., and Rosenfeld, M.G. (1989). Expression of a large family of POU-domain regulatory genes in mammalian brain development. Nature *340*, 35-41.

Heavner, W., and Pevny, L. (2012). Eye development and retinogenesis. Cold Spring Harb Perspect Biol *4*.

Helms, A.W., Battiste, J., Henke, R.M., Nakada, Y., Simplicio, N., Guillemot, F., and Johnson, J.E. (2005). Sequential roles for Mash1 and Ngn2 in the generation of dorsal spinal cord interneurons. Development *132*, 2709-2719.

Hendrickson, A. (1992). A morphological comparison of foveal development in man and monkey. Eye (Lond) *6 (Pt 2)*, 136-144.

Hendrickson, A. (2016). Development of Retinal Layers in Prenatal Human Retina. Am J Ophthalmol *161*, 29-35 e21.

Hendrickson, A., and Kupfer, C. (1976). The histogenesis of the fovea in the macaque monkey. Invest Ophthalmol Vis Sci *15*, 746-756.

Hendrickson, A., Possin, D., Kwan, W.C., Huang, J., and Bourne, J.A. (2016). The temporal profile of retinal cell genesis in the marmoset monkey. J Comp Neurol *524*, 1193-1207.

Hendrickson, A.E., and Yuodelis, C. (1984). The morphological development of the human fovea. Ophthalmology *91*, 603-612.

Henrique, D., Hirsinger, E., Adam, J., Le Roux, I., Pourquie, O., Ish-Horowicz, D., and Lewis, J. (1997). Maintenance of neuroepithelial progenitor cells by Delta-Notch signalling in the embryonic chick retina. Curr Biol *7*, 661-670.

Herr, W., Sturm, R.A., Clerc, R.G., Corcoran, L.M., Baltimore, D., Sharp, P.A., Ingraham, H.A., Rosenfeld, M.G., Finney, M., Ruvkun, G.*, et al.* (1988). The POU domain: a large conserved region in the mammalian pit-1, oct-1, oct-2, and Caenorhabditis elegans unc-86 gene products. Genes Dev *2*, 1513-1516.

Hoang, T., Wang, J., Boyd, P., Wang, F., Santiago, C., Jiang, L., Yoo, S., Lahne, M., Todd, L.J., Jia, M.*, et al.* (2020). Gene regulatory networks controlling vertebrate retinal regeneration. *370*, eabb8598.

Hodson, D.J., Shaffer, A.L., Xiao, W., Wright, G.W., Schmitz, R., Phelan, J.D., Yang, Y., Webster, D.E., Rui, L., Kohlhammer, H.*, et al.* (2016). Regulation of normal B-cell differentiation and malignant B-cell survival by OCT2. Proc Natl Acad Sci U S A *113*, E2039-2046.

Hojo, M., Ohtsuka, T., Hashimoto, N., Gradwohl, G., Guillemot, F., and Kageyama, R. (2000). Glial cell fate specification modulated by the bHLH gene Hes5 in mouse retina. Development *127*, 2515-2522.

Holt, C.E., Bertsch, T.W., Ellis, H.M., and Harris, W.A. (1988). Cellular determination in the Xenopus retina is independent of lineage and birth date. Neuron *1*, 15-26.

Homem, C.C., Repic, M., and Knoblich, J.A. (2015). Proliferation control in neural stem and progenitor cells. Nat Rev Neurosci *16*, 647-659.

Honma, Y., Kiyosawa, H., Mori, T., Oguri, A., Nikaido, T., Kanazawa, K., Tojo, M., Takeda, J., Tanno, Y., Yokoya, S.*, et al.* (1999). Eos: a novel member of the Ikaros gene family expressed predominantly in the developing nervous system. FEBS Lett *447*, 76-80.

Hori, K., and Hoshino, M. (2012). GABAergic neuron specification in the spinal cord, the cerebellum, and the cochlear nucleus. Neural Plast *2012*, 921732.

Hori, N., Nakano, H., Takeuchi, T., Kato, H., Hamaguchi, S., Oshimura, M., and Sato, K. (2002). A dyad oct-binding sequence functions as a maintenance sequence for the unmethylated state within the H19/Igf2-imprinted control region. J Biol Chem *277*, 27960-27967.

Hoshino, A., Ratnapriya, R., Brooks, M.J., Chaitankar, V., Wilken, M.S., Zhang, C., Starostik, M.R., Gieser, L., La Torre, A., Nishio, M.*, et al.* (2017). Molecular Anatomy of the Developing Human Retina. Dev Cell *43*, 763-779 e764.

Hyer, J., Mima, T., and Mikawa, T. (1998). FGF1 patterns the optic vesicle by directing the placement of the neural retina domain. Development *125*, 869-877.

Islam, M.M., Li, Y., Luo, H., Xiang, M., and Cai, L. (2013). Meis1 regulates Foxn4 expression during retinal progenitor cell differentiation. *2*, 1125-1136.

Isshiki, T., Pearson, B., Holbrook, S., and Doe, C.Q. (2001). Drosophila neuroblasts sequentially express transcription factors which specify the temporal identity of their neuronal progeny. Cell *106*, 511-521.

Jadhav, A.P., Cho, S.H., and Cepko, C.L. (2006a). Notch activity permits retinal cells to progress through multiple progenitor states and acquire a stem cell property. Proc Natl Acad Sci U S A *103*, 18998-19003.

Jadhav, A.P., Mason, H.A., and Cepko, C.L. (2006b). Notch 1 inhibits photoreceptor production in the developing mammalian retina. Development *133*, 913-923.

Javed, A., and Cayouette, M. (2017). Temporal Progression of Retinal Progenitor Cell Identity: Implications in Cell Replacement Therapies. Front Neural Circuits *11*, 105.

Javed, A., Mattar, P., Lu, S., Kruczek, K., Kloc, M., Gonzalez-Cordero, A., Bremner, R., Ali, R.R., and Cayouette, M. (2020). Pou2f1 and Pou2f2 cooperate to control the timing of cone photoreceptor production in the developing mouse retina. Development *147*.

Jean, D., Bernier, G., and Gruss, P. (1999). Six6 (Optx2) is a novel murine Six3-related homeobox gene that demarcates the presumptive pituitary/hypothalamic axis and the ventral optic stalk. Mech Dev *84*, 31-40.

Jensen, A.M., and Raff, M.C. (1997). Continuous observation of multipotential retinal progenitor cells in clonal density culture. Dev Biol *188*, 267-279.

Jeon, C.J., Strettoi, E., and Masland, R.H. (1998). The major cell populations of the mouse retina. J Neurosci *18*, 8936-8946.

Jessell, T.M. (2000). Neuronal specification in the spinal cord: inductive signals and transcriptional codes. Nat Rev Genet *1*, 20-29.

Jia, L., Oh, E.C., Ng, L., Srinivas, M., Brooks, M., Swaroop, A., and Forrest, D. (2009). Retinoid-related orphan nuclear receptor RORbeta is an early-acting factor in rod photoreceptor development. Proc Natl Acad Sci U S A *106*, 17534-17539.

John, L.B., Yoong, S., and Ward, A.C. (2009). Evolution of the Ikaros gene family: implications for the origins of adaptive immunity. J Immunol *182*, 4792-4799.

Johns, P.R., and Easter, S.S., Jr. (1977). Growth of the adult goldfish eye. II. Increase in retinal cell number. J Comp Neurol *176*, 331-341.

Jones, M.K., Lu, B., Girman, S., and Wang, S. (2017). Cell-based therapeutic strategies for replacement and preservation in retinal degenerative diseases. Prog Retin Eye Res *58*, 1-27.

Jorstad, N.L., Wilken, M.S., Grimes, W.N., Wohl, S.G., VandenBosch, L.S., Yoshimatsu, T., Wong, R.O., Rieke, F., and Reh, T.A. (2017). Stimulation of functional neuronal regeneration from Müller glia in adult mice. Nature *548*, 103-107.

Jorstad, N.L., Wilken, M.S., Todd, L., Finkbeiner, C., Nakamura, P., Radulovich, N., Hooper, M.J., Chitsazan, A., Wilkerson, B.A., Rieke, F.*, et al.* (2020). STAT Signaling Modifies Ascl1 Chromatin Binding and Limits Neural Regeneration from Muller Glia in Adult Mouse Retina. Cell Rep *30*, 2195-2208.e2195.

Kambadur, R., Koizumi, K., Stivers, C., Nagle, J., Poole, S.J., and Odenwald, W.F. (1998). Regulation of POU genes by castor and hunchback establishes layered compartments in the Drosophila CNS. Genes Dev *12*, 246-260.

Kanai, M.I., Okabe, M., and Hiromi, Y. (2005). seven-up Controls switching of transcription factors that specify temporal identities of Drosophila neuroblasts. Dev Cell *8*, 203-213.

Kang, J., Goodman, B., Zheng, Y., and Tantin, D. (2011). Dynamic regulation of Oct1 during mitosis by phosphorylation and ubiquitination. PLoS One *6*, e23872.

Karcavich, R., and Doe, C.Q. (2005). Drosophila neuroblast 7-3 cell lineage: a model system for studying programmed cell death, Notch/Numb signaling, and sequential specification of ganglion mother cell identity. J Comp Neurol *481*, 240-251.

Katoh, K., Omori, Y., Onishi, A., Sato, S., Kondo, M., and Furukawa, T. (2010). Blimp1 suppresses Chx10 expression in differentiating retinal photoreceptor precursors to ensure proper photoreceptor development. J Neurosci *30*, 6515-6526.

Kautzmann, M.A., Kim, D.S., Felder-Schmittbuhl, M.P., and Swaroop, A. (2011). Combinatorial regulation of photoreceptor differentiation factor, neural retina leucine zipper gene NRL, revealed by in vivo promoter analysis. J Biol Chem *286*, 28247-28255.

Kaya, K.D., Chen, H.Y., Brooks, M.J., Kelley, R.A., Shimada, H., Nagashima, K., de Val, N., Drinnan, C.T., Gieser, L., Kruczek, K.*, et al.* (2019). Transcriptome-based molecular staging of human stem cell-derived retinal organoids uncovers accelerated photoreceptor differentiation by 9-cis retinal. Mol Vis *25*, 663-678.

Kechad, A., Jolicoeur, C., Tufford, A., Mattar, P., Chow, R.W.Y., Harris, W.A., and Cayouette, M. (2012). Numb is required for the production of terminal asymmetric cell divisions in the developing mouse retina. J Neurosci *32*, 17197-17210.

Kefalov, V., Fu, Y., Marsh-Armstrong, N., and Yau, K.W. (2003). Role of visual pigment properties in rod and cone phototransduction. Nature *425*, 526-531.

Kelley, C.M., Ikeda, T., Koipally, J., Avitahl, N., Wu, L., Georgopoulos, K., and Morgan, B.A. (1998). Helios, a novel dimerization partner of Ikaros expressed in the earliest hematopoietic progenitors. Curr Biol *8*, 508-515.

Kelley, M.W., Turner, J.K., and Reh, T.A. (1994). Retinoic acid promotes differentiation of photoreceptors in vitro. Development *120*, 2091-2102.

Kim, J., Wu, H.H., Lander, A.D., Lyons, K.M., Matzuk, M.M., and Calof, A.L. (2005). GDF11 controls the timing of progenitor cell competence in developing retina. Science *308*, 1927-1930.

Kim, S., Lowe, A., Dharmat, R., Lee, S., Owen, L.A., Wang, J., Shakoor, A., Li, Y., Morgan, D.J., Hejazi, A.A.*, et al.* (2019). Generation, transcriptome profiling, and functional validation of cone-rich human retinal organoids. Proc Natl Acad Sci U S A *116*, 10824-10833.

Kirsch, M., Fuhrmann, S., Wiese, A., and Hofmann, H.D. (1996). CNTF exerts opposite effects on in vitro development of rat and chick photoreceptors. Neuroreport *7*, 697-700.

Kirsch, M., Schulz-Key, S., Wiese, A., Fuhrmann, S., and Hofmann, H. (1998). Ciliary neurotrophic factor blocks rod photoreceptor differentiation from postmitotic precursor cells in vitro. Cell Tissue Res *291*, 207-216.

Kirstetter, P., Thomas, M., Dierich, A., Kastner, P., and Chan, S. (2002). Ikaros is critical for B cell differentiation and function. Eur J Immunol *32*, 720-730.

Kiyota, T., Kato, A., Altmann, C.R., and Kato, Y. (2008). The POU homeobox protein Oct-1 regulates radial glia formation downstream of Notch signaling. Dev Biol *315*, 579-592.

Klemm, J.D., Rould, M.A., Aurora, R., Herr, W., and Pabo, C.O. (1994). Crystal structure of the Oct-1 POU domain bound to an octamer site: DNA recognition with tethered DNA-binding modules. Cell *77*, 21-32.

Klug, C.A., Morrison, S.J., Masek, M., Hahm, K., Smale, S.T., and Weissman, I.L. (1998). Hematopoietic stem cells and lymphoid progenitors express different Ikaros isoforms, and Ikaros is localized to heterochromatin in immature lymphocytes. Proc Natl Acad Sci U S A *95*, 657-662.

Ko, H.S., Fast, P., McBride, W., and Staudt, L.M. (1988). A human protein specific for the immunoglobulin octamer DNA motif contains a functional homeobox domain. Cell *55*, 135-144.

Kofler, N.M., Shawber, C.J., Kangsamaksin, T., Reed, H.O., Galatioto, J., and Kitajewski, J. (2011). Notch signaling in developmental and tumor angiogenesis. Genes Cancer *2*, 1106-1116.

Kohwi, M., and Doe, C.Q. (2013). Temporal fate specification and neural progenitor competence during development. Nat Rev Neurosci *14*, 823-838.

Kolb, H. (1995). S-Cone Pathways. In Webvision: The Organization of the Retina and Visual System, H. Kolb, E. Fernandez, and R. Nelson, eds. (Salt Lake City (UT)).

Komai, T., Iwanari, H., Mochizuki, Y., Hamakubo, T., and Shinkai, Y. (2009). Expression of the mouse PR domain protein Prdm8 in the developing central nervous system. Gene Expr Patterns *9*, 503-514.

Kong, W., Biddy, B.A., Kamimoto, K., Amrute, J.M., Butka, E.G., and Morris, S.A. (2020). CellTagging: combinatorial indexing to simultaneously map lineage and identity at single-cell resolution. Nat Protoc *15*, 750-772.

Konig, H., Pfisterer, P., Corcoran, L.M., and Wirth, T. (1995). Identification of CD36 as the first gene dependent on the B-cell differentiation factor Oct-2. Genes Dev *9*, 1598-1607.

Kriks, S., Lanuza, G.M., Mizuguchi, R., Nakafuku, M., and Goulding, M. (2005). Gsh2 is required for the repression of Ngn1 and specification of dorsal interneuron fate in the spinal cord. Development *132*, 2991-3002.

Krupnick, J.G., Gurevich, V.V., and Benovic, J.L. (1997). Mechanism of quenching of phototransduction. Binding competition between arrestin and transducin for phosphorhodopsin. J Biol Chem *272*, 18125-18131.

Kuehn, H.S., Boisson, B., Cunningham-Rundles, C., Reichenbach, J., Stray-Pedersen, A., Gelfand, E.W., Maffucci, P., Pierce, K.R., Abbott, J.K., Voelkerding, K.V.*, et al.* (2016). Loss of B Cells in Patients with Heterozygous Mutations in IKAROS. N Engl J Med *374*, 1032-1043.

Kunzevitzky, N.J., Almeida, M.V., Duan, Y., Li, S., Xiang, M., and Goldberg, J.L. (2011). Foxn4 is required for retinal ganglion cell distal axon patterning. Mol Cell Neurosci *46*, 731-741.

La Manno, G., Soldatov, R., Zeisel, A., Braun, E., Hochgerner, H., Petukhov, V., Lidschreiber, K., Kastriti, M.E., Lonnerberg, P., Furlan, A.*, et al.* (2018). RNA velocity of single cells. Nature *560*, 494-498.

La Vail, M.M., Rapaport, D.H., and Rakic, P. (1991). Cytogenesis in the monkey retina. J Comp Neurol *309*, 86-114.

Lahne, M., Nagashima, M., Hyde, D.R., and Hitchcock, P.F. (2020). Reprogramming Müller Glia to Regenerate Retinal Neurons. *6*, 171-193.

Lai, H.C., Seal, R.P., and Johnson, J.E. (2016). Making sense out of spinal cord somatosensory development. Development *143*, 3434-3448.

Langmead, B., and Salzberg, S.L. (2012). Fast gapped-read alignment with Bowtie 2. Nat Methods *9*, 357-359.

Latchman, D.S., Dent, C.L., Lillycrop, K.A., and Wood, J.N. (1992). POU family transcription factors in sensory neurons. Biochem Soc Trans *20*, 627-631.

Lee, C.Y., Wilkinson, B.D., Siegrist, S.E., Wharton, R.P., and Doe, C.Q. (2006). Brat is a Miranda cargo protein that promotes neuronal differentiation and inhibits neuroblast self-renewal. Dev Cell *10*, 441-449.

Lee, T., and Luo, L. (1999). Mosaic analysis with a repressible cell marker for studies of gene function in neuronal morphogenesis. Neuron *22*, 451-461.

Lennon, G., Auffray, C., Polymeropoulos, M., and Soares, M.B. (1996). The I.M.A.G.E. Consortium: an integrated molecular analysis of genomes and their expression. Genomics *33*, 151-152.

Levine, E.M., Roelink, H., Turner, J., and Reh, T.A. (1997). Sonic hedgehog promotes rod photoreceptor differentiation in mammalian retinal cells in vitro. J Neurosci *17*, 6277-6288.

Li, H., Kaminski, M.S., Li, Y., Yildiz, M., Ouillette, P., Jones, S., Fox, H., Jacobi, K., Saiya-Cork, K., Bixby, D*., et al.* (2014). Mutations in linker histone genes HIST1H1 B, C, D, and E; OCT2 (POU2F2); IRF8; and ARID1A underlying the pathogenesis of follicular lymphoma. Blood *123*, 1487-1498.

Li, S., Misra, K., Matise, M.P., and Xiang, M. (2005). Foxn4 acts synergistically with Mash1 to specify subtype identity of V2 interneurons in the spinal cord. *102*, 10688-10693.

Li, S., Misra, K., and Xiang, M. (2010). A Cre transgenic line for studying V2 neuronal lineages and functions in the spinal cord. Genesis *48*, 667-672.

Li, S., Mo, Z., Yang, X., Price, S.M., Shen, M.M., and Xiang, M. (2004). Foxn4 Controls the Genesis of Amacrine and Horizontal Cells by Retinal Progenitors. Neuron *43*, 795-807.

Li, S., and Xiang, M. (2011). Foxn4 influences alveologenesis during lung development. Dev Dyn *240*, 1512-1517.

Li, X., Erclik, T., Bertet, C., Chen, Z., Voutev, R., Venkatesh, S., Morante, J., Celik, A., and Desplan, C. (2013). Temporal patterning of Drosophila medulla neuroblasts controls neural fates. Nature *498*, 456-462.

Liem, K.F., Jr., Tremml, G., and Jessell, T.M. (1997). A role for the roof plate and its resident TGFbeta-related proteins in neuronal patterning in the dorsal spinal cord. Cell *91*, 127-138.

Lillien, L. (1995). Changes in retinal cell fate induced by overexpression of EGF receptor. Nature *377*, 158-162.

Lillycrop, K.A., Dawson, S.J., Estridge, J.K., Gerster, T., Matthias, P., and Latchman, D.S. (1994). Repression of a herpes simplex virus immediate-early promoter by the Oct-2 transcription factor is dependent on an inhibitory region at the N terminus of the protein. Mol Cell Biol *14*, 7633-7642.

Lillycrop, K.A., and Latchman, D.S. (1992). Alternative splicing of the Oct-2 transcription factor RNA is differentially regulated in neuronal cells and B cells and results in protein isoforms with opposite effects on the activity of octamer/TAATGARAT-containing promoters. J Biol Chem *267*, 24960-24965.

Liu, H., Etter, P., Hayes, S., Jones, I., Nelson, B., Hartman, B., Forrest, D., and Reh, T.A. (2008). NeuroD1 regulates expression of thyroid hormone receptor 2 and cone opsins in the developing mouse retina. J Neurosci *28*, 749-756.

Liu, I.S., Chen, J.D., Ploder, L., Vidgen, D., van der Kooy, D., Kalnins, V.I., and McInnes, R.R. (1994). Developmental expression of a novel murine homeobox gene (Chx10): evidence for roles in determination of the neuroretina and inner nuclear layer. Neuron *13*, 377-393.

Liu, S., Liu, X., Li, S., Huang, X., Qian, H., Jin, K., and Xiang, M. (2020a). Foxn4 is a temporal identity factor conferring mid/late-early retinal competence and involved in retinal synaptogenesis. Proc Natl Acad Sci U S A *117*, 5016-5027.

Liu, S.Q., Jiang, S., Li, C., Zhang, B., and Li, Q.J. (2014a). miR-17-92 cluster targets phosphatase and tensin homology and Ikaros Family Zinc Finger 4 to promote TH17-mediated inflammation. J Biol Chem *289*, 12446-12456.

Liu, T., Li, J., Yu, L., Sun, H.-X., Li, J., Dong, G., Hu, Y., Li, Y., Shen, Y., Wu, J.*, et al.* (2021). Cross-species single-cell transcriptomic analysis reveals pre-gastrulation developmental differences among pigs, monkeys, and humans. Cell Discovery *7*, 8.

Liu, Y.Z., Lillycrop, K.A., and Latchman, D.S. (1995). Regulated splicing of the Oct-2 transcription factor RNA in neuronal cells. Neurosci Lett *183*, 8-12.

Liu, Z., Li, W., Ma, X., Ding, N., Spallotta, F., Southon, E., Tessarollo, L., Gaetano, C., Mukouyama, Y.S., and Thiele, C.J. (2014b). Essential role of the zinc finger transcription factor Casz1 for mammalian cardiac morphogenesis and development. J Biol Chem *289*, 29801-29816.

Liu, Z., Naranjo, A., and Thiele, C.J. (2011). CASZ1b, the short isoform of CASZ1 gene, coexpresses with CASZ1a during neurogenesis and suppresses neuroblastoma cell growth. PLoS One *6*, e18557.

Liu, Z., Zhang, X., Lei, H., Lam, N., Carter, S., Yockey, O., Xu, M., Mendoza, A., Hernandez, E.R., Wei, J.S.*, et al.* (2020b). CASZ1 induces skeletal muscle and rhabdomyosarcoma differentiation through a feed-forward loop with MYOD and MYOG. Nat Commun *11*, 911.

Lloyd, A., and Sakonju, S. (1991). Characterization of two Drosophila POU domain genes, related to oct-1 and oct-2, and the regulation of their expression patterns. Mech Dev *36*, 87-102.

Loosli, F., Winkler, S., and Wittbrodt, J. (1999). Six3 overexpression initiates the formation of ectopic retina. Genes Dev *13*, 649-654.

Lu, B., Rothenberg, M., Jan, L.Y., and Jan, Y.N. (1998). Partner of Numb colocalizes with Numb during mitosis and directs Numb asymmetric localization in Drosophila neural and muscle progenitors. Cell *95*, 225-235.

Lu, Y., Shiau, F., Yi, W., Lu, S., Wu, Q., Pearson, J.D., Kallman, A., Zhong, S., Hoang, T., Zuo, Z.*, et al.* (2020). Single-Cell Analysis of Human Retina Identifies Evolutionarily Conserved and Species-Specific Mechanisms Controlling Development. Dev Cell *53*, 473-491 e479.

Luchina, N.N., Krivega, I.V., and Pankratova, E.V. (2003). Human Oct-1L isoform has tissue-specific expression pattern similar to Oct-2. Immunol Lett *85*, 237-241.

Luo, H., Jin, K., Xie, Z., Qiu, F., Li, S., Zou, M., Cai, L., Hozumi, K., Shima, D.T., and Xiang, M. (2012). Forkhead box N4 (Foxn4) activates Dll4-Notch signaling to suppress photoreceptor cell fates of early retinal progenitors. *109*, E553-E562.

Ma, L., Cantrup, R., Varrault, A., Colak, D., Klenin, N., Gotz, M., McFarlane, S., Journot, L., and Schuurmans, C. (2007). Zac1 functions through TGFbetaII to negatively regulate cell number in the developing retina. Neural Dev *2*, 11.

Malhas, A.N., Lee, C.F., and Vaux, D.J. (2009). Lamin B1 controls oxidative stress responses via Oct-1. J Cell Biol *184*, 45-55.

Mann, I.C. (1928). THE PROCESS OF DIFFERENTIATION OF THE RETINAL LAYERS IN VERTEBRATES. Br J Ophthalmol *12*, 449-478.

Marcucci, F., Murcia-Belmonte, V., Wang, Q., Coca, Y., Ferreiro-Galve, S., Kuwajima, T., Khalid, S., Ross, M.E., Mason, C., and Herrera, E. (2016). The Ciliary Margin Zone of the Mammalian Retina Generates Retinal Ganglion Cells. Cell Rep *17*, 3153-3164.

Marquardt, T., Ashery-Padan, R., Andrejewski, N., Scardigli, R., Guillemot, F., and Gruss, P. (2001). Pax6 is required for the multipotent state of retinal progenitor cells. Cell *105*, 43-55.

Mathers, P.H., Grinberg, A., Mahon, K.A., and Jamrich, M. (1997). The Rx homeobox gene is essential for vertebrate eye development. Nature *387*, 603-607.

Matsuda, T., and Cepko, C.L. (2007). Controlled expression of transgenes introduced by in vivo electroporation. Proc Natl Acad Sci U S A *104*, 1027-1032.

Matsuzaki, F., Ohshiro, T., Ikeshima-Kataoka, H., and Izumi, H. (1998). miranda localizes staufen and prospero asymmetrically in mitotic neuroblasts and epithelial cells in early Drosophila embryogenesis. Development *125*, 4089-4098.

Matsuzaki, M., and Saigo, K. (1996). hedgehog signaling independent of engrailed and wingless required for post-S1 neuroblast formation in Drosophila CNS. Development *122*, 3567-3575.

Mattar, P., Ericson, J., Blackshaw, S., and Cayouette, M. (2015). A conserved regulatory logic controls temporal identity in mouse neural progenitors. Neuron *85*, 497-504.

Mattar, P., Jolicoeur, C., Dang, T., Shah, S., Clark, B.S., and Cayouette, M. (2021). A Casz1-NuRD complex regulates temporal identity transitions in neural progenitors. Sci Rep *11*, 3858.

Mattar, P., Langevin, L.M., Markham, K., Klenin, N., Shivji, S., Zinyk, D., and Schuurmans, C. (2008). Basic helix-loop-helix transcription factors cooperate to specify a cortical projection neuron identity. Mol Cell Biol *28*, 1456-1469.

Mattar, P., Stevanovic, M., Nad, I., and Cayouette, M. (2018). Casz1 controls higher-order nuclear organization in rod photoreceptors. Proc Natl Acad Sci U S A *115*, E7987-E7996.

Maurange, C., Cheng, L., and Gould, A.P. (2008). Temporal transcription factors and their targets schedule the end of neural proliferation in Drosophila. Cell *133*, 891-902.

McDonald, J.A., and Doe, C.Q. (1997). Establishing neuroblast-specific gene expression in the Drosophila CNS: huckebein is activated by Wingless and Hedgehog and repressed by Engrailed and Gooseberry. Development *124*, 1079-1087.

Mears, A.J., Kondo, M., Swain, P.K., Takada, Y., Bush, R.A., Saunders, T.L., Sieving, P.A., and Swaroop, A. (2001). Nrl is required for rod photoreceptor development. Nat Genet *29*, 447-452.

Mikami, Y. (1939). Reciprocal Transformation of Parts in the Developing Eve-vesicle, with Special Attention to the Inductive Influence of Lens-ectoderm on the Retinal Differentiation. 動物学雑誌 *51*, 253-256.

Misra, K., Luo, H., Li, S., Matise, M., and Xiang, M. (2014). Asymmetric activation of Dll4-Notch signaling by Foxn4 and proneural factors activates BMP/TGFβ signaling to specify V2b interneurons in the spinal cord. *141*, 187-198.

Mitton, K.P., Swain, P.K., Chen, S., Xu, S., Zack, D.J., and Swaroop, A. (2000). The leucine zipper of NRL interacts with the CRX homeodomain. A possible mechanism of transcriptional synergy in rhodopsin regulation. J Biol Chem *275*, 29794-29799.

Mizeracka, K., DeMaso, C.R., and Cepko, C.L. (2013). Notch1 is required in newly postmitotic cells to inhibit the rod photoreceptor fate. Development *140*, 3188-3197.

Mizuguchi, R., Kriks, S., Cordes, R., Gossler, A., Ma, Q., and Goulding, M. (2006). Ascl1 and Gsh1/2 control inhibitory and excitatory cell fate in spinal sensory interneurons. Nat Neurosci *9*, 770-778.

Mizuguchi, R., Sugimori, M., Takebayashi, H., Kosako, H., Nagao, M., Yoshida, S., Nabeshima, Y., Shimamura, K., and Nakafuku, M. (2001). Combinatorial roles of olig2 and neurogenin2 in the coordinated induction of pan-neuronal and subtype-specific properties of motoneurons. Neuron *31*, 757-771.

Molnár, A., Wu, P., Largespada, D.A., Vortkamp, A., Scherer, S., Copeland, N.G., Jenkins, N.A., Bruns, G., and Georgopoulos, K. (1996). The Ikaros gene encodes a family of lymphocyte-

restricted zinc finger DNA binding proteins, highly conserved in human and mouse. J Immunol *156*, 585-592.

Montana, C.L., Kolesnikov, A.V., Shen, S.Q., Myers, C.A., Kefalov, V.J., and Corbo, J.C. (2013). Reprogramming of adult rod photoreceptors prevents retinal degeneration. Proc Natl Acad Sci U S A *110*, 1732-1737.

Montana, C.L., Lawrence, K.A., Williams, N.L., Tran, N.M., Peng, G.H., Chen, S., and Corbo, J.C. (2011). Transcriptional regulation of neural retina leucine zipper (Nrl), a photoreceptor cell fate determinant. J Biol Chem *286*, 36921-36931.

Monteiro, C.B., Midão, L., Rebelo, S., Reguenga, C., Lima, D., and Monteiro, F.A. (2016). Zinc finger transcription factor Casz1 expression is regulated by homeodomain transcription factor Prrxl1 in embryonic spinal dorsal horn late-born excitatory interneurons. Eur J Neurosci *43*, 1449-1459.

Moore, D.L., Blackmore, M.G., Hu, Y., Kaestner, K.H., Bixby, J.L., Lemmon, V.P., and Goldberg, J.L. (2009). KLF family members regulate intrinsic axon regeneration ability. Science *326*, 298-301.

Moran-Rivard, L., Kagawa, T., Saueressig, H., Gross, M.K., Burrill, J., and Goulding, M. (2001). Evx1 is a postmitotic determinant of v0 interneuron identity in the spinal cord. Neuron *29*, 385-399.

Morgan, B., Sun, L., Avitahl, N., Andrikopoulos, K., Ikeda, T., Gonzales, E., Wu, P., Neben, S., and Georgopoulos, K. (1997). Aiolos, a lymphoid restricted transcription factor that interacts with Ikaros to regulate lymphocyte differentiation. EMBO J *16*, 2004-2013.

Mu, X., Fu, X., Sun, H., Beremand, P.D., Thomas, T.L., and Klein, W.H. (2005). A gene network downstream of transcription factor Math5 regulates retinal progenitor cell competence and ganglion cell fate. Dev Biol *280*, 467-481.

Muller, T., Anlag, K., Wildner, H., Britsch, S., Treier, M., and Birchmeier, C. (2005). The bHLH factor Olig3 coordinates the specification of dorsal neurons in the spinal cord. Genes Dev *19*, 733-743.

Muller, T., Brohmann, H., Pierani, A., Heppenstall, P.A., Lewin, G.R., Jessell, T.M., and Birchmeier, C. (2002). The homeodomain factor lbx1 distinguishes two major programs of neuronal differentiation in the dorsal spinal cord. Neuron *34*, 551-562.

Muto, A., Iida, A., Satoh, S., and Watanabe, S. (2009). The group E Sox genes Sox8 and Sox9 are regulated by Notch signaling and are required for Muller glial cell development in mouse retina. Exp Eye Res *89*, 549-558.

Nakajima, A., Isshiki, T., Kaneko, K., and Ishihara, S. (2010). Robustness under functional constraint: the genetic network for temporal expression in Drosophila neurogenesis. PLoS Comput Biol *6*, e1000760.

Nelson, B.R., Hartman, B.H., Georgi, S.A., Lan, M.S., and Reh, T.A. (2007). Transient inactivation of Notch signaling synchronizes differentiation of neural progenitor cells. Dev Biol *304*, 479-498.

Nelson, B.R., Ueki, Y., Reardon, S., Karl, M.O., Georgi, S., Hartman, B.H., Lamba, D.A., and Reh, T.A. (2011). Genome-wide analysis of Muller glial differentiation reveals a requirement for Notch signaling in postmitotic cells to maintain the glial fate. PLoS One *6*, e22817.

Neophytou, C., Vernallis, A.B., Smith, A., and Raff, M.C. (1997). Muller-cell-derived leukaemia inhibitory factor arrests rod photoreceptor differentiation at a postmitotic pre-rod stage of development. Development *124*, 2345-2354.

Ng, L., Hurley, J.B., Dierks, B., Srinivas, M., Salto, C., Vennstrom, B., Reh, T.A., and Forrest, D. (2001). A thyroid hormone receptor that is required for the development of green cone photoreceptors. Nat Genet *27*, 94-98.

Ng, L., Lu, A., Swaroop, A., Sharlin, D.S., Swaroop, A., and Forrest, D. (2011). Two transcription factors can direct three photoreceptor outcomes from rod precursor cells in mouse retinal development. J Neurosci *31*, 11118-11125.

Ng, L., Ma, M., Curran, T., and Forrest, D. (2009). Developmental expression of thyroid hormone receptor beta2 protein in cone photoreceptors in the mouse. Neuroreport *20*, 627-631.

Nguyen, M., and Arnheiter, H. (2000). Signaling and transcriptional regulation in early mammalian eye development: a link between FGF and MITF. Development *127*, 3581-3591.

Nishida, A., Furukawa, A., Koike, C., Tano, Y., Aizawa, S., Matsuo, I., and Furukawa, T. (2003). Otx2 homeobox gene controls retinal photoreceptor cell fate and pineal gland development. Nat Neurosci *6*, 1255-1263.

Nornes, H.O., and Das, G.D. (1972). Temporal pattern of neurogenesis in spinal cord: cytoarchitecture and directed growth of axons. Proc Natl Acad Sci U S A *69*, 1962-1966.

Nornes, H.O., and Das, G.D. (1974). Temporal pattern of neurogenesis in spinal cord of rat. I. An autoradiographic study--time and sites of origin and migration and settling patterns of neuroblasts. Brain Res *73*, 121-138.

Novitch, B.G., Chen, A.I., and Jessell, T.M. (2001). Coordinate regulation of motor neuron subtype identity and pan-neuronal properties by the bHLH repressor Olig2. Neuron *31*, 773-789.

Novotny, T., Eiselt, R., and Urban, J. (2002). Hunchback is required for the specification of the early sublineage of neuroblast 7-3 in the Drosophila central nervous system. Development *129*, 1027-1036.

O'Neill, E.A., Fletcher, C., Burrow, C.R., Heintz, N., Roeder, R.G., and Kelly, T.J. (1988). Transcription factor OTF-1 is functionally identical to the DNA replication factor NF-III. Science *241*, 1210-1213.

Oh, E.C., Cheng, H., Hao, H., Jia, L., Khan, N.W., and Swaroop, A. (2008). Rod differentiation factor NRL activates the expression of nuclear receptor NR2E3 to suppress the development of cone photoreceptors. Brain Res *1236*, 16-29.

Oh, E.C., Khan, N., Novelli, E., Khanna, H., Strettoi, E., and Swaroop, A. (2007). Transformation of cone precursors to functional rod photoreceptors by bZIP transcription factor NRL. Proc Natl Acad Sci U S A *104*, 1679-1684.

Oliver, G., Mailhos, A., Wehr, R., Copeland, N.G., Jenkins, N.A., and Gruss, P. (1995). Six3, a murine homologue of the sine oculis gene, demarcates the most anterior border of the developing neural plate and is expressed during eye development. Development *121*, 4045-4055.

Onishi, A., Peng, G.-H., Poth, E.M., Lee, D.A., Chen, J., Alexis, U., de Melo, J., Chen, S., and Blackshaw, S. (2010). The orphan nuclear hormone receptor ERRβ controls rod photoreceptor survival. *107*, 11579-11584.

Ortin-Martinez, A., Nadal-Nicolas, F.M., Jimenez-Lopez, M., Alburquerque-Bejar, J.J., Nieto-Lopez, L., Garcia-Ayuso, D., Villegas-Perez, M.P., Vidal-Sanz, M., and Agudo-Barriuso, M. (2014). Number and distribution of mouse retinal cone photoreceptors: differences between an albino (Swiss) and a pigmented (C57/BL6) strain. PLoS One *9*, e102392.

Ortin-Martinez, A., Tsai, E.L., Nickerson, P.E., Bergeret, M., Lu, Y., Smiley, S., Comanita, L., and Wallace, V.A. (2017). A Reinterpretation of Cell Transplantation: GFP Transfer From Donor to Host Photoreceptors. Stem Cells *35*, 932-939.

Ouimette, J.F., Jolin, M.L., L'Honore, A., Gifuni, A., and Drouin, J. (2010). Divergent transcriptional activities determine limb identity. Nat Commun *1*, 35.

Ovando-Roche, P., West, E.L., Branch, M.J., Sampson, R.D., Fernando, M., Munro, P., Georgiadis, A., Rizzi, M., Kloc, M., Naeem, A.*, et al.* (2018). Use of bioreactors for culturing human retinal organoids improves photoreceptor yields. Stem Cell Res Ther *9*, 156.

Ozawa, Y., Nakao, K., Shimazaki, T., Shimmura, S., Kurihara, T., Ishida, S., Yoshimura, A., Tsubota, K., and Okano, H. (2007). SOCS3 is required to temporally fine-tune photoreceptor cell differentiation. Dev Biol *303*, 591-600.

Pan, D., Xia, X.X., Zhou, H., Jin, S.Q., Lu, Y.Y., Liu, H., Gao, M.L., and Jin, Z.B. (2020). COCO enhances the efficiency of photoreceptor precursor differentiation in early human embryonic stem cell-derived retinal organoids. Stem Cell Res Ther *11*, 366.

Pan, F., Yu, H., Dang, E.V., Barbi, J., Pan, X., Grosso, J.F., Jinasena, D., Sharma, S.M., McCadden, E.M., Getnet, D.*, et al.* (2009). Eos mediates Foxp3-dependent gene silencing in CD4+ regulatory T cells. Science *325*, 1142-1146.

Payne, K.J., Huang, G., Sahakian, E., Zhu, J.Y., Barteneva, N.S., Barsky, L.W., Payne, M.A., and Crooks, G.M. (2003). Ikaros isoform x is selectively expressed in myeloid differentiation. J Immunol *170*, 3091-3098.

Payne, K.J., Nicolas, J.H., Zhu, J.Y., Barsky, L.W., and Crooks, G.M. (2001). Cutting edge: predominant expression of a novel Ikaros isoform in normal human hemopoiesis. J Immunol *167*, 1867-1870.

Pearson, B.J., and Doe, C.Q. (2003). Regulation of neuroblast competence in Drosophila. Nature *425*, 624-628.

Pearson, R.A., Gonzalez-Cordero, A., West, E.L., Ribeiro, J.R., Aghaizu, N., Goh, D., Sampson, R.D., Georgiadis, A., Waldron, P.V., Duran, Y.*, et al.* (2016). Donor and host photoreceptors engage in material transfer following transplantation of post-mitotic photoreceptor precursors. Nat Commun *7*, 13029.

Perdomo, J., Holmes, M., Chong, B., and Crossley, M. (2000). Eos and pegasus, two members of the Ikaros family of proteins with distinct DNA binding activities. J Biol Chem *275*, 38347-38354.

Philippidou, P., and Dasen, J.S. (2013). Hox genes: choreographers in neural development, architects of circuit organization. Neuron *80*, 12-34.

Pierani, A., Brenner-Morton, S., Chiang, C., and Jessell, T.M. (1999). A sonic hedgehog-independent, retinoid-activated pathway of neurogenesis in the ventral spinal cord. Cell *97*, 903-915.

Pierani, A., Moran-Rivard, L., Sunshine, M.J., Littman, D.R., Goulding, M., and Jessell, T.M. (2001). Control of interneuron fate in the developing spinal cord by the progenitor homeodomain protein Dbx1. Neuron *29*, 367-384.

Pillai, A., Mansouri, A., Behringer, R., Westphal, H., and Goulding, M. (2007). Lhx1 and Lhx5 maintain the inhibitory-neurotransmitter status of interneurons in the dorsal spinal cord. Development *134*, 357-366.

Pituello, F. (1997). Neuronal specification: generating diversity in the spinal cord. Curr Biol *7*, R701-704.

Poche, R.A., Furuta, Y., Chaboissier, M.C., Schedl, A., and Behringer, R.R. (2008). Sox9 is expressed in mouse multipotent retinal progenitor cells and functions in Muller glial cell development. J Comp Neurol *510*, 237-250.

Pounds, S., and Dyer, M.A. (2008). Statistical analysis of data from retroviral clonal experiments in the developing retina. Brain Res *1192*, 178-185.

Powell, M.D., Read, K.A., Sreekumar, B.K., and Oestreich, K.J. (2019). Ikaros Zinc Finger Transcription Factors: Regulators of Cytokine Signaling Pathways and CD4(+) T Helper Cell Differentiation. Front Immunol *10*, 1299.

Provis, J.M., Diaz, C.M., and Dreher, B. (1998). Ontogeny of the primate fovea: a central issue in retinal development. Prog Neurobiol *54*, 549-580.

Pruijn, G.J., van Driel, W., and van der Vliet, P.C. (1986). Nuclear factor III, a novel sequence-specific DNA-binding protein from HeLa cells stimulating adenovirus DNA replication. Nature *322*, 656-659.

Qian, Y., Shirasawa, S., Chen, C.L., Cheng, L., and Ma, Q. (2002). Proper development of relay somatic sensory neurons and D2/D4 interneurons requires homeobox genes Rnx/Tlx-3 and Tlx-1. Genes Dev *16*, 1220-1233.

Quinlan, A.R., and Hall, I.M. (2010). BEDTools: a flexible suite of utilities for comparing genomic features. Bioinformatics *26*, 841-842.

Quirion, M.R., Gregory, G.D., Umetsu, S.E., Winandy, S., and Brown, M.A. (2009). Cutting edge: Ikaros is a regulator of Th2 cell differentiation. J Immunol *182*, 741-745.

Ramamurthy, V., Jolicoeur, C., Koutroumbas, D., Muhlhans, J., Le, Y.Z., Hauswirth, W.W., Giessl, A., and Cayouette, M. (2014). Numb regulates the polarized delivery of cyclic nucleotide-gated ion channels in rod photoreceptor cilia. The Journal of neuroscience : the official journal of the Society for Neuroscience *34*, 13976-13987.

Ramirez, F., Ryan, D.P., Gruning, B., Bhardwaj, V., Kilpert, F., Richter, A.S., Heyne, S., Dundar, F., and Manke, T. (2016). deepTools2: a next generation web server for deep-sequencing data analysis. Nucleic Acids Res *44*, W160-165.

Rapaport, D.H., Wong, L.L., Wood, E.D., Yasumura, D., and LaVail, M.M. (2004). Timing and topography of cell genesis in the rat retina. J Comp Neurol *474*, 304-324.

Ray, P., Torck, A., Quigley, L., Wangzhou, A., Neiman, M., Rao, C., Lam, T., Kim, J.Y., Kim, T.H., Zhang, M.Q.*, et al.* (2018). Comparative transcriptome profiling of the human and mouse dorsal root ganglia: an RNA-seq-based resource for pain and sensory neuroscience research. Pain *159*, 1325-1345.

Read, K.A., Powell, M.D., Baker, C.E., Sreekumar, B.K., Ringel-Scaia, V.M., Bachus, H., Martin, R.E., Cooley, I.D., Allen, I.C., Ballesteros-Tato, A.*, et al.* (2017). Integrated STAT3 and Ikaros Zinc Finger Transcription Factor Activities Regulate Bcl-6 Expression in CD4(+) Th Cells. J Immunol *199*, 2377-2387.

Reese, B.E., Necessary, B.D., Tam, P.P., Faulkner-Jones, B., and Tan, S.S. (1999). Clonal expansion and cell dispersion in the developing mouse retina. Eur J Neurosci *11*, 2965-2978.

Reményi, A., Tomilin, A., Pohl, E., Lins, K., Philippsen, A., Reinbold, R., Schöler, H.R., and Wilmanns, M. (2001). Differential dimer activities of the transcription factor Oct-1 by DNA-induced interface swapping. Mol Cell *8*, 569-580.

Rheaume, B.A., Jereen, A., Bolisetty, M., Sajid, M.S., Yang, Y., Renna, K., Sun, L., Robson, P., and Trakhtenberg, E.F. (2018). Single cell transcriptome profiling of retinal ganglion cells identifies cellular subtypes. Nat Commun *9*, 2759.

Rieder, S.A., Metidji, A., Glass, D.D., Thornton, A.M., Ikeda, T., Morgan, B.A., and Shevach, E.M. (2015). Eos Is Redundant for Regulatory T Cell Function but Plays an Important Role in IL-2 and Th17 Production by CD4+ Conventional T Cells. J Immunol *195*, 553-563.

Riesenberg, A.N., Liu, Z., Kopan, R., and Brown, N.L. (2009). Rbpj cell autonomous regulation of retinal ganglion cell and cone photoreceptor fates in the mouse retina. J Neurosci *29*, 12865-12877.

Ringuette, R., Atkins, M., Lagali, P.S., Bassett, E.A., Campbell, C., Mazerolle, C., Mears, A.J., Picketts, D.J., and Wallace, V.A. (2016). A Notch-Gli2 axis sustains Hedgehog responsiveness of neural progenitors and Muller glia. Dev Biol *411*, 85-100.

Roberts, M.R., Hendrickson, A., McGuire, C.R., and Reh, T.A. (2005). Retinoid X receptor (gamma) is necessary to establish the S-opsin gradient in cone photoreceptors of the developing mouse retina. Invest Ophthalmol Vis Sci *46*, 2897-2904.

Rocha-Martins, M., de Toledo, B.C., Santos-Franca, P.L., Oliveira-Valenca, V.M., Vieira-Vieira, C.H., Matos-Rodrigues, G.E., Linden, R., Norden, C., Martins, R.A.P., and Silveira, M.S. (2019). De novo genesis of retinal ganglion cells by targeted expression of Klf4 in vivo. Development *146*.

Roesch, K., Jadhav, A.P., Trimarchi, J.M., Stadler, M.B., Roska, B., Sun, B.B., and Cepko, C.L. (2008). The transcriptome of retinal Muller glial cells. J Comp Neurol *509*, 225-238.

Ruan, G.X., Barry, E., Yu, D., Lukason, M., Cheng, S.H., and Scaria, A. (2017). CRISPR/Cas9-Mediated Genome Editing as a Therapeutic Approach for Leber Congenital Amaurosis 10. Mol Ther *25*, 331-341.

Sagner, A., Zhang, I., Watson, T., Lazaro, J., Melchionda, M., and Briscoe, J. (2020). Temporal patterning of the central nervous system by a shared transcription factor code. 2020.2011.2010.376491.

Santos-Ferreira, T., Llonch, S., Borsch, O., Postel, K., Haas, J., and Ader, M. (2016). Retinal transplantation of photoreceptors results in donor-host cytoplasmic exchange. Nat Commun *7*, 13028.

Sapkota, D., Chintala, H., Wu, F., Fliesler, S.J., Hu, Z., and Mu, X. (2014). Onecut1 and Onecut2 redundantly regulate early retinal cell fates during development. Proc Natl Acad Sci U S A *111*, E4086-4095.

Satoh, S., Tang, K., Iida, A., Inoue, M., Kodama, T., Tsai, S.Y., Tsai, M.J., Furuta, Y., and Watanabe, S. (2009). The spatial patterning of mouse cone opsin expression is regulated by bone morphogenetic protein signaling through downstream effector COUP-TF nuclear receptors. J Neurosci *29*, 12401-12411.

Scheer, N., Groth, A., Hans, S., and Campos-Ortega, J.A. (2001). An instructive function for Notch in promoting gliogenesis in the zebrafish retina. Development *128*, 1099-1107.

Schmid, A., Chiba, A., and Doe, C.Q. (1999). Clonal analysis of Drosophila embryonic neuroblasts: neural cell types, axon projections and muscle targets. Development *126*, 4653-4689.

Schmidt, H., Rickert, C., Bossing, T., Vef, O., Urban, J., and Technau, G.M. (1997). The embryonic central nervous system lineages of Drosophila melanogaster. II. Neuroblast lineages derived from the dorsal part of the neuroectoderm. Dev Biol *189*, 186-204.

Schonemann, M.D., Ryan, A.K., Erkman, L., McEvilly, R.J., Bermingham, J., and Rosenfeld, M.G. (1998). POU domain factors in neural development. Adv Exp Med Biol *449*, 39-53.

Sekiya, T., Kondo, T., Shichita, T., Morita, R., Ichinose, H., and Yoshimura, A. (2015). Suppression of Th2 and Tfh immune reactions by Nr4a receptors in mature T reg cells. J Exp Med *212*, 1623-1640.

Sen, S.Q., Chanchani, S., Southall, T.D., and Doe, C.Q. (2019). Neuroblast-specific open chromatin allows the temporal transcription factor, Hunchback, to bind neuroblast-specific loci. Elife *8*.

Seroka, A.Q., and Doe, C.Q. (2019). The Hunchback temporal transcription factor determines motor neuron axon and dendrite targeting in Drosophila. Development *146*.

Shakya, A., Goren, A., Shalek, A., German, C.N., Snook, J., Kuchroo, V.K., Yosef, N., Chan, R.C., Regev, A., Williams, M.A.*, et al.* (2015). Oct1 and OCA-B are selectively required for CD4 memory T cell function. J Exp Med *212*, 2115-2131.

Shakya, A., Kang, J., Chumley, J., Williams, M.A., and Tantin, D. (2011). Oct1 is a switchable, bipotential stabilizer of repressed and inducible transcriptional states. J Biol Chem *286*, 450-459.

Sharma, M.D., Huang, L., Choi, J.H., Lee, E.J., Wilson, J.M., Lemos, H., Pan, F., Blazar, B.R., Pardoll, D.M., Mellor, A.L.*, et al.* (2013). An inherently bifunctional subset of Foxp3+ T helper cells is controlled by the transcription factor eos. Immunity *38*, 998-1012.

Shekhar, K., Lapan, S.W., Whitney, I.E., Tran, N.M., Macosko, E.Z., Kowalczyk, M., Adiconis, X., Levin, J.Z., Nemesh, J., Goldman, M.*, et al.* (2016). Comprehensive Classification of Retinal Bipolar Neurons by Single-Cell Transcriptomics. Cell *166*, 1308-1323 e1330.

Shen, C.P., Knoblich, J.A., Chan, Y.M., Jiang, M.M., Jan, L.Y., and Jan, Y.N. (1998). Miranda as a multidomain adapter linking apically localized Inscuteable and basally localized Staufen and Prospero during asymmetric cell division in Drosophila. Genes Dev *12*, 1837-1846.

Shimojo, H., Ohtsuka, T., and Kageyama, R. (2008). Oscillations in notch signaling regulate maintenance of neural progenitors. Neuron *58*, 52-64.

Siegert, S., Scherf, B.G., Del Punta, K., Didkovsky, N., Heintz, N., and Roska, B. (2009). Genetic address book for retinal cell types. Nat Neurosci *12*, 1197-1204.

Singh, M.S., Balmer, J., Barnard, A.R., Aslam, S.A., Moralli, D., Green, C.M., Barnea-Cramer, A., Duncan, I., and MacLaren, R.E. (2016). Transplanted photoreceptor precursors transfer proteins to host photoreceptors by a mechanism of cytoplasmic fusion. Nat Commun *7*, 13537.

Skeath, J.B., Zhang, Y., Holmgren, R., Carroll, S.B., and Doe, C.Q. (1995). Specification of neuroblast identity in the Drosophila embryonic central nervous system by gooseberry-distal. Nature *376*, 427-430.

Skene, P.J., Henikoff, J.G., and Henikoff, S. (2018). Targeted in situ genome-wide profiling with high efficiency for low cell numbers. Nat Protoc *13*, 1006-1019.

Srinivas, M., Ng, L., Liu, H., Jia, L., and Forrest, D. (2006). Activation of the blue opsin gene in cone photoreceptor development by retinoid-related orphan receptor beta. Mol Endocrinol *20*, 1728-1741.

Staudt, L.M., Clerc, R.G., Singh, H., LeBowitz, J.H., Sharp, P.A., and Baltimore, D. (1988). Cloning of a lymphoid-specific cDNA encoding a protein binding the regulatory octamer DNA motif. Science *241*, 577-580.

Staudt, L.M., Singh, H., Sen, R., Wirth, T., Sharp, P.A., and Baltimore, D. (1986). A lymphoid-specific protein binding to the octamer motif of immunoglobulin genes. Nature *323*, 640-643.

Stepchenko, A.G. (1992). The nucleotide sequence of mouse OCT-1 cDNA. Nucleic Acids Res *20*, 1419.

Stiles, J., and Jernigan, T.L. (2010). The basics of brain development. Neuropsychol Rev *20*, 327-348.

Sturm, R.A., and Herr, W. (1988). The POU domain is a bipartite DNA-binding structure. Nature *336*, 601-604.

Suzuki, N., Peter, W., Ciesiolka, T., Gruss, P., and Scholer, H.R. (1993). Mouse Oct-1 contains a composite homeodomain of human Oct-1 and Oct-2. Nucleic Acids Res *21*, 245-252.

Suzuki, T., Kaido, M., Takayama, R., and Sato, M. (2013). A temporal mechanism that produces neuronal diversity in the Drosophila visual center. Dev Biol *380*, 12-24.

Swaroop, A., Kim, D., and Forrest, D. (2010). Transcriptional regulation of photoreceptor development and homeostasis in the mammalian retina. Nat Rev Neurosci *11*, 563-576.

Takatsuka, K., Hatakeyama, J., Bessho, Y., and Kageyama, R. (2004). Roles of the bHLH gene Hes1 in retinal morphogenesis. Brain Res *1004*, 148-155.

Takebayashi, H., Ohtsuki, T., Uchida, T., Kawamoto, S., Okubo, K., Ikenaka, K., Takeichi, M., Chisaka, O., and Nabeshima, Y. (2002). Non-overlapping expression of Olig3 and Olig2 in the embryonic neural tube. Mech Dev *113*, 169-174.

Tanna, P., Strauss, R.W., Fujinami, K., and Michaelides, M. (2017). Stargardt disease: clinical features, molecular genetics, animal models and therapeutic options. Br J Ophthalmol *101*, 25-30.

Tantin, D. (2013). Oct transcription factors in development and stem cells: insights and mechanisms. Development *140*, 2857-2866.

Taranova, O.V., Magness, S.T., Fagan, B.M., Wu, Y., Surzenko, N., Hutton, S.R., and Pevny, L.H. (2006). SOX2 is a dose-dependent regulator of retinal neural progenitor competence. Genes Dev *20*, 1187-1202.

Thelie, A., Desiderio, S., Hanotel, J., Quigley, I., Van Driessche, B., Rodari, A., Borromeo, M.D., Kricha, S., Lahaye, F., Croce, J.*, et al.* (2015). Prdm12 specifies V1 interneurons through cross-repressive interactions with Dbx1 and Nkx6 genes in Xenopus. Development *142*, 3416-3428.

Thomas, R.M., Chen, C., Chunder, N., Ma, L., Taylor, J., Pearce, E.J., and Wells, A.D. (2010). Ikaros silences T-bet expression and interferon-gamma production during T helper 2 differentiation. J Biol Chem *285*, 2545-2553.

Tomilin, A., Reményi, A., Lins, K., Bak, H., Leidel, S., Vriend, G., Wilmanns, M., and Schöler, H.R. (2000). Synergism with the coactivator OBF-1 (OCA-B, BOB-1) is mediated by a specific POU dimer configuration. Cell *103*, 853-864.

Tran, K.D., and Doe, C.Q. (2008). Pdm and Castor close successive temporal identity windows in the NB3-1 lineage. Development *135*, 3491-3499.

Tran, K.D., Miller, M.R., and Doe, C.Q. (2010). Recombineering Hunchback identifies two conserved domains required to maintain neuroblast competence and specify early-born neuronal identity. Development *137*, 1421-1430.

Treacy, M.N., and Rosenfeld, M.G. (1992). Expression of a family of POU-domain protein regulatory genes during development of the central nervous system. Annu Rev Neurosci *15*, 139-165.

Trimarchi, J.M., Stadler, M.B., and Cepko, C.L. (2008). Individual retinal progenitor cells display extensive heterogeneity of gene expression. PLoS One *3*, e1588.

Turner, D.L., and Cepko, C.L. (1987). A common progenitor for neurons and glia persists in rat retina late in development. Nature *328*, 131-136.

Turner, D.L., Snyder, E.Y., and Cepko, C.L. (1990). Lineage-independent determination of cell type in the embryonic mouse retina. Neuron *4*, 833-845.

Ueki, Y., Wilken, M.S., Cox, K.E., Chipman, L.B., Bermingham-McDonogh, O., and Reh, T.A. (2015). A transient wave of BMP signaling in the retina is necessary for Müller glial differentiation. *142*, 533-543.

Umulis, D., O'Connor, M.B., and Othmer, H.G. (2008). Robustness of embryonic spatial patterning in Drosophila melanogaster. Curr Top Dev Biol *81*, 65-111.

Urbach, R., and Technau, G.M. (2003). Segment polarity and DV patterning gene expression reveals segmental organization of the Drosophila brain. Development *130*, 3607-3620.

Vacalla, C.M., and Theil, T. (2002). Cst, a novel mouse gene related to Drosophila Castor, exhibits dynamic expression patterns during neurogenesis and heart development. Mech Dev *118*, 265-268.

Vazquez-Arreguin, K., and Tantin, D. (2016). The Oct1 transcription factor and epithelial malignancies: Old protein learns new tricks. Biochim Biophys Acta *1859*, 792-804.

Vecino, E., Rodriguez, F.D., Ruzafa, N., Pereiro, X., and Sharma, S.C. (2016). Glia-neuron interactions in the mammalian retina. Prog Retin Eye Res *51*, 1-40.

Verrijzer, C.P., Alkema, M.J., van Weperen, W.W., Van Leeuwen, H.C., Strating, M.J., and van der Vliet, P.C. (1992). The DNA binding specificity of the bipartite POU domain and its subdomains. Embo j *11*, 4993-5003.

Virden, R.A., Thiele, C.J., and Liu, Z. (2012). Characterization of critical domains within the tumor suppressor CASZ1 required for transcriptional regulation and growth suppression. Mol Cell Biol *32*, 1518-1528.

Voronina, V.A., Kozhemyakina, E.A., O'Kernick, C.M., Kahn, N.D., Wenger, S.L., Linberg, J.V., Schneider, A.S., and Mathers, P.H. (2004). Mutations in the human RAX homeobox gene in a patient with anophthalmia and sclerocornea. Hum Mol Genet *13*, 315-322.

Wall, D.S., Mears, A.J., McNeill, B., Mazerolle, C., Thurig, S., Wang, Y., Kageyama, R., and Wallace, V.A. (2009). Progenitor cell proliferation in the retina is dependent on Notch-independent Sonic hedgehog/Hes1 activity. J Cell Biol *184*, 101-112.

Walther, C., and Gruss, P. (1991). Pax-6, a murine paired box gene, is expressed in the developing CNS. Development *113*, 1435-1449.

Wang, D., Yamamoto, S., Hijiya, N., Benveniste, E.N., and Gladson, C.L. (2000). Transcriptional regulation of the human osteopontin promoter: functional analysis and DNA-protein interactions. Oncogene *19*, 5801-5809.

Wang, J.H., Nichogiannopoulou, A., Wu, L., Sun, L., Sharpe, A.H., Bigby, M., and Georgopoulos, K. (1996). Selective defects in the development of the fetal and adult lymphoid system in mice with an Ikaros null mutation. Immunity *5*, 537-549.

Wang, S., Sengel, C., Emerson, M.M., and Cepko, C.L. (2014). A gene regulatory network controls the binary fate decision of rod and bipolar cells in the vertebrate retina. Dev Cell *30*, 513-527.

Wang, S.W., Kim, B.S., Ding, K., Wang, H., Sun, D., Johnson, R.L., Klein, W.H., and Gan, L. (2001). Requirement for math5 in the development of retinal ganglion cells. Genes Dev *15*, 24-29.

Wang, Y., Dakubo, G.D., Thurig, S., Mazerolle, C.J., and Wallace, V.A. (2005). Retinal ganglion cell-derived sonic hedgehog locally controls proliferation and the timing of RGC development in the embryonic mouse retina. Development *132*, 5103-5113.

Wässle, H., and Boycott, B.B. (1991). Functional architecture of the mammalian retina. Physiol Rev *71*, 447-480.

Watanabe, T., and Raff, M.C. (1990). Rod photoreceptor development in vitro: intrinsic properties of proliferating neuroepithelial cells change as development proceeds in the rat retina. Neuron *4*, 461-467.

Welby, E., Lakowski, J., Di Foggia, V., Budinger, D., Gonzalez-Cordero, A., Lun, A.T.L., Epstein, M., Patel, A., Cuevas, E., Kruczek, K.*, et al.* (2017). Isolation and Comparative Transcriptome Analysis of Human Fetal and iPSC-Derived Cone Photoreceptor Cells. Stem Cell Reports *9*, 1898-1915.

Wilson, S.I., Shafer, B., Lee, K.J., and Dodd, J. (2008). A molecular program for contralateral trajectory: Rig-1 control by LIM homeodomain transcription factors. Neuron *59*, 413-424.

Wolf, F.A., Angerer, P., and Theis, F.J. (2018). SCANPY: large-scale single-cell gene expression data analysis. Genome Biol *19*, 15.

Wong, L., Wood, E., Yasumura, D., LaVail, M., and Rapaport, D. (2002). The Timing, Sequence and Spatial Pattern of Cell Genesis in the Rat Retina. Investigative Ophthalmology & Visual Science *43*, 2681-2681.

Wong, L.Y., Hatfield, J.K., and Brown, M.A. (2013). Ikaros sets the potential for Th17 lineage gene expression through effects on chromatin state in early T cell development. J Biol Chem *288*, 35170-35179.

Wu, F., Bard, J.E., Kann, J., Yergeau, D., Sapkota, D., Ge, Y., Hu, Z., Wang, J., Liu, T., and Mu, X. (2021). Single cell transcriptomics reveals lineage trajectory of retinal ganglion cells in wild-type and Atoh7-null retinas. Nat Commun *12*, 1465.

Wu, L., Nichogiannopoulou, A., Shortman, K., and Georgopoulos, K. (1997). Cell-autonomous defects in dendritic cell populations of Ikaros mutant mice point to a developmental relationship with the lymphoid lineage. Immunity *7*, 483-492.

Wu, S.J., Furlan, S.N., Mihalas, A.B., Kaya-Okur, H., Feroze, A.H., Emerson, S.N., Zheng, Y., Carson, K., Cimino, P.J., Keene, C.D.*, et al.* (2020). Single-cell analysis of chromatin silencing programs in developmental and tumor progression. 2020.2009.2004.282418.

Wu, Y.Y., Chang, C.L., Chuang, Y.J., Wu, J.E., Tung, C.H., Chen, Y.C., Chen, Y.L., Hong, T.M., and Hsu, K.F. (2016). CASZ1 is a novel promoter of metastasis in ovarian cancer. Am J Cancer Res *6*, 1253-1270.

Xiao, D., Qiu, S., Huang, X., Zhang, R., Lei, Q., Huang, W., Chen, H., Gou, B., Tie, X., Liu, S.*, et al.* (2019). Directed robust generation of functional retinal ganglion cells from Müller glia. 735357.

Yadav, S.P., Hao, H., Yang, H.J., Kautzmann, M.A., Brooks, M., Nellissery, J., Klocke, B., Seifert, M., and Swaroop, A. (2014). The transcription-splicing protein NonO/p54nrb and three NonO-interacting proteins bind to distal enhancer region and augment rhodopsin expression. Hum Mol Genet *23*, 2132-2144.

Yan, W., Laboulaye, M.A., Tran, N.M., Whitney, I.E., Benhar, I., and Sanes, J.R. (2020). Molecular identification of sixty-three amacrine cell types completes a mouse retinal cell atlas. 2020.2003.2010.985770.

Yao, K., Qiu, S., Wang, Y.V., Park, S.J.H., Mohns, E.J., Mehta, B., Liu, X., Chang, B., Zenisek, D., Crair, M.C.*, et al.* (2018). Restoration of vision after de novo genesis of rod photoreceptors in mammalian retinas. Nature *560*, 484-488.

Yaron, O., Farhy, C., Marquardt, T., Applebury, M., and Ashery-Padan, R. (2006). Notch1 functions to suppress cone-photoreceptor fate specification in the developing mouse retina. Development *133*, 1367-1378.

Yoshida, N., Sakaguchi, H., Muramatsu, H., Okuno, Y., Song, C., Dovat, S., Shimada, A., Ozeki, M., Ohnishi, H., Teramoto, T.*, et al.* (2017). Germline IKAROS mutation associated with primary immunodeficiency that progressed to T-cell acute lymphoblastic leukemia. Leukemia *31*, 1221-1223.

Young, R.W. (1985a). Cell differentiation in the retina of the mouse. Anat Rec *212*, 199-205.

Young, R.W. (1985b). Cell proliferation during postnatal development of the retina in the mouse. Brain Res *353*, 229-239.

Yu, C., Mazerolle, C.J., Thurig, S., Wang, Y., Pacal, M., Bremner, R., and Wallace, V.A. (2006). Direct and indirect effects of hedgehog pathway activation in the mammalian retina. Mol Cell Neurosci *32*, 274-282.

Yu, W., Mookherjee, S., Chaitankar, V., Hiriyanna, S., Kim, J.-W., Brooks, M., Ataeijannati, Y., Sun, X., Dong, L., Li, T.*, et al.* (2017). Nrl knockdown by AAV-delivered CRISPR/Cas9 prevents retinal degeneration in mice. Nature Communications *8*, 14716.

Yukawa, K., Butz, K., Yasui, T., Kikutani, H., and Hoppe-Seyler, F. (1996). Regulation of human papillomavirus transcription by the differentiation-dependent epithelial factor Epoc-1/skn-1a. J Virol *70*, 10-16.

Zannino, D.A., and Sagerstrom, C.G. (2015). An emerging role for prdm family genes in dorsoventral patterning of the vertebrate nervous system. Neural Dev *10*, 24.

Zelinger, L., Karakulah, G., Chaitankar, V., Kim, J.W., Yang, H.J., Brooks, M.J., and Swaroop, A. (2017). Regulation of Noncoding Transcriptome in Developing Photoreceptors by Rod Differentiation Factor NRL. Invest Ophthalmol Vis Sci *58*, 4422-4435.

Zhang, Y., Ungar, A., Fresquez, C., and Holmgren, R. (1994). Ectopic expression of either the Drosophila gooseberry-distal or proximal gene causes alterations of cell fate in the epidermis and central nervous system. Development *120*, 1151-1161.

Zheng, M.H., Shi, M., Pei, Z., Gao, F., Han, H., and Ding, Y.Q. (2009). The transcription factor RBP-J is essential for retinal cell differentiation and lamination. Mol Brain *2*, 38.

Zhou, S., Flamier, A., Abdouh, M., Tetreault, N., Barabino, A., Wadhwa, S., and Bernier, G. (2015). Differentiation of human embryonic stem cells into cone photoreceptors through simultaneous inhibition of BMP, TGFbeta and Wnt signaling. Development *142*, 3294-3306.

Zibetti, C., Liu, S., Wan, J., Qian, J., and Blackshaw, S. (2019). Epigenomic profiling of retinal progenitors reveals LHX2 is required for developmental regulation of open chromatin. Commun Biol *2*, 142.

Zuber, M.E., Gestri, G., Viczian, A.S., Barsacchi, G., and Harris, W.A. (2003). Specification of the vertebrate eye by a network of eye field transcription factors. Development *130*, 5155-5167.

Zuber, M.E., Perron, M., Philpott, A., Bang, A., and Harris, W.A. (1999). Giant eyes in Xenopus laevis by overexpression of XOptx2. Cell *98*, 341-352.